Vascular Regulation of Embryonic Neurogenesis

Mathew Alec Jamshed Tata

Thesis submitted in fulfilment for the degree of Doctor of Philosophy

University College London (UCL)

Department of Cell and Developmental Biology

Supervisor: Prof Christiana Ruhrberg

Secondary Supervisor: Dr François Guillemot

DECLARATION

I, Mathew Alec Jamshed Tata, confirm that the work presented in this thesis is my own. Where information has been derived from other sources, I confirm that this has been indicated in the thesis.

ACKNOWLEDGEMENTS

I have enjoyed my PhD immensely and that is largely due to the wonderful people I've had the pleasure of working with. I start with thanking Christiana Ruhrberg who has been such an enthusiastic, engaging and above all supportive supervisor over the last few years. I would also like to extend my profound thanks to the members of the Ruhrberg group who have always been willing to lend a helping hand along the way. In particular, I must thank Alex Fantin who helped me out technically when I first joined the lab, as well as Alice Plein who has always had useful suggestions for challenging experiments. I am also very grateful to both Laura Denti and Valentina Senatore for their efforts with animal work. Finally, special thanks must go to Andy Joyce who has worked tirelessly to support my PhD research and endured several years of sitting next to me in the office.

I am thankful to other staff at the UCL Institute of Ophthalmology, including members of the Biological Resources Unit, as well as Peter Munro and Matthew Hayes in the Imaging Facility. Additionally, I am grateful to Ayad Eddaoudi and Stephanie Canning at the Institute of Child Health for their help with FACS experiments.

I would like to thank my family Philip, Amanda and Lauren who have always been there for me when I needed a boost or encouragement. I am also very grateful to Holly, who has been so supportive and loving throughout my PhD and kept me going during difficult times.

I would like to end by giving the very biggest thanks to my grandparents Jamshed and Renée. It makes me smile ear-to-ear to think that the trips to The Ridgeway and Kings' College when I was just a young boy would take me as far as doctoral training. Thank you for giving me those experiences that ultimately led me to do something as exciting as scientific research.

ABSTRACT

Neural progenitor cells (NPCs) in the embryonic nervous system generate a large number and variety of neurons in a process known as neurogenesis. NPCs reside in a regulatory 'niche' that provides an extensive array of diverse signals, and loss of any one of these signals can deplete the pool of NPCs and therefore impair neural development. These niche signals are most commonly studied in the forebrain, where a complex array of cell divisions yields a set of diverse NPCs. In contrast, little is known on the role of niche signals in regulating the behaviour of NPCs in the hindbrain, the evolutionary oldest part of the brain that is essential for many vital bodily functions. In the adult brain, blood vessels and the vascular growth factor VEGF-A regulate the behaviour of neural stem cells (NSC). However, it is not known whether either also regulates hindbrain neurogenesis. For my PhD research, I have used the mouse embryo hindbrain as a model to examine the role of blood vessels and VEGF-A receptors in developmental neurogenesis.

My studies have revealed that NPCs divide most actively during a period of extensive blood vessel growth in the hindbrain, that hindbrain NPCs reside within a well-vascularised germinal zone (GZ) and that they make physical contact with the GZ vasculature. To establish whether VEGF-A receptors or hindbrain blood vessels regulate the behaviour of hindbrain NPCs, I have analysed mouse embryos lacking the neurovascular cell surface receptor NRP1 in either the neural or endothelial lineages. I found that NRP1 regulates the proliferative behaviour of hindbrain NPCs through its role in promoting GZ vascularisation, but not as a receptor for VEGF-A in NPCs. I have further shown that GZ vasculature sustains the size of the NPC pool through the period of hindbrain neurogenesis and may do so by limiting the expression of pro-differentiation signals to set the pace of neurogenesis. Even though blood vessels are best know for their role in tissue oxygenation, my results also show that NRP1-dependent GZ vasculature does not regulate hindbrain NPC behaviour through its role in oxygenating the neuroepithelium.

In conclusion, my results identify an essential role for blood vessels in regulating NPC behaviour in the embryonic hindbrain and have increased our understanding of the regulatory niche that orchestrates developmental neurogenesis.

TABLE OF CONTENTS

DECLARATION 2

ACKNOWLEDGEMENTS 3

ABSTRACT 4

TABLE OF CONTENTS 5

LIST OF TABLES 9

LIST OF FIGURES 10

ABBREVIATIONS 13

Chapter 1 INTRODUCTION 16

1.1 The formation of the central nervous system 16

1.1.1 Mammalian neural progenitor cells 18

1.1.2 Structure of mammalian neural progenitor cells 24

1.1.3 Complex processes in neural progenitor cells 30

1.2 Regulation of neural progenitor cells 34

1.2.1 Transcriptional control of neural progenitor cells 34

1.2.2 Intrinsic regulation of neural progenitor cells by intracellular molecules 40

1.2.3 Extrinsic control of neural progenitor cells 42

1.3 VEGF in neural development 55

1.4 Vascularisation of the central nervous system (CNS) 58

1.4.1 Cellular and molecular interactions in CNS vascularisation 60

1.5 The mammalian stem cell niche 73

1.5.1 Embryonic stem cell niches in mammals 73

1.5.2 Postnatal stem cell niches in mammals 74

1.6 Aims and objectives of this study 80

Chapter 2 MATERIALS AND METHODS 81

2.1 Materials 81

2.1.1 General Laboratory Materials *81*

2.1.2 General Laboratory Solutions *81*

2.2 Methods 82

2.2.1 Animal Methods *82*

2.2.2 Immunolabelling *89*

2.2.3 Imaging *93*

2.2.4 Analysis of immunolabelling *93*

2.2.5 3-dimensional data visualisation *93*

2.2.6 Fluorescence-activated cell sorting (FACS) *94*

2.2.7 qRT-PCR *96*

2.2.8 Neurosphere culture *101*

2.2.9 Statistics *102*

Chapter 3 EMBRYONIC NEURAL PROGENITOR CELLS IN THE MOUSE HINDBRAIN RESIDE WITHIN A VASCULAR NICHE 103

3.1 Introduction 103

3.2 Results 104

3.2.1 The mouse hindbrain as a model for simultaneous visualisation of embryonic neural progenitors and sprouting blood vessels *104*

3.2.2 NPC mitotic activity correlates well with hindbrain angiogenesis *109*

3.2.3 The hindbrain germinal zone (GZ) is well-vascularised *114*

3.2.4 NPCs contact blood vessel plexi within and outside the hindbrain *117*

3.2.5 Hindbrain NPCs contact vessel-associated extracellular membrane *120*

3.2.6 Sox1-iCreER^{T2} mouse strain labels single hindbrain NPCs *122*

3.3 Discussion 126

3.4 Summary 129

Chapter 4 NRP1 REGULATES HINDBRAIN NEURAL PROGENITOR CELLS NON-CELL AUTONOMOUSLY THROUGH ITS ROLE IN GERMINAL ZONE VASCULARISATION 130

4.1 Introduction 130

4.2 Results 131

4.2.1 Developmental staging for studying neurogenesis 131

4.2.2 Neuropilin 1 is required for vascularisation of the hindbrain GZ..... 134

4.2.3 Cell survival is not compromised in NRP1-deficient hindbrains..... 137

4.2.4 Neuropilin 1 regulates the timing of hindbrain NPC mitosis 139

4.2.5 Neuropilin 1 maintains GZ organisation 143

4.2.6 NPC processes are mildly disorganised in NRP1-null hindbrains.... 146

4.2.7 Neuropilin 1 regulates NPC division non-cell autonomously through germinal zone vascularisation 151

4.2.8 Neuropilin 1 is not required cell autonomously by hindbrain NPCs to regulate mitotic activity..... 156

4.2.9 Neuropilins 1 and 2 redundantly regulate hindbrain NPC mitotic activity 157

4.2.10 Hindbrain NPCs express VEGFR2 in vitro but not in vivo 160

4.2.11 Microglia do not regulate hindbrain NPC mitosis 162

4.3 Discussion 164

4.4 Summary 171

Chapter 5 HINDBRAIN GERMINAL ZONE VASCULATURE REGULATES NEURAL PROGENITOR CELL SELF-RENEWAL..... 172

5.1 Introduction 172

5.2 Results 173

5.2.1 Loss of germinal zone vascularisation reduces neural progenitor cell cycle re-entry..... 173

5.2.2 Loss of germinal zone vascularisation induces premature neuronal differentiation..... 179

5.2.3 Cell cycle analysis of hindbrain NPCs by fluorescence-activated cell sorting (FACS) 183

5.2.4 Germinal zone vasculature regulates cell cycle progression in hindbrain NPCs..... 188

5.2.5 Germinal zone vasculature is essential for proper hindbrain growth 192

5.2.6 The SVP does not regulate hindbrain NPCs by relieving tissue hypoxia 194

5.2.7 Differential gene expression in the neuropilin 1-null hindbrain 198

5.2.8 Increased neurotrophin expression in the neuropilin 1-null hindbrain... 205

5.2.9 Potential angiocrine molecules regulating NPCs 207

5.3 Discussion 210

5.4 Summary 220

Chapter 6 FINAL CONCLUSIONS AND FUTURE WORK 221

6.1 Summary of Conclusions and Final Remarks 221

6.2 Future work 222

6.2.1 The spatial relationship between neurogenesis and angiogenesis 222

6.2.2 Role of NRPs and VEGF in NPCs 222

6.2.3 Neural lineage progression in the hindbrain 223

6.2.4 Angiocrine signalling from embryonic CNS vasculature 224

6.2.5 Functional analysis of vascular regulation of NPCs 224

Chapter 7 BIBLIOGRAPHY 225

Chapter 8 APPENDIX 262

LIST OF TABLES

Table 2.1 Genetic mouse strains and published reference. 83

Table 2.2 Olignonucleotide primers used for genotyping. 87

Table 2.3 PCR parameters for specific primer pairs......88

Table 2.4 Primary antibody parameters for immunolabelling......92

Table 2.5 Primary antibody parameters for FACS. 95

Table 2.6 Oligonucleotide primers designed for qRT-PCR......98

Table 2.7 Genes tested for in Qiagen RT^2 Profiler PCR Array (Neurogenesis). .99

Table 5.1 Differentially expressed genes in qRT-PCR array......204

Table 8.1 Fold change enrichment for all transcripts assayed for in qRT-PCR array......262

Table 8.2 Number of embryos analysed......265

LIST OF FIGURES

Figure 1.1 Schematic representation of the different NPC subtypes in the developing CNS. 19

Figure 1.2 Schematic representation of the structure of aRG. 29

Figure 1.3 INM in the developing CNS. 32

Figure 1.4 Cellular and molecular regulation of NPCs. 45

Figure 1.5 VEGF receptor binding. 65

Figure 1.6 Schematic representation of the interaction between neuroglial cells, microglia and endothelial cells during CNS vascularisation. 72

Figure 3.1 Temporal pattern of hindbrain vascularisation. 106

Figure 3.2 The mouse hindbrain as a model for simultaneous visualisation of NPCs and sprouting blood vessels. 107

Figure 3.3 The temporal pattern of hindbrain angiogenesis. 112

Figure 3.4 The temporal pattern hindbrain NPC mitosis. 113

Figure 3.5 Spatial relationship of blood vessel growth and NPC proliferation in the hindbrain. 116

Figure 3.6 NPC processes contact hindbrain vasculature. 119

Figure 3.7 NPC processes contact vascular ECM. 121

Figure 3.8 Mosaic labelling of NPCs in the forebrain and hindbrain. 124

Figure 4.1 *Nrp1*$^{-/-}$ embryos are developmentally delayed. 133

Figure 4.2 NRP1 regulates hindbrain GZ vascularisation. 136

Figure 4.3 Cell survival in the hindbrain is not impaired following constitutive loss of *Nrp1*. 138

Figure 4.4 NRP1 regulates hindbrain NPC proliferation. 141

Figure 4.5 NRP1 regulates the organisation of the hindbrain GZ. 145

Figure 4.6 $RC2^+$ processes and laminin expression in NRP1-deficient hindbrains. 150

Figure 4.7 NRP1 regulates NPC mitosis non-cell autonomously through its role in GZ vascularisation. 154

Figure 4.8 Semaphorin signalling through NRPs in NPCs regulates NPC mitosis. 159

Figure 4.9 VEGFR2 is expressed by hindbrain vessels and cultured hindbrain NPCs, but not by hindbrain NPCs *in vivo*. 161

Figure 4.10 Microglia do not regulate hindbrain NPC mitosis at 50s. 163

Figure 5.1 NPC cell cycle re-entry is impaired in hindbrains lacking GZ vasculature at 32s. 176

Figure 5.2 The proportion of cycling NPCs is normal in the *Nrp1*$^{-/-}$ hindbrains at 40s and 46s, but fewer cycling NPCs are present. 177

Figure 5.3 NPCs differentiate prematurely in the absence of GZ vasculature in *Nrp1*$^{-/-}$ and *Tie2-Cre; Nrp1*$^{c/-}$ hindbrains at 32s. 181

Figure 5.4 Reduced neurogenesis in *Nrp1*$^{-/-}$ hindbrains at 40s and 46s. 182

Figure 5.5 FACS analysis of hindbrain NPCs. 186

Figure 5.6 NPC cell cycle progression is perturbed at 36s, but not 32s, in *Nrp1*$^{-/-}$ hindbrains......190

Figure 5.7 Impaired GZ vascularisation compromises hindbrain growth......193

Figure 5.8 The SVP does not regulate NPCs by relieving tissue hypoxia......196

Figure 5.9 Differential gene expression of neurogenesis-associated transcripts in *Nrp1*-null hindbrains at 35s. 202

Figure 5.10 Increased expression of *Bdnf* and *Ntf3* in the *Nrp1*-null hindbrain at 32s......206

Figure 5.11 Screening candidate molecules for angiocrine signalling. 209

Figure 5.12 Working model for the role of blood vessels in hindbrain neurogenesis......212

ABBREVIATIONS

aIP	apical intermediate progenitor
aRG	apical radial glia
AP	apical progenitor
BBB	blood-brain barrier
BCIP	5-bromo-4-chloro-3'-indoylphosphate salt, 50mg/ml in 100% DMF
bIP	basal intermediate progenitor
bRG	basal radial glia
BSA	bovine serum albumin
bp	base
BP	basal progenitor
cDNA	complementary DNA
CNS	central nervous system
CSF	cerebrospinal fluid
DABCO	1,4-diazabicyclo-[2.2.2]octane
DAPI	4'-6'diamidino-2-phenylindole
DG	dentate gyrus
dNTP	deoxynucleoside triphosphate
DMEM	Dulbecco's modified eagle medium
DMF	dimethylformamide
DNA	deoxyribonucleic acid
DNAse	deoxyribonuclease
DP	deeper vascular plexus
DTT	dithiothreitol
E	embryonic day
ECM	extracellular matrix
EDTA	ethyldiaminotetraacetic acid, disodium salt
FBM	facial branchiomotor neuron
FBS	fetal bovine serum
G	gauge
GE	ganglionic eminence
GnRH	gonadotrophin-releasing hormone
GPCR	G protein-coupled receptor

GZ	germinal zone
h	hour
HCl	hydrochloric acid
IB4	Isolectin B4 (*bandeirea simplicifolia*)
INM	interkinetic nuclear migration
kb	kilobase
l	litre
LGE	lateral ganglionic eminence
LOT	lateral olfactory neuron
LV	lateral ventricle
M	molar
µ	micro
m	milli
min	minute
miRNA	micro RNA
mRNA	messenger RNA
MW	molecular weight
NBT	nitro-blue tetrazolium chloride, 75 mg/ml in 70% DMF
NE	neuroepithelial cells
NGS	normal goat serum
NPC	neural progenitor cell
NRP1/2	neuropilin 1/2
NSC	neural stem cell
OB	olfactory bulb
P	pial surface
PBS	phosphate buffered saline
PBT	1X PBS + Triton X-100
PCR	polymerase chain reaction
PFA	paraformaldehyde
PNP	Perineural vascular plexus
PNS	peripheral nervous system
RGC	retinal ganglion cell
RMS	rostral migratory stream
RPC	retinal progenitor cell
RNA	ribonucleic acid

RNAse	ribonuclease
RNAseq	RNA sequencing
rpm	rotations per minute
RT	room temperature
RV	radial vessel
qRT-PCR	quantitative real-time PCR
(35)s	35 somites
(10) s	(10) seconds
SAPs	subapical progenitor
SDS	sodium dodecyl sulphate
SEMA3	class III semaphorin
SGZ	subgranular zone
SSC	saline sodium citrate buffer
SVP	subventricular plexus
SVZ	subventricular zone
TAE	tris acetate EDTA
TAPs	transit amplifying progenitors
TE	tris EDTA buffer
TF	transcription factor
TM	transmembrane
Tris	tris (hydroxymethyl) aminomethane
tRNA	transfer RNA
V	ventricular surface
VEGF	vascular endothelial growth factor
(v/v)	volume to volume ratio
VZ	ventricular zone
(w/v)	weight to volume ratio
YFP	yellow fluorescent protein

Chapter 1 INTRODUCTION

1.1 The formation of the central nervous system

The formation of the vertebrate central nervous system (CNS) begins early in embryogenesis when germ layer specification takes place (Spemann and Mangold, 1924). Of these germ layers, the early ectoderm separates into the presumptive epidermis and the presumptive neural ectoderm, and it is from the neural ectoderm that the CNS derives. The neural ectoderm develops into the neuroepithelium, which will ultimately generate the neurons and glia of the CNS, as well as the peripheral nervous system (PNS) and neural crest. The neuroepithelium begins as a thin epithelial sheet known as the neural plate, but progressively folds to establish the neural tube along the anterior-posterior axis of the embryo. The neural tube remodels significantly during the process of 'neurulation' to form the forebrain, midbrain and hindbrain from the anterior segment and the spinal cord from the posterior segment.

Neuroepithelial cells are the first embryonic neural progenitor cells and populate the neural tube (Rakic, 1995). They divide and differentiate to produce a diverse range of functionally specialised cells in both neural and glial lineages. Furthermore, neuroepithelial cells and their derivatives often migrate away from their initial birthplace and can acquire specific identities based on their location along the rostrocaudal and dorsoventral axes. The process by which neurons are generated from different neural progenitor cell subtypes is termed 'neurogenesis'.

Neurogenesis is a highly orchestrated process that is regulated both by intrinsic transcriptional machinery and extrinsic signalling mechanisms (Paridaen and Huttner, 2014). The formation of glia, specifically astrocytes and oligodendrocytes, is termed 'gliogenesis' and occurs in parallel with neurogenesis. In addition to neurons and glia, various other populations of cells colonise the developing CNS, such as tissue-resident immune cells called microglia, as well as the endothelial cells and pericytes that form blood vessels.

Both embryonic neurogenesis and blood vessel growth in the CNS have been studied *in vivo* to elucidate cellular and tissue dynamics, as well as *in vitro* to explore

the underlying molecular mechanisms. Whilst *in vitro* models have helped to define molecular interactions through cell biological and biochemical methods, usually in a homogenous, single type of primary cells, such analyses do not accurately recapitulate the complex cell-cell interactions and extracellular environment within the growing nervous system. Analysis carried out *in vivo* in a number of vertebrate and invertebrate model species, often through genetic loss-of-function studies, have therefore been used to confirm the physiological functions of a multitude of molecular mechanisms initially identified *in vitro*. Together, both means of analysis have therefore been invaluable in documenting the myriad of cellular and molecular interactions that underlie neural development.

Although neurogenesis and CNS vascularisation have typically been studied independently of each other, recent research has identified neurovascular crosstalk during CNS development and in the adult. For example, neural progenitors and endothelial cells are regulated by overlapping sets of extrinsic signals, which are discussed extensively later in this thesis. There is also a growing body of evidence to suggest that neural progenitor cells, post-mitotic neurons and glia direct vascularisation in the CNS. However, there have been relatively few demonstrations of reciprocal regulation, whereby developmental CNS vascularisation may regulate neurogenesis in mechanisms beyond the obvious role of vessels in maintaining tissue homeostasis. This is a particularly important question given several recent demonstrations of vascular regulation of neurogenesis in the postnatal mammalian brain.

Below, I will outline the current core cell and molecular biology knowledge of vertebrate neural progenitor cells, with particular emphasis on their ‘stem cell niche’, including the membrane-bound and diffusible factors that regulate their behaviour. I will also describe current knowledge of the cellular and molecular mechanisms that ensure CNS vascularisation. Finally, I will discuss current understanding of the niche that controls adult neural stem cells and how blood vessels contribute to this regulatory environment.

1.1.1 Mammalian neural progenitor cells

Neural progenitor cells (referred to as NPCs hereafter) in the mammalian nervous system are subdivided into a variety of classes according to each subtype's capacity for self-renewal and clonal capacity. The current strategy for NPC subtype identification in the developing mammalian CNS is based predominantly on morphological and behaviour criteria. Even though a few molecular markers are available to distinguish specific NPC sub-populations, some progenitor subtypes share expression of these markers. Therefore, it has been recently suggested that current classification of mammalian NPCs should be performed using subcellular and morphological, rather than molecular, attributes to distinguish the different subtypes involved in generating the CNS across many different vertebrate model species (Taverna et al., 2014). The three proposed key criteria consist of the (a) location of mitosis relative to the surface of the brain ventricles, (b) the degree of polarity across the cell and the (c) capacity for proliferation. Subtle combinations of these varying criteria help to roughly mark out at least six different NPC classes in the developing rodent CNS (**Figure 1.1**) and have aided research aimed at interrogating and manipulating just one or two of these subtypes.

Interestingly, these criteria have come under scrutiny in recent years with increased focus on the specific adaptations of NPCs in the brain of species with increased CNS growth and cognitive function, such as primates (Florio et al., 2015). In some cases, some additional NPC subtypes are present the developing CNS of species with perceived higher cognitive function and thus, the very presence of some NPCs may be directly linked to brain evolution (e.g. LaMonica et al., 2012).

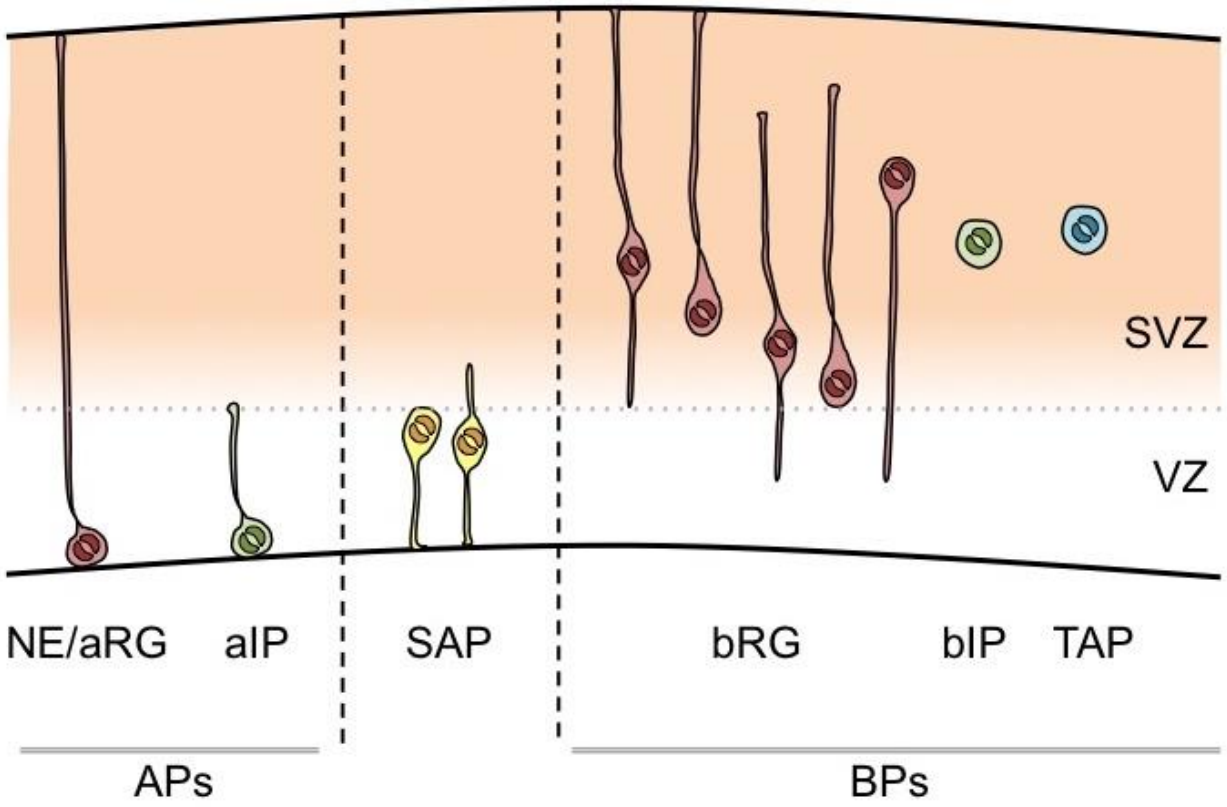

Figure 1.1 Schematic representation of the different NPC subtypes in the developing CNS.

Radial glia shown in red, subapical progenitors in yellow and intermediate progenitors in green and blue. Abbreviations: APs, apical progenitors; BPs, basal progenitors; aRG, apical radial glia; aIP, apical intermediate progenitor; SAP, subapical progenitor; bRG, basal radial glia; bIP, basal intermediate progenitor; VZ, ventricular zone; SVZ, subventricular zone.

1.1.1.1 *Classification of NPCs by their location during mitosis*

The neural tube displays an intrinsic polarity across the epithelium, with one side forming the ventricular surface and the other forming the pial surface with a basal lamina. This polarity is present throughout gestation and thus permits easy definition of 'apical' and 'basal' NPC types. Apical progenitors (APs) divide either at, or very close to, the ventricle in the aptly termed 'ventricular zone' (VZ). These progenitors are linked by a belt of adherens junctions that extends across the length of the neuroepithelium and possess a small but important area of plasma membrane that is in direct contact with the cerebrospinal fluid (CSF) in the ventricle. This is termed the 'apical plasma membrane' and its asymmetric inheritance during NPC mitosis significantly influences the types of progeny that are generated (Kosodo et al., 2004). In contrast, basal progenitors (BPs) divide further away from the VZ and are not linked via a belt formed by adherens junctions. Mitosis of BPs occurs most commonly in the 'subventricular zone' (SVZ), and, accordingly, BPs also lack an apical plasma membrane that is in contact with the CSF (Betizeau et al., 2013). Upon establishment of a large pool of BPs, the SVZ of the developing forebrain becomes highly mitotic and thus complements the VZ as another region of NPC division.-The evolution of the neocortex from lower to higher vertebrates, and its expansion in terms of surface area, is attributed to the presence of BPs with a greater proliferative capacity (Lui et al., 2011, LaMonica et al., 2012, Ostrem et al., 2014).

Although NPC subtypes of the embryonic CNS are defined as either APs or BPs based on their location at the time of mitosis, 'subapical progenitors' (SAPs) possess some properties that are characteristic of either APs or BPs (Pilz et al., 2013). Whilst SAPs undergo mitosis in a non-ventricular region, they make contact with the apically positioned adherens junction belt. However, it is not known whether they possess an apical plasma membrane (Pilz et al., 2013).

1.1.1.2 Classification by cell polarity and cell polarity markers

Different subtypes of NPCs have been defined within the general classifications of APs versus BPs based on the presence of polarity-specific determinants (Taverna et al., 2014). For example, CD133, also known as prominin-1, is localised to the primary cilium in APs (described later in **1.1.2.3**) and is therefore apically restricted, making it one of the few molecular markers available for identifying and purifying APs (Roper et al., 2000). Basolateral proteins, like N-Cadherin, demark the opposing region of the plasma membrane in NPCs and best define apical-basal cell polarity at the time of mitosis (Betizeau et al., 2013, Kadowaki et al., 2007). Mitosis is used as the specific time window for determining apicobasal polarity as this represents the temporal checkpoint for the differential inheritance of cellular constituents, such as apical plasma membrane, by prospective daughter cells. It is this process which ultimately governs cell fate following cell division.

Other cytoarchitectural criteria, which were initially used to characterise polarised and non-polarised NPCs, dynamically change during interphase. These consist of apically- and basally-targeted processes that form contacts at or near either surface of the neural tube (Noctor et al., 2002, Rakic, 1972). These processes are thin and elongated extensions of the cell body that act to physically tether NPCs within the neuroepithelium via endfeet, as well as to receive extrinsic signals (discussed in greater detail in **1.2.3**). Owing to the dynamic nature of process extension, the presence of apical and basal processes is defined specifically during mitosis in order to establish NPC polarity (Taverna et al., 2014).

Based on the above criteria, the group of APs consists of the initial neuroepithelial cells (NE) as well as apical radial glia (aRG) and apical intermediate progenitors (aIPs), whilst BPs are basal radial glia (bRG), basal intermediate progenitors (bIPs) and transit amplifying progenitors (TAPs) (Gal et al., 2006, Fietz et al., 2010, Taverna et al., 2014). In addition, the aforementioned characteristics of NPC polarity also help define two distinct forms of SAPs, present in both bipolar and unipolar forms (Pilz et al., 2013).

All three AP sub-classes (NE, aRG and aIPs) extend a process each towards both sides of the neuroepithelium and are considered bipolar as a result. NE and aRG project processes to the nearby ventricular surface and the more distant pial basement membrane, whilst aIPs only project a basal process as far as the VZ boundary.

In contrast to APs, all BPs lack contact with the apical surface and are therefore considered to lack an intrinsic apical-basal polarity across the cell (Fietz et al., 2010, Miyata et al., 2004, Hansen et al., 2010, Betizeau et al., 2013). Unusually, bRG variably possess a monopolar or bipolar morphology at the time of mitosis, depending on whether they extend either one or both the apical and basal process, respectively. However, the apical process of bRG does not enter the VZ, as is observed in APs. TAPs are multipolar and can extend several short processes in any direction during interphase, before becoming nonpolar during cell division (Fietz et al., 2010, Miyata et al., 2004, Hansen et al., 2010).

The polarised nature of SAPs is less well understood. Whilst SAPs possess adherens junctions found in the apical belt of the VZ, it has not been identified whether they also possess an apical plasma membrane. Furthermore, SAPs can project both apical and basal processes, or just the apical process, during cell division (Pilz et al., 2013).

These findings demonstrate the considerable heterogeneity of process organisation and polarization in the overall NPC classes of APs and BPs, as well as within more specific sub-classes, such as SAPs, and at specific times in the cell cycle, such as in TAPs.

1.1.1.3 Classification by proliferative capacity

Specific NPC subtypes undergo a finite number of successive rounds of cell division and therefore have a limited capacity for self-renewal (Taverna et al., 2014, Noctor et al., 2004). In addition, some NPCs are only able to divide once, and this represents a third criterion for further classification of mammalian NPCs. Specifically, aIPs and bIPs undergo one single mitosis to generate two post-mitotic

neurons (Noctor et al., 2004). All other subtypes of APs and BPs divide twice or more before undergoing a self-consuming division that yields neurons or glia.

1.1.1.4 Division modes for NPCs

Embryonic NPCs divide either symmetrically or asymmetrically. Symmetric divisions produce identical daughter cells: either another 'copy' of the dividing cell (symmetric proliferative) or two more committed progeny (symmetric consumptive; (Taverna et al., 2014). The earliest APs, NE and aRG, undergo symmetric proliferative divisions to expand the pool of stem and progenitor cells before the onset of neuron generation (Noctor et al., 2004). TAPs also undergo symmetric proliferative divisions, expanding the pool of TAPs in a process that is hypothesised to underlie the expansion of the SVZ and cortex in the brain (Hansen et al., 2010). Following a symmetric consumptive division, neither daughter cell shares the identity of their mother cell, and this mode of division eventually exhausts the NPC sub-class of the mother cell. For example, one aRG can divide into two bIPs, and then one bIP into two neurons (Haubensak et al., 2004, Miyata et al., 2004, Noctor et al., 2004).

Asymmetric divisions can either be self-renewing or self-consuming (Taverna et al., 2014). Self-renewing divisions produce one daughter cell identical to its mother, and one more differentiated daughter cell, whilst self-consuming divisions produce two non-identical daughter cells that are more differentiated than the mother cell. Self-renewing divisions in the rodent CNS are characteristic of both aRG and bRG and are also either neurogenic, when the non-identical daughter becomes a neuron, or differentiative, when the non-identical daughter is a more differentiated NPC subtype. aRG can divide asymmetrically in a self-renewing differentiative division to produce one identical copy of themselves, as well as a more differentiatied BP (Noctor et al., 2004, Kosodo et al., 2008). Alternatively, aRG and bRG can undergo a self-renewing neurogenic division to produce another copy of the mother cell, as well as a neuron (Noctor et al., 2004, Kosodo et al., 2008). Asymmetric consumptive divisions, as with symmetric consumptive divisions, also exhaust the mother cell's NPC class, as neither daughter cell shares an identity with the mother (Taverna et al., 2014, Hansen et al., 2010).

The variety of division modes available to NPCs establishes an extensive number of lineages from which different types of neurons are generated. Live-imaging in organotypic slice culture assays have helped trace these lineages *in situ* and improve the understanding of species differences in neural lineage progression (Loulier et al., 2014, Taverna et al., 2012, Chen and LoTurco, 2012).

1.1.2 Structure of mammalian neural progenitor cells

1.1.2.1 The apical endfoot

The symmetry of NPC cell division determines the inheritance of specific cellular structures and subcellular components that ultimately dictates daughter cell fate (see **Figure 1.2**). Thus, a symmetric division is defined as a division that leads to the equal inheritance of such fate-determining components, whilst asymmetric divisions are those that cause an unequal allocation of such determinants to the daughter cells (Knoblich, 2001).

Several apical-basal cues can be differentially inherited during cell division and control the respective fate determination of each newly formed cell. One such example is the apical endfoot of APs, which is composed of apical plasma membrane and the adherens junctional belt. Despite only representing a very small (1-2%) fraction of the whole plasma membrane, the apical plasma membrane contains the primary cilium, which protrudes into the ventricle, and is highly influential in defining daughter cell fate following mitosis (Kosodo et al., 2004). The apical endfoot of APs also represents a signalling hub for ventricular signals that modulate NPC behaviour (Johansson et al., 2013, Lehtinen and Walsh, 2011). Thus, unequal inheritance of these structures amongst daughter cells provides the molecular basis for division symmetry and fate determination (e.g. Alexandre et al., 2010).

Altogether, the apical surface, which faces the ventricle, is made up cumulatively of the apical plasma membrane of all NE and aRG in the neuroepithelium. The ventricle itself is filled with CSF, which is rich in nutrients and soluble cues that maintain NPC homeostasis and regulate their behaviour through membrane-bound receptors (Lehtinen and Walsh, 2011; discussed in **1.2.3)**.

1.1.2.2 Apical junctional complexes

The apical junctional belt ensures separation of apical and basolateral membrane and promotes structural adhesion between APs. Furthermore, the apical junctional belt, as well as the endfeet at the end of basal process in aRG, contains gap junctions that allow intercellular signalling. Apical junctional complexes maintain cell polarity by acting in both structural and signalling capacities. Typical components of cell junctions like cadherins and catenins are vital to maintain polarisation and cell identity in aRG and NE by ensuring cohesion between APs (Aaku-Saraste et al., 1996, Kim et al., 2010, Chenn and Walsh, 2002, Zhang et al., 2010a, Marthiens et al., 2010). Cadherin homo-oligomers also help coordinate cytoskeletal dynamics through both α- and β-catenin (Suzuki and Takeichi, 2008). Furthermore, WNT signal-mediated inhibition of β-catenin degradation allows β-catenin to translocate to the nucleus and modulate the transcription of genes important for both proliferation and differentiation (see **1.2.3.3**; Wodarz and Nusse, 1998).

NE and aRG are also linked at both apical and basal endfeet via gap junctions to facilitate neuronal migration following detachment from the apical surface and intercellular communication (Elias and Kriegstein, 2008). Small molecule exchange through these connexin-rich channels coordinates neurogenesis in the developing forebrain, such as through the coupling of intracellular calcium concentrations across APs, which synchronises interkinetic nuclear migration (INM; discussed in **1.1.3.1**) across the neuroepithelium (Owens and Kriegstein, 1998, Liu et al., 2008).

1.1.2.3 The primary cilium

One of the most important components found in the apical plasma membrane is the primary cilium, which protrudes out into the lumen of the ventricle as an ‘antenna’ to detect CSF-based signals (Lehtinen and Walsh, 2011). The primary cilium is linked to the centrosome via the older of its two centrioles, the mother centriole, that forms the basal body. During S-phase, the two centrioles are duplicated, and each centrosome subsequently forms one pole of the mitotic spindle. Each centrosome is distinct from the other, given the asymmetric inheritance of the mother centriole, and this is significant in the context of mammalian NPCs. In

dividing aRG, the centrosome containing the mother centriole is inherited by the daughter cell that remains an aRG after an asymmetric self-renewing division (Paridaen et al., 2013, Wang et al., 2009). Conversely, the centrosome containing the daughter centriole is inherited by the more differentiated daughter cell. Therefore, asymmetric inheritance of the centrosome (and thus the original centriole pair) is tightly linked to daughter cell fate during asymmetric cell division (Paridaen et al., 2013, Wang et al., 2009). The ciliary membrane is also inherited preferentially by the daughter cell retaining the mother cell identity during asymmetric cell division and promotes regeneration of the primary cilium over the sibling cell (Paridaen et al., 2013).

Interestingly, the cilium is found on the basolateral plasma membrane in the more differentiated daughter cell (e.g. BPs or post-mitotic neurons) during the onset of delamination, before migration across the neuroepithelium takes place (Wilsch-Brauninger et al., 2012). Therefore, this alteration in localisation may expose the cilium to basolateral signals.

1.1.2.4 The basal process

The vast majority of the plasma membrane of NE and aRG is basolateral in identity and surrounds the nucleus, cell body and much of both processes. The basolateral plasma membrane area increases during neural development in line with the thickening of the cortical wall. It is separated into two subcompartments: the basolateral plasma membrane and the distal segment of the basal process (Taverna and Huttner, 2010). The basolateral plasma membrane is made up of the proximal segment of the basal process and also holds the nucleus during INM, whilst the distal segment is extremely thin and extends across the entire neuroepithelium to the pial basement membrane (Noctor et al., 2001, Miyata et al., 2001).

This distal segment is a stereotypical feature of aRG, and never contains the nucleus during INM, as well as in bRG and some SAPs also (Taverna et al., 2014). In APs, the formation of the basal process (from the total basolateral plasma membrane) occurs with the switch from NE to aRG, and its function extends beyond its key role as a substrate for neuronal migration (Rakic, 1972). The basal process permits

sensitivity of signals originating from the basal portion of the neuroepithelium, such as laminin from the extracellular matrix (ECM) in the basement membrane and retinoic acid from the pia (Loulier et al., 2009, Siegenthaler et al., 2009). It therefore acts as a signalling hub, much like the apical plasma membrane, to help orchestrate fate specification and neurogenesis. The basal process also displays asymmetric inheritance during mitosis and is generally passed on to the daughter cell retaining the capacity to proliferate (Miyata et al., 2001, Konno et al., 2008, LaMonica et al., 2013, Alexandre et al., 2010).

Projected at the end of the basal process, the basal endfoot contacts the pial surface directly and is the region of the NPC most exposed to signals originating from the lamina. In addition to anchoring NPCs to the pial surface via integrins, the basal endfoot transduces signals from the ECM to the nucleus that regulate cell proliferation (Haubst et al., 2006, Fietz et al., 2010). The basal endfoot can sustain pro-proliferative signals by functioning readily as a site for protein synthesis, and therefore acting as a pool for cues that promote NPC expansion (Tsunekawa et al., 2012).

1.1.2.5 The mitotic spindle

The mitotic spindle is a crucial component of NPCs and is primarily responsible for regulating the mode of division (Shitamukai and Matsuzaki, 2012). Mutations in genes coding for the spindle machinery, such as microtubules or the centrosomes, have a profound influence on overall brain growth; thus, they compromise the growth of the cerebrum in a group of human diseases known as ‘microcephalies’ (Bond and Woods, 2006, Woods et al., 2005). Such mutations often deplete the NPC population and consequently reduce overall neuron number (Morin et al., 2007, Konno et al., 2008).

In early NPCs that are the most capable of self-renewal amongst all NPC subtypes, namely NE and aRG, the spindle is typically orientated perpendicular to the apical-basal axis of the cell to ensure equal partitioning of apical-basal polarity-based cues like the apical plasma membrane (Fish et al., 2006, Konno et al., 2008). However, spindle orientation, in relation to the apical-basal axis, varies considerably

across the developing CNS, with oblique or even horizontal (i.e. parallel to the apical-basal axis) cleavage planes (Wilcock et al., 2007, Pilz et al., 2013). The latter two spindle orientations often occur concomitantly with divisions generating bRG and reflect a shift from bipolar APs to monopolar BPs (Pilz et al., 2013, Gertz et al., 2014, Shitamukai et al., 2011, LaMonica et al., 2012). Conversely, bRG undergo asymmetric cell divisions, but the spindle is rarely orientated completely perpendicular to the apical-basal axis. Instead, it is more commonly orientated horizontally, allowing asymmetric inheritance of basal polarity cues following cell division (LaMonica et al., 2013). The characterisation of mitotic spindle orientation in BPs, such as IPs and TAPs, however, is poor.

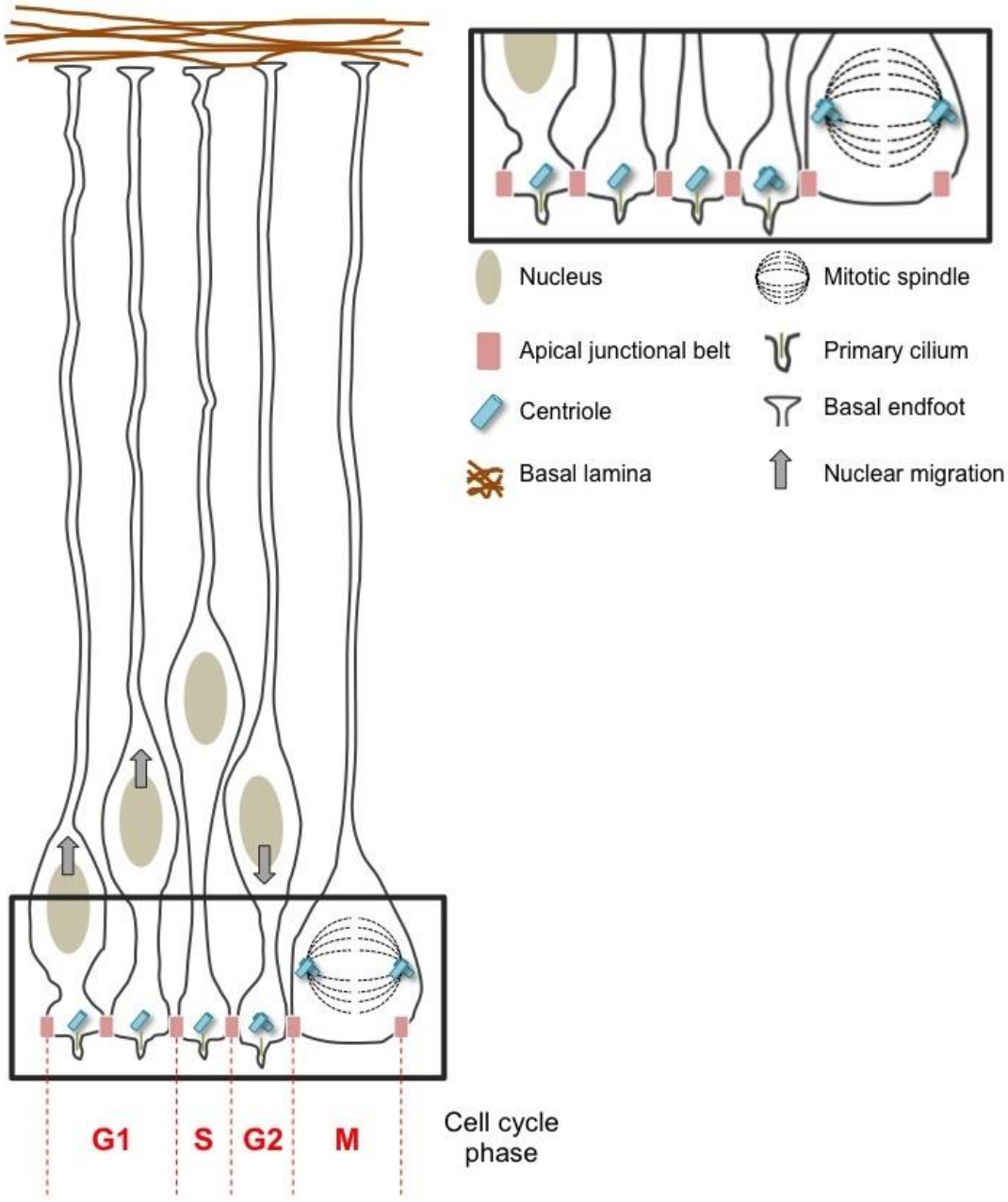

Figure 1.2 Schematic representation of the structure of aRG.

Organisation of subcellular structures in aRG undergoing interkinetic nuclear migration (see below). Arrows denote direction of nuclear migration during specific phases of the cell cycle.

1.1.3 Complex processes in neural progenitor cells

1.1.3.1 Interkinetic nuclear migration

Interkinetic nuclear migration (INM) is a hallmark of both NE and aRG, whereby the nucleus moves along the apicobasal axis of the cell in synchrony with the cell cycle (Sauer, 1935; **Figure 1.3**). In both NPC subtypes, mitosis occurs at the ventricular surface, S-phase occurs more basally, and the G1 and G2 phases occur during the apical-to-basal and basal-to-apical migration, respectively (Sauer, 1935, Taverna and Huttner, 2010). The asynchrony of NE and aRG undergoing INM therefore produces a pseudostratified appearance of the VZ.

Both the microtubule and actin cytoskeleton comprise the machinery that is required for INM (Schenk et al., 2009, Cappello et al., 2011, Norden et al., 2009). Accordingly, mutations in genes encoding microtubule-based motor proteins impair neural development and can lead to lissencephaly in human patients, a condition characterised by a complete lack of cerebral gyrification (Faulkner et al., 2000). INM during G1 is driven by both actomyosin- and microtubule-based motors, but may also occur passively due to nuclear displacement induced by apically migrating nuclei during G2 (Schenk et al., 2009, Kosodo et al., 2011).

Blocking cell cycle progression abrogates the stereotypical migration of NPC nuclei (Murciano et al., 2002). This synchrony results from various cell cycle-dependent proteins that regulate INM, such as the microtubule-associated protein TPX2, which accumulates in the apical endfoot during G2 and promotes microtubule-dependent, apically directed nuclear migration (Kosodo et al., 2011). Whilst abrogating cell cycle progression impairs INM, perturbing INM through pharmacological blockade of the actomyosin machinery does not reciprocally compromise cell cycle progression or cytokinesis (Schenk et al., 2009).

The specific function of INM in governing NPC behaviour is not fully understood. It has been proposed that pseudostratification maximises the number of NPCs that can undergo mitosis at the apical surface (Smart, 1972). Alternatively, the ‘nuclear resident hypothesis’ suggests that INM allows NPC nuclei to sample

different extracellular environments in the apical and basal regions of the developing neuroepithelium (Taverna and Huttner, 2010; described extensively in **1.2.3**). In agreement with this idea, the zebrafish Notch ligands Delta B and Delta C are expressed in a gradient to drive self-renewal of apically positioned progenitors in the developing zebrafish neuroepithelium (Del Bene et al., 2008). Genetic perturbation of INM in a manner that prolongs the positioning of NPC nuclei in more basal regions results in premature cell cycle exit and a switch to neurogenic divisions (Del Bene et al., 2008). Furthermore, the distance migrated basally during INM correlates directly with the likelihood of progenitors undergoing a neurogenic division (Baye and Link, 2007). Therefore, INM is likely to influence NPC fate by regulating exposure of progenitor nuclei to proliferative versus neurogenic signals.

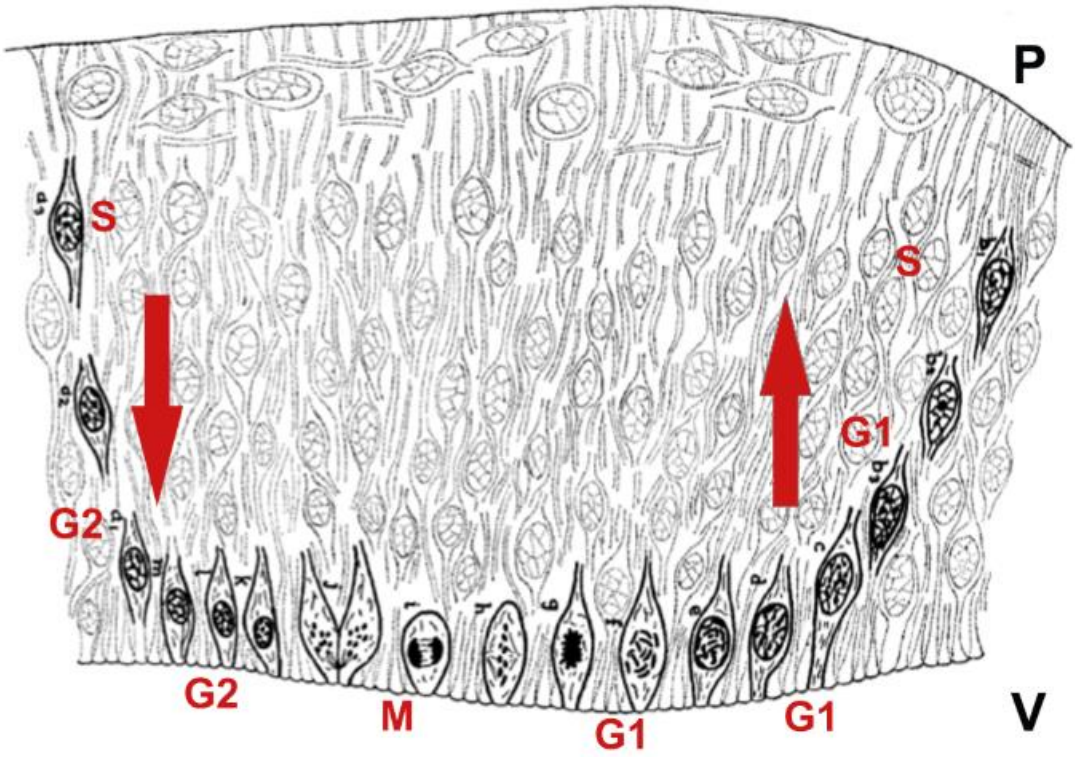

Figure 1.3 INM in the developing CNS.

Drawing of INM in the mammalian neural tube. Cell cycle phase shown next to NPC nuclei shown in red, arrows denote direction of nuclear migration. P, pial surface; V, ventricular surface. Adapted from “Mitosis in the neural tube” (Sauer, 1935).

1.1.3.2 Nucleokinesis in the basal compartment

INM is undertaken exclusively by NE and aRG, but not by SAPs and BPs. However, BPs also show specific patterns of nuclear migration, such as in newly formed BPs migrating from the VZ to form the SVZ (Schenk et al., 2009). In addition, bRG and SAPs undergo a fast nuclear movement, normally in the basal direction, immediately prior to mitosis known as mitotic somal translocation (MST) but the molecular mechanism or developmental function of MST is not known (Betizeau et al., 2013, Hansen et al., 2010, LaMonica et al., 2013, Pilz et al., 2013).

1.1.3.3 Cell cycle length

Cell cycle length regulates neurogenesis in the developing mammalian CNS. Analysis of neurogenic and proliferative progenitors indicates that the normal lengthening of G1 phase and subsequently, the entire cell cycle in the embryonic forebrain precedes the onset of neurogenesis, whilst forced G1 phase reduction increases NPC self-renewal (Lukaszewicz et al., 2005, Calegari and Huttner, 2003, Calegari et al., 2005, Pilaz et al., 2009, Lukaszewicz et al., 2002, Lange et al., 2009). Patterns of G1 phase duration vary with the capacity for self-renewal/differentiation in different NPC subtypes such as aRG and bIPs (Arai et al., 2011, Calegari et al., 2005). Moreover, S-phase is longer during proliferative, self-renewing divisions in these subtypes (Arai et al., 2011). It has been hypothesised that a longer S-phase facilitates greater fidelity of DNA replication, which is important when NPCs undergo many successive divisions to generate radial units (Arai et al., 2011).

The shift in the relative duration of specific cell cycle phases and the cell cycle overall prior to differentiation observed in the forebrain is not necessarily observed in other parts of the brain. In the chick spinal cord, motoneuron-specified NPCs have a longer cell cycle whilst undergoing self-renewing divisions but then cycle more quickly during the switch to neurogenic divisions (Saade et al., 2013). In contrast to the forebrain, G1 phase typically remains the same length in relation to the other cell cycle phases between both division modes, whilst the relative duration of S-phase decreases upon the switch to neurogenesis (Saade et al., 2013). Thus, cell cycle length

and phase duration vary considerably between NPCs in different regions of the developing CNS.

1.2 Regulation of neural progenitor cells

1.2.1 Transcriptional control of neural progenitor cells

1.2.1.1 Control by transcription factors

NPC identity and fate determination, as well as the timing of neurogenesis, are controlled by specific transcription factors (TFs). Some of the TFs that maintain the earliest, self-renewing NPC populations (i.e. APs) are members of the *Sex determining region Y-box* (Sox) gene family. SOX2 is the most widely studied of the three main SOXB TFs (the others being SOX1 and SOX3), is commonly used as a molecular marker of NE and plays a vital role in the early establishment of APs. SOX2 initially functions in the early embryo to maintain pluripotency in embryonic stem cells, before specifying neuroectoderm from ectoderm following gastrulation (Wood and Episkopou, 1999, Avilion et al., 2003, Zhao et al., 2004, Masui et al., 2007).

In the chick spinal cord, SOX2 is expressed in proliferative NPCs, and its expression is downregulated during the final cell cycle before a terminal cell division, as highlighted by mutually exclusive expression of SOX2 and neuronal markers (Graham et al., 2003). Forced SOX2 expression results in a robust inhibition of neuronal differentiation whilst inhibition of SOX2-induced gene expression leads to delamination of NPCs from the VZ and premature cell cycle exit. (Graham et al., 2003) Interestingly, this latter defect could be rescued by forced expression of SOX1, suggesting a functional redundancy in maintaining NPC identity amongst SOXB TFs (Graham et al., 2003). In rodents, $SOX2^+$ NPCs readily form 'neurospheres' - floating *in vitro* aggregates of neural stem and progenitor cells with a great capacity for self-renewal (Ellis et al., 2004). Neurospheres derived from $SOX2^+$ NPCs can generate both neurons and glia in agreement with the role of SOX2 in maintaining the earliest and most pluripotent NPCs (Ellis et al., 2004).

Like SOX2, SOX1 also promotes neural determination from ectoderm and marks dividing NPCs of the neural tube (Pevny et al., 1998). Forced SOX1 expression can even compensate for loss of niche-derived retinoic acid signals to drive neural specification of cultured ectodermal cells. However, its expression is also concomitant with differentiation in NPCs, and thus SOX1 does not unequivocally promote stemness in NPCs in the same manner as SOX2 (Pevny et al., 1998). In avian NPC cultures derived from the telencephalon, SOX1 drives both stemness initially and then neuronal commitment after prolonged expression (Kan et al., 2007). In support of this, SOX1 is also expressed in adult mouse hippocampal neural stem cells (NSCs) during activation from quiescence, therefore contributing to neurogenesis both embryonically and postnatally (Venere et al., 2012).

SOX3 is more restricted to later stages in neural development in mice. For example, NPCs require SOX3 for proper formation of the hypothalamus-pituitary axis (Rizzoti et al., 2004). Conversely, SOX3 functions earlier in frog and chick development. In the former species, SOX3 activates SOX2 expression and induces commitment to the neural lineage from ectodermal cells, but then blocks neurogenesis as a downstream effector of Notch signalling (Rogers et al., 2009). In adult mice, SOX3 is transiently expressed in NSCs prior to differentiation and is even maintained in some post-mitotic neurons (Wang et al., 2006). Thus, SOX3 contributes more to neurogenesis than maintenance of stemness in the adult mammalian brain. The function of SOX family TF homologs is conserved across different species and genetic ablation of *Sox2* or *SoxNeuro* results in a severely underdeveloped CNS in *Xenopus* and *Drosophila* respectively, due to impaired NPC expansion (Kishi et al., 2000, Buescher et al., 2002).

In addition to the three SOXB1 transcription factors, the Pax family of TFs also contributes considerably to murine CNS development by regulating both lineage specification and NPC maintenance. Similar to the SOXB1 family, expression of Pax TFs first takes place during neurulation, when PAX2, PAX5, PAX6 and PAX8 promote regionalisation of the neural tube (Pfeffer et al., 2002, Matsunaga et al., 2000). PAX6 induces neural determination in human ectoderm, yet it is not required for this process in mice, a difference that may contribute to increased expansion and convolution of the gyrencephalic brain in higher-order species (Zhang et al., 2010b).

PAX6 is the best characterised Pax TF in maintaining NPC stemness and is expressed solely by APs and not BPs (Gotz et al., 1998). PAX6 is required for normal cell cycling and morphology of APs and by promoting cell cycle re-entry, PAX6 ensures long-term neurogenic potential in aRG (Heins et al., 2002). In addition, it also balances self-renewal versus differentiation by regulating transcription of a battery of essential neurogenesis genes (Sansom et al., 2009). Furthermore, PAX6 enhances the expression of key subcellular components whose differential inheritance in newly formed daughter cell NPCs influences division symmetry. SPAG5, a microtubule-associated protein, is a direct transcriptional target of PAX6, and PAX6 promotes symmetric NPC divisions and anchorage to the apical surface through its regulation of SPAG5 (Asami et al., 2011).

Notch signalling forms a vital part of stemness maintenance in stem and progenitor cells both within and outside the CNS, during development, as well as in adult life (discussed in greater detail in **1.2.3.5**). The core downstream effectors of Notch signalling at the transcriptional level in NPCs are the Hes family of TFs, which exist in antagonistic relationships with proneural TFs to ensure correct timing of NPC differentiation. HES1 and HES3 are expressed consistently in NE along the neuraxis, although the latter's expression is replaced by HES5 upon switching from NE to aRG (Hatakeyama et al., 2004). HES1 and HES5 subsequently mark almost the entirety of the murine CNS from midway through gestation and maintain the NPC population prior to differentiation. Expression of HES1/5 is inversely proportional to the expression of the proneural TF ASCL1 (see below), and thus the downregulation of both HES1 and HES5 initiates neural differentiation in NPCs (Ishibashi et al., 1995, Hatakeyama et al., 2004). HES3 also acts in concert with HES1/5, and all are required for normal CNS development (Ohtsuka et al., 1999, Ohtsuka et al., 2001, Hatakeyama et al., 2004). The transcriptional antagonism between HES1 and ASCL1 regulates NPC fate decisions through an oscillatory mechanism (Imayoshi et al., 2013) and by oscillating between high and low levels of both TF, NPCs remain 'primed' for either self-renewing or neurogenic divisions (Kageyama et al., 2015). In agreement, fluctuating expression of ASCL1 in an oscillatory manner drives consecutive NPC divisions in the ventral telencephalon, whilst prolonged ASCL1 expression initiates neurogenesis (Imayoshi et al., 2013). In contrast, OLIG2, a TF that promotes

commitment to the oligodendrocyte lineage, is asynchronous with HES1 expression (Imayoshi et al., 2013).

Whilst SOX, PAX and HES family TFs largely maintain features of stemness, such as continued cell cycling, self-renewing divisions and specific subcellular structures, proneural TFs are responsible for initiating the process of differentiation and neurogenesis. The best studied are the basic helix-loop-helix (bHLH) TFs mouse achaete-scute homolog 1 (ASCL1 or MASH1) and Neurogenins 1 and 2 (NGN1/2). Although ASCL1 and NGN1/2 are expressed in spatially distinct domains, all three are crucial for neuronal differentiation in NPCs and are most abundant in the apical region of the neuroepithelium (Sommer et al., 1996, Guillemot et al., 1993, Lo et al., 1991). Their potency in inducing neurogenesis is underlined by the fact that forced expression of ASCL1 or NGN1 is capable of inducing neural differentiation and maturation in a cultured cancer cell line (Farah et al., 2000). Similar to HES1 repression of ASCL1 expression, PAX6 inhibits transcription of NGN2 to maintain stemness and delay differentiation (Gotz et al., 1998, Scardigli et al., 2003).

Within the forebrain, NGN1 and NGN2 are expressed primarily in the dorsal pallium and are required for expression of another pair of proneural TFs known as NEUROD1 and NEUROD2 (Neurogenic differentiation 1/2; (Sommer et al., 1996). NEUROD1/2 activate transcription of neuron-specific genes, such as βIII-tubulin, by binding E-Box sites within their promoter region (Farah et al., 2000, Boutin et al., 2010). These TFs are expressed in cells terminally committed to becoming neurons, whilst their upstream transcriptional regulators, NGN1/2, are expressed earlier and more transiently. ASCL1 functions more commonly in neurogenesis in the ganglionic emminence and in the ventral forebrain (although its expression is observed in different areas of the developing CNS; (Casarosa et al., 1999). In the medial ganglionic emminence, ASCL1 ensures correct timing of neuron formation via its antagonistic relationship with HES1, as well as the eventual establishment of subsets of neurons in the basal ganglia and cerebral cortex (Casarosa et al., 1999, Imayoshi et al., 2013).

Although ASCL1 and NGN2 expression is normally spatially restricted, each is able to partially compensate for the others absence to maintain neurogenesis (Fode

et al., 2000). Ectopic ASCL1 can substitute for NGN2 in the dorsal thalamus of *Ngn2*$^{-/-}$ mutants with respect to the numbers of neurons formed, but NPCs are misspecified to neurons with a more ventral identity (such as GAD67^{+} interneurons; (Fode et al., 2000). Therefore, the regional specificity of proneural TF expression appears to enable specification of different neuronal subtypes, in addition their general role in initiating neuronal differentiation.

A number of TFs regulate the onset of gliogenesis. Two main classes of glia are generated in the mammalian CNS: oligodendrocytes, which are responsible for ensheathing axons, and astrocytes, which maintain brain homeostasis and the blood-brain barrier. OLIG1 and OLIG2 initiate NPC commitment to the oligodendrocyte lineage, as ectopic expression of either gene across the forebrain increases the numbers of oligodendrocytes generated (Lu et al., 2000, Takebayashi et al., 2000). OLIG2 is also required for the specification of various neuronal subtypes. For example, OLIG2 acts in combination with NGN2 to promote motor neuron differentiation in the developing spinal cord, and also acts downstream of SHH signalling in the rodent telencephalon to specify neurons across the embryonic rodent CNS (Lu et al., 2000, Novitch et al., 2001).

Members of the Hes family of TFs maintain NPC stemness when expressed earlier in development but then mark NPCs committed to the astrocyte lineage when expressed later on (Wu et al., 2003). In the chick spinal cord, Hes TFs induce astrocyte specification of NPCs through co-operation with the TF NF1A. NF1A is indispensable to astrogliogenesis and is antagonized by OLIG2, in a mechanism presumably designed to ensure appropriate formation of both astrocytes and oligodendrocytes (Deneen et al., 2006).

1.2.1.2 Epigenetic control

Whilst various TFs either promote stemness or induce differentiation in NPCs, changes in DNA acetylation and methylation also take place during either process. For example, histone acetylases (HATs) and histone deacetylases (HDACs) catalyse the addition or removal of an acetyl group onto a histone in order to induce changes in coiling of the DNA molecule. Generally, acetylation activates gene expression whilst

deacetylation represses gene expression. DNA methylation is, in contrast, a common DNA 'silencing' mechanism utilised to repress the expression of genes.

In the context of embryonic neurogenesis, HDACs repress the switch to neuronal differentiation, as well as the restriction of NPCs to glial cell fates (Jung et al., 2008, Balasubramaniyan et al., 2006). HDACs form part of the REST transcription repressor complex, which acts in NPCs to inhibit expression of neuronal genes and maintain stemness (Ballas et al., 2005). HDACs also associate with TFs to repress their target genes, such as the TF TLX, which typically promotes neuronal differentiation through its target genes *p21* and *Pten* but is prevented from doing so when bound to an HDAC (Sun et al., 2007).

The best-characterised methylation mechanism regulating gene expression is the cytosine methylation of CpG dinucleotides, which inhibits binding of TFs to their target gene sequences. In NPCs, DNA methylation maps tightly to patterns of local histone methylation and increases upon differentiation (Meissner et al., 2008). DNA methyltransfereases (DNMTs), such as DNMT1, mediate the methylation of CpG dinucleotides and as a result, regulate the onset of neurogenesis (Fan et al., 2005). Extracellular signalling can induce both histone and DNA methylation in NPCs. FGF2 can potentiate the CNTF-derived induction of the astroglial cell fate by modulating methylation around astrocyte-specific genes like *Gfap* and *S100* (Song and Ghosh, 2004). Furthermore, bone morphogenetic protein (BMP) and Notch signalling are also known to regulate astroglial specification across the CNS by regulating methylation in a similar manner (Akizu et al., 2010, Namihira et al., 2009).

1.2.1.3 Non-coding RNAs

Non-coding RNAs, particularly microRNAs (miRNAs), play a key role in regulating embryonic neurogenesis. miRNAs are roughly 21-nucleotide long RNA molecules and are generated by RNAses such as Drosha and Dicer. Mature miRNAs are then transported to mRNA to prevent their translation and thus promote gene silencing post-transcriptionally (Djuranovic et al., 2012).

The action of the RNAse enzyme DICER1 is particularly vital to NPC regulation as it produces miRNAs by cleaving double-stranded RNA (De Pietri Tonelli et al., 2008, Kawase-Koga et al., 2010). Two miRNAs generated through Dicer, miR-124 and miR-9, promote neuronal differentiation by inhibiting activation of the TF STAT3 (Krichevsky et al., 2006). Additionally, both repress the HDAC-containing REST complex known to promote NPC stemness (Packer et al., 2008, Visvanathan et al., 2007). Targets of miR-124-induced gene silencing include β1-integrin and γ1 laminin, which both contribute to NPC identity, whist miR-9 suppresses expression of *Foxg1* to induce NPC differentiation into Cajal-Retzius cells in the murine embryonic cortex (Cao et al., 2007, Shibata et al., 2011).

1.2.2 Intrinsic regulation of neural progenitor cells by intracellular molecules

Intrinsic control of NPC identity and behaviour is also driven by non-transcriptional mechanisms through the action of intracellular molecules. As I have discussed previously, many different subcellular structures and processes modulate neurogenesis. For example, apicobasal polarity defines the symmetry of NPC divisions and the identity of the progeny that are generated. Additionally, on going processes, such as INM, also define whether NPCs undergo self-renewing or differentiative divisions. Below I will discuss key molecules required for these mechanisms that ultimately govern progenitor cell behaviour.

Centrosomal proteins like ASPM and CDK5RAP2 are vital to normal cortical expansion (Bond et al., 2002, Bond et al., 2005). Both are critical to spindle function and are required for aRG self-renewal (Bond et al., 2002, Bond et al., 2005). Components of the apical domain are also integral to NPC fate determination. In addition to the primary cilium and apical junctional belt, the PAR3-PAR6-aPKC complex (or PAR-PKC complex) represents a subcellular structure involved in defining the division mode in NPCs. Much of the original evidence on the role of the PAR-aPKC complex in NPCs comes from experiments in *C. elegans* and *Drosophila*, although more recent work indicates conservation of its function in more complex species (Costa et al., 2008). In *Drosophila*, the PAR-aPKC complex ensures correct apicobasal polarization of epithelia, whilst in mice the PAR3 subcomponent is vital

for Notch signalling-induced NPC self-renewal (Siller and Doe, 2009, Bultje et al., 2009).

The PAR-aPKC complex relays information on polarity through the apically localized Pins protein. The mammalian orthologues of Pins, known as LGN, is required to regulate AP expansion by ensuring the correct orientation of the mitotic spindle in a planar configuration to facilitate self-renewing cell divisions (Konno et al., 2008). Furthermore, proteins LIS1 and NDE1 are both crucial to ensuring correct positioning of LGN at the mitotic spindle and thus maintain normal NPC division planes, neuronal migration and overall cortical expansion, as highlighted by their mutation in microcephalies (Feng and Walsh, 2004, Pawlisz and Feng, 2011, Vallee and Tsai, 2006, Tai et al., 2002).

The GEF protein DOCK7 links microtubule organisation during INM to cell fate. DOCK7 negatively regulates the expansion of the AP pool in the developing mouse neocortex by promoting the transition from aRG to BPs, and then ultimately to neurons, by slowing the apical-basal progression of nuclei during INM (Yang et al., 2012). DOCK7 does this by antagonising the microtubule-growth promoting and microtubule-stabilizing roles of another protein called TACC3 that normally enables nuclear movement (Yang et al., 2012). Owing to the role of INM in fate determination, DOCK7 therefore acts a molecular bridge between the speed of INM and the switch from self-renewing to neurogenic divisions.

Two proteins asymmetrically localized during NPC mitosis are TRIM32 and NUMB. Whilst TRIM32 has been better characterised in *Drosophila*, the mammalian orthologue of NUMB is required for asymmetric division in the developing mammalian CNS (Zhong et al., 1997, Shen et al., 2002). Mammalian NUMB regulates neuronal differentiation in the developing rodent brain in two distinct ways (Zhong et al., 2000, Li et al., 2003, Petersen et al., 2002, Petersen et al., 2004). First, NUMB localizes to adherens junctions found in the apical endfeet of aRG to ensure proper distribution of junctional cadherins and cell polarity (Rasin et al., 2007). Secondly, NUMB interacts with mammalian PAR3 to asymmetrically partition NOTCH signalling into dividing NPCs, thus preferentially inhibiting differentiation in one daughter cell to drive self-renewal (Bultje et al., 2009).

The RNA-binding proteins MUSASHI 1 and 2 act in a similar fashion to miRNAs by silencing gene expression post-transcriptionally. MUSASHI 1 specifically is expressed in early NPCs and maintains self-renewing divisions by destabilizing the mRNA cap during translation when bound to specific mRNAs associated with neuronal differentiation, such as m-numb, an antagonist of Notch signalling (Kawahara et al., 2008, Imai et al., 2001, Sakakibara et al., 1996).

The Id (inhibitor of differentiation) proteins complement the Musashi proteins by silencing the expression of proneural genes to delay differentiation. On the one hand, they function as dominant negative inhibitors of bHLH TFs by forming inactive heterodimers with these TFs (Benezra et al., 1990). On the other hand, Id proteins sequester DNA-binding E-proteins that proneural TFs, like NGN2, must bind to initiate expression of target genes, such as NEUROD1 (Benezra et al., 1990, Lyden et al., 1999). Id proteins can therefore indirectly repress neuronal differentiation in the developing mouse neocortex. Id proteins can also positively regulate the activity of stemness-maintaining bHLH TFs. HES1 expression in the chick hindbrain represses the switch from self-renewing to differentiative divisions but retains a negative feedback autoregulatory mechanism to ensure that neurogenesis occurs in a timely manner (Bai et al., 2007). ID1 and ID3 release HES1 from autoregulation, subsequently maintaining low expression of proneural TFs indirectly (through the oscillatory antagonism between Hes family and proneural TFs) and promoting expansion of the NPC pool (Bai et al., 2007, Jung et al., 2010).

1.2.3 Extrinsic control of neural progenitor cells

In addition to the transcriptional and intracellular determinants that balance NPC self-renewal with differentiation and neurogenesis, a large number of extracellular signalling molecules modulate NPC behaviour. Indeed, this regulation of NPCs often involves increasing the abundance or function of the transcriptional and subcellular molecules mentioned previously. These extracellular signals, originating from neighbouring cells, extra-neural tissue outside the CNS, as well as systemically through the CSF, are collectively termed the neurogenic ‘niche’, and orchestrate neural development spatiotemporally. Listed below are key examples of extrinsic,

niche-derived signals that regulate NPC behaviour and control the switch from self-renewing or differentiative or neurogenic cell divisions (**Figure 1.4**).

1.2.3.1 FGF and EGF

NPC proliferation and stemness are regulated by many secreted factors. Amongst them, basic Fibroblast growth factor (bFGF) and Epidermal growth factor (EGF) are amongst the best characterised. Experiments based around the isolation and culture of NPCs from the embryonic rodent CNS indicate that both factors act in developmental neurogenesis as mitogens for NPC subtypes found throughout the period of neural development and across the entire neuraxis. For example, both transient and sustained periods of FGF stimulation *in vitro* elicit considerable levels of NPC proliferation via elevated phosphorylation of cAMP (Tao et al., 1997, Qian et al., 1997, Lukaszewicz et al., 2002, Ciccolini and Svendsen, 1998).

Single intracerebroventricular injections of FGF2 at mid-gestation also significantly increase the proportion of dividing NPCs, highlighting the mitogenic potency of FGF signalling (Vaccarino et al., 1999). FGFs drive NPC proliferation through upregulation of cyclin D2 expression, as well as by decreasing expression of the cyclin-dependent kinase inhibitor p27(kip1) (Vaccarino et al., 1999). Various FGF isoforms are capable of maintaining NPC survival, such as FGF2, FGF4 and FGF8b, and do so through FGFR3 (Vaccarino et al., 1999). However, FGF-mediated proliferation can be completely antagonized by the action of neurotrophins, such as NT-3, as it induces NPC differentiation even in the presence of FGFs (Ghosh and Greenberg, 1995; discussed in greater detail in **1.2.3.7**).

FGF ligands and receptors (FGFRs) exhibit some functional redundancy and only after simultaneous deletion of either all isoforms of FGF2 or FGFRs 1, 2 and 3, is CNS development considerably disrupted (Ortega et al., 1998, Paek et al., 2009). Genetic manipulation of either FGF ligands or receptors demonstrates that FGF signalling is essential to proper formation of the mouse cortex by mediating both proliferation and cell survival in NPCs (Ortega et al., 1998, Paek et al., 2009).

The role of FGF signalling in mammalian CNS development is perhaps demonstrated clearly in the human disease Thanatophoric dysplasia (Lin et al., 2003). Mutations in the *Fgfr3* gene that render it constitutively active result in gross brain abnormalities, such as an enlarged cerebrum resulting from increased proliferation and survival of NPCs within the cortical VZ (Lin et al., 2003). In contrast, patients exhibit smaller cerebella, suggesting that FGF ligands have varying proficiencies for promoting NPC proliferation across the CNS (Lin et al., 2003).

FGF signalling is also important for the commitment of NPCs towards glial cell fates, as well as the specification of certain neuronal subtypes. The decision between either neuronal or oligodendroglial and astroglial fates is dose-dependent, whereby low concentrations of FGF promote proliferation and eventual neurogenesis in cultured cortical NPCs, whilst higher levels of FGF drive the generation of both glial subtypes (Qian et al., 1997, Hajihosseini and Dickson, 1999, Bartlett et al., 1998). FGF also plays an inductive role for specifying cultured NPCs to become tyrosine hydroxylase (TH)-positive dopaminergic neurons when co-stimulated with glial cell-conditioned media (Daadi and Weiss, 1999). Furthermore, FGF signalling through FGFR1 is required for proper specification of parvalbumin-expressing cortical interneurons, whilst the specification of other subtypes, such as GABAergic neurons of the ganglionic emminence is not affected in the *Fgfr1*$^{-/-}$ mouse embryonic cortex (Smith et al., 2014).

EGF signalling is not as fundamental as FGF stimulation to sustain mammalian NPC proliferation *in vivo* or *in vitro*, indicated by the reduced responsiveness of NPCs to EGF at earlier developmental time points compared to FGF (Kornblum et al., 1997, Kilpatrick and Bartlett, 1995). EGF signalling is important, however, for maintaining proliferation in the embryonic striatum and promotes cell survival of cultured striatal NPCs (Kornblum et al., 1998). Yet, striatal NPCs isolated from EGFR-null embryos still proliferate in the presence of FGF signalling, indicating that FGF signals can compensate for EGF in specific regions of the CNS (Kornblum et al., 1998). EGF-responsive NPCs express TH *in vivo*, indicating that EGF helps specify dopaminergic neurons as well (Kornblum et al., 1997).

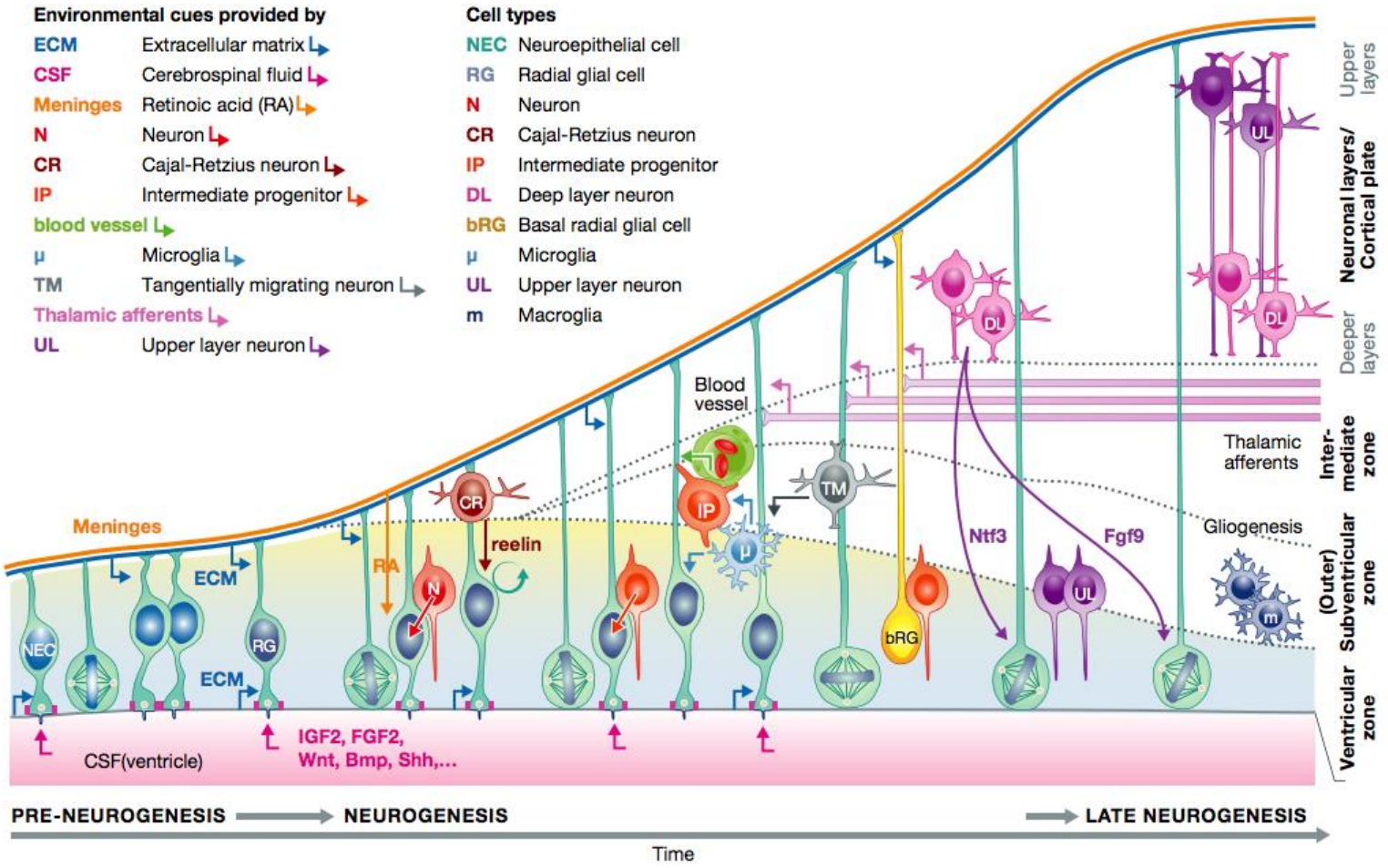

Figure 1.4 Cellular and molecular regulation of NPCs.

Schematic representation of niche signalling for NPCs in the embryonic mammalian forebrain. Adapted from "The cell biology of neurogenesis: toward an understanding of the development and evolution of the neocortex" (Paridaen and Huttner, 2014)

1.2.3.2 Sonic hedgehog

Another secreted factor, Sonic hedgehog (SHH), acts as both a potent mitogen for NPCs and an essential morphogen involved in regionalisation of progenitors across the developing CNS. SHH belongs to the hedgehog multigene family that signals through the primary cilium in a wide variety of embryonic cell types during development and is indispensable for embryogenesis. The receptor Patched (PTCH), which normally sequesters and inhibits the function of another transmembrane receptor, the GPCR-like Smoothened (SMO) protein, releases SMO once bound by SHH. Release of SMO from repression by PTCH subsequently reduces the proteolytic degradation of the GLI family of proteins, allowing accumulation of the GLI2/3 complex that activates expression of various SHH-signalling target genes.

SHH drives proliferation and prevents differentiation of NPCs in the murine neural tube, and ectopic SHH expression doubles the rate of mitosis in NPCs at mid-gestation (Rowitch et al., 1999). SHH enhances NPC proliferation by upregulating expression of proto-oncogenic NMYC, which itself increases expression of cyclin D1 that consequently drives cell cycle progression (Kenney et al., 2003, Oliver et al., 2003). Furthermore, in the developing cerebellum, newborn Purkinje cells maintain proliferation of granule cell precursors by releasing SHH (Dahmane and Ruiz i Altaba, 1999). SHH also promotes the identity of both early and more lineage-committed NPCs at various stages of CNS development. For example, SHH is crucial for the establishment of early forming $PAX6^{+}$ APs and thus overall expansion of the nervous system, given that more differentiated NPCs and post-mitotic neurons derive from APs (Ericson et al., 1997). On the other hand, SHH is also required to induce specific progenitor domains in the developing spinal cord that give rise to interneuron and motoneuron populations (Ericson et al., 1997).

SHH signalling synergizes with both EGF and FGF signalling to promote proliferation *in vitro*, as well as to maintain the NPC pool size *in vivo* (Palma and Ruiz i Altaba, 2004, Zhu et al., 1999). SHH cooperation with FGF signalling extends to other functions as well, such as in the induction of subtype-specific domains. These

include dopaminergic neurons when combined with FGF8, and serotonergic neurons with FGF4 (Ye et al., 1998).

In vitro, SHH and BMP signals antagonize one another, by either driving neurogenesis and oligodendrogliogenesis (SHH) or astrogliogenesis (BMP2; Zhu et al., 1999). WNT signalling (see below) can also antagonise SHH signalling, but at later stages of neural development during the establishment of NPC-specific domains (Alvarez-Medina et al., 2008).

1.2.3.3 Wnt signalling

Wingless-int or 'Wnt' proteins are secreted ligands whose signalling was first identified in carcinogenesis (Polakis, 2012). In canonical Wnt signalling, a Wnt ligand binds a member of the Frizzled (FZ) family of receptors, which form co-receptor complexes with either LRP5 or LRP6. This complex consequently becomes stabilized upon binding of Wnt and subsequently prevents the proteolytic degradation of β-catenin, allowing β-catenin to accumulate in the cytoplasm and translocate to the nucleus where it acts as a transcriptional activator in conjunction with the TCF/LEF family of TFs.

Wnt ligands are expressed across the entire developing chick and murine CNS, in particular WNT1, WNT3A and WNT4, with the former being fundamental to the expansion of NPCs responsible for generating the mouse midbrain and cerebellum (Hollyday et al., 1995, McMahon and Bradley, 1990). Conversely, WNT3A promotes proliferation of hippocampus-forming NPCs at the caudomedial margin, as well as of primary cortical NPCs derived from the SVZ (Lee et al., 2000, Kalani et al., 2008). WNT3A stimulates formation of the hippocampus through its activation of the TF LEF1, which is vital to the generation of dentate gyrus granule cells (Galceran et al., 2000).

The pro-proliferative and stemness effects of Wnt signals derive from their activation of β-catenin-mediated expression of cyclins D1 and D2, which sustain cell cycle re-entry and prevent neuronal differentiation (Chenn and Walsh, 2002, Megason

and McMahon, 2002). Thus, Wnt signalling directly controls the switch from self-renewing to neurogenic divisions (Chenn and Walsh, 2002).

Like SHH, Wnt signalling exhibits an array of interactions with other pathways governing embryonic neurogenesis and dorsal-ventral patterning of the developing CNS. For example, Wnt signalling stimulates proliferation more robustly in dorsal regions of the embryonic cortex and also in the spinal cord, where it performs cross-antagonism with BMP signalling (Megason and McMahon, 2002, Ille et al., 2007, Ikeya et al., 1997). Wnt also promotes proliferation of NPCs in the dorsal developing avian spinal cord following the dorsal specification of these progenitors by BMPs (Chesnutt et al., 2004).

Although typically antagonistic during the specification of discrete neuronal subtypes, Wnt signals synergize with SHH, as well as with FGF, to promote the formation and subsequent expansion of NPCs found in the SVZ of the developing cortex (Viti et al., 2003). Thus, FGF and SHH signals promote differentiation into BPs, which then proliferate upon Wnt stimulation (Viti et al., 2003). Conversely, FGF signalling inhibits Wnt-induced differentiation of NPCs by preventing Wnt-stimulated β-catenin/LEF TF complexes from binding to the NGN1 promoter (Israsena et al., 2004).

1.2.3.4 VIP, IGF, LIF, CNTF and PDGF

Vasoactive intestinal peptide (VIP) is a neuropeptide hormone that acts in a variety of different organs during adulthood. VIP drives proliferation in forebrain APs by decreasing cell cycle length, upregulating expression of *Mcph1* and *Chk1* and therefore ensuring cell cycle re-entry (Gressens et al., 1994, Passemard et al., 2011). Insulin-like growth factor (IGF1) reaches cortical NPCs via the CSF to promote the self-renewal of striatal NPCs by maintaining cell cycle re-entry as well (Lehtinen et al., 2011, Hodge et al., 2004, Arsenijevic et al., 2001, Popken et al., 2004). IGF1 is necessary for maintaining proliferation of these progenitors, independently of FGF and EGF signalling.

The peptide hormone ciliary neurotrophic factor (CNTF) and the cytokine leukaemia inhibitory factor (LIF) are both enriched in regions of inflammation postnatally and promote neuronal survival (Blesch et al., 1999, Arakawa et al., 1990). Developmentally, both signal through a receptor complex containing a gp130 subunit, and CNTF/LIF/gp130 signalling is vital for sustaining NPC self-renewal in the lateral ganglionic emminence by enhancing Notch signalling in NPCs there (Gregg and Weiss, 2005, Chojnacki et al., 2003). In the lateral ganglionic emminence, increasing gradients of either CNTF or LIF normally correlate with a decreasing gradient of NPC differentiation; in contrast both factors positively regulate differentiation in spinal cord progenitors (Gregg and Weiss, 2005). LIF also regulates commitment of NPCs to astroglial fates in the developing cortex and hippocampus by interacting with BMP signals to promote the assembly of a complex comprised of STAT3, SMAD1 and the transcriptional co-activator p300 (Nakashima et al., 1999, Koblar et al., 1998).

Platelet-derived growth factor (PDGF) is a potent mitogen in many cell types during adulthood, such as cells of the retinal pigment epithelium. Yet in contrast, PDGF induces neuronal differentiation in NPCs of the mid-gestational rat cortex (Hinton et al., 1998, Williams et al., 1997). PDGF signals are even able to override CNTF-induced proliferation of rat cortical NPCs by inhibiting self-renewal, implicating PDGF as a highly proficient differentiation factor in the developing rodent CNS (Park et al., 1999).

1.2.3.5 Notch signalling

Notch signalling maintains stemness by driving expression of Notch target genes, primarily the Hes family of TFs. Upon binding of a Notch ligand, such as Delta or Jagged, Notch receptors release the Notch intracellular domain (NICD) into the cytoplasm, which binds to the DNA-binding protein CSL to act as a transcriptional activator in the nucleus (Kopan and Ilagan, 2009). Notch ligands (both secreted and membrane-associated) and receptors are expressed widely by NPCs across the developing mammalian CNS but are restricted to distinct NPC subtypes and in a salt-and-pepper pattern (Mizutani et al., 2007). FGF promotes stemness by inducing the expression of the Notch receptor NOTCH1 in NPCs and therefore sensitises progenitors to stimulation by Notch ligands (Rash et al., 2011).

Notch signalling between APs, such as aRG, employs a mechanism known as 'lateral inhibition'. Lateral inhibition through Notch signalling is underpinned by the oscillatory relationship between Hes and proneural TFs (Shimojo et al., 2008). For example, increasing expression of the proneural TF NGN2 during periods of low Notch signalling promotes expression of the Notch ligand Delta like 1 (DLL1) to stimulate Notch signalling and target gene expression in a neighbouring NPC (Shimojo et al., 2008). Mutual activation of Notch signalling in adjacent NPCs, combined with the temporal oscillation of Hes family TFs, therefore maintains stemness amongst NPCs.

Many components of the canonical Notch signalling pathway play fundamental roles in maintaining NPC identity (Chambers et al., 2001, Hitoshi et al., 2002, Imayoshi et al., 2010). Variations in Notch signalling between NPC subtypes exist as a result of differential expression of Notch signalling mediators. For example, the Notch effector C-promoter binding factor (CBF1) is expressed primarily in aRG, but not in more differentiated NPC classes, suggesting that CBF1 demarks cells of increased proliferative capacity (Mizutani et al., 2007). Conversely, the E3 ubiquitin ligase mind bomb-1 (MIB1) is expressed in basally positioned, non-aRG NPCs, as well as in post-mitotic neurons and ensures proper endocytosis of Notch signals (Yoon et al., 2008). $MIB1^{+}$ cells present Notch ligands to aRG on filopodia-like extensions and are required to ensure the timely generation of more differentiated NPC subtypes, as well as to sustain neurogenesis (Yoon et al., 2008). PROX1, a transcriptional repressor, is expressed in the domain between NOTCH1-positive NPCs and post-mitotic neurons (Kaltezioti et al., 2010). Within this compartment, PROX1 expression inhibits NOTCH1 expression and drives differentiation into more committed NPCs, such as in BPs (Kaltezioti et al., 2010).

1.2.3.6 Integrins

Integrins assemble in the plasma membrane as heterodimers composed of one member each from the alpha and beta subunit families, and interact with the ECM. Integrins are responsible for mediating the interaction of NPCs with the basement membrane at the pial surface, as well as with other cells, to anchor progenitors to the

appropriate anatomical position. Furthermore, integrins transduce ECM signals to regulate NPC behaviour.

Integrins were first implicated in developmental neurogenesis during the migration of newly-formed neurons across the developing cortex (Anton et al., 1999). Migrating neurons use α3β1 integrin for adhesion to the basal process of aRG as they move down into the cortical plate (Anton et al., 1999). However, only the alpha subunit is required for the process of migration, as mutant embryos lacking β1 integrin in the developing cortex show no such defect (Graus-Porta et al., 2001). Instead, β1 integrin is essential for anchorage of the basal endfoot of NPCs to the pial basement membrane (Graus-Porta et al., 2001). Loss of this anchorage through genetic ablation of either β1 integrin or its laminin ligand LAMA2 increases apoptosis in the cortex (Graus-Porta et al., 2001, Radakovits et al., 2009). Integrins are also crucial for adhesion at the apical surface of the developing mammalian CNS. LAMA2 interacts with β1 integrin to maintain NPC anchorage at the ventricle, and pharmacological perturbation of this interaction specifically at the apical surface results in detachment of the apical endfoot (Loulier et al., 2009). This subsequently perturbs INM and results in both a complete loss of horizontal division planes amongst dividing NPCs, as well as cortical layering defects (Loulier et al., 2009).

α5β1 integrin expression correlates strongly with expression of the NPC marker NESTIN in multipotent and self-renewing NPCs *in vitro* and is stimulated by both EGF and bFGF, but decreases following neuronal differentiation (Yoshida et al., 2003, Suzuki et al., 2010). These findings are supported by *in vivo* evidence that transcripts of ECM-based genes, as well as genes encoding integrins, are enriched in and around NPCs with increased capacity for self-renewal (Fietz et al., 2012).

Integrin signalling can also promote NPC self-renewal in a non-cell autonomous manner. Constitutive activation of β1 integrin in a small proportion of NPCs in the developing avian mesencephalon induced proliferation of non-VZ associated progenitors considered to be the avian equivalent of SAPs (Long et al., 2016). Organotypic slice culture experiments demonstrated that activation of β1 integrin in NPCs induces secretion of WNT7A, which signals in a paracrine

manner to adjacent or near-by SAPs and stimulates expression of the ECM protein Decorin (Long et al., 2016). Although not fully explored yet in NPCs, Decorin typically interacts with other proliferation-inducing pathways, such as in the developing kidney, and is hypothesised to mediate differentiation in the embryonic avian CNS (Long et al., 2016). Thus, integrin expression in one NPC subtype can regulate the behaviour and lineage commitment of another neighbouring subtype (i.e. non-cell autonomously).

Integrins can also act as receptors for non-ECM ligands. α5β3 integrin promotes the expansion of bIPs by inducing cell cycle re-entry at the expense of neurogenic divisions. The ligand in this instance is not a component of ECM and is instead thyroid hormone, suggesting that integrins may act to transduce systemic endocrine signals and not just those originating locally from ECM (Stenzel et al., 2014). However, whilst it is proposed that thyroid hormone signalling through integrin induces cell cycle re-entry in bIPs, this NPC class is not commonly believed to undergo self-renewing divisions (see **1.1.1.3**; Noctor et al., 2004, Taverna et al., 2014). Thus, additional work is required to establish whether this represents a novel feature of bIPs or alternatively, whether a different BP subtype actually expands in this instance.

1.2.3.7 Neurotrophins

The neurotrophins brain-derived neurotrophic factor (BDNF) and neurotrophin 3 (NT3) activate a variety of intracellular signalling pathways in both post-mitotic neurons and NPCs, and function potently as pro-survival factors in the nervous system (Segal, 2003). Whilst BDNF and NT3 signal through the transmembrane receptors TRKB and TRKC, respectively, both also bind to the TRK co-receptor p75NTR (Segal, 2003). Both neurotrophins and their respective TRK receptors are expressed across the developing rodent cortex. BDNF expression gradually increases in parallel with the progression of neurogenesis, whereas NT-3 expression gradually diminishes (Fukumitsu et al., 1998, Maisonpierre et al., 1990).

EGF-generated neurospheres derived from the ventral murine telencephalon commit to neurogenesis after a single exposure to BDNF *in vitro*, dependent on

p75NTR, indicating its strong differentiative potential (Ahmed et al., 1995, Hosomi et al., 2003, Vicario-Abejon et al., 1995). Furthermore, exogenous administration of BDNF, in the form of an intraventricular injection at embryonic day (e) 16, increases neuron production in the developing rat telencephalon (Fukumitsu et al., 1998).

BDNF action works in parallel with that of the gaseous molecule nitrous oxide (NO), whose synthesis correlates with differentiation across the embryonic CNS (Bredt and Snyder, 1994). NO was originally characterised as a cytostatic and differentiative factor and is now commonly thought to work in a feedback mechanism with neurotrophins (Peunova and Enikolopov, 1995). For example, NO inhibits the secretion of neurotrophins from cultured hippocampal neurons by inhibiting protein kinase G-dependent calcium release (Canossa et al., 2002). Additionally, NO abolishes BDNF release by baroreceptor neurons *in vitro* by reducing BDNF expression (Hsieh et al., 2010).

Conversely, BDNF stimulation increases expression of the neural NO synthase (nNOS) in differentiating neurons generated from murine telencephalic NPCs (Cheng et al., 2003). nNOS-derived NO subsequently inhibits proliferation and drives neuronal differentiation in adjacent NPCs in a paracrine manner (Cheng et al., 2003). The suggestion that BDNF and NO act redundantly is supported by the observations of cultured NPCs following pharmacological blockade of NO synthesis. Blocking NO production in NPCs increases BDNF expression, possibly as a compensatory mechanism, to ensure timely neuronal differentiation in the absence of the cytostatic effects of NO (Lameu et al., 2012). This blockade of NO signalling *in vitro* results in a three-fold increase in p75NTR expression, thus potentiating the sensitivity of cultured NPCs to extracellular neurotrophins to maintain the generation of neurons (Lameu et al., 2012).

NT3 promotes differentiation in the avian neural tube, both *in vitro* and *in vivo*, as well as in cultured NPCs from the rodent brain (Averbuch-Heller et al., 1994, Vicario-Abejon et al., 1995) and does so by potently driving the switch from self-renewing to neurogenic cell division (Ghosh and Greenberg, 1995). Accordingly, NT3 inhibits FGF2-mediated proliferation of NPCs in a dose-dependent manner by inhibiting the PI3K/AKT and GSKβ signalling pathways, as well as by lengthening

the G1 phase through decreased expression of cyclin D2 (Ghosh and Greenberg, 1995, Jin et al., 2005). In the developing murine forebrain, NT3 is typically expressed by post-mitotic neurons within the cortical plate under the control of the transcriptional repressor SIP1, and signals to APs in a feedback mechanism (Parthasarathy et al., 2014). Neuron-derived NT3 promotes differentiation of $PAX6^+$ APs to $TBR2^+$ BPs, and also drives the formation of neurons in the upper layers the cortex (Parthasarathy et al., 2014). Thus, NT3 induces both neurogenic and differentiative divisions in multipotent murine APs.

1.2.3.8 Other regulatory mechanisms

The chemokine CXCL12 is released by the meninges during neurogenesis to guide the tangential migration of Cajal-Retzius cells across the cortex by signalling through CXCR4 (Borrell and Marin, 2006). Cajal-Retzius cells themselves influence cortical NPCs from an early point in CNS development. These neurons are produced at the onset of murine neurogenesis in the embryonic cortex and migrate to the most basal region of the neuroepithelium in layer I (Soriano and Del Rio, 2005). Cajal-Retzius cells express the secreted signal Reelin, which was initially demonstrated to mediate neuronal migration (Dulabon et al., 2000, Hartfuss et al., 2003, Lakoma et al., 2011). In addition, Reelin signalling enhances Notch signalling in aRG by increasing NICD expression in forebrain VZ NPCs and subsequently drives self-renewal and inhibits differentiation of APs (Lakoma et al., 2011). Thus, newborn Cajal-Retzius cells sustain NPC expansion via long-range Reelin signals.

Neurotransmitters can also regulate NPC cell cycle progression. Gabba-aminobutyric acid (GABA) and glutamate typically have opposing effects in neurophysiology but both play similar roles in regulating VZ proliferation during early phases of cortical development (Haydar et al., 2000, Luk et al., 2003). Thus, GABA and glutamate reduce DNA synthesis and antagonize the proliferative effects of FGF2 at comparatively later stages, during peak neuron production (LoTurco et al., 1995, Antonopoulos et al., 1997). Dopamine signals can also promote or inhibit cell cycle progression in the developing brain, such as in the lateral ganglionic emminence, depending on which dopamine receptor is predominantly activated (Ohtani et al., 2003). For example, activation of the D1 receptor promotes cell cycle

lengthening in the VZ of the LGE, leading to increased differentiative or neurogenic cell divisions, whilst D2-like receptor activation promotes NPC cell cycle re-entry and self-renewal (Ohtani et al., 2003).

Finally, immune cells have also been shown to play a role in neurogenesis across many different species. Microglia are tissue-resident macrophages in the developing and adult CNS and are present in the embryonic rodent cortex from as early as e11, when they help to maintain NPC proliferation (Antony et al., 2011, Cunningham et al., 2013). However, pharmacologic blockade of microglial recruitment to the cortical VZ and SVZ increases NPC proliferation, potentially through reduced phagocytosis of progenitors by microglia (Cunningham et al., 2013).

1.2.3.9 Embryonic NPCs and blood vessels

The mechanisms by which blood vessels regulate NPCs of the embryonic rodent CNS were poorly defined prior to my research project. Initial studies showed that $TBR2^+$ BPs in the developing cortex cluster preferentially around the growing vessel network there (Stubbs et al., 2009, Javaherian and Kriegstein, 2009). However, findings published towards the end of my PhD indicated that vasculature regulates NPCs either through relief of tissue hypoxia or by acting as a physical tether for NPC processes (Tan et al., 2016, Lange et al., 2016). I will discuss these regulatory mechanisms in greater detail later in my thesis and compare them to my own findings.

1.3 VEGF in neural development

Despite being initially characterised as potent inducers of blood vessel growth (discussed in greater detail in **1.4.1.1**), members of the vascular endothelial growth factor (VEGF) family also regulate neural development. Both *in vivo* and *in vitro* models have shown that VEGF, particularly VEGF-A, promotes neuronal survival, migration and maturation. Moreover, some evidence suggests that VEGF-A and VEGF-C play a role in regulating NPC behaviour.

1.3.1.1 VEGF-A regulates neuronal migration

Both the facial branchiomotor neurons (FBMs) of the embryonic hindbrain and the granule cells of the cerebellum require VEGF-A for correct chemotaxis (Schwarz et al., 2004, Ruiz de Almodovar et al., 2010). However, VEGF-A signalling in either cell type differs with respect to the required VEGF isoform, as well as the receptor. Whilst FBM axons are guided outside of the CNS by class 3 semaphorins (SEMA3), VEGF164 signals through the transmembrane, non-tyrosine kinase receptor neuropilin 1 (NRP1) on the FBM cell body (Schwarz et al., 2004). Increased expression of non-NRP1 binding VEGF120, at the expense of VEGF164, results in misplaced FBM soma in rhombomere 5 rather than rhombomere 6 (Schwarz et al., 2004). Conversely, ECM-binding VEGF188 guides newborn granule cells via its interaction with VEGFR2, a VEGF receptor tyrosine kinase, from their birthplace in the external granule cell layer to the Purkinje cell layer (Ruiz de Almodovar et al., 2010).

1.3.1.2 VEGF-A regulates axon guidance

Although VEGF-A/NRP1 signalling does not appear to be required for correct guidance of axons in the PNS, it is necessary for guidance of retinal ganglion cell (RGCs) axons in the developing mouse brain (Vieira et al., 2007, Schwarz et al., 2004, Erskine et al., 2011). RGCs project contralaterally in species lacking overlap in the visual field, such as in fish. In contrast, species with an overlap in vision, such as in mice and humans, possess a small number of RGC axons that project ipsilaterally. Thus, the path of RGC axons at the optic chiasm in the diencephalon is finely tuned by an extensive array of molecules (Erskine et al., 2011). Contralateral RGC axons are guided across the chiasm via VEGF164/NRP1 signalling to innervate the correct hemisphere (Erskine et al., 2011). Depletion of either VEGF164 or NRP1 increased ipsilateral projection across the optic chiasm (Erskine et al., 2011). In contrast, neither VEGFR2 or perineural blood vessels are required for correct RGC axon guidance. On the other hand, commissural axons in the murine spinal cord use VEGF-A as a guidance molecule for midline crossing via VEGFR2 (Ruiz de Almodovar et al., 2011). Both pharmacological blockade as well as genetic manipulation of

commissural axon-expressed VEGFR2 result in reduced axon turning *in vitro* and misplaced axons *in vivo*, respectively (Ruiz de Almodovar et al., 2011).

1.3.1.3 VEGF-A is a survival factor for embryonic and postnatal neurons

Several studies have implicated VEGF-A as an important neuroprotective factor during motoneuron degeneration. In a model of low VEGF-A expression across the whole animal, mutant mice demonstrate late-onset, progressive degeneration of motoneurons (Oosthuyse et al., 2001). Endogenous VEGF-A is also protective during either ischaemia- or AMPA-induced degeneration (Oosthuyse et al., 2001, Lambrechts et al., 2003, Tovar et al., 2007). Moreover, it has been shown since that direct infusion of exogenous VEGF-A directly protects newborn neurons in the dentate gyrus after focal cerebral ischaemia in a vessel-independent manner (Sun et al., 2003).

The best unequivocal demonstration of VEGF-A in a direct neuroprotective role, independently of vessel-derived neuroprotection, was provided from studies into a migrating population of neurons responsible for synthesising gonadotrophin releasing hormone (Cariboni et al., 2011). These GnRH neurons migrate from their birthplace in the olfactory epithelium to the hypothalamus in the forebrain. Neural-specific loss of NRP1 results in increased GnRH neuron cell death and fewer GnRH neurons reach the hypothalamus (Cariboni et al., 2011). Both neural-specific *Vegfr2* and endothelial-specific *Nrp1* mutants show no changes in GnRH neuron apoptosis, indicating that VEGF164 signals through NRP1 to promote cell survival in migrating GnRH neurons independently of CNS vascularisation, although it has not been established whether NRP1 requires a co-receptor to mediate this function (Cariboni et al., 2011). Furthermore, treatment of immortalized GnRH neurons *in vitro* with recombinant VEGF164 significantly reduces levels of apoptosis during serum starvation (Cariboni et al., 2011). However, it is not clear which intracellular signalling pathways transduce VEGF164 signals to increase cell survival.

1.3.1.4 VEGF and embryonic NPCs

Although there have been several demonstrations of VEGF-A- and VEGF-C-induced neurogenesis in the adult (see **1.5.2.2**), evidence of a role for VEGF in directly regulating embryonic NPCs is sparse. Murine cortices with reduced VEGF-A isoform diversity exhibit decreased proliferation and stemness in cortical NPCs, although it was not defined whether VEGF-A-stimulated blood vessel growth regulated NPC behaviour (Darland et al., 2011). Secondly, vascular-derived VEGF-A was suggested to regulate different aspects of cortical development, and mutant embryos lacking VEGF-A expression specifically by *Tie2*-expressing endothelial cells exhibited differentiation defects and severe cortical delamination (Li et al., 2013). It is, however, also not clear whether the phenotypes observed in this study result from loss of direct VEGF-A signalling to NPCs or indirectly by promoting vascular growth within the CNS.

Studies of the developing chick retina suggest that VEGF-A promotes proliferation of retinal NPCs, independently of its vascular role through VEGFR2 (Hashimoto et al., 2006). In addition, the formation of neurospheres derived from e14 cortical NPCs is enhanced by VEGF-A/VEGFR2 signalling (Wada et al., 2006). This appears to be through improved cell survival, mediated by the NF-κB (Wada et al., 2006).

Contrastingly, VEGF-C plays a clear and direct role in regulating NPCs in the developing CNS of both the mouse and the frog (Le Bras et al., 2006). Morpholino-induced knockdown of VEGF-C in frogs reduces proliferation of VEGFR3-expressing NPCs in a vessel-independent manner. Furthermore, *Vegfc*$^{-/-}$ and *Vegfc*$^{+/-}$ mouse embryos possess fewer oligodendrocyte progenitor cells in the optic nerve and VEGF-C stimulates proliferation of VEGFR3^{+} oligodendrocyte precursors *in vitro* (Le Bras et al., 2006).

1.4 Vascularisation of the central nervous system (CNS)

The embryonic CNS is vascularised by the invasion of blood vessels from a perineural vascular plexus (PNP), which resides outside of the brain and spinal cord.

This ingression of vessels from outside of the CNS, and then into other areas of the neural parenchyma, follows a process known as 'angiogenesis' in which new blood vessels sprout from pre-existing ones. This process is distinct from 'vasculogenesis', where blood vessels form *de novo* from endothelial cells in so-called 'blood islands', and intussusceptive angiogenesis where a single blood vessel splits into two. Blood vessel ingression into the neural tube is followed by extensive sprouting and remodelling until a vascular network is formed. Remarkably, vascularisation occurs without perturbing the complex cytoarchitecture of the developing neurogenic niches or newly forming neural networks. This results from extensive neurovascular crosstalk that patterns CNS vasculature (discussed below; see **Figure 1.6**).

The mouse embryo hindbrain is widely used as a model system to study developmental angiogenesis in the mammalian CNS and gives an overview of specific cellular and molecular mechanisms regulating the blood vessel growth within these organs (Fantin et al., 2013b). Vascularisation of the mouse hindbrain begins around e9.5, when vessel sprouts emerge from the PNP and extend radially towards the VZ, where NPCs release vascular growth factors (Fantin et al., 2010). From e10.25, these radial vessels turn at near right angles to extend parallel to the hindbrain surface. The subventricular vascular plexus (SVP) forms when sprouts from neighbouring radial vessels anastomose – a process that is mediated by tissue resident macrophages (Fantin et al., 2010, Fantin et al., 2013a, Ruhrberg et al., 2002). During this phase, pericytes invest the vessel sprouts and eventually ensheath the endothelial cells to provide structural support and instructive signals (Gerhardt and Betsholtz, 2003). By e12.5, the SVP has formed an extensive vascular network, and is followed by additional angiogenic sprouting in deeper, more basal layers of the CNS (Fantin et al., 2010, Ruhrberg et al., 2002).

The mouse postnatal retina is also used as another model for studying CNS vascularisation and follows a similar pattern of blood vessel growth to the hindbrain, albeit after birth (Tata et al., 2015). The following cellular and molecular mechanisms of CNS vascularisation will therefore be explained in the context of both developing hindbrain and postnatal retina models.

1.4.1 Cellular and molecular interactions in CNS vascularisation

During angiogenesis, tip cells respond to different signals by initiating endothelial migration, whilst stalk cells follow behind the tip cell and proliferate and induce lumen formation to form the main body of new vessel sprouts. Early studies linked tip and stalk cell behaviours to signalling by VEGF-A. NPCs within the embryonic brain secrete VEGF-A to stimulate angiogenic sprouting (Gerhardt et al., 2003, Haigh et al., 2003, Ruhrberg et al., 2002).

Subsequent experiments demonstrated that VEGF signalling interacts with the Notch pathway to regulate the proportion of tip cells versus stalk cells in retinal angiogenesis (Hellstrom et al., 2007, Leslie et al., 2007, Suchting et al., 2007). Studies of chimeric embryoid bodies and developing vasculature within the mouse retina further suggested that tip/stalk cell phenotypes and associated functionalities are plastic and switch dynamically over time (Jakobsson et al., 2010).

In agreement with a key role for VEGF in tip cell induction in both the hindbrain and postnatal retina, high levels of VEGFR2 are expressed in tip cells relative to neighbouring stalk cells to promote tip cell-mediated vessel sprouting (Jakobsson et al., 2010). Furthermore, tip cell fusion, known as vessel 'anastomosis' is mediated by tissue resident macrophages in vascularisation of both mouse and fish CNS (Fantin et al., 2010). Macrophages act independently of VEGF-A, but synergize with VEGF-induced vessel sprouting to promote vascular network formation. Recent work identified additional regulators of vessel sprouting and tip cell behaviour, which are discussed in greater detail below.

In addition to the general principles of angiogenesis described above, specialised interactions between endothelial and non-endothelial CNS cells generate a unique structure termed the neurovascular unit. Within the neurovascular unit, endothelial cells form strong junctions with one another and interact with other cell types, such as pericytes, astrocytes and microglia, to create the blood brain barrier (BBB). The BBB maintains CNS homeostasis and is also believed to regulate blood flow and synaptic activity within the brain. For example, a hallmark of CNS vessels is the presence of the glucose transporter GLUT1. Mutations in the *GLUT1* gene

underlie a rare autosomal dominant disorder termed GLUT1 deficiency syndrome, which is characterized by pathologically low levels of glucose within the cerebrospinal fluid, due to reduced glucose transport across the BBB (Seidner et al., 1998).

1.4.1.1 VEGF and hypoxia inducible factors (HIFs)

Various neural cell types produce VEGF-A, and neuroglial-secreted VEGF-A is required for the ingression of blood vessels into the developing neural tube across different vertebrate species (Bussmann et al., 2011, Haigh et al., 2003, James et al., 2009, Raab et al., 2004). VEGF-A mRNA is differentially spliced to produce isoforms with varying affinities for the surrounding ECM, and their bioavailability is further regulated by proteolytic mechanisms (Park et al., 1993, Houck et al., 1992). The human isoforms of VEGF-A are termed VEGF121, VEGF165 and VEGF189, reflecting the number of amino acid residues present in the mature protein. VEGF121 is the most diffusible, VEGF189 binds ECM the most efficiently and VEGF165 has intermediate properties. Cleavage of VEGF189 by matrix metalloproteases (MMPs) leads to the generation of VEGF113, which is subsequently released from the matrix. The corresponding isoforms in mouse are one amino acid residue shorter and thus termed VEGF112, VEGF120, VEGF164 and VEGF188, respectively. The isoforms also differ in their ability to interact with specific receptors (see below).

Genetic manipulations that restrict expression of VEGF-A to only a single isoform at the expense of the other isoforms do not prevent the entry of vasculature into the neural tube, but instead perturb vessel patterning and morphogenesis within the CNS. Accordingly, blood vessels within the hindbrain and retina of *Vegfa*$^{120/120}$ mice, which only express VEGF120, have a larger diameter and branch infrequently (Ruhrberg et al., 2002, Stalmans et al., 2002). Conversely, vessels in *Vegfa*$^{188/188}$ mice expressing only the VEGF188 isoform are thin and over-branched (Stalmans et al., 2002). In the avian neural tube, forced over-expression of the matrix-binding VEGF165 or VEGF189 in a localized manner also results in ectopic vessel ingression at the site of electroporation, whilst ectopic expression of the more diffusible VEGF121 does not lead to this effect (James et al., 2009). Furthermore, local VEGF-A blockade in the same model by forced expression of soluble VEGFR1 (sFLT1),

which acts a decoy for VEGF-A in the interstitial fluid, prevents vascular ingression (James et al., 2009). In the neonatal mouse retina, a collection of the three murine VEGF-A isoforms is synthesized and displayed by a network of astrocytes located beneath the expanding retinal vascular plexus, as well as by RGCs and neural cells within the inner nuclear layer.

In addition to receiving paracrine VEGF-A signals from neuroglial cells for angiogenesis, endothelial cells themselves are thought to be a key source of VEGF-A to promote vascular homeostasis in the long term (Lee et al., 2007). VEGF-A expression in endothelial cells in the murine retinal vascular plexus is induced by the transmembrane protein cysteine-rich motor neuron 1 (CRIM1) to maintain blood vessel stability (Fan et al., 2014). In addition, as previously mentioned, endothelium-derived VEGF-A has also been shown to be important for the development of the correct cytoarchitecture of the developing mammalian cortex (Li et al., 2013).

The hypoxia-inducible transcription factors HIF1A and HIF2A, known regulators of *Vegfa* transcription, induce angiogenesis in response to reduced tissue oxygenation (Carmeliet et al., 1998). For example, HIF1A is expressed abundantly in the neuroretina, especially by retinal progenitor cells (RPCs), and the deletion of HIF1A from the neuroretina severely perturbs retinal angiogenesis. However, HIF1A does not regulate VEGF-A expression in RPCs; instead, it induces the expression of the astrocyte mitogen PDGF-A to drive the formation of the astrocyte network that then promotes vascularisation of the retina (Nakamura-Ishizu et al., 2012).

1.4.1.2 VEGF tyrosine kinase receptors

VEGF-A binds three tyrosine kinase receptors that are all crucial for angiogenesis. These are VEGFR1 (FLT1), VEGFR2 (FLK1 or KDR) and VEGFR3 (FLT4; displayed in **Figure 1.5**)

VEGFR2 is the main signal transducing VEGF receptor in endothelial cells *in vitro* and is vital for endothelial cell survival and blood vessel formation *in vivo*. Heterozygous loss of *Vegfa* expression causes embryonic lethality at e9.5 in the mouse and due to their early embryonic lethality, $Vegfr2^{+/-}$ and $Vegfr2^{-/-}$ mice are not

suitable to study the specific functions of VEGFR2 signalling in CNS vascular development (Ferrara et al., 1996). However, the use of a function-blocking antibody or the selective ablation of VEGFR2 in endothelial cells, has revealed that VEGFR2 is essential for tip cell formation and vascular outgrowth in the mouse retina (Benedito et al., 2012, Gerhardt et al., 2003, Okabe et al., 2014, Zarkada et al., 2015). Moreover, retinal neurons express VEGFR2 abundantly to sequester and subsequently titrate the levels of VEGF-A in the retina (Okabe et al., 2014). This limits angiogenesis in the outer retinal layers, consequently restricting blood vessel growth to the inner retinal layer during formation of the primary plexus (Okabe et al., 2014). Endothelial VEGFR2 is also a critical mediator of VEGF-induced Notch signalling in sprouting retinal vasculature (Jakobsson et al., 2010).

VEGFR3 is best known as a VEGF-C receptor during lymphangiogenesis but is also highly expressed in angiogenic sprouts. In addition, genetic targeting of VEGFR3 is embryonic lethal at e10.5 due to severe vascular defects (Dumont et al., 1998). VEGFR3 function in angiogenesis is, however, not completely understood. On the one hand, function-blocking antibodies against VEGFR3 decreases sprouting, vessel density, vascular branching and endothelial cell proliferation in the mouse retina (Tammela et al., 2008). This finding is supported by a similar phenotype observed in animals with a heterozygous deletion of its ligand VEGF-C (Tammela et al., 2011). On the other hand, however, the specific deletion of VEGFR3 in endothelial cells causes excessive vessel sprouting and branching in both the mouse embryonic hindbrain and postnatal retina (Tammela et al., 2011). Thus, it has been proposed that VEGFR3 positively regulates angiogenesis induced by VEGF-C, but simultaneously inhibits excessive angiogenesis by enhancing Notch signalling in response to macrophage-secreted VEGF-C, to drive the fusion and stabilisation of vascular sprouts (Tammela et al., 2011).

Vegfr1$^{-/-}$ embryos lacking both forms (soluble and membrane-bound) of the receptor die at e9.5 due to abnormal vascular development caused by excessive endothelial cell proliferation, yet mice lacking only the intracellular kinase domain are healthy (Hiratsuka et al., 1998). These findings indicate an important function for sFLT1 in modulating VEGF bioavailability to VEGFR2. Accordingly, sFLT1 negatively regulates vascular sprout formation and branching morphogenesis during

developmental angiogenesis (Kearney et al., 2004). Furthermore, the global deletion of *Vegfr1* in postnatal mice augmented both VEGFR2 accumulation and signalling, and therefore enhanced angiogenesis in both the retina and brain (Ho et al., 2012).

Despite the fact that the soluble VEGFR1 isoform inhibits angiogenesis by sequestering VEGF, an *in vitro* study indicated that full length VEGFR1 (containing the tyrosine kinase domain) also signals in endothelial cells (Autiero et al., 2003). Thus, VEGFR1/VEGFR2 heterodimerisation enhances VEGFR2 trans-phosphorylation when endothelial cells are co-stimulated with both placental growth factor (PGF) and VEGF. A role for VEGFR1 signalling in endothelial cells is also supported by the observation that mice genetically manipulated to express only sFLT1 at the expense of the transmembrane isoform have reduced VEGFR2 signalling, fewer endothelial cells and thinner vessels (Hiratsuka et al., 2005). Taken together, these observations of VEGFR1 signalling suggest that vascular defects in full VEGFR1 knockout mice reflect the net effect of losing a strongly anti-angiogenic function carried by sFLT1 and a relatively weaker proangiogenic role for the full-length isoform.

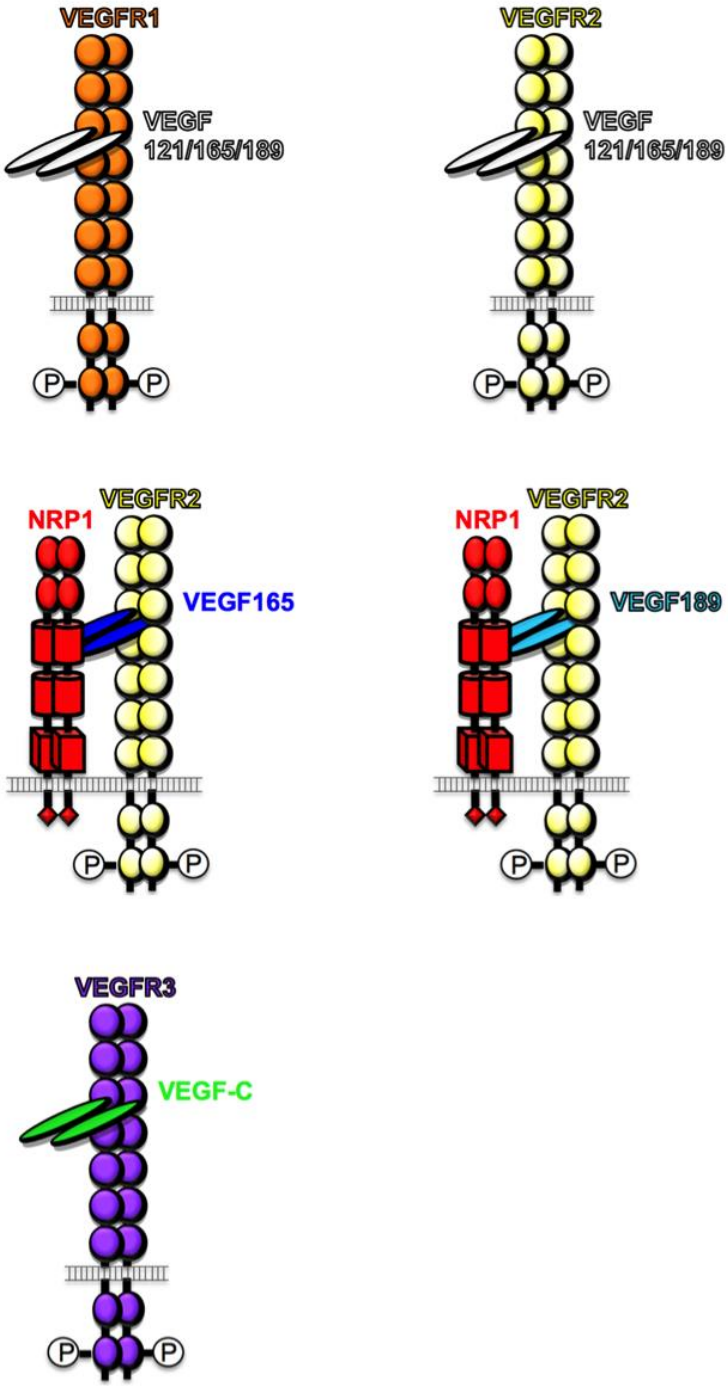

Figure 1.5 VEGF receptor binding.

Schematic representation of typical VEGF-VEGF receptor binding during CNS vascularisation. VEGFR1 (orange) and VEGFR2 (yellow) both bind all three isoforms of VEGF-A (white). NRP1 (red) can bind VEGF165 (dark blue) and VEGF189 (light blue) whilst in a co-receptor complex with VEGFR2. VEGFR3 (purple) binds VEGF-C (green).

1.4.1.3 Neuropilins (NRPs), neuropilin-binding VEGF isoforms and semaphorins

Both Neuropilins were initially identified as transmembrane receptors required for different aspects of neural development but are also essential for the vascularisation of the mouse spinal cord, hindbrain, forebrain and retina (Kawasaki et al., 1999, Gerhardt et al., 2004, Gu et al., 2003, Fantin et al., 2014, Raimondi et al., 2014, Fantin et al., 2015). In contrast, other regions located outside the CNS, such as the perisomitic space, are well-vascularised in the absence of NRP1, and the vasculature in these regions show only minor morphological defects (Ruhrberg et al., 2002). It is not known why NRP1 is especially important for CNS vascularisation, but is less important for some other vessel networks.

Both of the classical NRP1 ligands, SEMA3 and VEGF165, have been implicated as regulators of endothelial cell behaviour through NRP1 binding *in vitro* and *in vivo*. VEGF121 can also bind NRP1 *in vitro*, although it does so with a 50-fold lower affinity than VEGF165, as it lacks an exon 7-encoded domain that enhances NRP1 binding (Parker et al., 2012). This finding was supported by analyses using the hindbrain model that showed that VEGF121 is not able to bind NRP1 at detectable levels *in vivo* (Tillo et al., 2015). Moreover, VEGF121 cannot bind and signal through NRP1 to compensate for loss of VEGF165 and VEGF189 (Cariboni et al., 2011, Erskine et al., 2011). Whilst these observations in neural models suggest that VEGF121 is also unlikely to signal through NRP1 during vascular development *in vivo*, it has been difficult to demonstrate this directly due to the presence of VEGF121-binding VEGFR1 and VEGFR2 in endothelial cells. In addition to VEGF165, VEGF189 is also able to bind to and signal through NRP1 *in vivo*; however, this has so far only been shown for neurons (Tillo et al., 2015).

Analysis of mouse knockout embryos lacking SEMA3A revealed that this NRP1 ligand is dispensable for brain vascularisation, as well as blood vessel formation elsewhere in the developing mouse (Bouvree et al., 2012, Vieira et al., 2007). Likewise, inactivation of semaphorin binding to NRP1 does not impact on brain angiogenesis or vascular development in the early mouse embryo, even if functional compensation by NRP2 is also prevented (Gu et al., 2005, Vieira et al., 2007).

Interestingly, SEMA3F has been described to act to repel angiogenesis during vascularisation of the retina (Buehler et al., 2013). Whilst SEMA3A expression is seen exclusively in the inner retina, SEMA3F expression is restricted to the outer retina and retinal pigment epithelium, where it inhibits sprouting angiogenesis to maintain the physiological avascularity in the outer retina (Buehler et al., 2013). It is presently unknown whether NRP2, the receptor for SEMA3F, is involved in this process.

SEMA3E is the only member of the class 3 semaphorin family that does not bind to a neuropilin receptor, and instead binds directly to the plexin PLXND1 (Gu et al., 2005). In the developing mouse retinal vasculature, high levels of VEGF secreted from the avascular retinal periphery induce PLXND1 expression in endothelial cells at the vascular front via VEGFR2 (Kim et al., 2011). Neuroretinal SEMA3E signals to endothelial PLXND1 to upregulate DLL4 expression at the vascular front, which in turn enhances endothelial Notch signalling to block the formation of tip cells and tip cell filopodia (Kim et al., 2011). Despite the fact that SEMA3E does not directly bind to NRP1, NRP1 can convert SEMA3E/PLXND1-mediated axonal repulsion into attraction in CNS neurons, but it is unclear whether such a mechanism exists in endothelial cells as well (Chauvet et al., 2007).

Despite the lack of brain vascularisation defects in semaphorin/NRP signalling mutants, loss of NRP1 from endothelial cells causes vascular patterning defects in the brain that are similar to those caused by loss of NRP1 in all cells. It was therefore proposed that the vascular phenotype of mice lacking NRP1 in endothelial cells results from defective VEGF signalling through NRP1 (Gu et al., 2005). However, *Vegfa*$^{120/120}$ mice lacking heparin/neuropilin binding VEGF isoforms have less severe CNS vascular defects than mice lacking NRP1 (Ruhrberg et al., 2002) (Gerhardt et al., 2004). Furthermore, mice that possess a mutation that specifically blocks VEGF binding to NRP1 have milder defects in CNS angiogenesis than *Nrp1*-null or endothelial-specific *Nrp1*-null mice (Fantin et al., 2014, Gelfand et al., 2014). Two different mouse mutants have been generated that carry point mutations in the VEGF-binding domain of NRP1: Y297A or D320K (Gelfand et al., 2014, Fantin et al., 2014). The former mutants also have low NRP1 expression levels that caused minor defects in hindbrain vascular complexity, whilst the D320K mutation did not

impair vascularisation of either the embryonic or the postnatal forebrain (Gelfand et al., 2014, Fantin et al., 2014). Both mutants showed similar reductions in both vascular extension and artery/vein formation in the retinal vessel plexus in agreement with the phenotype observed in *Vegfa*$^{120/120}$ mice lacking the NRP1-binding VEGF isoform VEGF164 (Gelfand et al., 2014, Fantin et al., 2014, Stalmans et al., 2002).

The observation of only mild reductions of vessel growth in VEGF-binding deficient NRP1 mutants suggests that NRP1 modulates CNS angiogenesis through additional, semaphorin- and VEGF-independent mechanisms. In agreement, it was recently shown that NRP1 enhances CNS angiogenesis by promoting ECM signalling (Raimondi et al., 2014). The ECM component and integrin ligand fibronectin (FN) induces cytoskeletal remodelling in cultured endothelial cells through a pathway that depends on the interaction of NRP1 with both the non-receptor tyrosine kinase ABL1, as well as the small RHO-GTPase CDC42 (Raimondi et al., 2014, Fantin et al., 2015). Both proteins regulate the actin cytoskeleton to drive retinal angiogenesis where FN is deposited ahead of the vascular front by astrocytes and around growing blood vessels. Pharmacological inhibition of ABL kinase or CDC42 activity in the postnatal retina perturbed vessel patterning similarly, but less severely than the genetic targeting of NRP1 in retinal endothelial cells (Fantin et al., 2015, Raimondi et al., 2014). This is due to the fact that VEGF-A also signals through NRP1 in retinal angiogenesis; therefore, NRP1 functions as both an ECM and VEGF-A receptor during blood vessel growth in the eye. However, it is not currently known which specific ECM components bind NRP1 during retinal angiogenesis, and whether a similar pathway exists in other areas of the CNS, such as in the hindbrain. NRP1 has also been demonstrated to be an effector of Notch activation to modulate TGFβ signalling responsible for tip-stalk cell specialisation during retinal angiogenesis (Aspalter et al., 2015).

1.4.1.4 Wnt signalling

A growing number of studies have demonstrated that Wnt signalling is an integral part of vascular development in the developing brain and postnatal retina. As previously discussed (see **1.2.3.3**), the Wnt-β-catenin pathway controls the proliferation and specification of embryonic NPCs through TCF-mediated gene

expression. The signalling pathway is also responsible for promoting vessel outgrowth and maturation in the developing neural tube, guided by parenchymal WNT7A and 7B (Daneman et al., 2009, Stenman et al., 2008). Moreover, Wnt signals from the neuroepithelium are also required to stabilise the nascent BBB by upregulating expression of GLUT1 and tight junction genes of the claudin family in the endothelium (Daneman et al., 2009, Stenman et al., 2008, Ma et al., 2013, Liebner et al., 2008, Zhou et al., 2014).

The non-WNT ligand norrin activates the β-catenin pathway through its receptors FZ4 and LRP5, analogous to the canonical Wnt signalling pathway, to drive retinal vascularisation (Xu et al., 2004). A similar receptor complex operates in the neural tube, although, LRP6 is able to compensate for LRP5 in this tissue, unlike in the retina (Ye et al., 2009, Wang et al., 2012, Zhou et al., 2014). In genetically mosaic retinal vessels, wildtype endothelial cells initially protect neighbouring *Fz4*$^{-/-}$ endothelial cells, but endothelial cells lacking FZ4 are progressively lost (Wang et al., 2012). This observation suggests that a quality control mechanism may selectively eliminate endothelial cells defective in Wnt signalling, possibly to protect the integrity of the blood retinal barrier (Wang et al., 2012). This mechanism may be mediated by receptors DR6 and TROY, both transcriptional targets of β-catenin, which are required for brain angiogenesis and BBB formation (Tam et al., 2012). However, it has not been established which ligand(s) activate DR6 and TROY during developmental blood vessel growth.

1.4.1.5 Orphan seven transmembrane (7-TM) receptors

Various 7-TM receptors, whose endogenous ligands have not yet been identified and are therefore defined as ‘orphan’ GPCR proteins, also drive CNS angiogenesis. One such example is the orphan 7-TM receptor GPR126. GPR126 signalling forms an integral part of vascular development, by promoting endothelial cell proliferation, migration and lumen formation *in vitro*, as well as during angiogenesis *in vivo*, by promoting VEGFR2 expression through STAT5/GATA2-mediated transcription (Cui et al., 2014). Another orphan 7-TM receptor, GPR124, is essential for correct vascularisation of the neural tube (Cullen et al., 2011, Anderson et al., 2011, Kuhnert et al., 2010). *Gpr124*$^{-/-}$ mice have delayed vessel ingression into

the developing neural tube from the PNP and vasculature that eventually extends into the neural tube forms abnormal glomeruloid tufts that, in spite of pericyte recruitment, are prone to haemorrhages (Kuhnert et al., 2010, Daneman et al., 2010). Accordingly, forced overexpression of endothelial GPR124 causes hypervascularisation within the adult neocortex (Kuhnert et al., 2010).

Rather than by promoting endothelial cell proliferation, GPR124 instead enhances vessel sprout directionality by activating CDC42 to remodel the actin cytoskeleton (Kuhnert et al., 2010). GPR124 may also modulate CNS angiogenesis by regulating the DLL4, TGFβ and/or WNT signalling pathways (Anderson et al., 2011). Analysis of gene expression in forebrain endothelium in *Gpr124*$^{-/-}$ mutants indicated that DLL4 expression and activation of the TGFβ pathway are negatively regulated by GPR124 (Anderson et al., 2011). The role of GPR124 as a coactivator of canonical Wnt signalling has been explored in more detail for CNS angiogenesis. GPR124 interacts genetically with both WNT7A and WNT7B to enhance Wnt signalling through either FZ1 or FZ4 together with LRP5 or LRP6 (Posokhova et al., 2015, Zhou and Nathans, 2014). In agreement with a role for GPR124 in enhancing the Wnt-β-catenin pathway, global loss of GPR124 leads to a severe malformations in the vessel network of the embryonic cortex, which could be rescued through forced stabilization of β-catenin (Zhou and Nathans, 2014). Norrin is more important in canonical Wnt signalling via FZ4 and LRP5 in the hindbrain and spinal cord, and is not expressed in the forebrain (Zhou and Nathans, 2014, Ye et al., 2011). Yet, forced norrin expression in the forebrain can rescue angiogenesis defects in *Gpr124*$^{-/-}$ knockout mice, suggesting that CNS vascular patterning relies on the specific spatiotemporal expression pattern of these ligands, rather than a definite requirement for either WNT7A/B or norrin signals (Zhou and Nathans, 2014).

1.4.1.6 Other mechanisms

Various integrins are required for neurovascular cell adhesion during brain and retinal angiogenesis (McCarty, 2009). Neuroglial expression of ITGAV and ITGB8 maintains CNS angiogenesis, as well as vascular stability (Arnold et al., 2012, Arnold et al., 2014, Hirota et al., 2011, McCarty et al., 2005, McCarty et al., 2002, Zhu et al., 2002). Vascularisation of the developing brain is also driven by hedgehog

signalling to regulate vessel sprouting and eventual BBB establishment. SHH is required for the induction of motor neurons in the neural tube, which themselves express the angiogenic factor angiopoietin 1 (ANG1) to induce vessel ingression (Nagase et al., 2005). Furthermore, SHH signalling from BBB-associated astrocytes promotes BBB stability by initiating expression of junctional proteins in BBB endothelial cells (Alvarez et al., 2011).

ANG1 is expressed at high levels by motor neurons at a time when its main receptor TIE2 is expressed in endothelial cells within the neural tube, and both promote vessel ingression from the PNP and vascular patterning (Nagase et al., 2005, Sato et al., 1995, Suri et al., 1996). Both ANG1 and the alternative TIE2 ligand ANG2 are required for vascularisation of the retina, where the former enhances angiogenesis independently of TIE2 and the latter regulates vascular remodelling (Gale et al., 2002, Lee et al., 2013, Hackett et al., 2000).

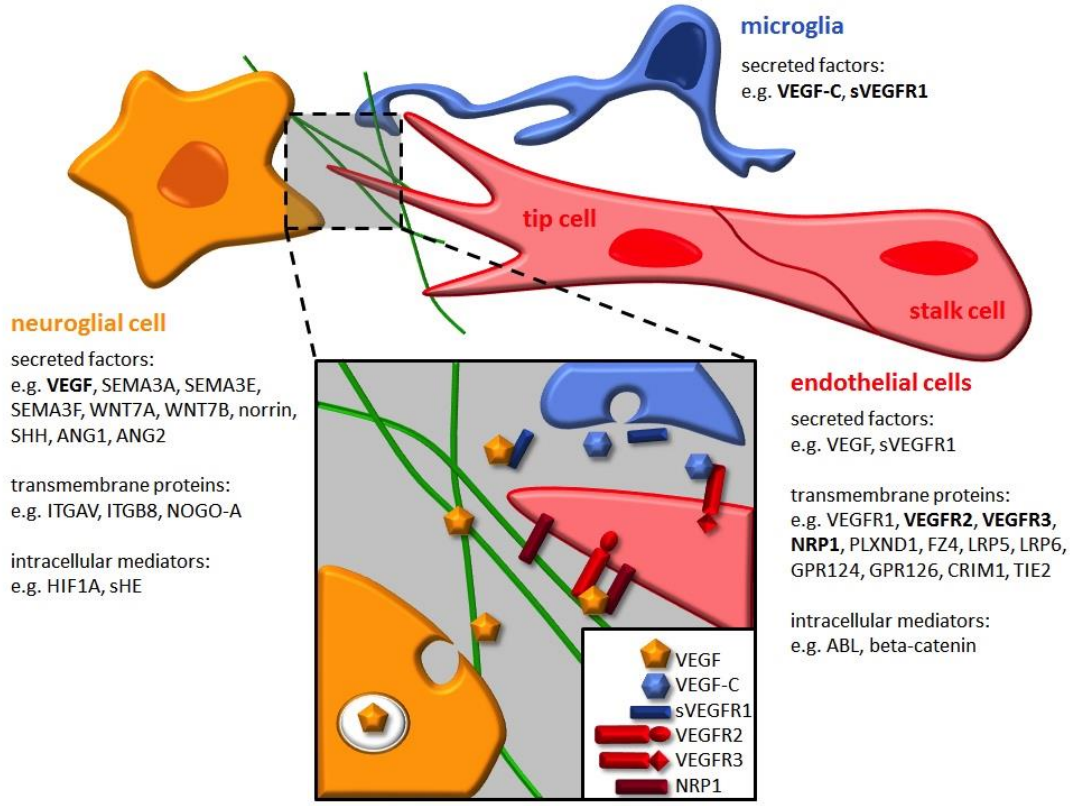

Figure 1.6 Schematic representation of the interaction between neuroglial cells, microglia and endothelial cells during CNS vascularisation.

Examples of secreted, transmembrane and intracellular signalling molecules are displayed under each cell type. Grey box illustrates role of VEGF family of ligands and receptors during blood vessel growth in CNS. Green fibres denote ECM. Adapted from "Vascularisation of the central nervous system" (Tata et al., 2015).

1.5 The mammalian stem cell niche

The term 'stem cell niche' refers to a complex regulatory microenvironment that physically surrounds stem or progenitor cells. The niche ensures that stem and progenitor cells are 'anchored' in a specific anatomical location within a tissue and also regulates the behaviour of such cell types through signals that may take the form of diffusible cues, cell membrane-bound ligands, ECM-derived molecules or metabolic parameters. The stem and progenitor cells integrate these signals in order to match their behaviour to physiological requirements.

During embryogenesis, the stem cell niche sustains stem and progenitor cell proliferation and differentiation in order to generate a tissue or organ. During adulthood, the niche is instead required to maintain tissue homeostasis, induce tissue expansion or enable tissue regeneration. Importantly, the processes promoting stem cell activity have to be balanced with the need to prevent premature exhaustion of the stem cell pool and excessive or abnormal proliferation that may result in pathology.

In this section, I will briefly discuss some of the best-studied mammalian stem cell niches to highlight conserved mechanisms that regulate the behaviour of stem and progenitor cells. I will focus particularly on the niche responsible for regulating adult neural stem cells as a direct comparison for the niche required for maintaining embryonic neurogenesis.

1.5.1 Embryonic stem cell niches in mammals

During mammalian embryogenesis, extensive and elaborate tissue and organ growth is required to generate an entire organism in often-short gestational periods. For example, the neural ectoderm is only specified from the ectodermal layer from around e7 in the mouse, and thus the murine CNS has to expand sufficiently over only 11 days *in utero* to enable life after birth (Avilion et al., 2003). This is facilitated by a vast array of signals that co-ordinately direct NPC growth and differentiation to give rise to an extensive and elaborate set of functionally diverse neurons. Furthermore, a subpopulation of embryonic NPCs has to specialise to become NSCs, exemplifying

the need for maintaining NPC stemness across gestation (Fuentealba et al., 2015, Furutachi et al., 2015).

1.5.2 Postnatal stem cell niches in mammals

1.5.2.1 Intestinal and epidermal stem cells

In contrast to embryonic progenitors, which enable organ formation and growth, adult stem and progenitor cells are required to maintain already-formed tissues. As such, niche regulation of adult progenitors is often required to restrain their proliferation to ensure the long-term preservation of germinative cell types.

The first adult stem cell niche to be studied in great detail was that of the intestine. In the mammalian small intestine and colon, stem cells reside in intestinal 'crypts', within which enteroendocrine, goblet and tuft cells and absorptive enterocytes are all derived from a lineage originating from $LGR5^+$ stem cells (Barker, 2014). A number of known molecular mechanisms regulate intestinal stem cells. For example, neighbouring Paneth cells promote self-renewal and proliferation of $LGR5^+$ stem cells through paracrine EGF, WNT3, DLL4 and TGF-α signals in co-culture experiments (Sato et al., 2011), and the genetic ablation of Paneth cells results in a dramatic loss of intestinal stem cells *in vivo* (Sato et al., 2011). Paneth cells also link $LGR5^+$ stem cell behaviour to nutrient levels, thus integrating information on calorific intake with gut physiology; in particular, heightened dietary intake activates the mammalian target of rapamycin (mTORC1) in Paneth cells, inducing the production of paracrine factor cyclic ADP ribose that subsequently enhances proliferation of intestinal stem cells (Yilmaz et al., 2012). Thus, $LGR5^+$ stem cells can be regulated in their niche by signals originating from their immediate neighbours, as well as through systemic cues transduced by neighbouring cells.

Melanocyte and hair follicle stem cells of the epidermal bulge are similarly regulated by a complex niche microenvironment (Hsu et al., 2014). Hair follicle stem cells ensure constant renewal of the skin epithelia and enable cell replacement during wound healing. Diffusible signals, such as IGF, EGF and FGF, as well as ECM proteins like laminin 5, maintain the stemness and colony-forming capacity of

epidermal stem cells (Lewis et al., 2010, Jones and Watt, 1993, Guo et al., 1993, Rheinwald and Green, 1977). Epidermal stem cell differentiation is promoted by Notch signalling, which simultaneously increases expression of genes characteristic of cells within the more differentiated spinous layers and inhibits those found in stem cells (Blanpain et al., 2006).

1.5.2.2 Neural stem cells of the subventricular zone

Adult neurogenesis has received increasing interest in the last decade as the potential therapeutic value of understanding NSC biology to treat neurodegenerative diseases has become clearer (Goldman, 2016). In the postnatal mammalian brain, new neurons are generated in two key regions, the subventricular zone (SVZ) bordering the lateral ventricles and the dentate gyrus (DG) in the hippocampus (discussed in **1.5.2.3**). The SVZ has been studied extensively owing to the comparatively large number of neurons produced there, as well as its responsiveness to brain injury (Benner et al., 2013).

In the rodent SVZ, several thousand NSCs, known as type B1 cells, line the walls of the CSF-filled lateral ventricles. Type B1 cells usually exist in a quiescent state but undergo expansion and neurogenesis after activation (Codega et al., 2014, Doetsch et al., 2002). Following activation, type B1 cells differentiate into transit-amplifying progenitors, more commonly known as type C cells or TAPs. Type C cells are able to divide symmetrically three times, thus expanding the pool of progenitor cells in a short space of time (Ponti et al., 2013). Type C cells differentiate further into neuroblasts, also known as type A cells, which migrate in the rostral migratory stream (RMS) to their destination in the olfactory bulb (OB), where they terminally differentiate into olfactory interneurons (Doetsch et al., 1999).

Many different factors control two key processes in NSCs in both neurogenic niches: activation from quiescence (i.e. exit from G_0) or proliferation. NSC quiescence in the SVZ, much like stemness in the embryonic CNS, is maintained by Notch signalling through the transcriptional regulator RBPJ (Aguirre et al., 2010, Imayoshi et al., 2010). Furthermore, autocrine BMP signals prevent NSCs from entering the cell cycle, but are antagonised by noggin from ependymal cells, which

potently induces stem cell activation and neurogenesis (Lim et al., 2000). As ependymal cells line the CSF-filled ventricle, it is hypothesised that signalling mechanisms like noggin may act to link B1 cell activation with systemic physiology. IGF2 circulates within the postnatal CSF and stimulates the expansion of B1 cells, similar to its role in increasing NPC self-renewal in the developing rodent cortex (Arsenijevic et al., 2001, Lehtinen et al., 2011). It is unclear, however, whether IGF2 increases activation of NSCs or instead acts as mitogen. EGF regulates neurogenesis in the SVZ later in the neural lineage by stimulating proliferation of TAPs (Aguirre et al., 2010). The initiation of EGFR expression is synchronised with the activation of B1 cells and becomes increasingly abundant after their differentiation into type C cells (Codega et al., 2014). B1 cell behaviour is also directly modulated by neurotransmitter release. For example, both dopaminergic and serotonergic neurons activate B1 cell proliferation (Tong et al., 2014, Hoglinger et al., 2004). However, local GABA release from neuroblasts inhibits cell cycle entry and thus maintains stem cell quiescence (Liu et al., 2005a).

In addition to the mechanisms discussed, a large number of vessel-derived factors are required for neurogenesis in the SVZ. All three VEGF receptor tyrosine kinases have been implicated in regulating various stages of the lineage originating from B1 cells. For example, exogenous VEGF-A infusion into the lateral ventricles stimulates NSC proliferation and cell cycling through VEGFR2 (Jin et al., 2002). This effect is independent of any changes to vasculature in or around the neurogenic niche, as cortical stem cell cultures that are devoid of endothelial cells are expanded by recombinant VEGF-A (Jin et al., 2002, Schanzer et al., 2004). Furthermore, VEGF-C signals through VEGFR3 to activate B1 cells and enhance neurogenesis independently of blood vessels (Calvo et al., 2011). VEGFR1 has also been implicated in SVZ neurogenesis, although it is not clear how it specifically contributes to the generation of OB interneurons (Wittko et al., 2009). Whilst it is detectable in the plasma membrane of B1 cells and in the RMS, where it may transduce signals, it has also been suggested that sFLT1 functions in the SVZ as a VEGF-A trap to limit extracellular VEGF-A levels (Wittko et al., 2009).

Several studies showed that endothelial cells in the SVZ niche express soluble factors that regulate the behaviour B1 cells. Pigment epithelium-derived factor

(PEDF) is secreted by both SVZ ependymal and endothelial cells and directly promotes NSC self-renewal by enhancing Notch signalling (Ramirez-Castillejo et al., 2006, Andreu-Agullo et al., 2009). By increasing expression of Notch transcriptional targets, such as HES1, and inhibiting expression of proneural ASCL1, PEDF promotes symmetric instead of asymmetric divisions in NSCs, thus expanding the pool of B1 cells (Andreu-Agullo et al., 2009). NT3 is also secreted by endothelial cells in the SVZ, but regulates adult NSCs in a different manner to that in the developing CNS. Whilst NT3 promotes cell cycle exit and neuronal differentiation of NPCs, vascular as well as CSF-derived NT3 maintains quiescence and prevents cell cycle entry of B1 cells (Delgado et al., 2014). This is explained by the observation that niche-derived NT3 phosphorylates eNOS in B1 cells, with the resulting increase in intracellular NO acting as a cytostatic factor for NSCs (Delgado et al., 2014).

BDNF is a vessel-derived neurotrophin in the adult avian brain; thus, angiogenesis in the higher vocal cord centre of the adult male songbird stimulates the growth of new capillaries, which express BDNF to increase neurogenesis (Louissaint et al., 2002). In the rodent brain, BDNF instead regulates the migration of type A cells towards the olfactory bulb. Neuroblasts migrate long distances down the RMS, aided by vessel networks along their migratory path (Thored et al., 2007, Bovetti et al., 2007). Neuroblasts are attracted to these vessels by chemotactic gradients of stromal-derived factor 1 (SDF1) and BDNF, which are secreted by endothelial cells (Kokovay et al., 2010, Snapyan et al., 2009). *In vitro* studies suggested that SDF1 increases the motility of neuroblasts, whilst BDNF acts as a chemoattractant.

SVZ vessels also regulate B1 cells via membrane-bound or ECM-derived signals. B1 cells contact vessels close to the walls of the lateral ventricle via endfoot protrusions and require vessel anchorage to remain physically tethered to their position within the neurogenic niche (Mirzadeh et al., 2008, Niola et al., 2012). Blood vessels themselves possess a lamina containing ECM molecules, such as LAMA5, which allows B1 cells to adhere to endothelial cells *in vitro* through its interaction with NSC-expressed α6β1 integrin (Shen et al., 2008). Blocking the association of LAMA5 with α6β1 integrin dissociates B1 cells from co-cultured endothelial cells and promotes NSC activation (Shen et al., 2008). Additionally, blood vessels regulate NSC quiescence via Notch and Ephrin signalling through endfoot protrusions (Ottone

et al., 2014). Both JAG1, a Notch ligand, and EPHRINB2 are localized to the plasma membrane of endothelial cells contacting B1 cell endfeet, and signal synergistically to NSCs to prevent cell cycle entry by reducing expression of cyclins D1 and E1 (Ottone et al., 2014).

1.5.2.3 Neural stem cells of the dentate gyrus

In the subgranular zone (SGZ) of the DG, NSCs are radial glia-like stem cells known as type 1 cells. Type 1 cells demonstrate astrocyte characteristics, such as the expression of glial fibrillary acid protein (GFAP), and they exist in either a quiescent or activated state, similar to NSCs in the SVZ (Encinas et al., 2011). Following activation and then proliferation, type 1 cells differentiate into the TAPs of the DG, known as type 2 cells. Type 2 cells are $TBR2^{+}$, similar to the BPs of the embryonic mammalian CNS, and they are highly proliferative in response to neurogenic stimuli, such as exercise (Hodge et al., 2008). Type 2 cells then differentiate further into type 3 cells, analogous to type A cells of the SVZ. Type 3 cells have a limited capacity for proliferation and eventually migrate to the granule cell layer, where they exit the cell cycle and differentiate into post-mitotic granule cells, which contribute to the memory processes in mammals.

Notch-RBPJ and BMP signalling maintain quiescence and stemness in type 1 cells of the DG, analogous to NSCs in the SVZ (Ables et al., 2010, Ehm et al., 2010, Bonaguidi et al., 2008, Mira et al., 2010). Furthermore, the behaviour of NSCs in the DG is regulated by a number of different neuronal inputs. On the one hand, long-term potentiation at synapses with granule cells increases the proliferation of a subset of SGZ progenitor cells, although it is not known which stem or progenitor subtype expands in response to increased neural activity (Bruel-Jungerman et al., 2006). On the other hand, it is known that type 2 cells receive direct GABAergic inputs from elsewhere in the hippocampus (Tozuka et al., 2005). Unusually, type 2 cells are depolarized by GABAergic stimulation, which induces expression of NEUROD1 and promotes neuronal differentiation (Tozuka et al., 2005). Furthermore, glutamatergic/NMDAR stimulation of NSCs in the DG, likely type 1 cells, induces NEUROD1 whilst inhibiting HES1 and ID2 expression, thereby promoting neuronal differentiation (Deisseroth et al., 2004).

Vascular cues also regulate hippocampal neurogenesis. Infusion of recombinant VEGF-A into the CSF of the adult rodent brain drives NSC activation in the SGZ, whilst VEGF-C signals through VEGFR3 in type 1 cells to promote cell cycling (Han et al., 2015, Jin et al., 2002). VEGF-A also promotes neuronal plasticity in newborn granule cells independently of its role in stimulating SGZ angiogenesis (Licht et al., 2011). Finally, NSCs in the DG extend endfeet to nearby blood vessels, and thus may receive vessel-bound signals for maintaining quiescence and stemness in a manner similar to B1 cells (Filippov et al., 2003).

1.6 Aims and objectives of this study

The precise regulation of NPC behaviour is crucial to ensure proper CNS development. As little is known on the role of the vascular niche in regulating hindbrain NPC behaviour, the overarching aim of my PhD research was to determine whether blood vessels and/or vascular factors regulate NPC behaviour and therefore neurogenesis in the mouse embryo hindbrain. To achieve this aim, I pursued three specific objectives.

My first objective was to define the spatiotemporal pattern of blood vessel growth relative to NPC proliferation and organisation in the developing hindbrain GZ to determine whether growing vasculature has the potential to regulate neurogenesis (**Chapter 3**).

My second objective was to use genetic mouse mutants to manipulate blood vessel growth, as well as VEGF-A and semaphorin signalling in NPCs, to distinguish the relative importance of these factors in hindbrain neurogenesis (**Chapter 4**). Thus, I have analysed NPC mitotic activity in hindbrains lacking the neurovascular receptor NRP1 in specific cell types to distinguish whether NRP1 functions cell autonomously in NPCs, or whether it regulates hindbrain NPCs non-cell autonomously by promoting formation of the SVP that vascularises the GZ. I complemented this approach by examining NPC mitotic activity in mutants lacking semaphorin signalling through both neuropilins.

My third objective was to elucidate molecular and cellular mechanisms by which GZ vasculature regulates hindbrain NPCs (**Chapter 5**). Accordingly, I determined the pattern of NPC self-renewal and neuron formation in hindbrains with defective GZ vascularisation and assessed whether hindbrain blood vessels regulate NPCs through a role in tissue oxygenation. Finally, I examined whether the expression of several signalling molecules known to regulate embryonic or adult NPCs is regulated by vasculature or vessel-derived signals in the neurogenic hindbrain.

Chapter 2 MATERIALS AND METHODS

2.1 Materials

2.1.1 General Laboratory Materials

All chemicals were obtained from Sigma Aldrich, except where indicated otherwise. Glassware was obtained from VWR International and plastic items were purchased from Corning or Nunc.

2.1.2 General Laboratory Solutions

Water was used after purification by a MilliRo 15 Water Purification System (Millipore) and, where necessary, water was further purified using the Milli-Q reagent Grade Water Ultrafiltration System (Millipore). RNAse and DNAse-free water was supplied by Sigma Aldrich and absolute ethanol, methanol and isopropanol were obtained from Fischer Scientific.

1X PBS: 137 mM NaCl, 3 mM KCl, 10 mM Na_2HPO_4, 1.8 mM KH_2PO_4, pH 7.2

4% (w/v) formaldehyde: freshly prepared freshly from paraformaldehyde in 1X PBS

1X PBT: 1X PBS + 0.1% (v/v) Triton X-100

1X TE: 10 mM Tris-HCl, 1 mM EDTA, pH 8.0

1X TAE: 40 mM Tris-acetate, 1 mM EDTA, pH 8.0

1X TBS: 25 mM Tris pH 7.5, 150 mM NaCl, 3 mM KCl

2.2 Methods

2.2.1 Animal Methods

All animal research was carried out according to institutional ethical review and United Kingdom Home Office (ASPA 1986) guidelines.

2.2.1.1 Animal Maintenance and Husbandry

To generate embryos of a defined gestational age, mice were paired in the evening and the presence of a vaginal plug the following morning was defined as e0.5.

2.2.1.2 Genetic mouse strains

I used wildtype mice on CD1 and C57Bl/6 genetic backgrounds (Charles River Laboratories). The majority of *Nrp1*-null mice were on a CD1 genetic background, whilst a small number analysed were on a JF1 genetic background. All other strains were on C57Bl/6 genetic backgrounds. Please see **Table 2.1** for details on the genetic mouse strains used.

Table 2.1 Genetic mouse strains and published reference.

Genetic mutation	Reference
Nes-Cre	(Petersen et al., 2004)
Nrp1-null (*Nrp1*$^{-/-}$)	(Kitsukawa et al., 1997)
Nrp1 flox (*Nrp1*$^{c/c}$)	(Gu et al., 2003)
Nrp1$^{Sema/Sema}$	(Gu et al., 2002)
Nrp2-null (*Nrp2*$^{-/-}$)	(Giger et al., 2000)
Pu.1 null (*Pu.1*$^{-/-}$)	(McKercher et al., 1996)
Rosa^{tdTomato}	(Madisen et al., 2010)
Rosa^{YFP}	(Srinivas et al., 2001)
Sox1-iCreER^{T2}	(Tata et al., 2016 – Provided by Prof. N. Kessaris)
Tie2-Cre	(Kisanuki et al., 2001)

2.2.1.3 Tissue-specific gene targeting

To selectively delete genes in specific cell types, a genetic approach based on the *Cre/lox* recombination system was used (reviewed in (Nagy, 2000). This method uses the properties of the enzyme CRE recombinase, which was initially identified in the P1 bacteriophage. This enzyme catalyses the recombination between its two 34 bp recognition sites, which are known as *loxP* (locus of recombination) sites (Hamilton and Abremski, 1984). By flanking a specific DNA sequence with these sites, the CRE enzyme is able to bind and create either an inversion or deletion of the intervening sequence depending on the orientation of the *loxP* sites. This recombination is then made cell type-specific by creating a transgene in which *Cre* is expressed under the control of a tissue-specific promoter. The enzyme, therefore, will only be expressed and sequence deletion will only take place in the cell type of interest. For instance, to delete *Nrp1* in endothelial and microglial cells, mice with a *Cre* transgene under the control of the endothelial *Tie2* promoter (Kisanuki et al., 2001) were mated to mice that were heterozygous for the *Nrp1*-null allele, and the then the subsequent *Tie2-Cre; $Nrp1^{+/-}$* offspring were then mated with mice homozygous for the "floxed" (i.e. flanked by *loxP*) NRP1 allele ($Nrp1^{c/c}$) to generate *Tie2-Cre; $Nrp1^{c/-}$* mice. The heterozygous null background was chosen to maximise the number of endothelial cells lacking NRP1, as *Cre*-mediated recombination is not 100% effective and therefore may not be able to delete both *Nrp1* alleles in every endothelial cells (see Gu et al., 2003).

2.2.1.4 Temporally regulated Cre activation

To temporally control the expression of *Sox1-Cre*, I analysed mice containing the *Sox1-iCreER^{T2}* transgene. This transgene consists of a *Cre* gene and a mutant murine oestrogen receptor (*ERT*) that encodes a fusion protein (*CreER^{T2}*) that is expressed under the control of the *Sox1* promoter (see **2.2.1.3**). Unlike the normal oestrogen receptor, which binds to 17'-oestradiol, the CRE-ER^{T2} recombinase binds to the synthetic compound 4-hydroxytamoxifen (tamoxifen; Danielian et al., 1998). CRE-ER^{T2} is normally sequestered within the cytoplasm by the cytoplasmic protein HSP90 (Mattioni et al., 1994, Picard, 1994); however, upon tamoxifen binding to the receptor, this interaction is prevented and the enzyme translocates to the nucleus.

Therefore, *Cre*-mediated DNA recombination will only occur after tamoxifen has been administered to the mouse. To analyse embryonic tissue labelling in *Sox1-iCreER*^{T2} mice, I collaborated with Prof. Nicoletta Kessaris, who delivered the tamoxifen to pregnant females that had been mated with *Rosa*^{tdTomato} males by oral gavage 24 h before sacrifice and embryo dissection. I prepared the tamoxifen solution by dissolving tamoxifen in peanut oil to 2 mg/ml. Pregnant females were administered a tamoxifen dose of 20 mg per kilogram of body weight to achieve a sufficient level of mosaic cell labelling.

2.2.1.5 Compound mutant mice

To generate compound *Nrp1*$^{Sema/Sema}$*;Nrp2*$^{-/-}$ mouse mutants, mice heterozygous for the *Nrp1*^{Sema} mutation were crossed to mice heterozygous for the *Nrp2*-null allele. Subsequently, offspring heterozygous for both mutations were mated, providing mice homozygous for both mutant alleles at a probability of 1/16.

2.2.1.6 Genotyping of mouse strains

The majority of genotyping was performed by Andy Joyce with the assistance of Laura Denti and Valentina Senatore from the Ruhrberg group. DNA was extracted either from embryonic tail snips or adult ear punches using a previously published method (Laird et al., 1991). Cells were lysed by incubating them overnight at 55ºC in 500 µl of lysis buffer (100 mM Tris-HCl pH 8.5, 5 mM EDTA, 0.2% SDS, 200 mM NaCl) with freshly added proteinase K (100 µg/ml) from a frozen stock solution. Following enzymatic digestion, DNA was precipitated by adding 1 ml of 100% ethanol, and collected following 3 min centrifugation at 13000 rpm at room temperature. The supernatant was decanted and DNA was resuspended in 70% ethanol and collected following another centrifugation using the aforementioned conditions. Subsequently, ethanol was decanted and DNA was air dried for 10 mins at room temperature before being reconstituted in 100 µl TBE buffer (2 mM Tris pH 8.0, 0.2 mM EDTA) for 5-30 min at 55ºC.

The genomic DNA was amplified by PCR using primers specific to the DNA sequence of interest (see **Table 2.2**) on a BioRad C1000 Touch Thermal Cycler. For

each PCR reaction, 2 µl of DNA were added to 8 µl Megamix (Microzone, containing *Taq* polymerase, 1.1X reaction buffer, 200 µM dNTPs, loading dye) and 0.1 µg of both the forward and reverse primer and amplified using the appropriate annealing temperature and number of amplification cycles to obtain DNA pieces of the predicted size (see **Table 2.3**).

The PCR products were analysed using electrophoresis through a 2% (weight/volume) agarose in TAE gel containing 2 µl of nucleic acid staining solution, RedSafe (iNtRON). For each reaction, a negative control consisting of 2 µl sterile water instead of the DNA solution was used, as well as a positive control consisting of 2 µl of previously validated DNA.

Table 2.2 Olignonucleotide primers used for genotyping.

Gene	Primer	Sequence	Amplicon size (bp)
Nes-Cre	Nes8F1	5'-GAATACCCTCGCTTCAGCTC-3'	300
	CreB	5'-GCATTTTCCAGGTATGCTCAG-3'	
Nrp1, Nrp1^{c}	NP1Neo	5'-CGTGATATTGCTGAAGAGCTTGGC-3'	486 (wildtype) 700 (mutant)
	NP1F	5'-CAATGACACTGACCAGGCTTATCATC-3'	
	NP1R	5'-GATTTTTATGGTCCCGCCACATTTGTC-3'	
Nrp1^{Sema}	P1	5'-AGGCCAATCAAAGTCCTGAAAGACAGTCCC-3'	200 (wildtype) 400 (mutant)
	P2	5'-AAACCCCCTCAATTGATGTTAACACAGCCC-3'	
	Zac2	5'-GTGTGCTGATCTGGGAAGGTAGGCAG-3'	
	Zac3	5'-GGAGACGGGAGCAACCAGAGTGC-3'	
Nrp2	NP2Neo	5'-CAGTGACAACGTCGAGCACAG-3'	462 (wildtype) 800 (mutant)
	NP2F	5'-TCAGGACACGAAGTGAGAAGC-3'	
	NP2R	5'-GCTCAATGTAGCTAAGTGGAGGG-3'	
Pu.1	KO2	5'-GCCCCGGATGTGCTTCCCTTATCAAAC-3'	1170 (wildtype) 980 (mutant)
	920	5'-GCCCCGGATGTGCTTCCCTTATCAAAC-3'	
Rosa^{tdTomato}	Tom wt F	5'-GGCATTAAAGCAGCGTATCC-3'	297
	Tom wt R	5'-CTGTTCCTGTACGGCATGG-3'	
Rosa^{YFP}	F1	5'-AAAGTCGCTCTGAGTTGTTAT-3'	650
	R1	5'-GGAGCGGGAGAAATGGATATG-3'	
Sox1-iCreER^{T2}	iCre 250 S	5'-GAGGGACTACCTCCTGTACC-3'	630
	iCre880AS	5'-TGCCCAGAGTCATCCTTGGC-3'	
Tie2-Cre	Tie2Pro	5'-CCCTGTGCTCAGACAGAAATGAGA-3'	850
	Cre2	5'-GTGGCAGATGGCGCGGCAACACCATT-3'	

Table 2.3 PCR parameters for specific primer pairs.

Gene	Hot Start	Denaturing	Annealing	Extension	Cycles	End
Nrp1, *Nrp1^{c}*	94°C, 3 min	94°C, 40 s	66°C, 1 min	72°C, 1 min	35	72°C, 5 min
Nrp1^{Sema}	94°C, 3 min	94°C, 30 s	69°C, 1 min	72°C, 1 min	35	72°C, 5 min
Nrp2	94°C, 3 min	94°C, 1 min	66°C, 1 min	72°C, 1 min	35	72°C, 5 min
Pu.1	94°C, 3 min	94°C, 40 s	60°C, 1 min	72°C, 2 min	35	72°C, 5 min
Rosa^{tdTomato}	94°C, 4 min	94°C, 30 s	61°C, 45 sec	72°C, 1 min	35	72°C, 10 min
Rosa^{tdTomato}	94°C, 3 min	94°C, 1 min	60°C, 1 min	72°C, 1 min	34	72°C, 5 min
Sox1-iCreER^{T2}	94°C, 4 min	94°C, 30 s	62°C, 45 sec	72°C, 1 min	33	72°C, 10 min
Nes-Cre, *Tie2-Cre*	94°C, 3 min	94°C, 1 min	67°C, 1 min	72°C, 1 min	32	72°C, 5 min

2.2.1.7 Tissue fixation

Pregnant females were culled by cervical dislocation in accordance to Home Office and institutional animal guidelines. The gravid uterus was excised and placed in ice-cold 1X PBS. Using fine Dumont forceps, the embryos were dissected from the uterus and yolk sac. To remove hindbrains, embryos were dissected as published previously (Fantin et al., 2013b).

Embryonic tissue collected for immunolabelling was fixed in 4% formaldehyde for 2 h at 4°C. Following fixation, all samples were rinsed briefly twice with 1X PBS at RT to remove any residual formaldehyde and either processed immediately or stored in 1X PBS at 4°C (short-term). Samples stored for the long-term were dehydrated in a methanol gradient comprised of 25%, 50% and 75% (v/v) absolute methanol in 1X PBS and then stored in 100% methanol at -80°C until use. Samples were then rehydrated using the same methanol gradient when processed for immunolabelling or embedding in OCT or agarose.

2.2.2 Immunolabelling

2.2.2.1 Cryosectioning

After fixation, tissue was washed in 1X PBS and dehydrated in cryoprotection solution (30% sucrose and 0.2% sodium azide in 1X PBS). Once tissue had equilibrated and therefore sunk in the solution, samples were placed into optimal cutting temperature embedding compound (OCT, Sakura Tissue-Tek) and rapidly frozen by floating moulds containing sample and OCT on propan-2-ol cooled to -40°C with dry ice. Following this step, samples were stored at -20°C for the short term or at -80°C for the long-term or immediately sectioned into 10 μm thick slices using a histology cryostat (Leica CM1850). The sections were collected on Superfrost Plus slides (VWR International), air-dried for 1 h at RT and then either stored at -20°C or immediately processed for immunolabelling.

2.2.2.2 Vibratome sectioning

Alternatively, following fixation, tissue was washed in 1X PBS and embedded in 3% molten agarose (prepared in Millipore water). After the agarose had set, samples were sectioned at 70 μm using a Vibratome (1000Plus Sectioning System, IntraCel). Sections were collected into 1X PBS in a 24-well plate and immunolabelled as floating sections.

2.2.2.3 Immunolabelling of wholemounts

Samples were initially washed with 10% [v/v] serum-free block (DAKO) in 1X PBT or in 1X PBT for 1 h at 4ºC to permeabilise the tissue and enhance antibody penetration, whereby the blocking reagent was used to prevent non-specific binding of secondary antibodies to the sample. After blocking, the primary antibodies (see **Table 2.4** for full list) were diluted in 1X PBT and applied to samples overnight at 4°C. The antibody solution was removed and slides were washed 5 times with 1X PBT for 1 h each at 4ºC. Secondary antibodies raised against the host species primary antibody were diluted 1:200 in 1X PBT (see **Table 2.4** for primary antibody host species). Samples were incubated with secondary antibody solution overnight at 4°C in the dark to protect the fluorophores. Samples were washed 5 times with 1X PBS for 1 h each and then post-fixed for 10 min with 4% formaldehyde (both at 4ºC). Tissue was then flatmounted into 'pockets' on a glass slide, which were prepared as follows: two layers of black electrical tape were stuck onto the glass slide and using a scalpel, pockets of an appropriate size were cut. For thick samples, I used 3 layers of tape. Samples were then placed inside these pockets and mounted using the SlowFade kit (ThermoFisher Scientific).

2.2.2.4 Immunolabelling of floating sections

Samples were blocked and immunolabelled as described for wholemount samples. PBT washes were instead performed 3 times for 15 min each. Prior to post-fixation, sections were counterstained with 0.02% (v/v) 4',6-diamidino-2-phenylindole dihydrochloride (DAPI, Sigma Aldrich) in PBS for 1 min at RT in the dark to visualise cell nuclei. Sections were post-fixed for 5 mins with 4%

formaldehyde at 4ºC, transferred to glass microscope slides, gently dehydrated then mounted using 90% (v/v) glycerol in distilled water.

2.2.2.5 Immunolabelling of cryosections

Slides were initially washed with 1X PBS to remove OCT. Using a PAP-PEN (Daido Sangyo), a hydrophobic barrier was drawn around the tissue sections, which prevents loss of staining solution. Cryosections were blocked, immunolabelled, counterstained and post-fixed as described for floating sections. Sections were then mounted using Mowiol solution. Mowiol solution was made by incubating 6 g of glycogen and 2.4 g of Mowiol 4-88 (Calbiochem) in 6 ml of distilled water for 2 h at RT and then adding 12 ml of 0.2 M Tris, pH 8.5, and 2.5% (w/v) DABCO (1,4-diazabicyclo-[2.2.2]octane, Sigma), and incubating for several hours at 55°C until dissolved.

2.2.2.6 BrdU labelling

To analyse cell proliferation *in vivo*, bromodeoxyuridine (BrdU, Sigma Aldrich) was injected into mice. BrdU is a synthetic analogue of thymidine and thus becomes incorporated into DNA in dividing cells. Pregnant females were injected intraperitoneally with 300 mg/kg of BrdU (10 mg/ml) and culled at the required time after injection. Immunostaining for BrdU was carried out as described in **2.2.2.4** and **2.2.2.5**. However, the BrdU antibody can only access BrdU after DNA has been denatured. Therefore, staining for BrdU first included a denaturation step, which constituted serial incubations of tissue sections with 1 M HCl for 10 min at room temperature, followed by 2 M HCl for 10 min at RT and then 10 min at 37°C. Subsequently, the acid was neutralised by incubating samples in 0.1M sodium tetraborate buffer (pH 8.5) for 10 min at RT. The denaturation step is damaging for many epitopes and thus immunolabelling for other markers was performed first, followed by the acid treatment and then the BrdU antibody staining.

Table 2.4 Primary antibody parameters for immunolabelling.

Primary Antibody	Company	Dilution	Species	Secondary Antibody	Blocking Solution
IB4	Sigma Aldrich	1:250	n/a (biotinylated)	streptavidin	PBT only
anti-BrdU	Abcam	1:250	rat	goat anti-rat	PBT only
anti-cleaved CASPASE 3	Cell Signalling	1:200	rabbit	goat anti-rabbit	10% NGS in PBT
anti-GLUT1	Millipore	1:200	rabbit	goat anti-rabbit	PBT only
anti-Ki67	BD Biosciences	1:100	mouse	goat anti-mouse	10% Dako in PBT
anti-LAMA1	Sigma Aldrich	1:30	rabbit	goat anti-rabbit	PBT only
anti-NRP2	R&D Systems	1:100	goat	FAB anti-goat	10% Dako in PBT
anti-pHH3	Millipore	1:400	rabbit	goat anti-rabbit	PBT only
anti-VEGFR2	R&D Systems	1:200	goat	FAB anti-goat	10% Dako in PBT
anti-RC2	DSHB	1:10	mouse IgM	goat anti-mouse IgM	PBT only
anti-RFP	MBL	1:500	rabbit	goat anti-rabbit	10% NGS in PBT
anti-SOX2	Millipore	1:200	rabbit	goat anti-rabbit	PBT only
anti-TUJ1	Covance	1:250	rabbit	goat anti-rabbit	PBT only

2.2.3 Imaging

Fluorescently labelled samples were imaged using an LSM710 laser scanning confocal microscopes (Zeiss). Images were processed with ImageJ (NIH) and Adobe Photoshop CS6 (AdobeSystems, Inc.).

2.2.4 Analysis of immunolabelling

The levels of angiogenesis in each sample were determined by quantifying $IB4^+$ tip cells in two 0.2 mm^2 areas per hindbrain hemisegment following wholemount immunolabelling. The number of mitotic NPCs was defined similarly from 0.25 mm^2 sample areas. Vascular coverage of the hindbrain germinal zone was calculated by determining the percentage of the germinal zone area occupied by $IB4^+$ blood vessels in 70 μm floating sections. The germinal zone was delineated by the basal boundary of $BrdU^+$ cells following a 1 h pulse and the ventricular surface. The depth of the germinal zone was calculated by taking the average of the distances between the basal boundary of the germinal zone and the ventricular surface at peri-midline, medial and lateral positions per hindbrain segment. Average values from each hindbrain segment were then averaged again to obtain the germinal zone depth for that embryo. The number of apoptotic cells was defined by counting cleaved caspase-3^+ cells in five 10 μm hindbrain cryosections per embryo. The number of cycling NPCs was determined by quantifying the percentage of $Ki67^+$ $BrdU^+$ cells amongst all $BrdU^+$ cells from three cryosections sections per embryo. The rate of neuronal differentiation in the hindbrain was defined by quantifying the percentage of the $DAPI^+$ area occupied by $TUJ1^+$ immunolabelling in three cryosections per embryo using ImageJ. Similarly, the level of neural GLUT1 expression (i.e. CNS hypoxia) was determined by quantifying the percentage of the $DAPI^+$ area occupied by GLUT1 immunolabelling and then subtracting the $IB4^+$ $GLUT1^+$ area to exclude vascular GLUT1 expression in the BBB.

2.2.5 3-dimensional data visualisation

3D volume reconstructions were generated from z stacks acquired from laser scanning confocal microscopy using Imaris software (Bitplane).

2.2.6 Fluorescence-activated cell sorting (FACS)

Tissues were isolated and homogenised in ice-cold FACS buffer composed of RPMI1640 medium (Life Technologies) containing 2.5% (v/v) FBS, 2.38 g/L HEPES and 1.5 g/L sodium hydrogen carbonate. Thus, embryonic tissue was homogenised by repeated passing through a 21 G needle syringe with RPMI buffer and then a 23 G needle syringe. To generate single cell suspensions, homogenates were passed through a 40 μm filter. Cell cycle analysis was based on a previously defined protocol (Goodell et al., 1996). Briefly, cell suspensions were incubated with 10 μg/ml Hoechst 33342 (Sigma Aldrich) in FACS buffer for 30 mins at 37ºC in the dark. Cell suspensions were then spun at 5000 rpm at 4 ºC for 5 mins and Hoechst-containing FACS buffer was aspirated. The cell pellet was then resuspended in FACS buffer containing 0.5% (v/v) 0.5 mg/ml Fc block (BD Pharmingen) for 5 mins at room temperature with agitation, to prevent non-specific antibody binding. Fluorochrome-conjugated primary antibodies were then added to single cell suspensions (see **Table 2.5** for details of antibodies used). Labelled cells were analysed with a BD FACSAria III (BD Biosciences). Dead and non-singlet cells were sorted out by analysing forward and side scatter patterns whilst samples from unstained, single antibody and fluorescence-minus-one controls were used to identify appropriate fluorescence voltage and gate parameters (Tung et al., 2007). Fluorescence-minus-one controls were samples labelled with all but one antibody, which were then compared to a sample that was only labelled with the missing antibody from the FMO. Comparison of FACS dot plots between the FMO and single antibody control helped exclude signal from other fluorescently conjugated antibodies that may cross over into the detection channel. Sorted cells were analysed using FACS DIVA software (BD Biosciences).

Table 2.5 Primary antibody parameters for FACS.

Primary Antibody	Manufacturer	Dilution	Fluorochrome
CD11b (ITGAM)	BD Pharmingen	2 µl per 10^6 cells	PerCp Cy5.5
CD31 (PECAM)	BD Pharmingen	4 µl per 10^6 cells	APC
CD133 (PROM-1)	Miltenyi Biotec	7 µl per 10^6 cells	PE
CD56 (NCAM)	R&D Biosystems	4 µl per 10^6 cells	Alexa Fluor 488

2.2.7 qRT-PCR

All solutions were maintained RNAse free by using fresh filtered pipette tips and autoclaved 1.5ml tubes. In addition, RNase-free PBS was used for dissecting hindbrains whilst forceps were washed in a solution of 3% H_2O_2 for 1 min prior to use to eliminate possible RNase contamination. H_2O_2 was rinsed off forceps with RNase-free water.

2.2.7.1 RNA extraction

Total RNA was extracted from samples using the RNeasy Micro kit (Qiagen) according to the manufacturer's instructions. Briefly, tissue samples were homogenised with a 23 G needle syringe in 350 µl of RLT lysis buffer containing 10 µl/ml β-mercaptoethanol. An equal volume of 70% (v/v) ethanol was added to lysates and solutions were transferred to individual spin columns. RNA was transferred to membranes by centrifuging columns at 8500 rpm for 15 s. Subsequently, membrane-bound RNA was washed with 350 µl of RW1 buffer. Genomic DNA was removed by digestion with DNase 1 solution for 15 min at RT and a subsequent wash with 350 µl of RW1 buffer. Membrane-bound RNA was first washed with 500 µl of RPE buffer and then 80% (v/v) ethanol. Finally, RNA was eluted in 14 µl of RNAse free water.

2.2.7.2 Reverse transcription

First strand cDNA synthesis was performed using the SuperScript Transcriptase III kit (Invitrogen). For each reaction 500 ng to 1 µg of RNA, 250 ng of random primers and 1 µl of 10 mM dNTPs were mixed and the volume was adjusted to 13 µl with water. The mixtures were heated to 65°C for 5 min and chilled on ice for 1 min. 4 µl of 5X First-Strand Buffer, 1 µl of 0.1 M DTT, 1 µl of RNaseOUT and 1 µl of SuperScript III polymerase (200 units/µl) were added to each sample. Subsequently, samples were incubated sequentially for 10 min at 25°C, 50 min at 42°C and 10 min at 70°C. Finally, cDNA quality and concentration were determined using a NanoDrop 1000 spectrometer (Thermo Scientific). Unless qPCR reactions were performed immediately, cDNA was stored at -20°C.

2.2.7.3 Quantitative Real Time PCR (qRT-PCR)

qRT-PCR was performed on a 96-well plate using a 7900HT Fast Real-Time PCR System (Applied Biosystems). For each reaction 12.5 µl of Power SYBR Green PCR Master Mix (Applied Biosystems) were added to 250 ng of cDNA solution and 1.5 µM of the forward and reverse oligonucleotide primer, which were designed using the Primer3 software (Howard Hughes Medical Institute) and synthesised to order by Sigma Aldrich (see **Table 2.6**). For each gene, the reaction was performed in triplicate, and for each primer pair a no template control was included. Alternatively, qRT-PCR was performed on a 96-well RT^2 Profiler PCR Array plate ('Mouse Neurogenesis' Array, Qiagen; see **Table 2.7**). For each plate, 600 ng of cDNA (at a volume of 102 µl) from three embryos was pooled and added to 1350 µl of RT^2 SYBR Green Mastermix (Qiagen) and 1248 µl RNAse free-water, and the resulting solution was split equally amongst the wells.

After a 10 min enzyme activation step at 95°C, 40 PCR cycles consisting of a 15 s denaturation step at 95°C followed by an annealing and extension step at 60°C for 1 min were carried out. Data was collected using the Sequence Detector Software (SDS version 2.4; Applied Biosystems) and the presence of primer dimer formation was excluded by examining dissociation curves and DNA amplification in no template controls. Expression levels were extrapolated from PCR data using DART-PCR software (Peirson et al., 2003) and normalised using *Actb* expression as a reference. Final data was presented as a fold change from control samples. Alternatively, expression values for genes examined using the RT^2 Profiler PCR Array plate were calculated manually using online Qiagen expression analysis software and normalised using *Hsp90ab1* expression as a reference.

Table 2.6 Oligonucleotide primers designed for qRT-PCR.

Gene	Primer	Sequence	Amplicon size (bp)
Actb	Actb-F	5'-AAGGCCAACCGTGAAAAGAT-3'	110
	Actb-R	5'-GTGGTACGACCAGAGGCATAC-3'	
Bdnf	Bdnf-F	5'-CGACATCACTGGCTGACACT-3'	162
	Bdnf-R	5'-GCAGAAAGAGTAGAGGAGGCTC-3'	
Ccnd1	Ccnd1-F	5'-AAGCTCAAGTGGAACCTGGC-3'	166
	Ccnd1-R	5'-CATTTCCAACCCACCCTCCA-3'	
Dll1	Dll1-F	5'-CTCTGTGTTCTGCCGACCTC-3'	168
	Dll1-R	5'-TTGCACTCCCCTGGTTTGTC-3'	
Hif1a	Hif1a-F	5'-AAACCACCCATGACGTGCTT-3'	182
	Hif1a-R	5'-GAGCGGCCCAAAAGTTCTTC-3'	
Jag1	Jag1-F	5'-CTTTGCTGGTGGAGGCCTG-3'	169
	Jag1-R	5'-TCATCACAGGTCACTCGGATC-3'	
Jag2	Jag2-F	5'-AACTCCTTCTACCTGCCGC-3'	165
	Jag2-R	5'-GGTGTCATTGTCCCAGTCCC-3'	
Kdr	Kdr-F	5'-TCACCGAGAACAAGAACAAA-3'	190
	Kdr-R	5'-TCCTATATCCTACAACCACAA-3'	
Nos1	Nos1-F	5'-CGCCAAAACCTGCAAAGTCC-3'	160
	Nos1-R	5'-CCTCCAGCCGTTCAATGAGT-3'	
Nos3	Nos3-F	5'-AAGGTGATGAGCTCTGTGGC-3'	166
	Nos3-R	5'- GTACTCAGCCGGTACCTCTG-3'	
Ntf3	Ntf3-F	5'-CCACCAGGTCAGAGTTCCAG-3'	150
	Ntf3-R	5'-GGTTGCCCACATAATCCTCCA-3'	
Serpinf1	Serpinf1-F	5'-CGAGAAAGACGACCCTCCAG-3'	191
	SerpinF1-R	5'-CAAGTTCTGGGTCACGGTCA-3'	
Vegfa	Vegfa-F	5'-CAGATCATGCGGATCAA-3'	100
	Vegfa-R	5'-TTGTTCTGTCTTTCTTTG-3'	

Table 2.7 Genes tested for in Qiagen RT^2 Profiler PCR Array (Neurogenesis).

Gene	Description
Ache	Acetylcholinesterase
Adora1	Adenosine A1 receptor
Adora2a	Adenosine A2a receptor
Alk	Anaplastic lymphoma kinase
Apbb1	Amyloid beta (A4) precursor protein-binding, family B, member 1
Apoe	Apolipoprotein E
App	Amyloid beta (A4) precursor protein
Artn	Artemin
Ascl1	Achaete-scute complex homolog 1 (Drosophila)
Bcl2	B-cell leukemia/lymphoma 2
Bdnf	Brain derived neurotrophic factor
Bmp2	Bone morphogenetic protein 2
Bmp4	Bone morphogenetic protein 4
Bmp8b	Bone morphogenetic protein 8b
Cdk5r1	Cyclin-dependent kinase 5, regulatory subunit 1
Cdk5rap2	CDK5 regulatory subunit associated protein 2
Chrm2	Cholinergic receptor, muscarinic 2, cardiac
Creb1	CAMP responsive element binding protein 1
Cxcl1	Chemokine (C-X-C motif) ligand 1
Dcx	Doublecortin
Dlg4	Discs, large homolog 4 (Drosophila)
Dll1	Delta-like 1 (Drosophila)
Drd2	Dopamine receptor D2
Dvl3	Dishevelled 3, dsh homolog (Drosophila)
Efnb1	Ephrin B1
Egf	Epidermal growth factor
Ep300	E1A binding protein p300
Erbb2	V-erb-b2 erythroblastic leukemia viral oncogene homolog 2, neuro/glioblastoma derived oncogene homolog (avian)
Fgf2	Fibroblast growth factor 2
Flna	Filamin, alpha
Gdnf	Glial cell line derived neurotrophic factor
Gpi1	Glucose phosphate isomerase 1
Grin1	Glutamate receptor, ionotropic, NMDA1 (zeta 1)
Hdac4	Histone deacetylase 4
Hes1	Hairy and enhancer of split 1 (Drosophila)
Hey1	Hairy/enhancer-of-split related with YRPW motif 1
Hey2	Hairy/enhancer-of-split related with YRPW motif 2
Heyl	Hairy/enhancer-of-split related with YRPW motif-like
Il3	Interleukin 3
Mdk	Midkine
Mef2c	Myocyte enhancer factor 2C
Mll1	Myeloid/lymphoid or mixed-lineage leukemia 1
Mtap2	Microtubule-associated protein 2
Ndn	Necdin
Ndp	Norrie disease (pseudoglioma) (human)
Neurod1	Neurogenic differentiation 1
Neurog1	Neurogenin 1
Neurog2	Neurogenin 2
Nf1	Neurofibromatosis 1
Nog	Noggin
Notch1	Notch gene homolog 1 (Drosophila)
Notch2	Notch gene homolog 2 (Drosophila)

Nr2e3	Nuclear receptor subfamily 2, group E, member 3
Nrcam	Neuron-glia-CAM-related cell adhesion molecule
Nrg1	Neuregulin 1
Nrp1	Neuropilin 1
Nrp2	Neuropilin 2
Ntf3	Neurotrophin 3
Ntn1	Netrin 1
Odz1	Odd Oz/ten-m homolog 1 (Drosophila)
Olig2	Oligodendrocyte transcription factor 2
Pafah1b1	Platelet-activating factor acetylhydrolase, isoform 1b, subunit 1
Pard3	Par-3 (partitioning defective 3) homolog (C. elegans)
Pax3	Paired box gene 3
Pax5	Paired box gene 5
Pax6	Paired box gene 6

Pou3f3	POU domain, class 3, transcription factor 3
Pou4f1	POU domain, class 4, transcription factor 1
Ptn	Pleiotrophin
Rac1	RAS-related C3 botulinum substrate 1
Robo1	Roundabout homolog 1 (Drosophila)
Rtn4	Reticulon 4
S100a6	S100 calcium binding protein A6 (calcyclin)
S100b	S100 protein, beta polypeptide, neural
Shh	Sonic hedgehog
Slit2	Slit homolog 2 (Drosophila)
Sod1	Superoxide dismutase 1, soluble
Sox2	SRY-box containing gene 2
Sox3	SRY-box containing gene 3
Stat3	Signal transducer and activator of transcription 3

Tgfb1	Transforming growth factor, beta 1
Th	Tyrosine hydroxylase
Tnr	Tenascin R
Vegfa	Vascular endothelial growth factor A
Actb	Actin, beta
B2m	Beta-2 microglobulin
Gapdh	Glyceraldehyde-3-phosphate dehydrogenase
Gusb	Glucuronidase, beta
Hsp90ab1	Heat shock protein 90 alpha (cytosolic), class B member 1
MGDC	Mouse Genomic DNA Contamination
RTC	Reverse Transcription Control
RTC	Reverse Transcription Control
RTC	Reverse Transcription Control
PPC	Positive PCR Control
PPC	Positive PCR Control
PPC	Positive PCR Control

2.2.8 Neurosphere culture

2.2.8.1 Neurosphere derivation

Hindbrains were dissected from e10.5 embryos and placed briefly in ice-cold 'N2 media' composed of DMEM:F12 with L-glutamine and HEPES, 1% (v/v) N2 supplement (both Gibco) and 1% (v/v) Penicillin/Streptomycin (Thermo Fisher). In order to dissociate neural progenitor cells and produce a single-cell suspension, hindbrains were then transferred to 'dissociation media' composed of N2 media containing 1mg/ml Collagenase/Dispase (Roche) and 0.5mg/ml DNase (Sigma). Hindbrains were incubated in dissociation media at 37ºC for 30 min, shaking once after 15 min. Hindbrains were triturated by passing 20 times each sequentially through P1000 and P200 filter pipette tips and a 10 µl sample was checked with a haemocytometer to confirm that a single cell suspension had been achieved. Single cell suspensions of dissociated hindbrains were then centrifuged at 4000 rpm at room temperature for 5 min and all dissociation media was aspirated. Cell pellets were resuspended in 500 µl 'neurosphere media' composed of N2 media containing 2% (v/v) B27 supplement (Gibco), bFGF and EGF (both 20ng/ml, RnD Systems). $5x10^4$ cells were plated into a total volume of 500 µl neurosphere media in a 24-well plate (Corning) and incubated at 37ºC/4% CO_2 overnight. 200 µl of neurosphere media was replaced with fresh neurosphere media at 37ºC the following morning, and then 250 µl neurosphere media was replaced every three days thereafter. Neurosphere cultures were continually incubated at 37ºC/4% CO_2 for the duration of their time *in vitro*.

2.2.8.2 Passaging of neurospheres

Neurosphere cultures were monitored every other day to check for the presence of floating spheres of expanded neural stem and progenitor cells. Small neurospheres appeared after 2-3 days *in vitro* (DIV) and had grown large enough to passage after 7 DIV. The contents of each well were transferred to 2 ml round-bottomed tubes and centrifuged at 4000 rpm at room temperature for 5 min. Neurosphere media was aspirated and cell pellets were resuspended with TrypLE Select (Gibco) and incubated at 37ºC for 30 min to dissociate neurospheres. A 10 µl

sample was checked with a haemocytometer to confirm that a single cell suspension had been achieved. Single cell suspensions of dissociated hindbrains were then centrifuged at 4000 rpm at room temperature for 5 min and all TrypLE Select was aspirated. Cell pellets were resuspended in 500 µl neurosphere media and plated and nourished with fresh neurosphere media as previously mentioned. Neurosphere cultures were only maintained for 14DIV and for one passage. After 14 DIV, neurospheres and media were centrifuged at 13000 rpm for 5 mins at 4ºC. All neurosphere media was aspirated and cell pellets were resuspended in RLT lysis buffer containing 10 µl/ml β-mercaptoethanol for subsequent RNA extraction (see **2.2.7.1**).

2.2.9 Statistics

Results are expressed as mean ± standard deviation unless specified. For all statistical analyses, I used a 2-tailed, unpaired Student's *t* test. *P* values of less than 0.05 were considered significant. I used the following abbreviations to refer to whether two discrete data sets were significantly different from one another: (not significant) ns: $P \geq 0.05$; (significant) *: $P < 0.05$, **: $P < 0.01$, *** $P < 0.001$.

In almost all cases, at least three animals were used in comparative studies to be able to perform Student's *t* tests. The number of embryos analysed in each individual experiment are listed in **Table 8.2**.

Chapter 3 EMBRYONIC NEURAL PROGENITOR CELLS IN THE MOUSE HINDBRAIN RESIDE WITHIN A VASCULAR NICHE

3.1 Introduction

Both the cytoarchitecture and lamination of the developing cortex in the rodent brain are relatively well defined. At the apical surface, the neuroepithelium interfaces with the fluid-filled ventricle, whilst at the basal surface, the neuroepithelium is separated from the mesenchyme by the basement membrane in the form of the meninges. The VZ and SVZ at the apical surface contain NPCs passing through INM and the cell cycle, thus generating additional progenitor cells, as well as immature neurons. These neurons then pass through the intermediate and marginal zones, before settling in their final destination in the cortical plate on the pial side. The ventricular lumen and pial basement membrane are key sources of signals to regulate NPC behaviour (for example, Lehtinen et al., 2011, Loulier et al., 2009). In addition, niche signals targeted to specific NPC populations emanate from other cell types within the neuroepithelium, such as from post-mitotic neurons, other NPC classes, microglia as well as from blood vessels in the forebrain (Lakoma et al., 2011, Yoon et al., 2008, Cunningham et al., 2013, Tan et al., 2016).

Whilst the emergence and function of these different niche components have been characterised reasonably well during CNS development, the spatiotemporal relationship of blood vessels with NPCs is still poorly defined. Whilst BPs of the developing forebrain are positioned and divide in close proximity to cerebrovasculature (Javaherian and Kriegstein, 2009), it has not been determined how vessels map spatially around cycling NPCs and whether vessels organise similarly around other NPC subtypes elsewhere in the CNS. During the course of my studies, characterisation of forebrain vascularisation by another group indicated that blood vessels begin to occupy the CNS mid-way through gestation (Lange et al., 2016). Yet it was also not established whether the peak phases of both angiogenesis and neurogenesis correlate with each other temporally.

I have used the mouse hindbrain as a model system to study the timing and spatial spatial patterning of vascularisation in the embryonic mammalian brain. The hindbrain is ideally suited to this task, as flatmount preparations allow simultaneous and organ-wide visualisation of both blood vessels and NPCs alongside each other (

Figure 3.2). Furthermore, previous work in my laboratory has characterised the pattern of blood vessel growth extensively in the hindbrain (see **1.4**; **Figure 3.1**), and a variety of mouse mutants are available that alter hindbrain vascularisation (Fantin et al., 2013b, Ruhrberg et al., 2002, Fantin et al., 2013a). Finally, the process of neurogenesis in the developing mouse hindbrain is fairly understudied in this part of the mammalian CNS, with very little known about hindbrain NPCs. This is of particular interest given that hindbrain architecture is highly conserved amongst vertebrates, it being the evolutionarily oldest region of the brain (Lumsden and Krumlauf, 1996). The embryonic hindbrain represents the brainstem and cerebellar primordia, regulates core physiology and is innervated by several cranial nerves. Thus, use of the hindbrain as a model for studying embryonic neurogenesis will provide insight into the development of a core region in the CNS. I have therefore characterised the spatiotemporal relation of NPC mitosis and angiogenesis in the hindbrain (**Chapter 3**) and then gone on to examine how vascular disruption alters hindbrain neurogenesis (**Chapter 4** and **Chapter 5**).

3.2 Results

3.2.1 The mouse hindbrain as a model for simultaneous visualisation of embryonic neural progenitors and sprouting blood vessels

The embryonic mouse hindbrain possesses a well-characterised pattern of blood blood vessel growth (**Figure 3.1**) that can be visualized effectively by both wholemount and cross-sectional immunolabelling (

Figure 3.2; Fantin et al., 2013b). Additionally, and in contrast to the developing cortex, wholemount imaging of the embryonic hindbrain also permits interrogation of the entire vascular network and clear definition of the anatomical positioning of vessel plexi in the hindbrain parenchyma. Wholemount staining with endothelial cell-bound isolectin B4 and antibodies for the mitotic marker phospho-histone H3

(known hereafter as IB4 and pHH3, respectively) at the stage of e11.5/45 somite pairs (s) illustrates the striking spatial proximity between dividing cells in the hindbrain VZ and the underlying SVP (

Figure 3.2B; *en face* view as illustrated in far-right cartoon in

Figure 3.2A). As the $pHH3^+$ cells are located at the ventricular surface and express the NPC marker SOX2 (Aquino et al., 2008, Fantin et al., 2010), they are mitotic NPCs, as observed in other parts of the CNS, where mitotic cells in the VZ are almost always APs (Taverna et al., 2014, Haubensak et al., 2004) and express SOX2 (Aquino et al., 2008).

By mounting the hindbrain *en face* and employing laser scanning confocal microscopy for imaging, I observed that mitotic NPCs are located apically to the SVP, which is undergoing a rapid phase of vessel sprout fusion at 45s (

Figure 3.2B). 3-dimensional reconstructions of confocal z stacks illustrate this relationship well, in particular when these reconstructions were rotated by 90^o to achieve a *pseudo*-sagittal perspective of both $pHH3^+$ NPCs and $IB4^+$ endothelium (see middle and right-hand panels in

Figure 3.2B'). This perspective provides not only an excellent viewpoint of both cell populations, but also highlights the filopodia extending from endothelial cells up towards the ventricle and in between NPCs (right-hand panel in

Figure 3.2B'). These filopodia extend occasionally as far as the mitotic NPCs themselves and reflect the angiogenic response of endothelial cells to the high levels of progenitor-expressed VEGF-A emanating from the hindbrain VZ (Fantin et al., 2010, Ruhrberg et al., 2002). However, it is not presently known why blood vessel tip cells do not follow their filopodia to the ventricular surface.

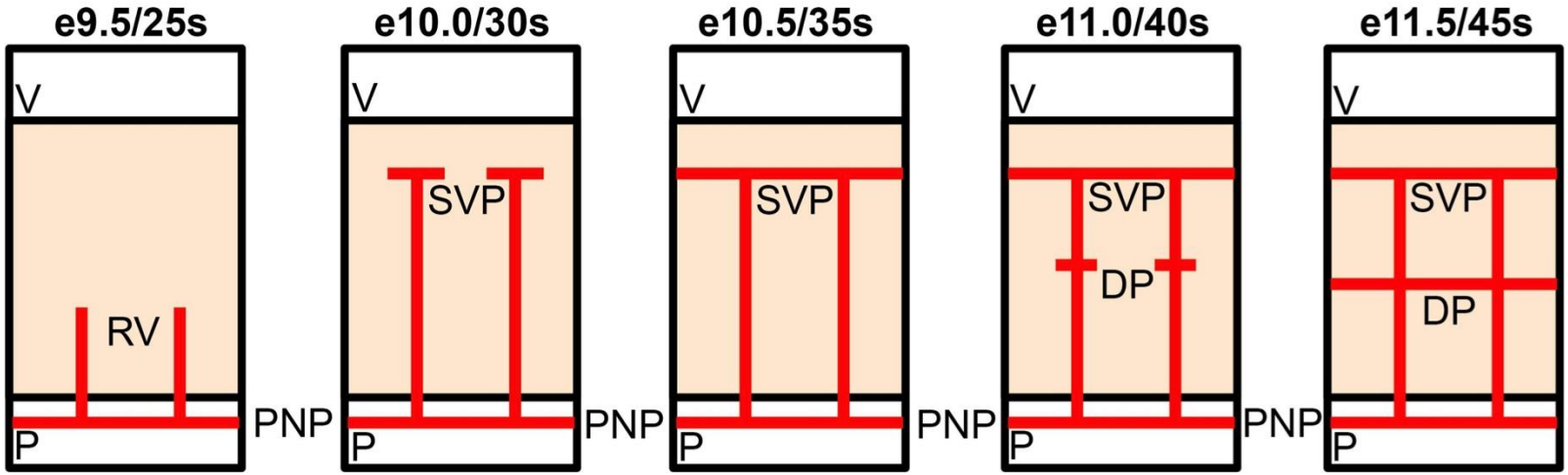

Figure 3.1 Temporal pattern of hindbrain vascularisation.

Schematic representation of hindbrain vascularisation from e9.5-e11.5 (25-45s) from a transverse perspective. Beige shaded box represents hindbrain neuroepithelium. Radial vessels sprout initially into the hindbrain from the PNP and sprout laterally near the ventricular surface to form the SVP. Later in development, a DP sprouts laterally from the radial vessels connecting with the SVP. Abbreviations: V, ventricle; P, pia; PNP, perineural vascular plexus; RV, radial vessels; SVP, subventricular vascular plexus; DP, deeper vascular plexus.

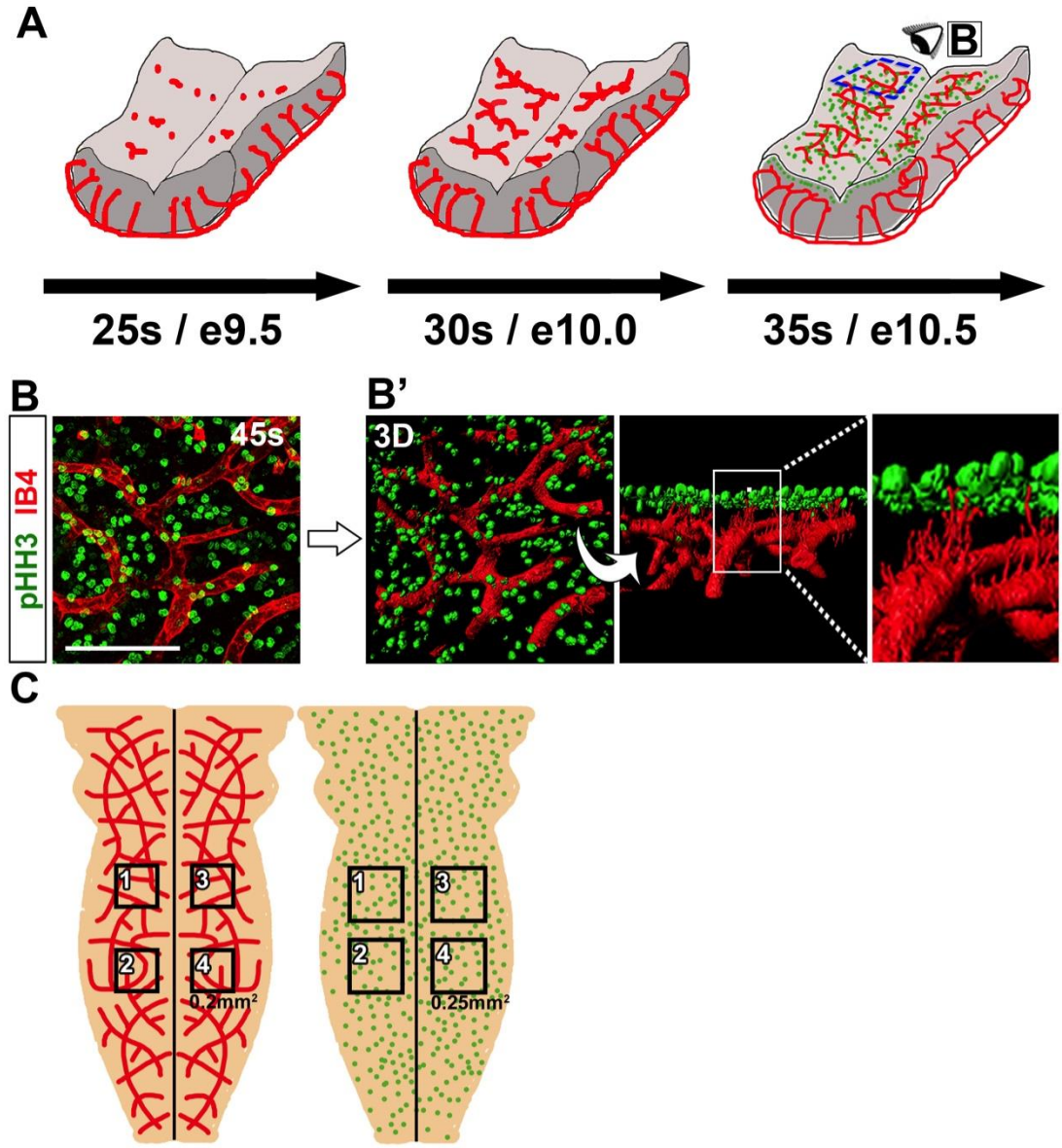

Figure 3.2 The mouse hindbrain as a model for simultaneous visualisation of NPCs and sprouting blood vessels.

(**A**) Schematic representation of flatmounted hindbrains at e9.5 and e10.0 (left and middle), as well as an e10.5 hindbrain (right) containing mitotic NPCs (green) and blood vessels (red). The blue box indicates the area imaged in (**B**), the eye illustrates the observer's point of view.

(**B,B'**) Maximal projection (xy) of a confocal z stack (**B**) through flatmounted 45s (e11.5) hindbrain after wholemount labelling with the dual vessel and microglia marker IB4 (red) and the mitotic marker pHH3 (green). Scale bar: 100 µm. 3D surface rendering (**B'**) illustrates the SVP beneath a layer of mitotic NPCs. 90°

rotation of the surface rendering in the left panel gives a *pseudo*-sagittal perspective of hindbrain NPCs and the SVP (show in middle panel). The higher magnification of the boxed area shows endothelial cell filopodia projecting between the mitotic NPCs towards the ventricular surface (right-hand panel).

(**C**) Schematic representation of sample areas used to determine angiogenesis (blood vessels shown in red) and NPC mitosis ($pHH3^+$ NPCs shown in green) following wholemount immunolabelling of the hindbrain (discussed in **2.2.4**).

3.2.2 NPC mitotic activity correlates well with hindbrain angiogenesis

Wholemount imaging of mitotic NPCs and cerebrovasculature in the mouse hindbrain demonstrated that both are positioned close to one another. However, this analysis did not address whether the development of each tissue occurs at similar time points in the developing rodent brain. I therefore carried out extensive characterisation of the time course of both sprouting angiogenesis and NPC cell division to determine when the two systems are most active (sampling strategy depicted in **Figure 3.1C**).

By labelling with IB4, I was able to observe blood vessel sprouts, identified by the presence of elongated $IB4^+$ tip cells with filopodial extensions, as well as tissue resident macrophages identified as single $IB4^+$ cells in the parenchyma, often in close proximity to blood vessels (**Figure 3.3A;** white and black arrowheads, respectively). Both blood vessels and macrophages were present in the hindbrain from as early as e9.5/25s onwards. However, I observed very few vessel sprouts at this stage (far-left panel in **Figure 3.3A**; **Figure 3.3B** e9.5/25s: 2±1.75 vessel sprouts/0.2mm^2). Half a day further into development, a surge in angiogenesis takes place in the hindbrain, with the number of vessel sprouts increasing over 12-fold as radial vessels begin to sprout laterally (**Figure 3.3B** e10.0/25s: 24.75±4.2 vessel sprouts/0.2mm^2) (Fantin et al., 2010). By e10.5/35s, vessel sprouting peaks as the nascent SVP extends laterally to cover the surface of the hindbrain (second-left panel in **Figure 3.3A**; **Figure 3.3B** e10.5/35s: 27.7±3.1 vessel sprouts/0.2mm^2). Thereafter, levels of sprouting subside when hindbrain blood vessels begin fusing with one another. Thus, the number of vessel sprouts has dropped off at e11.5/45s (**Figure 3.3B** e11.0/40s: 19.2±3.6 vessel sprouts/0.2mm^2; e11.5/45s: 15.8±2.8 vessel sprouts/0.2mm^2) as macrophages help to connect vessel sprouts for anastomosis (see a macrophage bridging two endothelial tip cells, labelled with black arrowhead in far-right panel of **Figure 3.3A**). Finally, vessel sprouting is negligible at e12.5/50s (**Figure 3.3B** e12.5/50s: 3.6±2.0 vessel sprouts/0.2mm^2) when the SVP remodels and matures (note the larger vessel calibre in the far-right panel of **Figure 3.3A**, compared to vessels in other panels).

Quantification of $pHH3^+$ NPCs in embryos from the CD1 genetic background revealed a similarly staged time course (**Figure 3.4**). Accordingly, the density of mitotic NPCs in the hindbrain VZ increases steadily from e9.5/25s (**Figure 3.4A,B**, e9.5/25s: 127±5.7 $pHH3^+$ VZ cells/0.25mm^2) in mice in the outbred, CD1 genetic background. In CD1 mice, the number of mitotic NPCs peak sharply at e11.0/40s **(Figure 3.4A,B** e11.0/25s: 219±5.8 $pHH3^+$ VZ cells/0.25mm^2). Mitosis in the hindbrain VZ subsequently declines rapidly thereafter, with rare cell divisions observed at e13.5/53s (**Figure 3.4B** e13.5/53s: 16±3.1 $pHH3^+$ VZ cells/0.25mm^2). Embryos in the inbred, C57BL/6 genetic background follow a similar pattern, although the peak in NPC mitosis occurs slightly earlier and is less sharp (**Figure 3.4C** e10.75/37s: 209±6.0 $pHH3^+$ VZ cells/0.25mm^2). The entire time course of NPC cell division therefore overlaps temporally with the period of hindbrain angiogenesis. Therefore, mitotic NPCs are, unsurprisingly, present in the hindbrain VZ prior to the initial radial vessel ingression as they populate the initial neuroepithelium across the developing CNS, as well as attract vessel ingression from the PNP by secreting pro-angiogenic VEGF-A (Ruhrberg et al., 2002). These findings further support the choice of the hindbrain as a suitable model for examining the possible role of blood vessels and/or vascular cues in embryonic neurogenesis.

Phosphorylation of histone H3 begins during prophase, spreads through the whole chromosomes and is completed by early metaphase and maintained until anaphase (Hans and Dimitrov, 2001). Dephosphorylation of histone H3 typically begins in anaphase and ends in early telophase, correlating with chromosome segregation (Hans and Dimitrov, 2001). Immunolabelling for the mitotic marker $pHH3^+$ distinguishes bright, mononuclear cells (wavy arrow in far-right panel of **Figure 3.4A**), corresponding to pre-anaphase VZ NPCs and dimmer, binuclear figures (arrow in far-right panel of **Figure 3.4A**), corresponding to mitotic NPCs between anaphase and telophase. I was therefore able to identify cells within distinct phases of mitosis by labelling only one antigen. In subsequent experiments, I therefore quantified the total cohort of mitotic NPCs as the sum of pre-anaphase and anaphase figures (the latter are depicted as red data points in **Figure 3.4B,C**). The time course of anaphase VZ cells is in good synchrony with that of all mitotic cells,

suggesting the speed of transition to anaphase is fairly constant across the period examined.

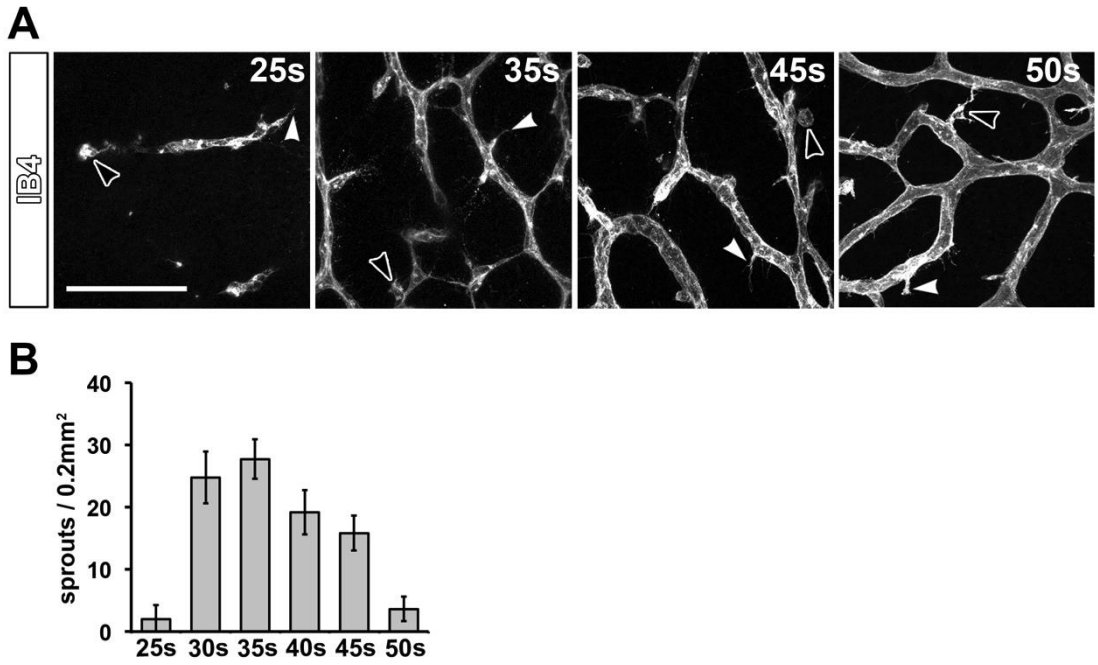

Figure 3.3 The temporal pattern of hindbrain angiogenesis.

(A-B) Time course of angiogenic vessel sprouting in the hindbrain. Maximal projection (xy) of confocal z stacks through flatmounted hindbrains at the indicated stages of the SVP after wholemount IB4 labelling (**A**) with accompanying quantification of vessel sprouts (see **2.2.4**; **B**) Scale bar: 100 μm. In (**A**), examples of tip cells at the front of vessel sprouts are indicated with arrowheads, examples of microglia with open arrowheads. Data are shown as mean ± standard deviation of the mean; n≥3 for each time point.

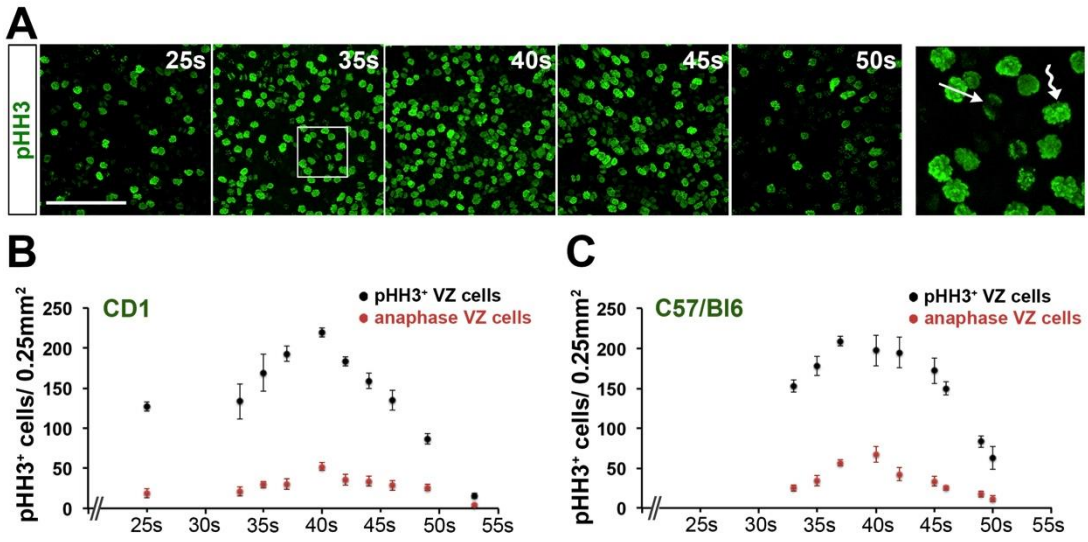

Figure 3.4 The temporal pattern hindbrain NPC mitosis.

(A-C) Time course of NPC proliferation in the hindbrain. Maximal projection (xy) of confocal z stacks through flatmounted hindbrains at the indicated stages after wholemount pHH3 staining (**A**) with accompanying quantification of mitotic and anaphase NPCs in the CD1 and C57BL6 backgrounds (**B,C**; see **2.2.4**). Scale bar: 100 µm. In (**A**), the boxed area is shown at higher magnification on the right to illustrate strongly labelled pre-anaphase NPCs (wavy arrow) and dimly labelled anaphase NPCs (arrow). Data are shown as mean ± standard deviation of the mean; n≥3 for each time point.

3.2.3 The hindbrain germinal zone (GZ) is well-vascularised

Although 3D-reconstruction of confocal micrographs from pHH3- and IB4-labelled labelled hindbrains permitted *pseudo*-sagittal observation of hindbrain NPCs in mitosis (see

Figure 3.2B'), it did not provide information on NPCs in INM. Thus, I labelled NPCs undergoing DNA replication during S-phase by injecting pregnant females with 300 mg kg^{-1} of the thymidine analogue BrdU 1 h prior to collecting embryos. I then cut transverse sections through the hindbrain across the main period of angiogenesis, from 25-50s, and labelled S-phase and mitotic NPCs with antibodies for BrdU and pHH3, respectively (**Figure 3.5**). Thick vibratome sections were cut to ensure that the morphology of hindbrain vessel networks could be observed in a single confocal z stack.

The analysis of such sections confirmed that at 25s, the hindbrain is largely avascular, as demonstrated by sparse vessel sprouting near the VZ at this time point (**Figure 3.3A,B**). Only a few radial vessels ('RV' in the top-left panel in **Figure 3.5**) have begun sprouting perpendicular to the ventricular surface, where mitotic, $pHH3^+$ NPCs reside. These radial vessels pass through a pseudostratified layer of S-phase NPCs similar to that observed in the mouse embryonic forebrain and the developing chick hindbrain (Guthrie et al., 1991, Smart, 1972). This pseudostratified pattern of $BrdU^+$ NPCs is also maintained throughout the main time course of hindbrain NPC mitosis (all panels in **Figure 3.5**).

By 35s, radial vessels have sprouted parallel to the ventricular surface and span almost the entire width of the embryonic hindbrain as the SVP (see top-right panel in **Figure 3.5**). The SVP passes through the area containing mitotic and S-phase NPCs, which is referred to as the germinal zone ('GZ') hereafter. In confirmation, SVP establishment in the hindbrain GZ occurs directly prior to the peak in NPC mitosis elucidated by wholemount $pHH3^+$ immunolabelling (**Figure 3.4** and **Figure 3.5**). Thus, actively cycling hindbrain NPCs reside in direct proximity to the newly formed blood vessel plexus. This proximity is maintained as far as 50s, where the hindbrain GZ remains occupied by the SVP.

The SVP remodels extensively towards the end of the time course (see lower panels in **Figure 3.5**). Whilst this remodelling results in the vessel bed switching from a flat, 2-dimensional plexus to a more 3-dimensional network, the GZ remains occupied by the SVP and is arguably even more vascularised. A deeper plexus sprouts from radial vessels more basally to the SVP and forms later, typically during the eleventh day of gestation (see lower-left panel in **Figure 3.5** and upper-middle panel in **Figure 4.6A**). This deeper plexus forms directly below the most basal point of $BrdU^+$ NPCs undergoing INM and remains there until at least 50s. Thus, the positioning of both the SVP and deeper plexus indicate that the GZ is a well-vascularised compartment of the hindbrain neuroepithelium.

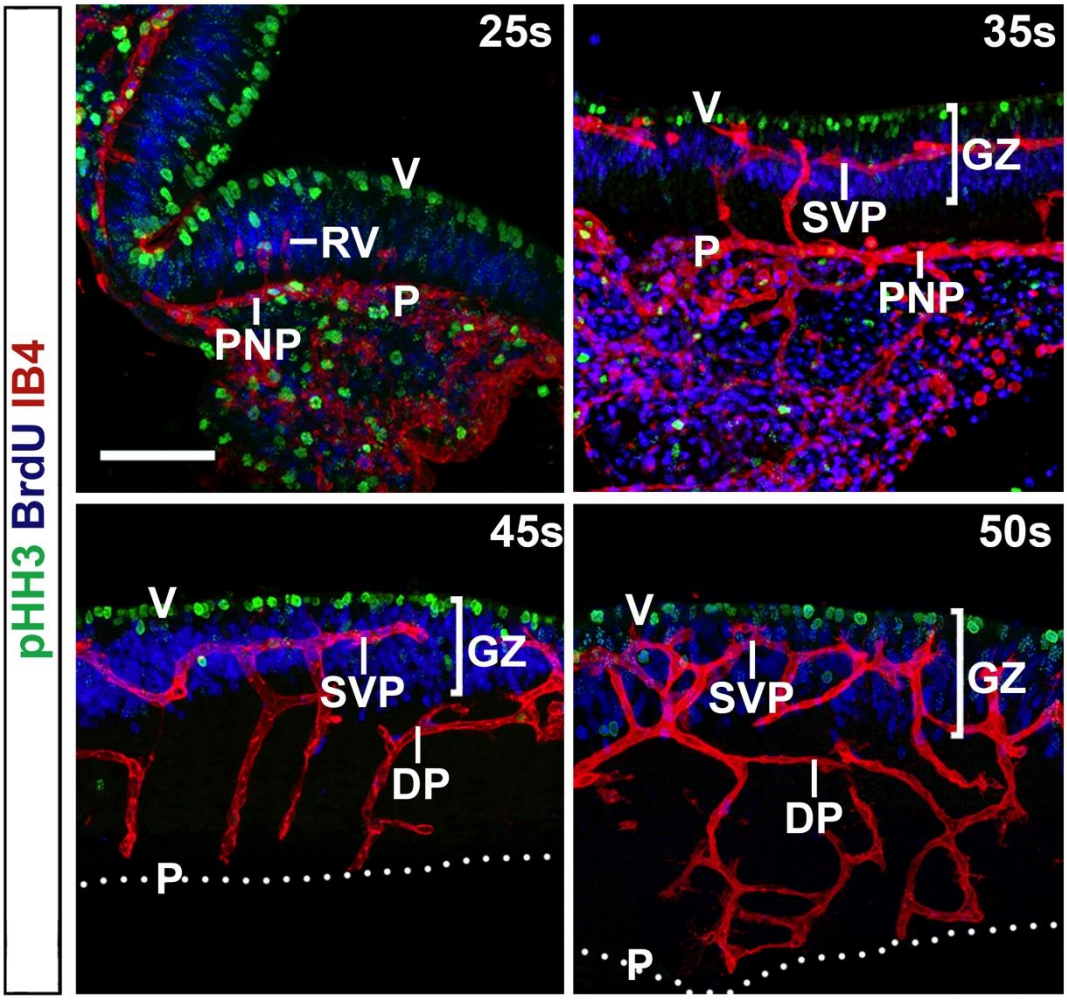

Figure 3.5 Spatial relationship of blood vessel growth and NPC proliferation in the hindbrain.

Confocal z stacks of 70 μm transverse sections of wild type hindbrains at the indicated stages after labelling with IB4 (red) together with antibodies for pHH3 (green) and BrdU (blue). Bracketed area denotes GZ containing mitotic ($pHH3^+$) and S-phase ($BrdU^+$) NPCs. Scale bar: 20 μm. Abbreviations: P, pial surface; V, ventricular surface; RV, radial vessel; SVP, subventricular vascular plexus; DP, deep plexus; PNP, perineural vascular plexus; GZ, germinal zone.

3.2.4 NPCs contact blood vessel plexi within and outside the hindbrain

Mammalian NPCs possess elongated processes that often terminate in endfeet. To investigate the morphologies of hindbrain NPC processes and examine their relationship with blood vessels in the hindbrain, I visualised processes by immunolabelling for an antigen of the intermediate filament nestin, which is found almost exclusively in neural cells, known as RC2. RC2 is used as a bonafide marker both embryonic NPCs and immature astrocytes (Misson et al., 1988). At 25s, when the hindbrain is largely avascular, RC2 labelling is only detectable in basal regions around the pial surface (far-left panel in **Figure 3.6A**; 25s, n = 2 embryos). The pattern of RC2 labelling appeared fibrous, similar to that observed in the mantle zone of the developing mouse cortex (Misson et al., 1988). However, by 35s, RC2 labelling extends across the entire apicobasal axis of the hindbrain (second-left panel in **Figure 3.6A**; 35s, n = 4 embryos). In particular, $RC2^+$ processes extend as single fascicles to the apical surface and denser bundles towards to the pial basement membrane at this stage. Thereafter, RC2 labels NPC processes that project to both surfaces of the hindbrain neuroepithelium (second- and far-right panels in **Figure 3.6A**). However, the organisation of NPC processes gradually changes over time, as the pattern of dense fasciculation seen in basally located processes from 25-35s gradually shifts to medial and then apical regions at 45s and 50s, respectively (45s, n = 3 embryos; 50s, n = 2).

NPC processes fasciculate most commonly in vascularised regions of the hindbrain from 35-50s (see panels corresponding to 35-50s in **Figure 3.6A**). I therefore examined the organisation of NPC processes specifically around the SVP at the time of its initial formation (see expansion box in second-left panel of **Figure 3.6A**, which is shown at higher magnification in **Figure 3.6B**). $RC2^+$ processes form densities that cluster on the nascent SVP, as well as around the radial vessels that initially sprout from the PNP (see upper- and lower left-hand panels in **Figure 3.6B**; 35s, n = 4 embryos). Orthogonal slices through a 20 μm-thick confocal z stack demonstrated that NPC densities directly appose the SVP, but do not possess the conventional appearance or morphology of NPC endfeet observed in the developing cortex (Misson et al., 1988). These observations demonstrate that $RC2^+$ NPC processes organise closely around the hindbrain SVP, making occasional contacts as

documented in the developing mouse cortex (Misson et al., 1988, Tan et al., 2016). Moreover, NPC processes are more fasciculated around hindbrain vasculature. Therefore, blood vessels may play an instructive role for NPC processes and act as an anchorage point for NPCs to attach to.

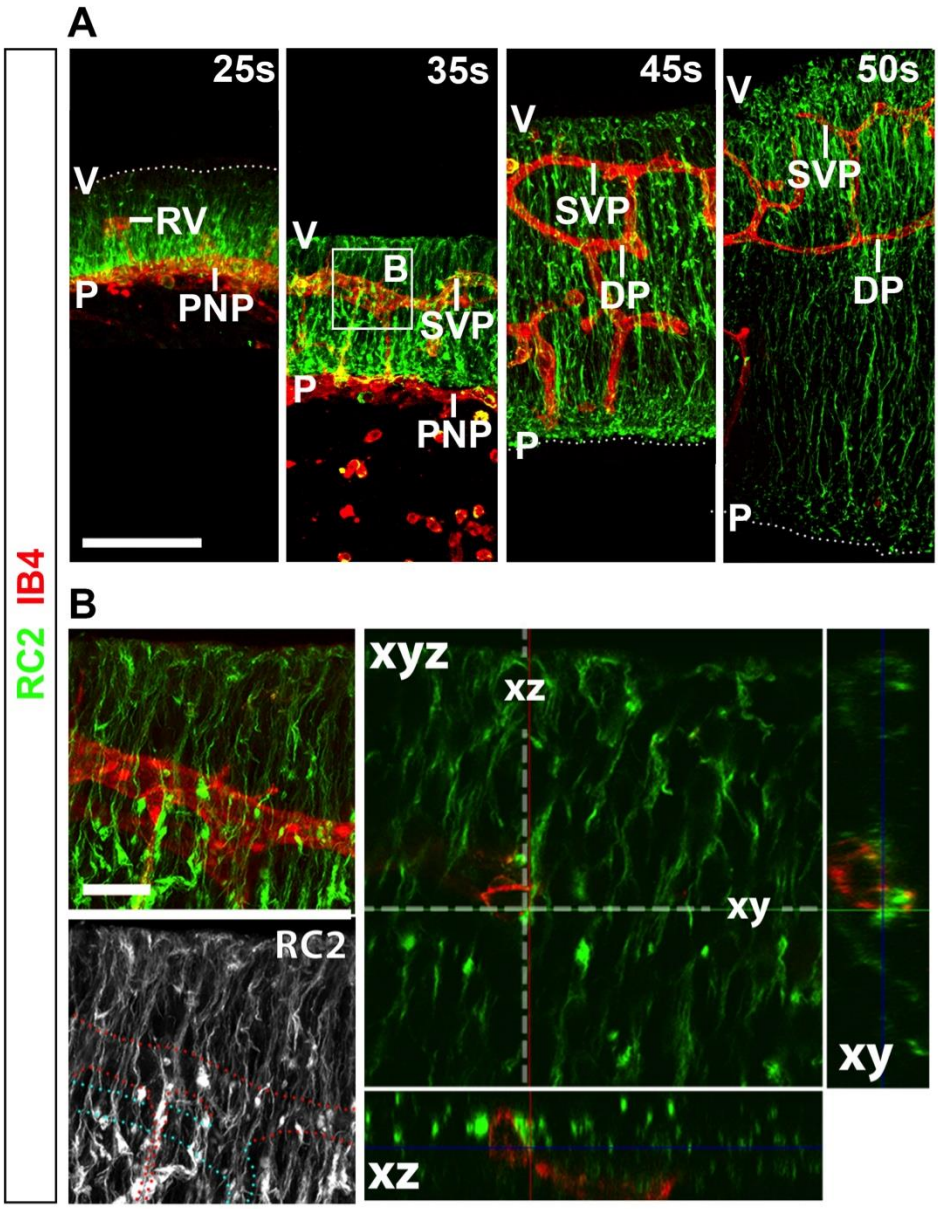

Figure 3.6 NPC processes contact hindbrain vasculature.

(**A-B**) Maximal projections (xy) of confocal z stacks of 70 µm transverse wild type hindbrain sections at the indicated stages, labelled with IB4 (red) and antibodies for the radial glia marker RC2 (green; **A**). Scale bar: 100 µm. The boxed area in (**A**) is shown at higher magnification in (**B**), with RC2 labelling only shown in grey scale in the lower left panel. Single (1.25 µm) optical section of the z stack shown in right panel. Flanking boxes display orthogonal xy and xz projections of single optical section; note how $RC2^{+}$ densities directly contact IB4+ vessels. Scale bar: 20 µm.

3.2.5 **Hindbrain NPCs contact vessel-associated extracellular membrane**

As NPC processes project endfeet onto the SVP, I hypothesized that progenitor endfeet may associate with components of the vessel-derived ECM. Stem and progenitor cells, such as NSCs and satellite cells in adult muscle possess functional contacts with vascular ECM in other stem cell niches (Christov et al., 2007, Shen et al., 2008). Here, I visualised vascular ECM with antibodies for laminin α1 (LAMA1) subunit, given its abundant expression in the basement membrane of endothelium in the adult brain (Yousif et al., 2013). At 25s (**Figure 3.7A**), $RC2^+$ NPC endfeet project onto the basement membrane surrounding the PNP (wavy arrow in bottom panel in **Figure 3.7A''**). However, sprouting radial vessels do not express LAMA1 at this stage and thus it is likely that blood vessels do not yet possess a basal lamina.

In contrast, all vessels within the embryonic hindbrain are ensheathed by a continuous $LAMA1^+$ ECM by 35s (**Figure 3.7B**). Single optical sections through a □□ μm-thick confocal z stack through the SVP at 35s reveal that $RC2^+$ densities contact the vessel-derived ECM directly with endfoot protrusions (arrow in **Figure 3.7B''**; observed in n = 2 embryos). Furthermore, processes interdigitate closely and wrap around the vessel plexus (bracketed region in **Figure 3.7B''**; observed in n = 2 embryos). These observations demonstrate that $RC2^+$ NPC processes and densities contact the $LAMA1^+$ ECM of the SVP immediately following its formation at 35s, raising the possibility that hindbrain NPCs make functional cell-cell contacts with blood vessels.

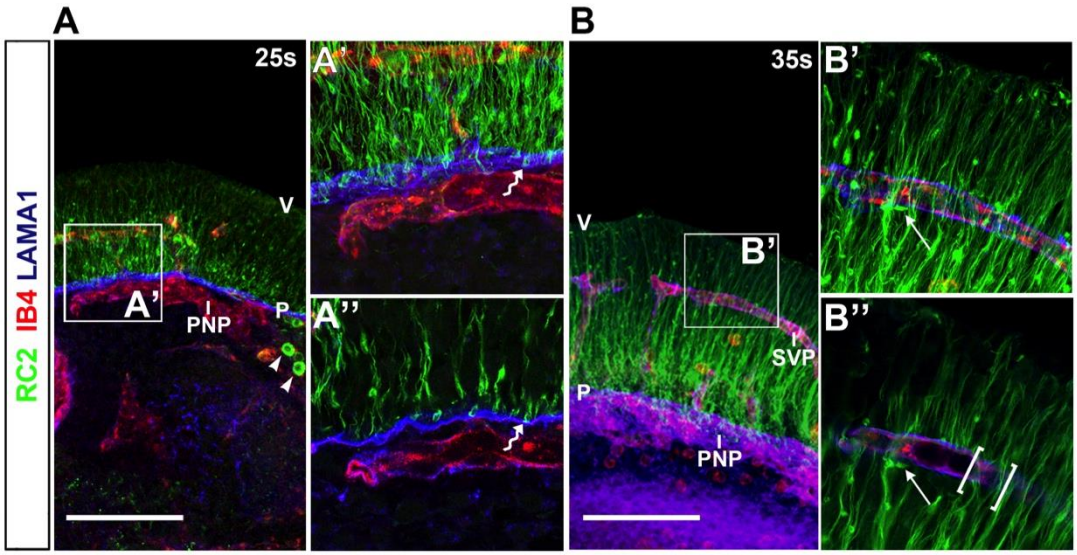

Figure 3.7 NPC processes contact vascular ECM.

(**A,B**) Confocal z stacks of 70 µm transverse sections of wild type hindbrains at the indicated stages after labelling with IB4 (red) together with antibodies for RC2 (green) and LAMA1 (blue). Scale bar: 20 µm. The boxed areas in (**A,B**) are shown in higher magnification adjacent to each panel (**A',B'**). Single (1.25 µm) optical sections from these projections are displayed underneath (**A",B"**). Arrowheads in (**A**) indicate IgM^+ microglia labelled with the secondary antibody used for RC2 detection. Arrows and curved arrow in (**B''**) denote NPC processes and density near SVP vessels. The wavy arrows in (**A',A''**) indicate NPC endfeet. Abbreviations: P, pial surface; V, ventricular surface; RV, radial vessel; SVP, subventricular vascular plexus; DP, deep plexus; PNP, perineural vascular plexus; GZ, germinal zone.

3.2.6 *Sox1-iCreER^{T2}* mouse strain labels single hindbrain NPCs

Due to the large number of NPCs in the developing brain, RC2 immunolabelling did not distinguish which processes and endfeet originate from which NPCs. Furthermore, this method of defining NPC morphology depends on the spatiotemporal expression of the RC2 antigen and therefore may not provide accurate information on NPC process extensions. I therefore used the *Sox1-iCreER^{T2}* transgene for mosaic labelling of NPCs at 35s in the mouse embryo hindbrain. *Sox1* is expressed in early hindbrain neuroectoderm at around e8.5/10s, during neural induction from primitive ectoderm and is therefore likely expressed by early hindbrain APs (Pevny et al., 1998). Low doses of tamoxifen were administered by Prof. Nicoletta Kessaris (UCL) to pregnant females 24 h before analysis to induce sparse recombination of the gene encoding the fluorescent tdTomato protein at the *ROSA26* locus, thus permitting single-cell analyses.

After titrating the appropriate dosage of tamoxifen required for sufficient mosaic labelling of murine NPCs to 20 mg kg^{-1}, I identified many individual tdTomato^{+} NPCs in the developing cortex at 50s when APs are most abundant (**Figure 3.8A**). NPC labelling was most prevalent in ventral regions, primarily in the lateral ganglionic emminence and ventral pallium (**Figure 3.8A**). Mosaic labelling was considerably sparser in the dorsal and medial pallium, but labelled NPCs in all the aforementioned regions appeared to be clustered around the emerging vessel network. Whilst labelling in the dorsomedial cortex was fairly sparse as well, I detected extensive tdTomato expression in the developing thalamus (right-hand side of **Figure 3.8A**).

Therefore, I proceeded to hindbrain analysis at 35s as this was the stage that I had observed NPC process association with vessels and vascular-associated ECM. In the 35s hindbrain, labelled NPC cell bodies and processes spanned across the neuroepithelium and were distinguishable near the newly formed SVP (**Figure 3.8B**). 0.5 μm-thick optical slices of z stacks taken at high magnification demonstrated that Sox1^{+} NPC processes wrap tightly around the SVP endothelium, although these processes do not associate directly with the endothelial cells as a small gap is present between both (see arrowheads in **Figure 3.8C',D'**), possibly

corresponding to the vascular basement membrane. Furthermore, elongated processes ran parallel to the pial surface in the basal region of the hindbrain, likely to be the mantle zone (clear arrowheads in **Figure 3.7**).

In order to improve the visualisation of NPC process organisation around the nascent SVP, I used 3D surface rendering of 70 μm-thick confocal z stacks from *Sox1-iCreER^{T2}; Rosa^{tdTomato}* hindbrain sections (**Figure 3.8E**). 3D reconstruction of immunolabelling demonstrated that the soma of hindbrain NPCs sit very close to the SVP, whilst densities project onto the vessel network, as mentioned previously (see **Figure 3.7** and curved arrowed in **Figure 3.8E'''**). Furthermore, surface rendering confirmed that hindbrain NPCs project endfeet onto the PNP, and that progenitor processes wrap firmly around the SVP (wavy and straight arrows in **Figure 3.8E'-E'''**, respectively). Thus, mosaic labelling of hindbrain NPCs supports the idea that NPCs contact cerebrovasculature and vascular-associated ECM through process extensions.

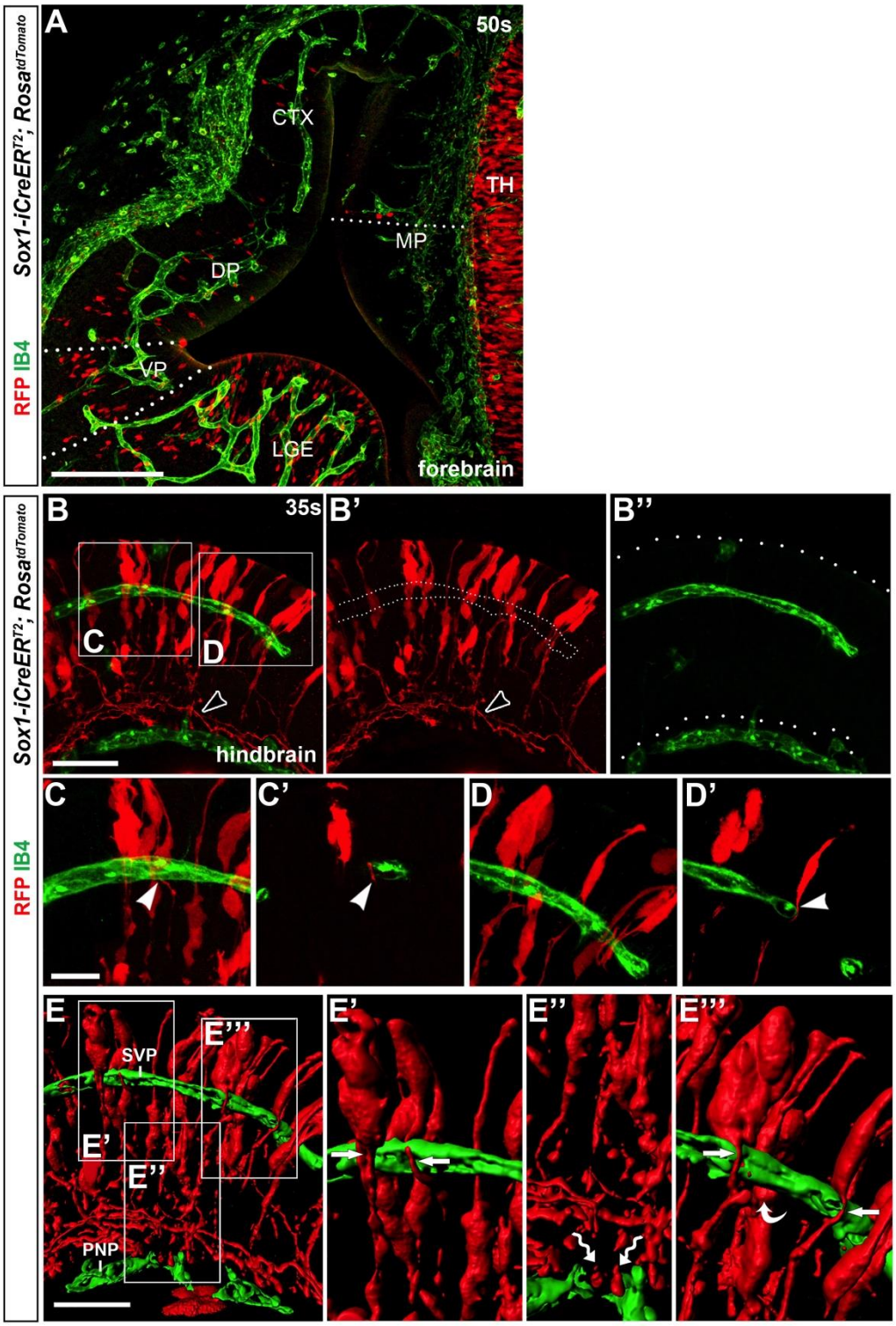

Figure 3.8 Mosaic labelling of NPCs in the forebrain and hindbrain.

(**A**) Maximal projection (xy) of confocal z stack of a 70 µm coronal *Sox1-iCreER^{T2}; RosatdTomato* 35s forebrain section after induction with 20 mg/kg of tamoxifen for 24 h, labelled with IB4 (green) and antibodies for RFP (red) to detect the tomato reporter. Dotted lines separate domains of the developing cortex. Scale bar: 200 µm.

Abbreviations: CTX, cortex; DP, dorsal pallium; LGE, lateral ganglionic emminence; MP, medial pallium; TH, thalamus; VP, ventral pallium.

(**B-D**) Maximal projections (xy) of confocal z stacks of a 70 μm transverse *Sox1-iCreER^{T2}; Rosa^{tdTomato}* 35s hindbrain section after induction with 20mg/kg of tamoxifen for 24 hours, labelled with IB4 (green) and antibodies for RFP (red) to detect the tomato reporter. Clear arrowheads in (**B,B'**) denote elongated, tangential cellular processes. Dotted lines in (**B'**) demarcate an SVP vessel, dotted lines in (**B''**) demarcate the hindbrain surfaces. The boxed areas in (**B**) are shown at higher magnification in (**C, D**) as a confocal z stack or single (1.25 μm) optical section of each z stack (**C',D'**). Arrowheads indicate RFP^{+} NPC processes contacting an SVP vessel. Scale bar: 50 μm (**B**), 20 μm (**C,D**).

(**E**) 3D surface rendering of the confocal z stack shown in (**B**). The boxed areas in (**E**) are shown in higher magnification in (**E'-E'''**). Arrows and curved arrow in (**E', E'''**) denote NPC processes and densities near SVP vessels. The wavy arrows in (**E''**) indicate NPC endfeet. Scale bar: 50 μm. Abbreviations: SVP, subventricular vascular plexus; PNP, perineural vascular plexus.

3.3 Discussion

Wholemount and transverse section immunolabelling demonstrates that the mouse mouse embryonic hindbrain is an excellent model system for simultaneous analysis of sprouting blood vessels and dividing NPCs. Flatmount preparation of the wholemount hindbrain allows quantification of angiogenic parameters (Fantin et al., 2013b), as well as mitotic NPC number at the ventricular surface (

Figure 3.2). Furthermore, quantification of mitotic NPCs in flatmounted hindbrains is easier than through analysis of tissue sections, owing to the fact a larger area of the VZ is visible and sufficiently thick enough confocal z stacks will account for the natural undulation of the ventricular surface. This is in stark contrast to the developing cortex, which is not amendable to similar analysis.

NPCs in the hindbrain divide over a considerably shorter space of time in comparison to those found in the embryonic forebrain (**Figure 3.4**; Haubensak et al., 2004). Whilst NPC cell division in the hindbrain finishes at e13.5, progenitors in the forebrain continue dividing until birth and even into adulthood in the form of slow-cycling NPCs that ultimately generate adult NSCs (Furutachi et al., 2015, Fuentealba et al., 2015). This discrepancy largely reflects the enhanced expansion of the cerebral cortex that forms from the developing forebrain, in comparison to the brainstem that forms from the hindbrain (Fernandez et al., 2016). Given the key role that the brainstem plays in core bodily functions, the need for timely neurogenesis during development is perhaps therefore greater in this area of the CNS in comparison to the cerebral cortex.

I have demonstrated that the temporal pattern of blood vessel sprouting in the hindbrain overlaps with that of dividing NPCs (**Figure 3.3** and **Figure 3.4**). Vessel ingression from the PNP occurs at a similar time in development as elsewhere in the embryonic murine CNS (Vasudevan et al., 2008, Nakao et al., 1988). Whilst the mitotic activity of hindbrain NPCs occurs from at least e9.5/25s up until e13.5/53s, angiogenesis takes place across a narrower time window. The latter is likely due to the necessary time required to establish and stabilize a vessel network within the

growing neuroepithelium, compared with the progressive expansion of NPCs from an initially small pool of NE.

It is therefore noteworthy that despite the longer time course of hindbrain NPC mitosis, the peak of progenitor cell division occurs extremely close to the point of maximum vessel sprouting in both genetic backgrounds analysed. This indicates two possibilities: (i) that no relationship exists between sprouting blood vessels and mitotic NPCs, and that both are coincidental, or (ii) that hindbrain vascularisation and NPC proliferation in the VZ are functionally linked. It is more likely that the latter possibility is true. Firstly, because NPCs attract radially ingressing vessels in the developing CNS via VEGF-A (Haigh et al., 2003). Secondly, NPC mitosis increases considerably after the surge in angiogenesis that results in the formation of the SVP. Thirdly, vasculature in the embryonic forebrain promotes the normal behaviour of NPCs there (Tan et al., 2016, Lange et al., 2016). These key observations demonstrate that both NPCs and blood vessels regulate one another in the developing mammalian CNS.

The pattern of GZ vascularisation in the developing hindbrain is reminiscent of that in the adult neurogenic stem cell niche (**Figure 3.5**). For example, a vessel plexus is established in close proximity to the walls of the lateral ventricles, where NSCs preferentially cluster around the blood vessel network (Tavazoie et al., 2008, Niola et al., 2012). NSCs not in direct contact with the vessel network via their cell body instead extend processes across the postnatal GZ to contact brain vasculature via endfeet (Tavazoie et al., 2008). This has also been suggested for the embryonic cortex, where NPC endfeet terminate on some occasions on blood vessels, whilst mitotic, $TBR2^{+}$ BPs are preferentially positioned around the blood vessels (Javaherian and Kriegstein, 2009, Misson et al., 1988, Tan et al., 2016). I have observed NPC endfeet clearly associating with the ECM that ensheaths the hindbrain SVP, as well as NPC processes wrapping around blood vessels (**Figure 3.6** and **Figure 3.7**). Mosaic analysis of *Sox1*$^{+}$ progenitors confirmed that hindbrain NPCs also project endfeet onto the PNP-associated basal lamina (**Figure 3.8**). It is unclear whether these contacts are functional and provide either structural anchorage or a regulatory input, as has been demonstrated in the embryonic forebrain (Tan et al.,

2016). Indeed, NPCs contact blood vessels with ITGB1 in the ventral forebrain to maintain cell division (Tan et al., 2016). Thus, the presence of a vascular ECM, which contains the ITGB1-ligand LAMA1 (Ettner et al., 1998), in contact with NPC processes supports the idea that vessel contact-based regulation of NPCs occurs in the hindbrain as well. I have not explored whether NPCs might contact pericytes in hindbrain vasculature or whether progenitor-endothelial cell association occurs in pericyte-free areas, akin to NSCs in the SVZ (Tavazoie et al., 2008).

I have shown that hindbrain NPCs also appear to undergo INM, as previously described in both the avian hindbrain and murine cortex (Guthrie et al., 1991, Smart, 1972). By labelling hindbrain NPCs with a short pulse of BrdU, I have demonstrated that migrating nuclei do not pass beyond the deeper vascular plexus after its formation at 45s. It is possible that the deeper plexus may act to restrict nuclear migration by either expressing repulsive signals or as a physical barrier to nuclear movement (Murciano et al., 2002, Taverna and Huttner, 2010).

Mosaic labelling of NPCs achieved through sparse recombination of *Sox1-iCreER^{T2}*-expressing cells also showed that progenitors in the hindbrain organise closely around the vessel plexus. This mouse strain has been used to label NPCs in both the chick and mouse spinal cord (Kicheva et al., 2014), and thus my demonstration of labelling in both the embryonic cortex and hindbrain suggests that it is a valuable tool for studying single NPC behaviour and morphology across the developing rodent CNS. Mosaic recombination in *Sox1-iCreER^{T2}* expressing cells at 25s also labelled tdTomato^{+} processes tangential to the basement membrane in the region that is usually populated by post-mitotic neurons. It is therefore possible that these processes belong to neurons generated from *Sox1*-expressing NPCs, in analogy to the processes of habenular projection neurons found near the pial membrane in the developing zebrafish brain (Bianco et al., 2008).

Given that I activated the *Sox1-iCreER^{T2}* transgene through administration of tamoxifen between e9.5/25s and e10.5/35s, this suggests further that hindbrain NPCs express SOX1 during this period analogous to the mammalian forebrain (Pevny et al., 1998). This transgene could therefore also be used to delete NPC-specific genes in the hindbrain.

3.4 Summary

In the mouse embryonic hindbrain, NPC mitosis and CNS vascularisation take place at similar points in development. Furthermore, the cell bodies and nuclei of cycling NPCs are positioned within a well vascularised GZ, and project processes that contact vessel-associated ECM. Therefore, hindbrain neurogenesis shares a spatiotemporal relationship with angiogenesis.

Chapter 4 NRP1 REGULATES HINDBRAIN NEURAL PROGENITOR CELLS NON-CELL AUTONOMOUSLY THROUGH ITS ROLE IN GERMINAL ZONE VASCULARISATION

4.1 Introduction

I have demonstrated that hindbrain NPCs are positioned within a vascularised compartment and that the time course of NPC division overlaps with a period of extensive vessel sprouting that forms the SVP (**Chapter 3**). Given that hindbrain neurogenesis therefore correlates spatiotemporally with CNS vascularisation, I therefore determined whether this relationship is functionally relevant.

Here I have examined whether hindbrain NPCs are directly regulated by VEGF-A or semaphorins, or indirectly by sprouting networks of blood vessels. I have first characterised NPC behaviour in mouse knockouts lacking NRP1 globally, as it plays equally important roles in neural development and CNS vascularisation. I have then tested whether NRP1 functions cell-autonomously in NPCs as a potential receptor for direct VEGF-A signalling. I have also determined whether semaphorin signalling through NRPs regulates NPC behaviour, as has been suggested previously (Arbeille et al., 2015). Finally, I have studied whether VEGF-A signals through VEGFR2 in NPCs.

I then analysed NPCs in embryos specifically lacking proper GZ vascularisation through loss of endothelial *Nrp1*, to determine whether blood vessels regulate neurogenesis via vessel-derived cues. Finally, I have studied whether hindbrain microglia, which also express NRP1, regulate NPCs as observed in the forebrain of both lissencephalic and gyrencephalic species. I have therefore examined NPC cell division in embryos lacking the transcription factor PU.1, which compromises the generation of monocyte-derived macrophages in the CNS (Scott et al., 1994).

4.2 Results

4.2.1 Developmental staging for studying neurogenesis

Typical staging of mouse embryos relies on estimating the time passed after a post-coital plug is found in females paired overnight. Whilst this may be sufficient for studying slower-forming tissues, or for making assessments of gross anatomy, I have found this to be inadequate for the study of neurogenesis in the embryonic hindbrain. Specifically, the time course of NPC cell division that I have plotted indicates that significant differences exist in the mitotic activity of hindbrains only one quarter of a day apart in development (see **Figure 3.4B,C**). As mice are paired at roughly 5 pm and checked for post-coital plugs at approximately 9 am the day after, the precise timing of fertilisation can range over half a day. In fact, I found that developmental stage can also vary between littermates, especially at younger ages (described previously in (Vieira et al., 2007).

To improve accuracy in staging embryos to generate more precise comparisons between genotypes, I have quantified the number of somite pairs found in each embryo (**Figure 4.1**). The number of somite pairs can be treated as an unequivocal validation of developmental age given that the rate of somitogenesis varies little between genetic mouse mutants, except in mice that lack expression of some circadian genes (Palmeirim et al., 1997). Based on classical Theiler staging (Theiler, 1989) according to specific morphological criteria, quantifying the number of somite pairs identifies a developmental delay in embryos lacking NRP1 in comparison to their wildtype littermates. At e9.5/25s, no difference in somite pair number exists between *Nrp1*$^{+/+}$ and *Nrp1*$^{-/-}$ embryos (data not shown). However, wildtype embryos possess roughly 2-3 somite pairs more than their *Nrp1*$^{-/-}$ littermates when analysed on e10.5 (left panel in **Figure 4.1**). In accordance with Theiler staging, this delay in somitogenesis equates to approximately one quarter of a day in wildtype mice.

The developmental delay in NRP1-null embryos increases thereafter, as mutant embryos possess roughly 4-5 fewer somites than wildtype littermates on

e11.5 and 3-4 fewer somites on e12.5 (middle and right panels in **Figure 4.1**). These correspond to delays of half a day and three-quarters of a day, respectively.

Nrp1$^{-/-}$ embryos also possess a smaller distance between crown and rump, suggesting that the difference in somite number results from a developmental delay, rather than a specific defect in somitogenesis (see dashed lines in **Figure 4.1**). Moreover, older *Nrp1*$^{-/-}$ embryos exhibit delayed limb development that also correlates with a reduced number of somites (A. Plein and C. Ruhrberg, unpublished observations). Thus, the developmental delay likely results from severe vascularisation defects that occur in the NRP1-null embryo (Kawasaki et al., 1999), as well as in extraembryonic structures like the placenta (A. Plein and C. Ruhrberg, unpublished observations).

The considerable difference in age at all three time points indicates the need to stage embryos accurately. I have therefore carried out all analyses of developmentally delayed embryos in this thesis with wildtype stage-matched embryos of a different litter from the same genetic background. This will eliminate the possibility of experimental bias resulting from comparisons made of embryos at different stages.

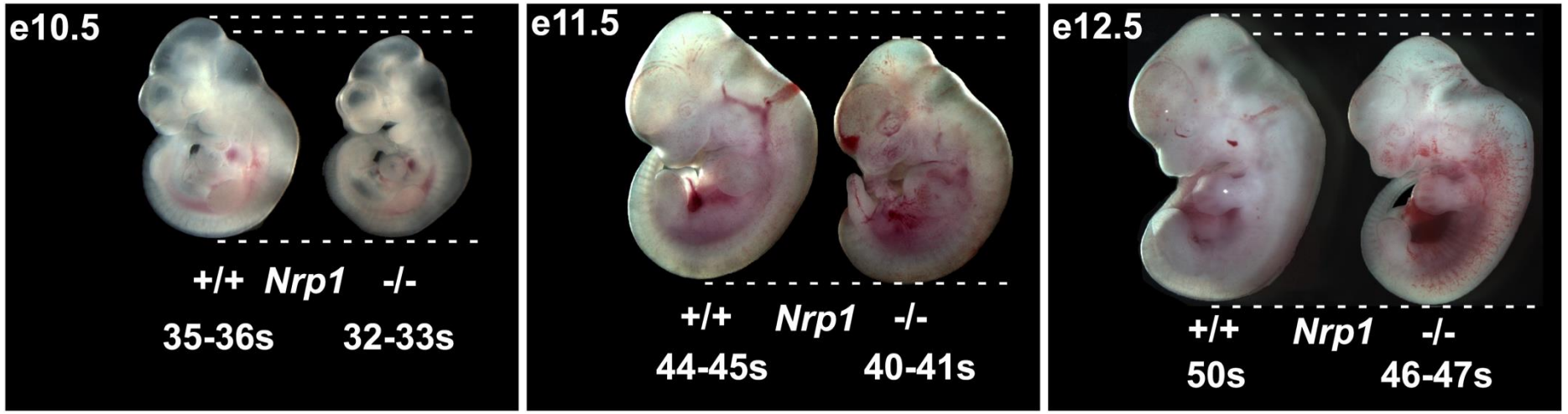

Figure 4.1 *Nrp1*$^{-/-}$ embryos are developmentally delayed.

Representative brightfield images of wildtype and *Nrp1*$^{-/-}$ littermates in the CD1 background at the indicated gestational ages. The typical range of somite pairs at that age is shown for each genotype below the image of the embryo. Dotted lines indicate the reduced crown-rump length of mutants.

4.2.2 Neuropilin 1 is required for vascularisation of the hindbrain GZ

As direct signalling through VEGFRs and blood vessel-derived signals regulate the behaviour of NSCs in the postnatal mammalian brain, I asked whether either or both mechanisms function in the developing CNS for NPCs. I chose initially to analyse embryos lacking NRP1 owing to its dual roles as a VEGF-A and SEMA3 receptor in the embryonic nervous system and as a pro-angiogenic receptor in sprouting endothelium. Our lab has demonstrated that embryos lacking NRP1 globally or in endothelial cells only fail to form a connected SVP in the hindbrain (Fantin et al., 2013a, Fantin et al., 2015). Moreover, NRP1 is expressed by hindbrain NPCs but its role in these cells has not been examined properly (Fantin et al., 2013a).

First, I determined whether hindbrain NPCs lack their stereotypical proximity to cerebrovasculature in full *Nrp1*$^{-/-}$ mutant embryos. Transverse vibratome sections through the wildtype hindbrain show that even at 32s, prior to the peak in SVP angiogenesis, the vessel plexus runs across the hindbrain and through the GZ (top left panel in **Figure 4.2A**). In contrast, NRP1-null embryos lack an SVP at the same time point and indeed, lack lateral vessel sprouting of any kind (bottom left panel in **Figure 4.2A**). Radial vessels ingress from the PNP but terminate instead as poorly invasive 'tufts' (see arrowhead in bottom left panel in **Figure 4.2A**) and very rarely extend beyond the basal-most limit of BrdU^{+} NPCs undergoing INM.

At 40s, the SVP in the wildtype hindbrain is fully formed and extends throughout the GZ (top right panel in **Figure 4.2A**) whilst the deeper plexus has also begun sprouting. Conversely, no recognisable SVP formed by 40s in *Nrp1*$^{-/-}$ hindbrains (bottom right panel in **Figure 4.2A**). A rudimentary network of vessels does form immediately below the GZ (see arrow in bottom right panel in **Figure 4.2A**) and occasional vessels sprout into the GZ. However, no deeper plexus forms (bottom right panel in **Figure 4.2A**). Radial vessels are also elongated and thinner in mutant compared to wildtype embryos (see arrow in bottom right panel in **Figure 4.2A**). Moreover, the rudimentary vessel network that does form in *Nrp1*$^{-/-}$ hindbrains contains mitotic endothelial cells (see black arrowhead in bottom right

panel in **Figure 4.2A**), whilst proliferative cells within the vasculature of wildtype hindbrains are rare at the stages examined (**Figure 3.4** and **Figure 4.2A**).

I quantified the vessel coverage in the GZ between 32-40s in transverse sections of the hindbrain by determining the percentage area occupied by blood vessels within the GZ (**Figure 4.2B**). Consistent with the findings discussed previously, the GZ in wildtype embryos is vascularised by 32s (**Figure 4.2B** *Nrp1*$^{+/+}$ 32s: 15.3±3.5%) and remains occupied by blood vessels thereafter (**Figure 4.2B** *Nrp1*$^{+/+}$ 36s: 17.1±1.4%; 40s: 16.4±2.4%). In contrast, the GZ of NRP1-null hindbrains was almost completely avascular at 32s (**Figure 4.2B** *Nrp1*$^{-/-}$ 32s: 1.1±0.4%, $p<0.001$) and was three times less vascularised compared to wildtype embryos at the peak of NPC mitosis at 40s (**Figure 4.2B** *Nrp1*$^{-/-}$ 36s: 3.5±3.1%; 40s: 4.9±4.3%; $p<0.001$ and $p<0.01$, respectively). These observations demonstrate that loss of NRP1 not only prevents formation of the hindbrain SVP, but also inhibits proper vascularisation of the GZ prior to and during the presumptive peak of NPC mitosis. Thus, *Nrp1*$^{-/-}$ embryos are well suited for studying whether blood vessels play a role in the niche that regulates embryonic neurogenesis.

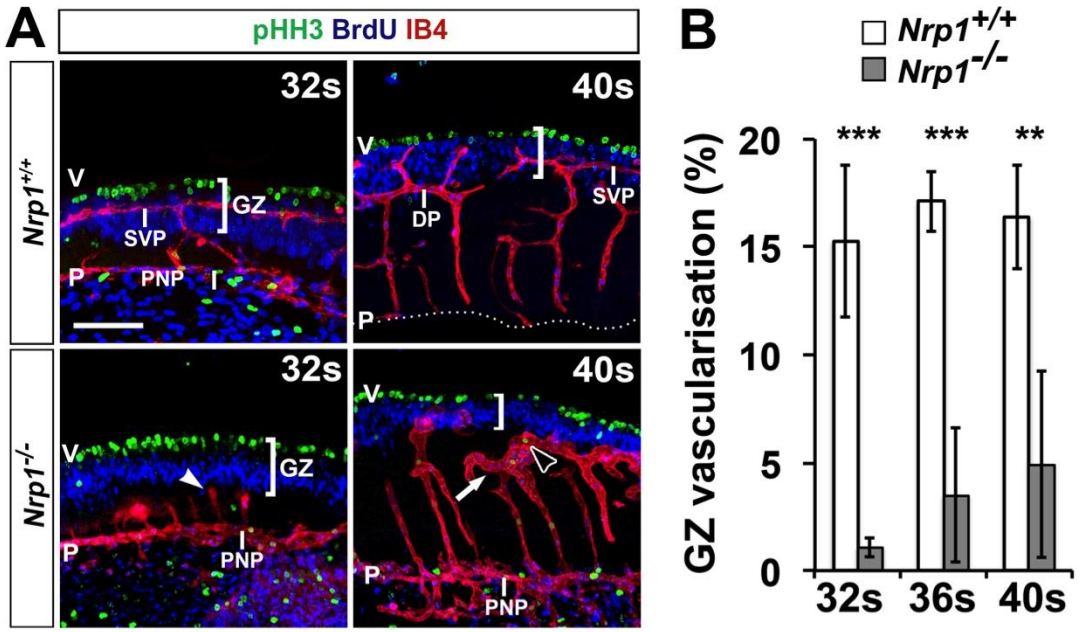

Figure 4.2 NRP1 regulates hindbrain GZ vascularisation.

(**A**) Maximal projections (xy) of confocal z stacks of 70 μm transverse hindbrain sections at the indicated stages after labelling for IB4 (red) together with antibodies for pHH3 (green) and BrdU (blue). Brackets denote GZ depth, the white arrowhead and straight arrow indicate a dead-ended radial vessel and an abnormal deep plexus, respectively. Black arrowhead denotes a mitotic cell in the abnormal vessel plexus. Scale bar: 100 μm. Abbreviations: P, pial surface; V, ventricular surface; SVP, subventricular vascular plexus; DP, deep plexus; PNP, perineural vascular plexus; GZ, germinal zone.

(**B**) Quantification of vascular coverage of the GZ (see **2.2.4**), quantified as $IB4^+$ area per $pHH3^+BrdU^+$ GZ area. Graph shows mean ± standard deviation of the mean, n≥3 for each time point and genotype; ** $p<0.01$, *** $p<0.001$.

4.2.3 Cell survival is not compromised in NRP1-deficient hindbrains

Impaired blood vessel growth and/or function compromises cell survival in the nervous system, such as in a mouse model of motoneuron degeneration (Oosthuyse et al., 2001) and development (Ferrara et al., 1996). Additionally, NRP1 promotes cell survival of migrating neurons in the forebrain (Cariboni et al., 2011). I asked, therefore, whether impaired vascularisation of the hindbrain or loss of NRP1 signalling in NPCs cells compromises cell survival in *Nrp1*-null embryos.

I performed immunolabelling of 10 μm transverse sections of the hindbrain for the apoptosis marker cleaved caspase-3 and quantified the number of apoptotic cells in stage-matched control and *Nrp1*$^{-/-}$ hindbrain sections. Despite the loss of NRP1 from all NPCs, as well as failed GZ vascularisation, I did not detect a decrease in cell survival up to and including at 46s (**Figure 4.3**). On the contrary, I observed a significant decrease in the number of apoptotic cells at 32s in *Nrp1*-deficient hindbrains (**Figure 4.3**, 32s *Nrp1*$^{+/+}$ 7.6±2.2 cleaved caspase-3^{+} cells per section vs. *Nrp1*$^{-/-}$ 3.1±0.6; $p<0.05$). Whilst the level of apoptosis returned to normal levels at 40s (**Figure 4.3**, 40s *Nrp1*$^{+/+}$ 7.9±1.5 cleaved caspase-3^{+} cells per section vs. *Nrp1*$^{-/-}$ 5.9±2.2; $p\geq0.05$), cell death in the hindbrain was again significantly reduced in *Nrp1*-deficient embryos at 46s (**Figure 4.3**, 46s *Nrp1*$^{+/+}$ 28.5±1.5 cleaved caspase-3^{+} cells per section vs. *Nrp1*$^{+/+}$ 21.7±1.6; $p<0.05$). I have not studied cell survival after this point, so cannot yet rule out the possibility of an increase in apoptosis in later stages of hindbrain development. Thus, these observations demonstrate that NRP1 loss does not increase cell death in the hindbrain, indicating that *Nrp1*$^{-/-}$ embryos represent an excellent model for studying vascular regulation of embryonic neurogenesis. Additionally, the decrease in cell death in mutant embryos points to greater cell survival that may potentially result from increased abundance of neurotrophic factors (see **Figure 5.10**).

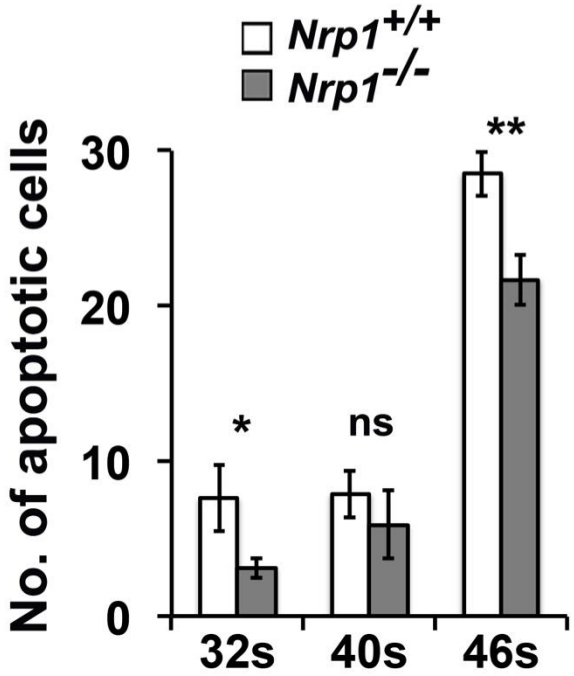

Figure 4.3 Cell survival in the hindbrain is not impaired following constitutive loss of *Nrp1*.

Quantification of the number of apoptotic (cleaved caspase 3^{+}) cells per 10 μm transverse hindbrain section in stage-matched control and *Nrp1*$^{-/-}$ embryos. 5 sections per embryo were analysed owing to the small number of apoptotic cells present in the hindbrain at the stages analysed (see **2.2.4**). All graphs show the mean ± standard deviation of the mean, n≥3 for each time point and genotype; ns (not significant) $p \geq 0.05$, * $p < 0.05$, ** $p < 0.01$.

4.2.4 Neuropilin 1 regulates the timing of hindbrain NPC mitosis

I next asked whether NRP1 may be required for regulating embryonic NPCs either directly as a VEGF-A or class 3 semaphorin receptor, or indirectly by promoting formation of the SVP. Indeed, both modes of regulation may not be mutually exclusive.

To determine whether NPC mitosis was altered in *Nrp1*$^{-/-}$ hindbrains, I performed wholemount immunolabelling for the mitotic marker pHH3 and determined the number of pHH3^{+} NPCs in the hindbrain VZ (see **2.2.4**). The number of pre-anaphase and anaphase NPCs (described in **Figure 3.4 The temporal pattern hindbrain NPC mitosis.** were counted individually in two 0.25mm^2 sample areas positioned midway along mediolateral axis of each hindbrain hemisegment (i.e. four samples per embryo). Prior to hindbrain vascularisation, when only a few radial vessels protrude into the hindbrain parenchyma (see **Figure 3.3A,B** and **Figure 3.5**), I did not detect any change in the density of pHH3^{+} NPCs in the VZ (**Figure 4.4B**, 25s *Nrp1*$^{+/+}$ 132±10.3 pHH3^{+} VZ cells/0.25 mm^2 vs. *Nrp1*$^{-/-}$ 126±14.3; p≥0.05), nor to the overall proportion of NPCs in anaphase (**Figure 4.4B**, 25s *Nrp1*$^{+/+}$ 15.4±4% NPCs in anaphase/total pHH3^{+} NPCs vs. *Nrp1*$^{-/-}$ 15.7±1%; p≥0.05).

However, after the onset in SVP formation at 32s, I observed an increase in the density of pHH3^{+} NPCs (**Figure 4.4B**, 32s *Nrp1*$^{+/+}$ 133±17.6 pHH3^{+} VZ cells/0.25 mm^2 vs. *Nrp1*$^{-/-}$ 162±10.6; p<0.05). Following the typical peak in angiogenesis in the wildtype hindbrain, I detected a significant increase in pHH3^{+} NPCs in the relatively avascular *Nrp1*$^{-/-}$ hindbrain (left hand panels in **Figure 4.4A**; **Figure 4.4B**, 36s *Nrp1*$^{+/+}$ 153±12 pHH3^{+} VZ cells/0.25 mm^2 vs. *Nrp1*$^{-/-}$ 215±16.2; p<0.01). This increase resulted from an expansion specifically in the proportion of NPCs in anaphase, which rose more than two-fold (**Figure 4.4C**, 36s *Nrp1*$^{+/+}$ 17±3% NPCs in anaphase/total pHH3^{+} NPCs vs. *Nrp1*$^{-/-}$ 36±4%; p<0.01). Supporting the notion that the surge in NPC mitoses was due to an increased number of NPCs resting in anaphase, I observed normal numbers of pre-anaphase NPCs in NRP1-null hindbrains at this stage (**Figure 4.4D**, 36s *Nrp1*$^{+/+}$ 127±7.8 pre-anaphase VZ cells/0.25 mm^2 vs. *Nrp1*$^{-/-}$ 139±16.8; p≥0.05).

This proportional increase in the density of $pHH3^+$ NPCs was transient, as the number of $pHH3^+$ NPCs, including those found to be pre-anaphase in the NRP1-null hindbrain were significantly less than in stage-matched wildtype embryos at 40s (middle panels in **Figure 4.4A**; **Figure 4.4B,D**, 40s *Nrp1*$^{+/+}$ 219±2.7 $pHH3^+$ VZ cells/0.25 mm^2, 166±4.3 pre-anaphase VZ cells/0.25 mm^2 vs. *Nrp1*$^{-/-}$ 162±9.2 $pHH3^+$ VZ cells/0.25 mm^2, 125±8.5 pre-anaphase VZ cells/0.25 mm^2; $p<0.001$ for both values). NRP1-null hindbrains contained significantly fewer $pHH3^+$ NPCs thereafter (right hand panels in **Figure 4.4A**; **Figure 4.4B**, 42s *Nrp1*$^{+/+}$ 183±6 $pHH3^+$ VZ cells/0.25 mm^2 vs. *Nrp1*$^{-/-}$ 111±24; 46s *Nrp1*$^{+/+}$ 135±12.6 vs. *Nrp1*$^{-/-}$ 82±8.8, $p<0.001$ at both stages). Thus, following the peak of hindbrain angiogenesis, the number of $pHH3^+$ NPCs increases prematurely and therefore, the entire time course of NPC mitotic activity appears to be shifted to earlier stages in the *Nrp1*$^{-/-}$ hindbrain thereafter. Unfortunately, due to the embryonic lethality caused by global loss of NRP1, I could not analyse *Nrp1*$^{-/-}$ embryos beyond 46s (collected on e12.5).

The percentage of NPCs in anaphase in NRP1-null embryos returned to normal levels at 40s and 42s (**Figure 4.4C**, 40s *Nrp1*$^{+/+}$ 24.4±1.1% NPCs in anaphase/total $pHH3^+$ NPCs vs. *Nrp1*$^{-/-}$ 22.8±1.7%; 46s *Nrp1*$^{+/+}$ 25±2% vs. *Nrp1*$^{-/-}$ 21±3, $p\geq0.05$ at both stages). Yet, the proportion of VZ NPCs in anaphase followed the previously described trend of decreasing mitotic activity at 46s, when *Nrp1*$^{-/-}$ hindbrains possessed 55% less anaphase NPCs amongst all mitotic progenitors compared to wildtype embryos (**Figure 4.4C**, 46s *Nrp1*$^{+/+}$ 21.5±5.6% NPCs in anaphase/total $pHH3^+$ NPCs vs. *Nrp1*$^{-/-}$ 9.7±1.5%; $p<0.01$). Therefore, loss of NRP1 causes an accumulation of NPCs in anaphase initially at 36s, but ultimately reduces numbers of mitotic NPCs in this phase of mitosis at later stages.

Altogether, these data demonstrate that NRP1 is essential for ensuring the temporal pattern of NPC mitosis in the embryonic hindbrain, including the number of mitotic NPCs, and to sustain NPC cell division into the latter stages of hindbrain development. In particular, NRP1 appears vital to ensuring that NPCs do not stall in the anaphase stage of mitosis around the presumptive point of SVP formation.

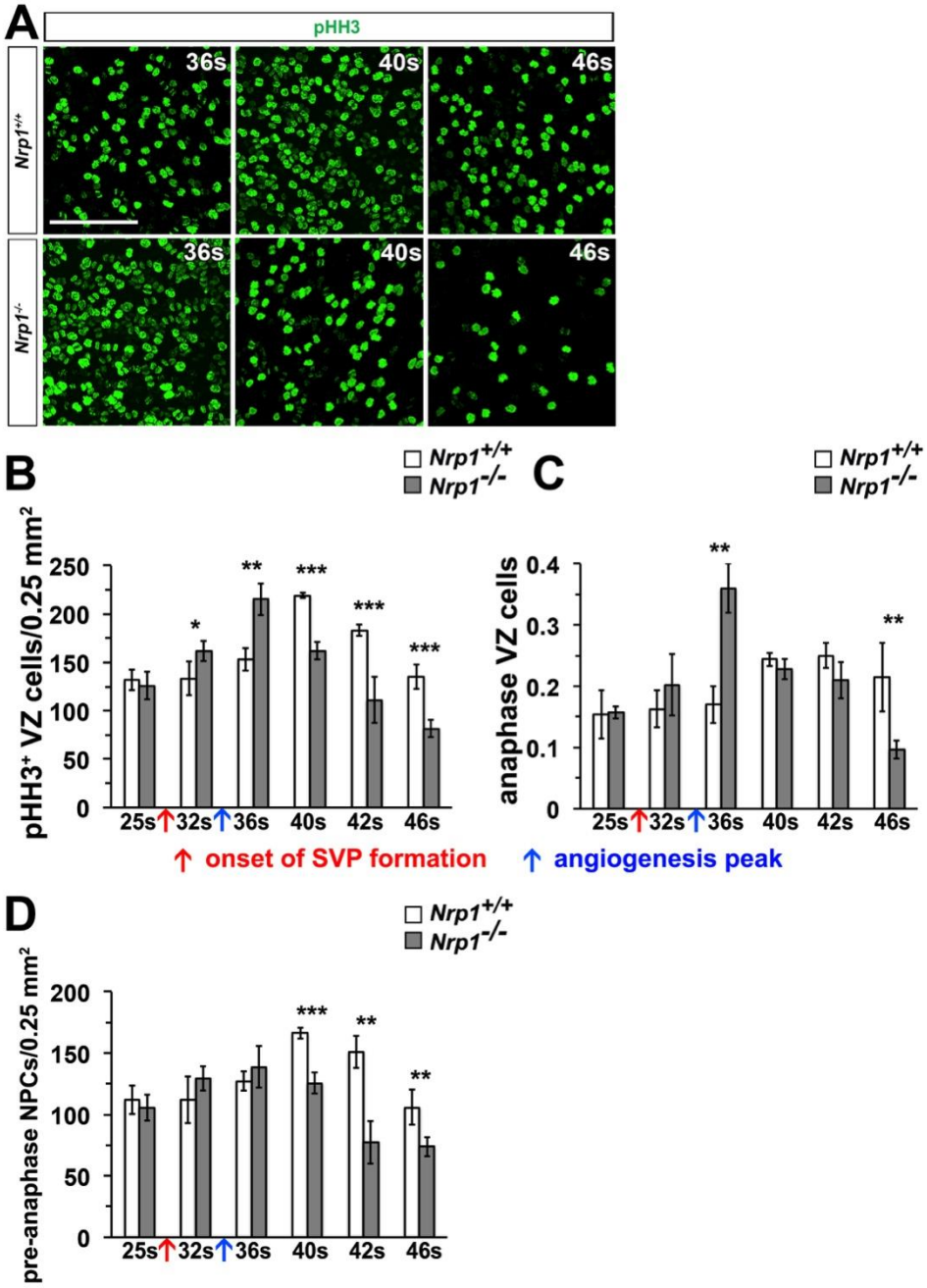

Figure 4.4 NRP1 regulates hindbrain NPC proliferation.

(**A**) Maximal projection (xy) of confocal z stacks of flatmounted wild type and *Nrp1*-null hindbrain VZ at the indicated stages after pHH3 labelling. Scale bar: 100 μm.

(**B-D**) Quantification of $pHH3^+$ mitotic NPCs per 0.25 mm^2 VZ at the indicated stages for *Nrp1*-null and stage matched control hindbrains. The total number of $pHH3^+$ NPCs per 0.25 mm^2 area (**B**), the proportion of NPCs in anaphase (**C**) and the total number of pre-anaphase NPCs per 0.25 mm^2 area (**D**). Red and blue arrows

indicate the onset of SVP formation and peak vessel sprouting in wildtype hindbrains, respectively.

All graphs show the mean ± standard deviation of the mean, $n \geq 3$ for each time point and genotype; * $p<0.05$, ** $p<0.01$, *** $p<0.001$.

4.2.5 Neuropilin 1 maintains GZ organisation

APs in the developing mammalian CNS perform INM as a vital process that influences fate determination. I have shown that hindbrain NPCs in S-phase are labelled by a 1 h pulse of BrdU and display a pseudostratified distribution of NPC nuclei undergoing INM (**Figure 3.5**) that is similar to elsewhere in the nervous system (Smart, 1972, Sauer, 1935). The migratory speed and distance travelled by NPC nuclei during INM correlates with cell cycle progression in NPCs and also exposes progenitors to different regulatory signals in fish (Del Bene et al., 2008).

As the loss of niche signalling can disrupt normal INM (Loulier et al., 2009) (Tsuda et al., 2010), I asked therefore whether NRP1 may also help to maintain INM and the overall organisation of NPCs within the GZ, in addition to its role in maintaining normal NPC mitotic activity. To assess the distribution of NPCs undergoing INM, I quantified the average thickness of the GZ in 70 μm-thick transverse sections at three discrete points across one hemisegment of wildtype and *Nrp1*$^{-/-}$ hindbrains: at (i) lateral, (ii) medial and (iii) peri-midline regions (illustrated in **Figure 4.5A**). The thickness at each point was defined as the distance along the apicobasal axis from the ventricular surface to the basal-most boundary of BrdU^{+} NPCs. The average of these three values was then used as a measure of the overall distribution of NPCs and their progression during INM.

At 32s, the GZ was substantially thicker across the *Nrp1*$^{-/-}$ mutant hindbrain (**Figure 4.2A; Figure 4.5B**, 32s *Nrp1*$^{+/+}$ 69.2±1.7 μm vs. *Nrp1*$^{-/-}$ 79.7±7.6 μm; $p<0.05$). The GZ became thinner at 36s in *Nrp1*$^{-/-}$ mutant hindbrains, thus returning to a similar thickness to that observed in wildtypes (**Figure 4.5B**, 36s *Nrp1*$^{+/+}$ 76±2.9 μm vs. *Nrp1*$^{-/-}$ 72.4±8 μm; $p\geq0.05$). However, the GZ of NRP1-null embryos compacted further until 40s, in contrast to the GZ in wildtype embryos, which further thickened (**Figure 4.2A; Figure 4.5B**, 40s *Nrp1*$^{+/+}$ 89±4.5 μm vs. *Nrp1*$^{-/-}$ 68.1±4.6 μm; $p<0.001$). Therefore, whilst the GZ becomes progressively thicker over the period of 32-40s, the GZ in NRP1-null embryos becomes gradually thinner. As NPC nuclei migrate further from the ventricular surface during INM in the absence of niche signalling (Loulier et al., 2009, Tsuda et al., 2010), this suggests that NRP1 may regulate INM in the mouse hindbrain.

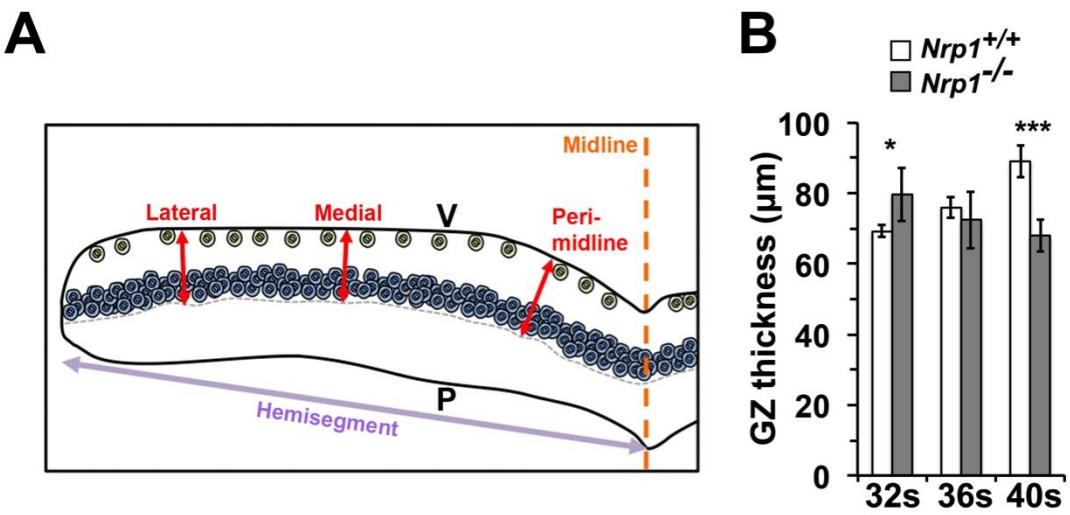

Figure 4.5 NRP1 regulates the organisation of the hindbrain GZ.

(**A**) Schematic representation of the method for quantifying hindbrain GZ thickness. The GZ thickness was defined as the average distance between the ventricular surface (V) and the basal-most point (grey dashed line) of $BrdU^+$ NPCs (blue cells) at lateral, medial and peri-midline points in a single hindbrain hemisegment (purple line). $pHH3^+$ cells in the VZ shown in green, orange line denotes midline; P, pial surface.

(**B**) Quantification of GZ thickness as defined as average thickness of the $BrdU^+$ GZ area (see **2.2.4**; representative images shown in **Figure 4.2**). Data shown represents the mean ± standard deviation of the mean, n≥3 for each time point and genotype; * $p<0.05$, *** $p<0.001$.

4.2.6 NPC processes are mildly disorganised in NRP1-null hindbrains

The majority of previous work on embryonic NPCs addresses the contact of NPC processes with the basal lamina at the pial surface (e.g. (Haubst et al., 2006). However, more recent research has shown that NPCs in the developing- and NSCs in the adult nervous systems contact blood vessels with endfoot protrusions that emerge from long processes (Misson et al., 1988, Tan et al., 2016, Mirzadeh et al., 2008, Ottone et al., 2014). I have observed that hindbrain NPCs also contact the SVP and associated lamina either via $RC2^{+}$ endfeet or processes that interdigitate and wrap around the nascent vessel network (see **Figure 3.6-Figure 3.8**).

In the SVZ of the adult rodent brain, disrupting the association between NSCs and blood vessels inhibits normal regulation of the cell cycle in NSCs and eventually leads to a reduced capacity for proliferation (Shen et al., 2008, Niola et al., 2012, Ottone et al., 2014). Given that loss of hindbrain vascularisation in *Nrp1*$^{-/-}$ mutants correlates with a precocious shift in NPC cell division, I examined whether blood vessels in the developing hindbrain act as a substrate for physical anchorage of NPCs that might be necessary for maintaining mitotic activity in progenitor cells (**Figure 4.6A,B**).

Labelling with RC2 in transverse sections of 32s wildtype hindbrain shows that NPC processes project to both surfaces of the neuroepithelium, with extensive fasciculation near the pial basement membrane (upper-left panel in **Figure 4.6A**). In addition, some $RC2^{+}$ densities clustered around the SVP. In the *Nrp1*$^{-/-}$ hindbrain, large areas lack blood vessels altogether (see Δ in lower panels in **Figure 4.6A**). However, at 32s, NPC processes in these regions appeared grossly normal. Greater process fasciculation was more prominent around poorly invasive radial vessels (chevron in lower-left panel in **Figure 4.6A**), but $RC2^{+}$ processes were still largely orientated correctly, extending along the apicobasal axis of the hindbrain.

At 40s, NPC processes extended across the hindbrain in both wildtype and NRP1-null embryos (middle panels in **Figure 4.6A**). In wildtype hindbrains, radial vessels feeding into the deeper plexus appeared to track perfectly with NPC processes in the basal compartment of the hindbrain (upper-middle panel in **Figure**

4.6A), whilst abnormal radial vessels in *Nrp1*$^{-/-}$ hindbrains were misaligned with NPC processes and angled towards the midline (wavy arrow in lower-middle panel in **Figure 4.6A**). Additionally, small regions of hindbrain still lacked vessel coverage and contained a disorganised mesh of RC2^{+} processes (Δ in lower-middle panel in **Figure 4.6A**). Moreover, processes also appeared somewhat tangled around the rudimentary and glomeruloid vessel network emerging in *Nrp1*$^{-/-}$ mutants. However, NPC morphology looked undisturbed in the apical- and basal-most compartments of the neuroepithelium. Therefore, NPC processes largely organise normally in vascularised regions of *Nrp1*$^{-/-}$hindbrains, but do not align properly with radial vessels sprouting from the PNP.

At 46s, avascular regions still remain in the NRP1-null hindbrain (fletched arrow in lower-right panel in **Figure 4.6A**). In these regions, NPC processes were severely disorganised and appeared to lose their normal alignment along the apicobasal axis. Processes were also tangled around the disorganised vessel network present but looked normal in most regions of hindbrain sections. In addition, some radial vessels were still poorly aligned with NPC processes in the basal compartment of the hindbrain, although this had improved in comparison to *Nrp1*$^{-/-}$ mutants at 40s (compare lower-middle and lower-right panels in **Figure 4.6A**). My observations of RC2 immunolabelling in the NRP1-null hindbrain indicate that whilst NRP1 does not appear important for gross organisation of NPC processes, process extension is mildly affected in regions either with abnormal vasculature or those lacking blood vessels altogether.

Analysis of only LAMA1 expression, demarking the ECM at the basal lamina as well as on cerebrovasculature, shows that expression of laminin α1 is normal in hindbrains lacking NRP1 (compare upper with lower panels in **Figure 4.6B**). This suggests that NRP1 does not regulate expression of LAMA1 and that despite being poorly organised, blood vessels generate ECM in the *Nrp1*$^{-/-}$ hindbrain.

These findings indicate that the organisation of NPC processes is not affected substantially by constitutive loss of NRP1 and is only perturbed in regions with impaired vascularisation. Vessels still retain LAMA1 expression in *Nrp1*$^{-/-}$ mutants,

suggesting that NPCs may still be able to associate with vascular ECM in spite of defective CNS angiogenesis.

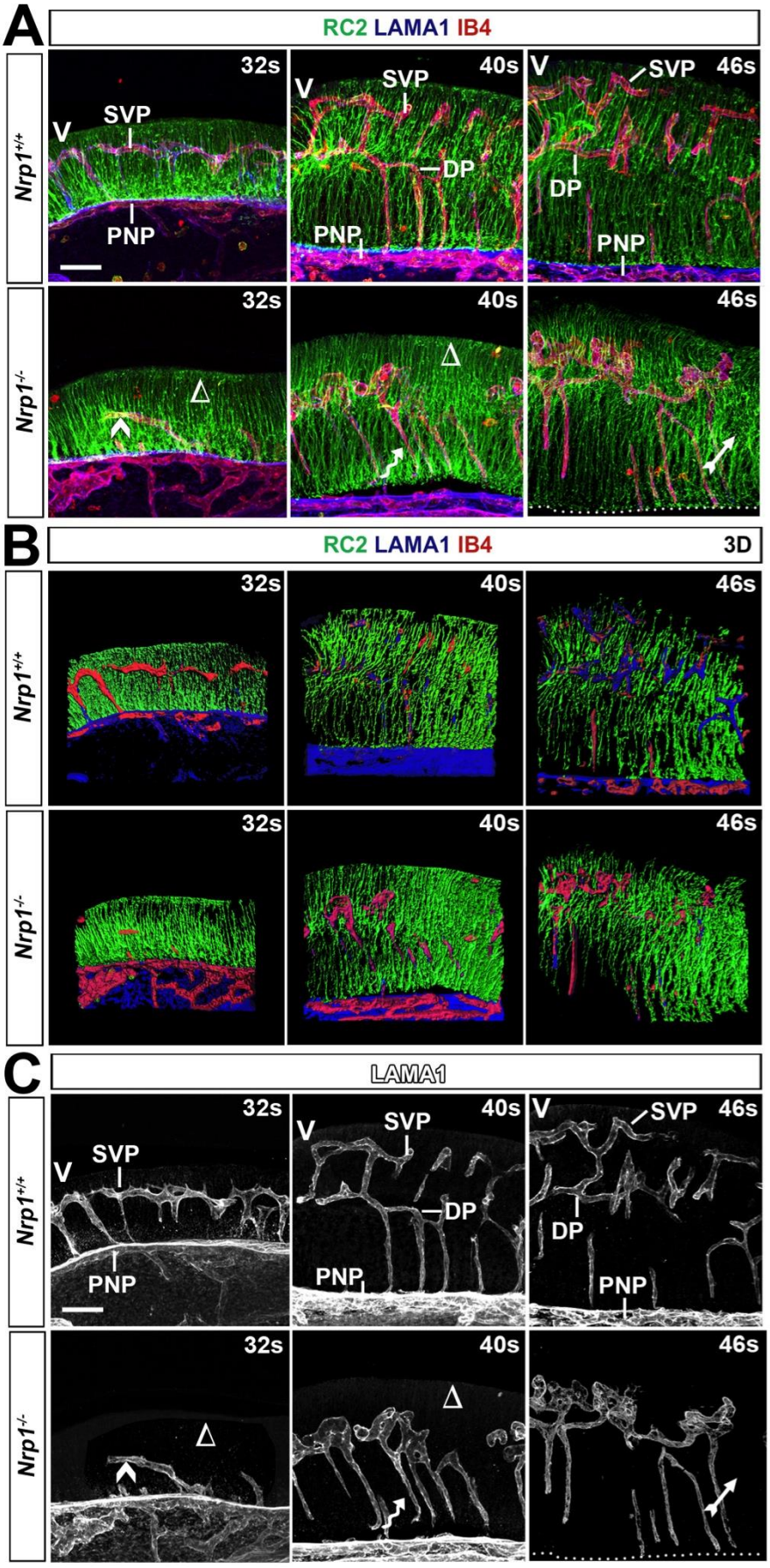
A
RC2 LAMA1 IB4
Nrp1+/+
Nrp1-/-
32s
40s
46s
V
SVP
DP
PNP
B
RC2 LAMA1 IB4
3D
C
LAMA1

Figure 4.6 RC2^{+} processes and laminin expression in NRP1-deficient hindbrains.

(**A**) Maximal projections (xy) of confocal z stacks of 70 μm transverse sections from stage-matched wildtype and *Nrp1*$^{-/-}$ hindbrains after labelling with IB4 (red) and antibodies for RC2 (NPC processes, green) and LAMA1 (extracellular matrix, blue).

(**B**) 3D surface renderings of images shown in (**A**) at indicated stages.

(**C**) LAMA1 staining is preserved in the vasculature of NRP1-deficient hindbrains.

Midline is to the left of each image; Δ denotes avascular regions; chevron indicates a poorly invasive radial vessel; wavy arrow denotes misaligned radial vessel; the feathered arrow indicates NPC process disorganisation. Scale bar: 100 μm. Abbreviations: P, pial surface; V, ventricular surface; SVP, subventricular vascular plexus; DP, deep plexus; PNP, perineural vascular plexus; GZ, germinal zone.

4.2.7 Neuropilin 1 regulates NPC division non-cell autonomously through germinal zone vascularisation

NRP1 is expressed by both NPCs and hindbrain endothelial cells (Fantin et al., 2013a). To distinguish between NPC- and endothelial-specific roles for NRP1, I studied the pattern of hindbrain NPC mitosis in embryos selectively lacking *Nrp1* in either the neural or endothelial lineage. Initially, I analysed *Tie2-Cre; Nrp1*$^{c/-}$ mutant embryos that lack NRP1 only in *Tie2*-expressing endothelium and microglia, as these mice fail to form a proper SVP (Fantin et al., 2013a). This would therefore determine whether the defects in NPC mitosis in *Nrp1*$^{-/-}$ mutants (**Figure 4.4**) stemmed from incomplete vascularisation of the hindbrain GZ. In comparison to embryos lacking NRP1 globally, however, *Tie2-Cre; Nrp1*$^{c/-}$ hindbrains retain a low level of vascularisation and form a basic but partially connected SVP at e12.5 (Fantin et al., 2013a). This is due to incomplete recombination of *Nrp1* by *Tie2-Cre*, resulting in endothelial cells that retain NRP1 expression and preferentially adopt the tip cell position to guide some vessel sprouts in the mouse hindbrain.

I first defined how blood vessel defects in the hindbrain GZ of *Tie2-Cre; Nrp1*$^{c/-}$ mutant embryos compared with that in full *Nrp1*$^{-/-}$ animals. Transverse sections through the hindbrain of endothelial NRP1 mutants at 32s reveals that whilst radial vessels sprout further in the neural parenchyma than in full *Nrp1*$^{-/-}$ embryos, the GZ still remains poorly vascularised (lower-left panel in **Figure 4.7A**). Moreover, despite the protrusion of some radial vessels into the GZ, no SVP has formed at this stage either. This is in contrast to stage-matched wildtype embryos on the same C57BL/6 genetic background in which an SVP already occupies the GZ at 32s (upper-left panel in **Figure 4.7A**). Towards the latter stages of hindbrain NPC mitosis at 48s, *Tie2-Cre; Nrp1*$^{c-/-}$ hindbrains are somewhat vascularised, with a rudimentary network of vessels present in the GZ of mutant embryos (see curved arrow in the lower-right panel in **Figure 4.7A**). These results indicate that similar to full *Nrp1*$^{-/-}$ mutants, *Tie2-Cre; Nrp1*$^{c/-}$ mutant embryos fail to form GZ vasculature at 32s, but there is a partial recovery of GZ vascularisation later in development, likely resulting from incomplete deletion of *Nrp1* in endothelial cells expressing *Tie2-Cre* (Fantin et al., 2013a). The organisation of $RC2^{+}$ processes was similar in endothelial *Nrp1* mutants to that in *Nrp1*$^{-/-}$ mutants (compare **Figure 4.7B** with **Figure 4.6A**).

NPC processes were largely unaffected and appeared normal at both 32s and 48s, with disorganisation only occurring in areas that either contain abnormal vessels or lack vasculature altogether (see asterisk in bottom-right panel in **Figure 4.7B**)

I next analysed the mitotic activity of hindbrain NPCs in *Tie2-Cre; Nrp1*$^{c/-}$ embryos that lack sufficient GZ vascularisation. Owing to cardiovascular defects (Plein et al., 2015), *Tie2-Cre; Nrp1*$^{c/-}$ mutant embryos also exhibit a developmental delay in comparison to wildtype littermates; therefore, I have compared mutants to stage-matched controls. At 36s, I observed significantly higher numbers of pHH3^{+} NPCs in mutant embryos (**Figure 4.7C**; left-hand graph in **Figure 4.7D**, 36s *Nrp1*$^{+/+}$ 178±10.4 pHH3^{+} VZ cells/0.25 mm^2 vs. *Tie2-Cre*; *Nrp1*$^{c/-}$ 201±10.8; $p<0.05$), although this increase was smaller than in full *Nrp1*$^{-/-}$ mutants, correlating with a less severe vascularisation phenotype. However, NPCs were also significantly less mitotic in *Tie2-Cre; Nrp1*$^{c/-}$ hindbrains compared to stage-matched controls at 42s (left-hand graph in **Figure 4.7D**, 42s *Nrp1*$^{+/+}$ 194±14.2 pHH3^{+} VZ cells/0.25 mm^2 vs. *Tie2-Cre*; Nrp1$^{c/-}$: 165±13.4; $p<0.05$). As with full *Nrp1*$^{-/-}$ mutants, NPCs were also significantly less mitotic thereafter in endothelial-null NRP1 embryos (left-hand graph in **Figure 4.7D**, 45s *Nrp1*$^{+/+}$ 167±14.7 pHH3^{+} VZ cells/0.25 mm^2 vs. *Tie2-Cre*; *Nrp1*$^{c/-}$ 143±6.4; 49s *Nrp1*$^{+/+}$ 98.5±12.8 vs. *Tie2-Cre*; *Nrp1*$^{c/-}$ 78±13.5, $p<0.01$ and $p<0.05$, respectively).

The proportion of mitotic NPCs in anaphase followed a similar pattern in endothelial- compared to full *Nrp1* mutants. At 36s, a significantly higher proportion of NPCs stalled in anaphase (right-hand graph in **Figure 4.7D**, 36s *Nrp1*$^{+/+}$ 19±0.6% anaphase NPCs cells/total pHH3^{+} NPCs vs. *Tie2-Cre*; *Nrp1*$^{c/-}$ 30±4.5%, $p<0.01$). Similar to full *Nrp1* mutant hindbrains, the proportion of mitotic NPCs in anaphase normalised during e11 (see 42s and 45s in right-hand graph in **Figure 4.7D**) before significantly decreasing in endothelial-specific *Nrp1* embryos at later stages (right-hand graph in **Figure 4.7D**, 49s *Nrp1*$^{+/+}$ 30±1.3% anaphase NPCs cells/total pHH3^{+} NPCs vs. *Tie2-Cre*; *Nrp1*$^{c/-}$ 20±1.3%, $p<0.001$).

Thus, as I observed in full *Nrp1*$^{-/-}$ mutants, NPCs in *Tie2-Cre*; *Nrp1*$^{c/-}$ mutant hindbrains stall in anaphase at 36s and then undergo a premature decline in mitosis thereafter. However, defects were less severe, potentially due to milder defects in

vessel growth in endothelial-specific *Nrp1* mutants compared to embryos lacking *Nrp1* globally. Therefore, the timing of NPC mitosis is perturbed in hindbrains lacking GZ vascularisation.

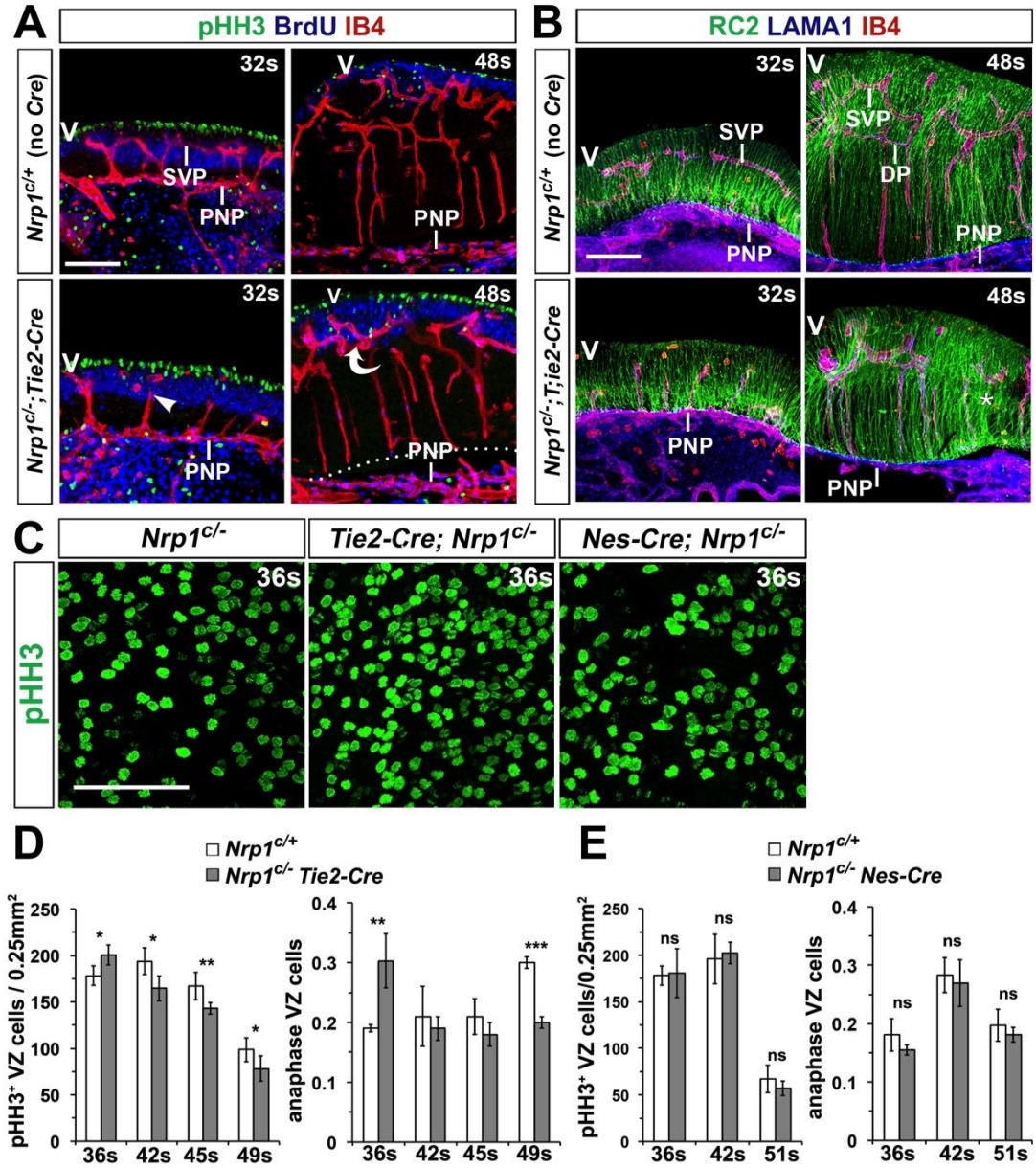

Figure 4.7 NRP1 regulates NPC mitosis non-cell autonomously through its role in GZ vascularisation.

(**A-C**) Maximal projections (xy) of confocal z stacks from 70 μm transverse sections of stage-matched *Tie2-Cre; Nrp1$^{c/-}$* and control hindbrains at the indicated stages after labelling with IB4 (red) and antibodies for pHH3 and BrdU (green and blue; **A**) or antibodies for RC2 and LAMA1 (green and blue; **B**), and through the VZ of flatmounted control, *Tie2-Cre; Nrp1$^{c/-}$* and *Nes-Cre; Nrp1$^{c/-}$* hindbrains at 36s after labelling with pHH3 (green, **C**). Arrowhead and curved arrow in (**A**) indicate blind-ended radial vessel and crude vessel plexus, respectively; asterisk in (**B**) indicates a region where NPC processes appear disorganised. The dotted lines in (**A**) demarcate pial hindbrain boundaries at 48s; separation of the hindbrain parenchyme from the

PNP in the perineural membrane is a sectioning artefact. Abbreviations: V, ventricular surface; SVP, subventricular vascular plexus; DP, deep plexus; PNP, perineural vascular plexus. Scale bars: 100 μm.

(**D,E**) Quantification of $pHH3^+$ mitotic NPCs per 0.25 mm^2 VZ at the indicated stages for *Tie2-Cre; Nrp1$^{c/-}$* and stage-matched control hindbrains (**D**) and *Nes-Cre; Nrp1$^{c/-}$* and littermate control hindbrains (**E**). The total number of $pHH3^+$ NPCs per 0.25 mm^2 area and the proportion of NPCs in anaphase are shown in the left- and right-hand graphs, respectively. All graphs show the mean ± standard deviation of the mean, $n \geq 3$ for each time point and genotype; ns (not significant) $p \geq 0.05$, * $p < 0.05$, ** $p < 0.01$, *** $p < 0.001$.

4.2.8 Neuropilin 1 is not required cell autonomously by hindbrain NPCs to regulate mitotic activity

To determine whether loss of NRP1 from NPCs impairs NPC mitosis, I analysed the density of mitotic NPCs in the hindbrain VZ of embryos lacking NRP1 in the neural lineage and compared this to mutant embryos lacking NRP1 globally. Prior work from my lab has shown that *Nes-Cre; Nrp1*$^{c/-}$ embryos lack NRP1 expression specifically in hindbrain NPCs, and indeed across the whole neuroepithelium, yet retain it in both endothelial and microglial lineages (Fantin et al., 2013a). As a result, the hindbrain SVP forms normally (Fantin et al., 2013a).

I used the *Nes-Cre* transgene to delete NRP1 from neural cells as its expression profile is ideally suited for studying hindbrain NPCs. Unlike the widely-used *Nestin-Cre* transgene, *Nes-Cre* is expressed across the whole CNS by e9.5/25s (Petersen et al., 2002). In addition, despite expression of *Nes-Cre* in somites (Petersen et al., 2002), *Nes-Cre; Nrp1*$^{c/-}$ embryos are not developmentally delayed compared to wildtype littermates and possess an identical number of somites (data not shown). The *Nes-Cre* transgene also labels pericytes (Iwayama et al., 2015) but NRP1 expression has not been detected in these cells.

Surprisingly, I did not detect differences in either the number of mitotic NPCs (left hand graph in **Figure 4.7E**) or the overall proportion of mitotic NPCs in anaphase (right hand graph in **Figure 4.7E**) between *Nes-Cre; Nrp1*$^{c/-}$ and wildtype littermates at any stages examined. For example, at 36s, when full *Nrp1*$^{-/-}$ mutant hindbrains demonstrate significantly higher levels of mitosis than in wildtype stage-matched controls, the number of NPCs in mitosis and the proportion of NPCs in anaphase were normal in *Nes-Cre; Nrp1*$^{c/-}$ embryos (**Figure 4.7C,E**). The level of NPC mitosis did not differ in *Nes-Cre; Nrp1*$^{c/-}$ mutants at 42s or 51s either, whereas the number of pHH3^{+} NPCs was significantly lower at these stages approximately in full *Nrp1*$^{-/-}$ mutants (compare **Figure 4.7E** with **Figure 4.4B**). Additionally, the proportion of anaphase cells amongst the total cohort of mitotic NPCs was unchanged in *Nes-Cre; Nrp1*$^{c/-}$ mutants (right-hand graph in **Figure 4.7E**). Therefore, these data demonstrate that abnormal mitotic activity in NPCs in the

Nrp1-null hindbrain is not caused by a loss of cell autonomous NRP1 signalling in NPCs.

4.2.9 Neuropilins 1 and 2 redundantly regulate hindbrain NPC mitotic activity

Having established that GZ vasculature regulates timely NPC mitosis, I asked whether NRP1 additionally plays a role in hindbrain NPCs, for example by acting as a receptor for a specific ligand. In particular, both NRPs function in spinal cord NPCs as semaphorin receptors to maintain normal spindle orientation and additionally, compensate for one another (Arbeille et al., 2015). In analogy, both may regulate hindbrain NPCs similarly in the hindbrain, given its anatomical proximity to the spinal cord. Furthermore, as neither semaphorin (Vieira et al., 2007) nor VEGF-A (Fantin et al., 2014 and A. Fantin, unpublished observations) signalling through either NRP is important for hindbrain angiogenesis, any defects observed in semaphorin- or VEGF-A-specific NRP1 mutants would indicate that NRPs may transduce cell autonomous signalling in NPCs.

To determine if NPC mitosis prematurely declines in the absence of semaphorin binding to NRP1 and/or NRP2, I analysed $Nrp1^{Sema/Sema}$ $Nrp2^{-/-}$ mutants. As the analysis of *Nrp1* and *Tie2-Cre;* $Nrp1^{c/-}$ mutants had identified defects towards the end of the neurogenesis time course (46s and 49s respectively; **Figure 4.4B** and **Figure 4.7D**), I also analysed $Nrp1^{Sema/Sema}$ $Nrp2^{-/-}$ mutants at a late stage of hindbrain neurogenesis (49s). I observed that the number of NPCs in mitosis was decreased in $Nrp2^{-/-}$ hindbrains (**Figure 4.8A**, 49s $Nrp2^{+/+}$ 128±8.1 $pHH3^{+}$ VZ cells/0.25 mm^2 vs. $Nrp2^{-/-}$ 107±14.8; p=0.057). However, dual loss of semaphorin signalling through both NRPs resulted in a significantly greater reduction in NPC mitosis (**Figure 4.8A**, 49s $Nrp1^{+/+}$ $Nrp2^{+/+}$ 128±8.1 $pHH3^{+}$ VZ cells/0.25 mm^2 vs. $Nrp1^{Sema/Sema}$ $Nrp2^{-/-}$ 78±9; p<0.001). These observations suggest that both NRPs act redundantly to maintain normal levels of NPC cell division at later stages of hindbrain development.

In contrast to global or endothelial *Nrp1* mutants, loss of NRP2 or compound deletion of semaphorin signalling through both NRPs did not significantly perturb the overall proportion of mitotic NPCs in anaphase (**Figure 4.8B**). However, I did

detect a small increase in the percentage of anaphase NPCs in *Nrp2*$^{-/-}$ embryos that was not statistically significant (**Figure 4.8B**, 49s *Nrp2*$^{+/+}$ 27±3% anaphase NPCs cells/total pHH3^{+} NPCs vs. *Nrp2*$^{-/-}$ 33±4%; p=0.07). Unexpectedly, however, NRP2 is not as widely expressed across the hindbrain neuroepithelium as NRP1 (Fantin et al., 2013a), and only appears to be present at the midline between 32-46s, as well as on axon fibres leaving the hindbrain at 46s (**Figure 4.8C**). Therefore, it is unclear how NRP2 can be important in maintaining hindbrain NPC mitosis given its limited expression pattern.

Overall, these observations indicate that both NRPs act redundantly by transducing semaphorin signals to maintain NPC mitosis at 49s, although NRP2 may be more influential in NPCs than NRP1. Indeed, I have not tested whether VEGF-A signals through NRP2. Future work is also needed to establish whether semaphorin signalling through both NRPs or VEGF-A signalling through NRP2 are required by hindbrain NPCs prior to the end stages of hindbrain development.

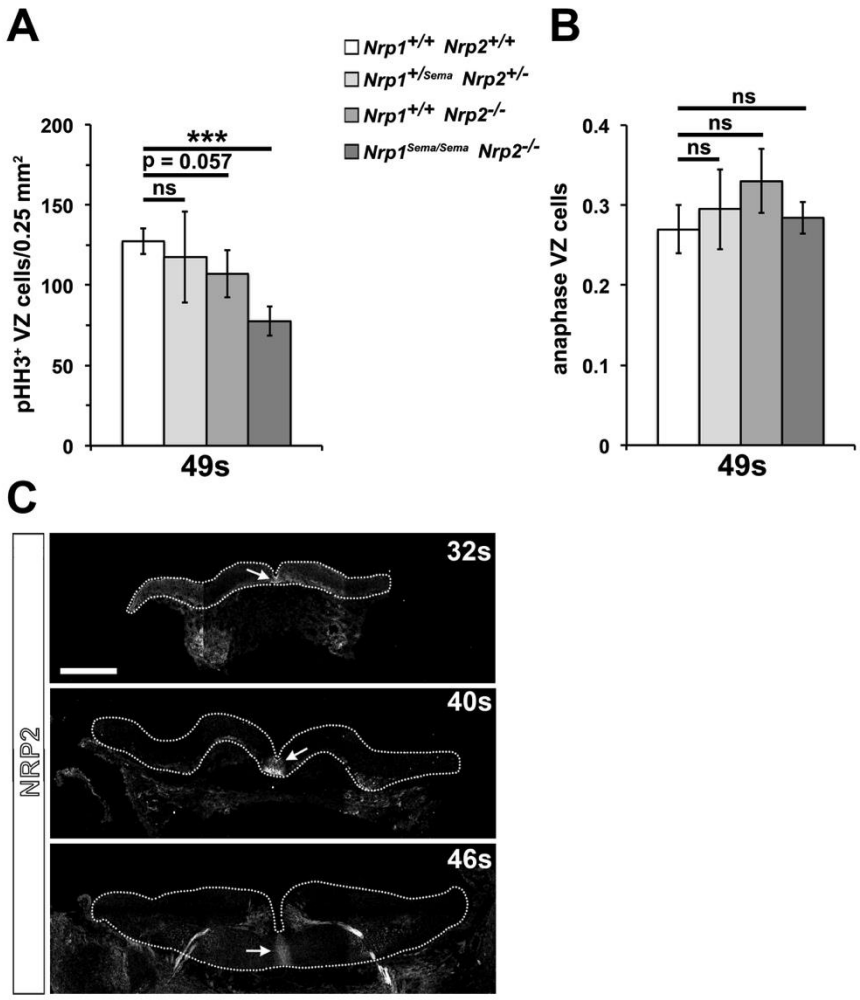

Figure 4.8 Semaphorin signalling through NRPs in NPCs regulates NPC mitosis.

(**A-B**) Quantification of mitotic NPCs in wildtype (*Nrp1*$^{+/+}$ *Nrp2*$^{+/+}$), *Nrp1*$^{+/Sema}$ *Nrp2*$^{+/-}$, *Nrp1*$^{+/+}$ *Nrp2*$^{-/-}$ and *Nrp1*$^{Sema/Sema}$ *Nrp2*$^{-/-}$ hindbrains. The total number of pHH3^{+} NPCs per 0.25 mm^2 area and the proportion of NPCs in anaphase are shown in (**A**) and (**B**), respectively. All graphs show the mean ± standard deviation of the mean, n≥2 for each time point and genotype. ns (not significant) p≥0.05, significant p<0.05.

(C) Maximal projection (xy) of confocal tile scan z stacks of 10 μm transverse sections of wildtype hindbrains after labelling for NRP2. Arrow indicates that NRP2 is expressed predominantly at the midline. Note that fluorescence in non-midline areas in top panel results from non-specific, background immunolabelling. Scale bar: 100 μm.

4.2.10 Hindbrain NPCs express VEGFR2 *in vitro* but not *in vivo*

I next asked whether VEGFR2 acts with NRP1 in partial redundancy to convey VEGF-A signals in hindbrain NPCs. By performing wholemount immunolabelling for $SOX2^+$ NPCs, $IB4^+$ endothelial cells and VEGFR2, I was able to define potential VEGFR2 expression in the VZ and SVP within the same confocal z stack obtained from a single hindbrain. At the ventricular surface, where $SOX2^+$ NPCs reside, VEGFR2 expression is completely absent across the main period of hindbrain development (e9.5-12.5; top panels in **Figure 4.9A**). In contrast, the $IB4^+$ SVP in the same hindbrains expresses VEGFR2 abundantly, as expected for actively sprouting and remodelling vasculature (Gerhardt et al., 2003) bottom panels in **Figure 4.9A**).

To determine whether expression of *Kdr*, which encodes the VEGFR2 protein, is a feature specific to hindbrain-derived, cultured NPCs, I performed PCR on cDNA generated from either hindbrain NPCs (*in vivo*) or neurospheres (NPCs propagated *in vitro*). $CD133^+$ hindbrain NPCs were isolated via fluorescence-activated cell sorting from e10.5 hindbrain (FACS; see **Figure 5.5A** for description of FACS isolation of NPCs) whilst neurospheres were generated by dissociating NPCs from e10.5 hindbrains and culturing them in neurosphere medium for 2 weeks to prevent contamination of endothelial cells (see **2.2.8** for full protocol). *Kdr* is not expressed in FACS-isolated hindbrain NPCs either, but upregulates in neurospheres (compare left and middle lanes in **Figure 4.9B**). These results agree with observations elsewhere in the developing mammalian CNS that VEGFR2 is not required by NPCs *in vivo* (Javaherian and Kriegstein, 2009, Haigh et al., 2003), but regulates neurosphere cultures *in vitro* (Wada et al., 2006).

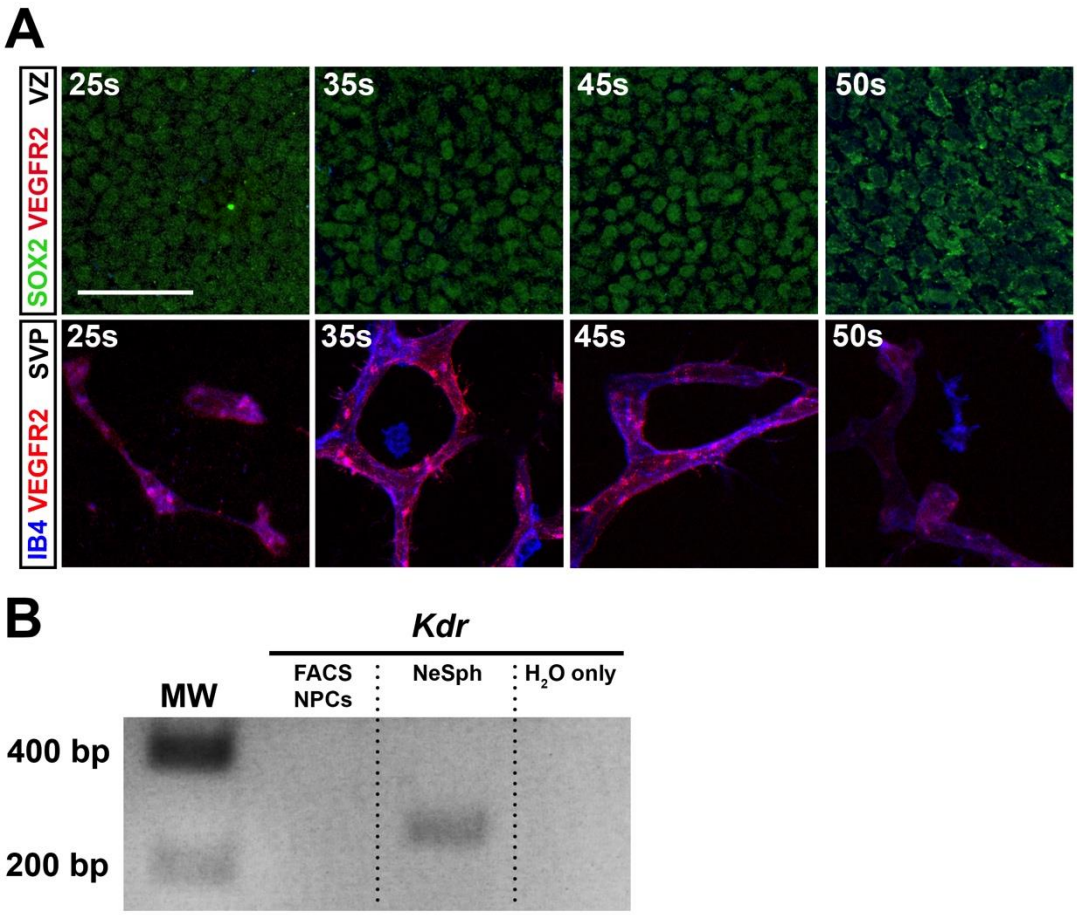

Figure 4.9 VEGFR2 is expressed by hindbrain vessels and cultured hindbrain NPCs, but not by hindbrain NPCs *in vivo*.

(**A**) Maximal projection (xy) of confocal z stacks through mouse embryo hindbrains at the indicated stages after wholemount immunolabelling with the dual vessel and microglia marker IB4 (red) together with antibodies for SOX2 (NPC nuclei marker; green) and the VEGF-A receptor VEGFR2 (blue) imaged at the level of the VZ (top panels) and SVP in the same hindbrain for each stage (bottom panels). Abbreviations: VZ, ventricular zone; SVP, subventricular vascular plexus. Scale bar: 100 μm.

(**B**) RT-PCR for *Kdr* from cDNA isolated from either FACS-isolated NPCs (FACS NPCs) or neurospheres (NeSph), with a no template (water; H_2O only) control. Molecular weight (MW) indicated on the left-hand side .

4.2.11 Microglia do not regulate hindbrain NPC mitosis

Microglia have an evolutionarily conserved role in forebrain neurogenesis, begin entering the hindbrain during the peak period of neurogenesis at around e10.5 and also express NRP1 (Fantin et al., 2010, Cunningham et al., 2013). Therefore, NRP1 may also regulate NPC mitosis through an additional, non-cell autonomous role in microglia. I therefore examined whether hindbrains lacking microglia possess similar defects in NPC mitosis as observed in full *Nrp1*$^{-/-}$ hindbrains by performing wholemount immunolabelling for pHH3 in both *Pu.1*$^{-/-}$ mutant and wildtype littermate embryos at the tail end of hindbrain neurogenesis.

However, I did not detect any significant difference in the level of NPC mitosis between *Pu.1*$^{-/-}$ embryos and controls at 50s (**Figure 4.10A**, *Pu.1*$^{+/+}$ 86±14.8 pHH3^{+} VZ cells/0.25 mm^2 vs. *Pu.1*$^{-/-}$ 93±15.9; p≥0.05). In addition, the proportion of mitotic NPCs in anaphase was normal in *Pu.1*$^{-/-}$ mutants (**Figure 4.10B**, 50s *Pu.1*$^{+/+}$ 28±4% anaphase NPCs cells/total pHH3^{+} NPCs vs. *Pu.1*$^{-/-}$ 29.5±4%, p≥0.05). Thus, it is unlikely that microglia are required to maintain NPC cell division to late stages of hindbrain neurogenesis. This analysis does not, however, exclude roles for microglia in other aspects of neurogenesis, or indeed potential regulation of NPC mitosis by hindbrain microglia at other stages.

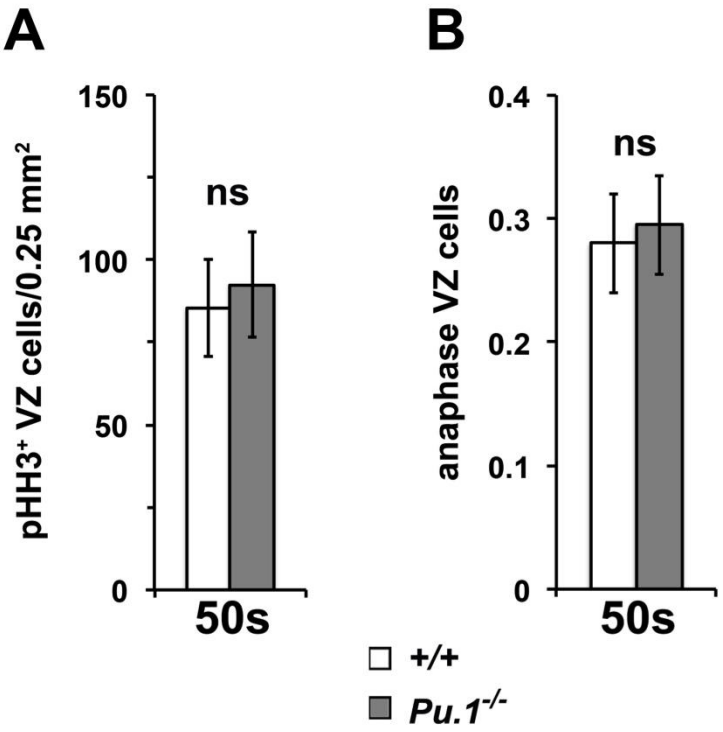

Figure 4.10 Microglia do not regulate hindbrain NPC mitosis at 50s.

(**A-B**) Quantification of mitotic NPCs in wildtype and *Pu.1*$^{-/-}$ hindbrains. The total number of pHH3^{+} NPCs per 0.25 mm^2 area and the proportion of NPCs in anaphase are shown in (**A**) and (**B**), respectively. All graphs show the mean ± standard deviation of the mean, n≥2 for each time point and genotype. ns (not significant) p≥0.05.

4.3 Discussion

The use of somite staging has been used historically for accurately defining periods of organogenesis and tissue morphogenesis during development (Theiler, 1989). During my PhD, I have used it similarly for precisely matching mutant embryos with defects in blood vessel growth with appropriate controls. I have shown that hindbrain NPCs divide rapidly and over a short space of time, and the trend in NPC mitosis changes significantly over just a few hours (**Figure 3.4**). This highlights the need for stage matching, as any difference determined between wildtype and NRP1-null embryos, for example (**Figure 4.1**), may partially or completely result from the developmental delay, and thus hinder analysis of neural development. Therefore, by precisely staging mutant embryos and comparing them to stage-matched wildtype animals from a different litter based on the number of somite pairs, I have eliminated any potential experimental bias arising from a delay in development.

I considered the possibility that NRP1 affects somitogenesis and therefore precludes accurate stage matching. However, this is unlikely for two key reasons. Firstly, NRP1 is not expressed by the paraxial mesoderm that makes up the somite, but instead by the neural crest cells that migrate past and between the somites (Schwarz et al., 2009). Secondly, embryos lacking NRP1 in endothelial and microglial cells only (*Tie2-Cre; Nrp1*$^{c/-}$) also possess a developmental delay in comparison to wildtype littermates. Therefore, it is likely that the delay results from severe cardiovascular defects observed in full and endothelial-specific *Nrp1* mutants and not from a role in regulating somitogenesis (Plein et al., 2015, Kawasaki et al., 1999).

NRP1 is crucial for vessel outgrowth and fusion in both the developing hindbrain and postnatal retina (Raimondi et al., 2014, Fantin et al., 2015). In the former, I have demonstrated that it is required for the formation of the SVP that is ideally situated to supply the GZ (**Figure 4.2**). However, despite the fact that filopodial extensions from endothelial cells project to the layer of mitotic NPCs (

Figure 3.2), it is not clear why the SVP does not form as close to the ventricular surface. NPCs may balance the effect of expressing pro-angiogenic

VEGF-A by secreting factors that are inhibitory towards further vessel growth, like sFLT1. Alternatively, an unknown anatomical landmark, such as a limiting membrane, may physically restrict radial vessels from sprouting as far as the ventricular surface. This possibility seems less likely, however, as it could also perturb hindbrain INM.

I have also shown that hindbrain GZ vascularisation occurs in a partially 'dose-dependent' manner with respect to NRP1 expression. Thus, the GZ contains some sparse vasculature at 32s following only partial recombination of NRP1 in *Tie2*-expressing blood vessels (*Tie2-Cre; Nrp1*$^{c/-}$ embryos, **Figure 4.7**) but is completely avascular when NRP1 is constitutively lost (*Nrp1*$^{-/-}$ embryos, **Figure 4.2**; (Fantin et al., 2013a). Whilst we can exclude roles for NRP1 in transducing both SEMA3 (Vieira et al., 2007) and VEGF-A (Fantin et al., 2014) signals during hindbrain angiogenesis, it is possible that an unidentified ligand promotes GZ vascularisation in addition to ECM signalling (Raimondi et al., 2014). Furthermore, NRP1 likely functions in a co-receptor complex during SVP formation, but no co-receptor has of yet been identified.

It is unclear, however, whether the loss of GZ vasculature in particular has a significant effect on normal NPC behaviour. Despite showing delayed outgrowth of radial vessels, poor GZ vascularisation and a rudimentary vessel network, equal numbers of radial vessels ingress into the *Nrp1*-null hindbrain (Fantin et al., 2015) and the neuroepithelium contains patent vasculature (see **Figure 4.2** and **Figure 4.6**). This vasculature is likely sufficient for tissue homeostasis, as cell survival is not compromised in *Nrp1*$^{-/-}$ embryos (**Figure 4.3**), indicating that defective angiogenesis does not render hindbrains ischaemic. Hindbrain NPCs in *Nrp1*$^{-/-}$ embryos may also receive sufficient blood flow for tissue oxygenation and/or potential angiocrine signalling, and impaired vascularisation of the GZ does not necessarily negate the delivery of either oxygen or secreted ligands that can diffuse long distances. This is exemplified by the long-range action of VEGF-A in both the embryonic (Ruhrberg et al., 2002) and postnatal CNS (Ruiz de Almodovar et al., 2010). Assessing the diffusible range of secreted factors, like with the small fluorescent molecule fluorescein, should help define whether vessel-derived cues are still able to reach the

entire neuroepithelium despite defects in angiogenesis. This method of defining the perfusable area around cerebrovasculature has been employed for studies of the SVZ, although the CSF there can also act as an additional route for the delivery of fluorescein to NSCs (Tavazoie et al., 2008). For these considerations, I have addressed the role of GZ vasculature in tissue oxygenation later in this thesis (see **5.2.6**).

Perineural blood vessels are required for regulating cell division in NSCs and loss of paracrine signalling from cerebrovasculature impairs long-term adult neurogenesis (Ottone et al., 2014, Shen et al., 2008, Delgado et al., 2014, Andreu-Agullo et al., 2009). My analysis of hindbrains that lack *Nrp1* either globally or in endothelial cells only demonstrates that the precise timing of NPC mitotic activity is regulated by the SVP that occupies the GZ (**Figure 4.4** and **Figure 4.7**). Yet, it is unclear what specifically causes the increase in $pHH3^{+}$ NPCs following the loss of NRP1 between 32-36s. This increase does not appear to be the result of a rise in NPC cell division; instead, progenitors in the hindbrain appear to stall in anaphase. The increased time spent in mitosis, therefore, may directly precede a switch to neurogenic divisions that ultimately deplete the NPC pool. This 'mitotic lag' that has been reported to perturb NPC behaviour in the developing forebrain (Pilaz et al., 2016). Prolonged mitosis in aRG results in the generation of neurons rather than APs, preventing any further expansion of the neural lineage. In this study, organotypic culture of forebrain sections was utilised to visualise NPC mitosis in real time (Pilaz et al., 2016). Unfortunately, however, immature blood vessels degenerate quickly *ex vivo* (Schwarz et al., 2004) and even *in vivo* postnatally (Licht et al., 2015), preventing this form of analysis for examining vascular regulation of NPCs.

Surprisingly, despite widespread expression across hindbrain NPCs, NRP1 does not modulate NPC mitotic activity directly (**Figure 4.7**), as documented for other membrane-bound receptors like NOTCH1 or p75NTR (Shimojo et al., 2008, Ahmed et al., 1995). I have shown that NPC mitosis is only perturbed after dual loss of semaphorin signalling through both NRPs, suggesting that NRP2 may indeed offset any loss in function resulting from the elimination of SEMA-NRP1 signalling (**Figure 4.8**). Moreover, NRP2 itself may actually be indispensable, as the decrease

in mitosis observed in *Nrp2*$^{-/-}$ hindbrains at 49s would likely become statistically significant with a greater sample size (n=2). This is somewhat surprising, however, given that NRP2 only appears to be expressed prominently at the midline from 32-46s and it is unclear how it can function in VZ NPCs given it is not expressed at the ventricular surface.

NRP1 may be required for normal orientation of the mitotic spindle in spinal cord NPCs that likely develop similarly to hindbrain NPCs given their anatomical proximity to one another (Arbeille et al., 2015). Yet, it is unclear whether one or both neuropilins are required for this process in the spinal cord as spindle orientation was only studied in embryos lacking semaphorin binding to both NRP1 and NRP2 (Arbeille et al., 2015). Whilst I have not examined mitotic spindle orientation of hindbrain NPCs in embryos selectively lacking *Nrp1* in the neural lineage, I have studied the pattern of NPC mitosis in these embryos and observed that the pattern of cell division is unchanged. In contrast, loss of SEMA3B, which is proposed to bind either one or both of NRP1 and NRP2 in the spinal cord, results in the precocious decline of mitosis in the spinal cord VZ at e11.5, as well as the premature generation of Islet1/2^{+} motoneurons (Arbeille et al., 2015). Unfortunately, it has not been defined unequivocally whether SEMA3B signals through NRP1 and/or NRP2 in NPCs. By analysing NPCs in *Nes-Cre; Nrp1*$^{c/-}$ spinal cords, future work could determine whether SEMA3B binds to NRP1, and whether SEMA3B signals solely through NRP1 or if NRP2 acts redundantly with NRP1 to ensure correct spindle orientation.

I have shown additionally that VEGF-A does not signal through the receptor tyrosine kinase VEGFR2, as VEGFR2 is not expressed by NPCs throughout the period of hindbrain neurogenesis (25-50s; **Figure 4.9**), despite being abundantly expressed by nearby endothelium. This finding is in agreement with the lack of VEGFR2 expression by non-endothelial cells in the embryonic forebrain (Javaherian and Kriegstein, 2009), suggesting that VEGF-A does not signal directly through its classical receptor in NPCs during development. Furthermore, conditional deletion of VEGFR2 in neural cells did not affect NPC proliferation in the forebrain of *Nes-Cre;*

Kdr$^{c/-}$ embryos, although efficient knockdown of VEGFR2 was not confirmed in these animals (Haigh et al., 2003).

These observations are in stark contrast to studies performed on embryonic NPCs propagated in culture, that require VEGF-A/VEGFR2 signalling to maintain cell survival and ensure expansion of NPCs *in vitro* (Wada et al., 2006). In agreement, I have shown that only cultured 'neurospheres' derived from hindbrain NPCs, not FACS-isolated NPCs, express *Kdr,* indicating that VEGFR2 may only be expressed once progenitors have been isolated from their position *in vivo* and propagated in culture. Placing NPCs in culture may separate them from a vital signalling mechanism from the surrounding niche that maintains cell survival and would normally negate the need for additional neuroprotective VEGF-A signals. Taken together, these results suggest that cell autonomous VEGF-A/VEGFR2 pro-survival signalling is likely to be a requirement of *in vitro* NPCs only.

These findings also indicate that VEGFR2 is unlikely to function in a co-receptor complex with NRP1 to convey VEGF-A signals in hindbrain NPCs. NRP1 may regulate other aspects of NPC behaviour cell autonomously in hindbrain NPCs that I have not studied during my PhD and therefore, NRP1 may yet operate as a VEGF-A receptor. However, VEGF-A signalling through NRP1 in neural cells has only been demonstrated in post-mitotic neurons that are actively sprouting axons or undergoing neuronal migration (Schwarz et al., 2004, Erskine et al., 2011).

INM progresses in phase with the NPC cell cycle and NPC nuclei travel further from towards the pial surface when G1 lengthens (Del Bene et al., 2008, Baye and Link, 2007). My analysis of the GZ in *Nrp1*$^{-/-}$ hindbrains shows that NPCs migrate further from the ventricular surface at 32s but I have not yet determined whether NRP1 maintains INM through a direct role in NPCs or by promoting the formation of the SVP (**Figure 4.5**).

NRP1 may directly regulate INM by transducing chemorepulsive semaphorin signals to limit basal migration of NPC nuclei, similar to those that restrict the migration of the soma of post-mitotic neurons (Tamamaki et al., 2003). However, this would not explain why NPC nuclei migrate less towards the pial surface at 40s

in *Nrp1*$^{-/-}$ embryos, causing the GZ to become significantly thinner, if NRP1-induced chemorepulsion is a continued requirement.

Alternatively, the SVP itself may regulate basally-directed INM. Firstly, the SVP could act as a physical barrier for NPCs undergoing INM, thus slowing the progression of NPC nuclei towards the pial surface. Indeed, it has been suggested previously that INM may be regulated by the physical restriction of migrating NPCs by surrounding cells (Taverna and Huttner, 2010). Secondly, the SVP may actually act as a migratory substrate for NPCs to enhance INM, similar to migrating neuroblasts along the RMS (Snapyan et al., 2009). However, this seems unlikely given that NPCs migrate further in *Nrp1*$^{-/-}$ hindbrains that lack vasculature. Live imaging of hindbrain NPCs undergoing INM could define whether the SVP directly regulates nuclear migration. However, as discussed previously, this is not yet attainable.

RC2^{+} NPC processes extend normally between the ventricular and pial surfaces in almost all regions of the hindbrain in NRP1-null embryos, but are mildly disorganised and entangled in regions with abnormal or absent blood vessels (**Figure 4.6**). However, I have not yet determined whether NRP1 regulates process organisation cell autonomously by enabling cell adhesion, or non-cell autonomously by promoting formation of the SVP that then acts a substrate for NPC anchorage.

NRP1 itself is hypothesized to mediate cell adhesion in the developing avian CNS and could therefore be required for process attachment to hindbrain vasculature (Shimizu et al., 2000, Takagi et al., 1995). NRP1 is expressed along the length of NPC processes during hindbrain development (Fantin et al., 2013a) so may also be required for adhesion to other NPCs, or even to facilitate the radial migration of newly-generated neurons (Noctor et al., 2001). Analysis of process organisation in *Nes-Cre; Nrp1*$^{c/-}$ embryos should demonstrate whether NPCs use NRP1 to tether themselves to blood vessels or indeed, to each other. Radial vessels may also require NRP1 to maintain alignment with NPC processes, given that radial vessels do not track properly with processes in the basal compartment of the *Nrp1*$^{-/-}$ hindbrain (**Figure 4.6**). NPCs may therefore facilitate radial vessel outgrowth from the PNP through a role cell adhesion, in addition to their role in stabilising immature vascular

networks (Ma et al., 2013). However, the ligand(s) responsible for NRP1-mediated cell adhesion is not yet known (Raimondi et al., 2016).

On the other hand, NRP1 may facilitate NPC attachment to hindbrain vasculature by promoting formation of the SVP. The disorganisation of processes in avascular regions of both *Nrp1*$^{-/-}$ and *Tie2-Cre; Nrp1*$^{c/-}$ hindbrains suggests that NPC processes may lose a vital anchorage point when angiogenesis is impaired, although I have not unequivocally established whether NPCs detach from blood vessels. As LAMA1 is still abundantly expressed by hindbrain blood vessels, NPCs may still be able to attach to the sparse vasculature that remains via laminin-integrin interactions, like those in the forebrain (Tan et al., 2016).

My analysis of mitotic NPCs in *Pu.1*$^{-/-}$ hindbrains suggests that microglia are not essential for sustaining NPC mitosis until later stages of hindbrain development, despite expressing NRP1 (Fantin et al., 2010). NPC mitosis remains at normal levels at 50s in embryos lacking all cells from the myeloid lineage, in contrast to the decline in cell division observed in embryos lacking NRP1 globally or in endothelial cells only at a similar stage (compare **Figure 4.4** and **Figure 4.7** with **Figure 4.10**). I have not examined whether microglia are required for regulating NPCs at earlier stages, such as at e11.5 when they are most abundant in the hindbrain during the period of vascular anastomosis (Fantin et al., 2010).

The SVP is poorly connected in the absence of microglia, as a result of reduced vessel fusion (Fantin et al., 2010), but this too does not appear to affect NPC mitosis at 50s. It seems more likely that the presence of endothelium in the GZ, rather than its correct organisation into a well-formed vessel plexus, is key to maintaining NPC mitosis into later stages of hindbrain development. Microglia themselves are sources of secreted factors, such as VEGF-C, but microglial VEGF-C has only been shown to play a role in postnatal retinal angiogenesis (Tammela et al., 2011). As VEGF-C regulates NPCs elsewhere in the developing vertebrate CNS (Le Bras et al., 2006), it is possible that it may be required also in the hindbrain. However, VEGF-C secreted by microglia clearly does not regulate NPC mitosis at 50s.

Specific roles for microglia also likely differ between the embryonic forebrain and hindbrain. Microglia actively maintain NPCs in both lissencephalic and gyrencephalic cortex during development, but may not possess the same function in the hindbrain that expands less and lacks BPs (Kwon and Hadjantonakis, 2007, Cunningham et al., 2013). In addition, microglia remain within the cortex long after birth (Cunningham et al., 2013) but depart from the hindbrain in mid-late gestation (A. Plein, unpublished observations), suggesting that microglia are required specifically by NPCs that are responsible for generating the cortex and keep expanding later into development (Fernandez et al., 2016).

4.4 Summary

NPC mitosis is regulated non-cell autonomously by NRP1, which promotes formation of GZ vasculature that sustains NPC cell division until later stages of the hindbrain neurogenesis time course. NPCs also undergo INM abnormally in *Nrp1*-null hindbrains whilst NPC processes are disorganised in hindbrains that lack timely SVP formation. Conversely, NRP1 is not required cell autonomously by NPCs for maintaining the normal pattern of mitosis and may function redundantly with NRP2 as a semaphorin receptor. These results indicate that GZ vascularisation is required to maintain normal levels of NPC proliferation and suggests that blood vessels in the embryonic CNS regulate NPCs through unidentified angiocrine signals.

Chapter 5 HINDBRAIN GERMINAL ZONE VASCULATURE REGULATES NEURAL PROGENITOR CELL SELF-RENEWAL

5.1 Introduction

NPCs balance self-renewal with differentiation, and prolonged self-renewal is essential for sustaining progenitor numbers later into development. Accordingly, premature loss of NPC self-renewal at early stages of neurogenesis results in depletion of NPC populations thereafter, compromising growth of the neuroepithelium (Hatakeyama et al., 2004, Sansom et al., 2009). I have observed a premature decline in the number of mitotic NPCs in hindbrains with impaired SVP formation (**Chapter 4**). It is therefore conceivable that the pool of NPCs becomes prematurely depleted in the absence of sufficient GZ vasculature due to the reduced self-renewal of early-formed progenitors. Alternatively, or additionally, NPCs may lose their capacity for cell division following the loss or reduction of mitogenic signals originating from hindbrain blood vessels. I have therefore determined whether NPCs lose their capacity to self-renew and whether reduction in NPC self-renewal impairs the overall growth of the hindbrain organ.

My observation of mitotic stalling of NPCs in *Nrp1*$^{-/-}$ and *Tie2-Cre*; Nrp1$^{c/-}$ hindbrains raises the possibility that loss of GZ vasculature alters cell cycle behaviour in NPCs. I have therefore determined the proportion of NPCs within each major cell cycle phase in stage-matched control and *Nrp1*$^{-/-}$ hindbrains and compared their expression of the gene encoding the cell cycle regulator cyclin D1.

Towards the end of my PhD research, it was demonstrated that vascularisation of the developing dorsal forebrain relieves local tissue hypoxia, which in turn allows aRG to differentiate into more fate-restricted BPs (Lange et al., 2016). Given that both the outgrowth of radial vessels and overall vascularisation are impaired in both *Nrp1*$^{-/-}$ and *Tie2-Cre*; Nrp1$^{c/-}$ hindbrains, I have examined whether defects in NPC proliferation may stem from reduced oxygenation of the neuroepithelium.

In the adult CNS, NSCs receive substantial angiocrine signalling from adjacent cerebrovasculature. I have therefore performed an expression screen to determine whether genes regulating neurogenesis extrinsically are differentially expressed in *Nrp1*$^{-/-}$ hindbrains. Finally, I have determined whether hindbrain blood vessels express a range of molecules known to regulate NPCs in the developing CNS.

5.2 Results

5.2.1 Loss of germinal zone vascularisation reduces neural progenitor cell cycle re-entry

Hindbrains lacking GZ vascularisation (in *Nrp1*$^{-/-}$ and *Tie2-Cre; Nrp1*$^{c/-}$ embryos) show a decline in mitotic activity after the time when the SVP is normally formed in wildtypes (**Figure 4.4** and **Figure 4.7**). This finding raises the possibility that NPCs undergo a premature loss of proliferative capacity and that NPC stemness may be regulated by vessel derived signals, analogous to those originating from the CSF to regulate NPCs in the forebrain (Megason and McMahon, 2002). To determine whether GZ vasculature sustains NPC mitotic activity, I have determined the proportion of NPCs that undergo self-renewal in full and endothelial-specific *Nrp1*-null hindbrains at 32s when the SVP normally forms.

I have defined NPC 'self-renewal' as the capacity for NPCs to re-enter the cell cycle to undergo further divisions. For this experiment, pregnant dams were administered 300 mg kg^{-1} of BrdU at approximately e9.5 before hindbrains were collected 24 hours later at the 32s stage (**Figure 5.1A**). BrdU would be incorporated into genomic DNA by all cell cycling NPCs at e9.5/25s, i.e. the majority of all hindbrain cells (note that most of the hindbrain is occupied by mitotic or S-phase NPCs in far left panel in **Figure 3.5**). I then immunolabelled 10 μm-thick transverse sections of stage-matched 32s stage-matched wildtype, *Nrp1*$^{-/-}$ and *Tie2-Cre; Nrp1*$^{c/-}$ hindbrains for BrdU and the proliferation marker Ki67. Ki67 is expressed in cells preparing to undergo cell division from roughly the end of G1 (Scholzen and Gerdes, 2000). Accordingly, cells double-labelled with BrdU and Ki67 24 h after initial BrdU administration are actively cycling NPCs. In contrast, Ki67^{-} BrdU^{+} cells are post-

mitotic cells, most likely differentiated neurons. I did not expect to observe $Ki67^+$ $BrdU^-$ cells, as all cycling NPCs should incorporate BrdU at e9.5 and ensure that all NPCs generated thereafter would be labelled with BrdU as well. Consistent with a loss of proliferative capacity later on in hindbrain development (**Figure 4.4** and **Figure 4.7**), I detected significantly fewer $Ki67^+$ NPCs (which were all also $BrdU^+$) in both *Nrp1* mutant strains compared to stage-matched controls (**Figure 5.1C**, $Ki67^+BrdU^+$ in all $BrdU^+$ at 32s: $Nrp1^{+/+}$ 84.5±5.9% vs. $Nrp1^{-/-}$ 59±6.3% vs. *Tie2-Cre*; $Nrp1^{c/-}$ 72.5±2%; $p<0.01$ for both vs. wildtype). I observed a significantly lower proportion of double-labelled NPCs in full $Nrp1^{-/-}$ mutants compared to endothelial-specific *Nrp1* hindbrains ($p<0.05$), likely because vascular defects are more severe in full NRP1 mutants compared to *Tie2-Cre*; $Nrp1^{c/-}$ embryos. Therefore, vascularisation of the GZ at 32s ensures that NPCs continue to cycle.

Interestingly, more single $BrdU^+$ cells were present at the pial basement membrane in both types of *Nrp1* mutants compared to controls, suggesting that NPCs exit the cell cycle and terminally differentiate earlier in hindbrains lacking GZ vasculature at or just before 32s (representative images shown in **Figure 5.1B**).

To determine whether NPC cell cycle re-entry is impaired also at 40s and 46s, I performed similar birth dating experiments in $Nrp1^{-/-}$ embryos, because their GZ vascularisation recovers less than that of endothelial-specific *Nrp1* mutants at later stages. Thus, pregnant dams were administered BrdU at e10.5 and e11.5 and hindbrains were analysed 24 h later (embryos were analysed at 40s and 46s because of the developmental delay; **Figure 5.2A**). Interestingly, the proportion of $Ki67^+$ $BrdU^+$ cells in all $BrdU^+$ cells was not different between wildtype and $Nrp1^{-/-}$ hindbrains at either stage (compare the size of yellow and red bars in **Figure 5.2B** at 40s and 46s).

Even though the proportion of cycling NPCs was unchanged at 40s and 46s, the total number of $BrdU^+$ cells and $Ki67^+$ NPCs in $Nrp1^{-/-}$ hindbrains was reduced in mutants compared to controls at 46s (**Figure 5.2C,D**, 46s $Nrp1^{+/+}$ 1289±154 $BrdU^+$ cells per section, 740±71 $Ki67^+$ NPCs per section vs. $Nrp1^{-/-}$ 589±98 $BrdU^+$ cells per section, 344±101 $Ki67^+$ NPCs per section; $p<0.01$ for both values). Indeed, transverse sections of *Nrp1*-null hindbrains contained visibly fewer BrdU-labelled

cells and basal, abventricular regions specifically lacked $BrdU^+$ cells (see Δ in representative images in **Figure 5.2E**). This suggests that fewer cell cycling NPCs are in S-phase at and following e11.5 (i.e. 24 h prior to analysis at 46s) to take up BrdU and agrees with the observation that fewer NPCs are in mitosis at this stage (**Figure 4.4**).

Taken altogether, these data indicate that the SVP is required to maintain NPC cell cycle re-entry at 32s and sustain the overall number of NPCs thereafter. Partial recovery of hindbrain vascularisation at 40s and 46s in *Nrp1*-null hindbrains may underlie the apparent restoration of normal cycling behaviour in NPCs that have escaped the earlier phase of increased cell cycle exit. Alternatively, later populations of NPCs may be less sensitive to signals provided by GZ vasculature than their earlier counterparts. In any case, this normalisation of cycling behaviour is unable to prevent depletion of the pool of cycling NPCs.

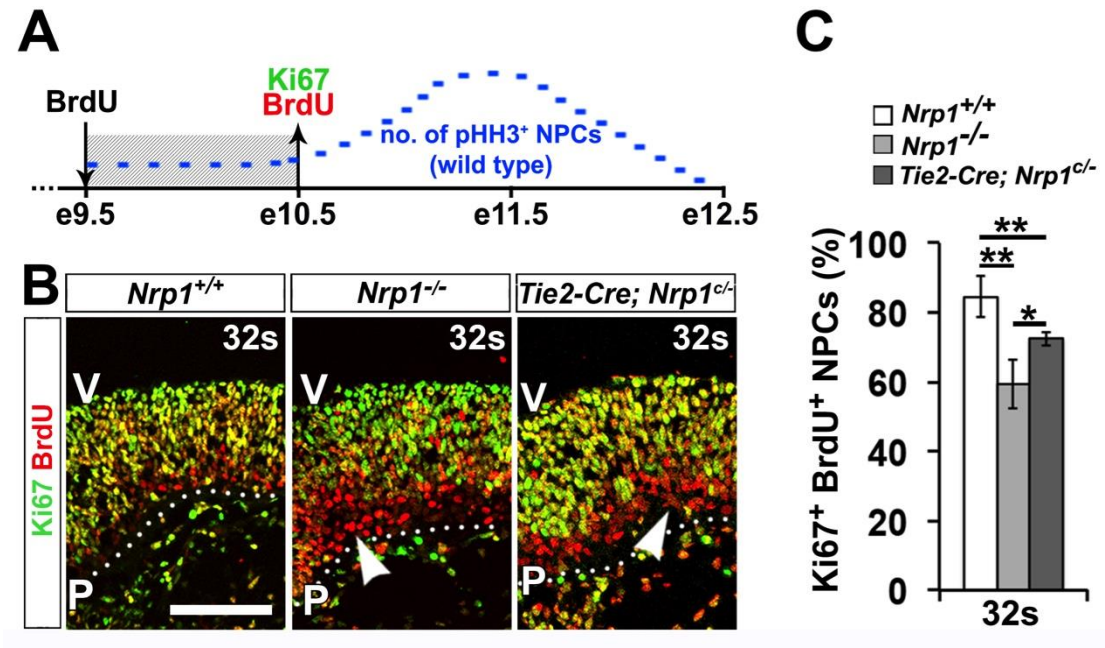

Figure 5.1 NPC cell cycle re-entry is impaired in hindbrains lacking GZ vasculature at 32s.

(**A**) Schematic representation of the BrdU birth dating strategy. Embryos received BrdU at approximately e9.5 and were analysed at 32s. The blue line represents the general trend of NPC mitosis across the main phase of hindbrain neurogenesis.

(**B**) 10 µm transverse sections from 32s stage-matched wildtype, *Nrp1*$^{-/-}$ and *Tie2-Cre; Nrp1*$^{c/-}$*; Tie2-Cre* hindbrains were labelled with antibodies for BrdU and Ki67. Dotted lines demarcate the basal hindbrain surface. Scale bar: 20 µm. Arrowheads indicate example of a Ki67^{-}/BrdU^{+} cell. Abbreviations: P, pial surface; V, ventricular surface.

(**C**) Proportion of Ki67^{+}BrdU^{+} in all BrdU^{+} cells (see **2.2.4**). Data are expressed as mean ± standard deviation of the mean; n≥3 for each genotype; * $p<0.05$, ** $p<0.01$.

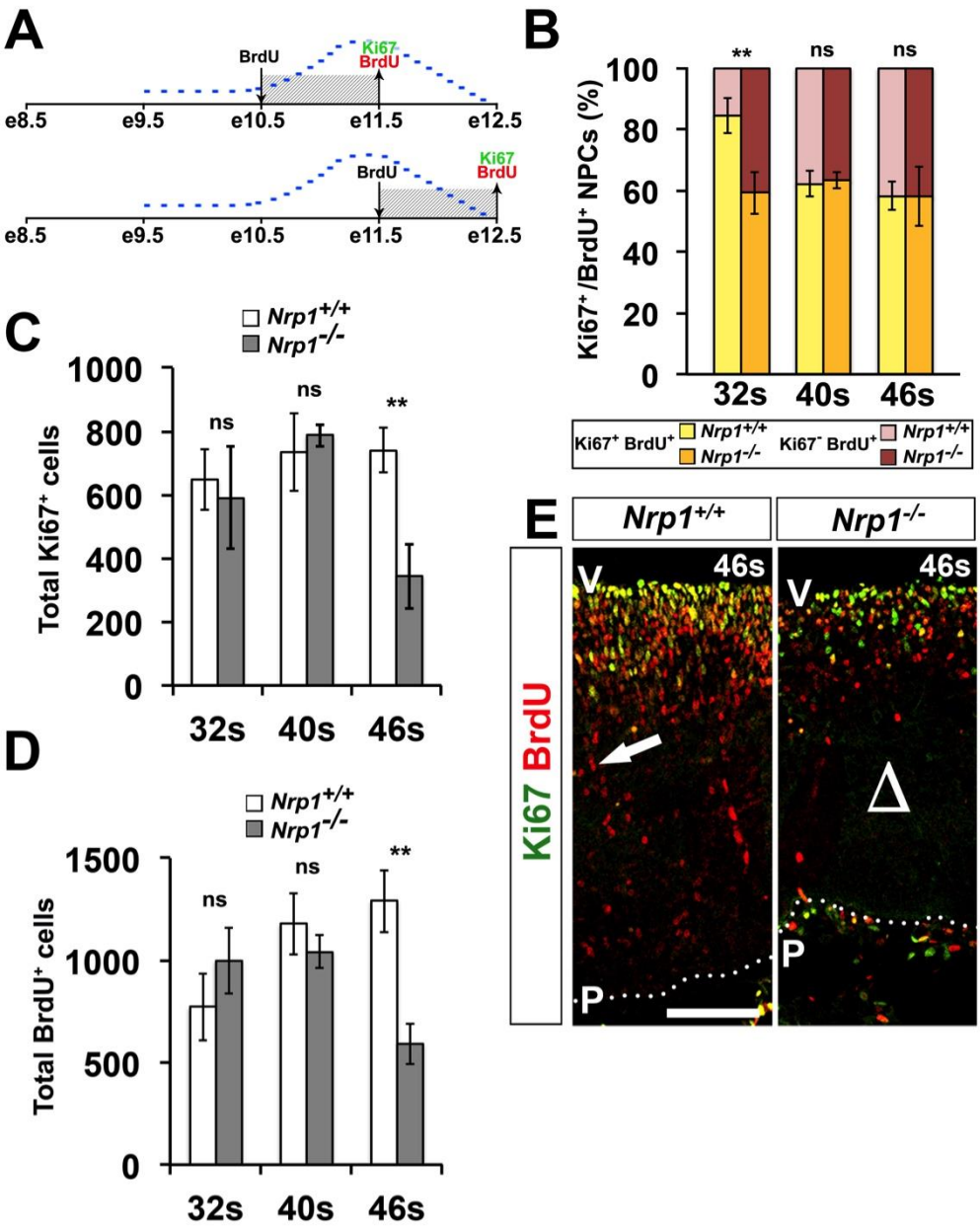

Figure 5.2 The proportion of cycling NPCs is normal in the *Nrp1*$^{-/-}$ hindbrains at 40s and 46s, but fewer cycling NPCs are present.

(**A**) Schematic representation of the BrdU birth dating strategy. Embryos received BrdU at either approximately e10.5 or e11.5 and were analysed 24 h later at e11.5 or e12.5, respectively. Owing to the developmental delay, *Nrp1*$^{-/-}$ mutants collected at e11.5 and e12.5 corresponded to 40s and 46s, respectively. The blue line represents the general trend of NPC mitosis across the main phase of hindbrain neurogenesis.

(**B-D**) Proportion of either $Ki67^{-}$ $BrdU^{+}$ (pink or red bars) or $Ki67^{+}$ $BrdU^{+}$ (yellow or amber bars) in all $BrdU^{+}$ cells (**B**). Total number of $BrdU^{+}$ cells following 24 h labelling at the indicated stages (**C**) and total number of $Ki67^{+}$ cells at the indicated stages (**D**). Data are expressed as mean ± standard deviation of the mean; n≥3 for each genotype; ns (not significant) p≥0.05, ** p<0.01.

(**E**) 10 μm transverse sections 46s stage-matched wildtype and *Nrp1*$^{-/-}$ hindbrains were labelled with antibodies for BrdU and Ki67. Dotted lines demarcate the basal hindbrain surface. Scale bar: 20 μm. Arrow indicates example of a $Ki67^{-}$ $BrdU^{+}$ cell away from the VZ, likely to be a radially migrating neuron. Δ illustrates the lack of $BrdU^{+}$ cells in the basal hindbrain at 46s. Abbreviations: P, pial surface; V, ventricular surface.

5.2.2 Loss of germinal zone vascularisation induces premature neuronal differentiation

As the 32s NRP1-null hindbrain contains fewer cycling NPCs, I hypothesized that it contained more NPCs undergoing neurogenic divisions. I therefore immunolabelled transverse sections of 32s stage-matched wildtype, *Nrp1*$^{-/-}$ and *Tie2-Cre; Nrp1*$^{c/-}$ hindbrains with the TUJ1 antibody for neuronal-specific βIII-tubulin, a common marker for differentiated neurons (Sullivan, 1988). To measure neuronal differentiation, I determined what percentage of the DAPI^{+} cross-sectional area of the 32s hindbrain was occupied by TUJ1 labelling.

Inversely correlating with reduced NPC self-renewal, I observed significantly more TUJ1^{+} immunolabelling at 32s in both full and endothelial-specific *Nrp1* mutants (**Figure 5.3A,B**, 32s *Nrp1*$^{+/+}$ 17.2±1.4% TUJ1^{+} area/DAPI^{+} area vs. *Nrp1*$^{-/-}$ 23.5±0.8% vs. *Tie2-Cre*; *Nrp1*$^{c/-}$ 23.2±3.2%; *Nrp1*$^{+/+}$ vs. *Nrp1*$^{-/-}$, $p<0.01$ and *Nrp1*$^{+/+}$ vs. *Tie2-Cre*; *Nrp1*$^{c/-}$, $p<0.05$). Whereas TUJ1 immunolabelling was restricted to the basal surface in control hindbrains, I detected ectopic TUJ1 expression in apical regions and even at the level of the VZ in both full and endothelial-specific *Nrp1* mutants (see arrows in representative images in **Figure 5.3A**). It would also be interesting, in the future, to expand this analysis to examine the production of neurons with pan-neuronal markers for their cell bodies, such as NeuN, or for specific neuronal subtypes, such as ISL1 for motor neurons (see **5.3**).

Whilst hindbrains lacking GZ vasculature have significantly more TUJ1 staining than controls at 32s, I found there to be significantly less TUJ1 expression in *Nrp1*-null hindbrains at both 40s and 46s (**Figure 5.4A**, 40s *Nrp1*$^{+/+}$ 54.1±3.2% TUJ1^{+} area/DAPI^{+} area vs. *Nrp1*$^{-/-}$ 47.3±2%; 46s *Nrp1*$^{+/+}$ 64.1±4.5% vs. *Nrp1*$^{-/-}$ 49.3±2.5%; $p<0.05$ and $p<0.01$, respectively). Therefore, *Nrp1*$^{-/-}$ hindbrains show a precocious decline in the formation of TUJ1^{+} neurons.

Furthermore, calculating the relative enrichment of TUJ1 in the hindbrain at 46s compared to that at 32s indicates that neurogenesis slows in *Nrp1*$^{-/-}$ hindbrains between 32-46s. NRP1-null embryos are only labelled with twice as much TUJ1 at 46s compared to 32s, in contrast to nearly four-fold enrichment in stage-matched

controls (**Figure 5.4B**, *Nrp1*$^{+/+}$ 3.7±0.26 factor increase in TUJ1^{+} area/DAPI^{+} area from 32s to 46s vs. *Nrp1*$^{-/-}$ 2.1±0.1 factor increase; $p<0.001$). These data demonstrate the hindbrain SVP restricts neuronal differentiation of NPCs at 32s, and ultimately sustains neurogenesis to later stages of development.

Immunolabelling was almost completely absent from the apical region of NRP1-null hindbrains at 46s, even though there is, surprisingly, widespread expression of TUJ1 along the entire apicobasal axis of the wildtype hindbrain (**Figure 5.4C**). Instead, large amounts of TUJ1^{+} cells appeared to accumulate midway along the apicobasal axis of the NRP1-null hindbrain, raising the possibility that neurons were unable to migrate to their correct position in the neuroepithelium. NRP1 may therefore be required for correct positioning of neurons in the hindbrain along the apicobasal axis. I have not yet examined whether this defect is recapitulated in hindbrains lacking NRP1 in the endothelial or neural lineage.

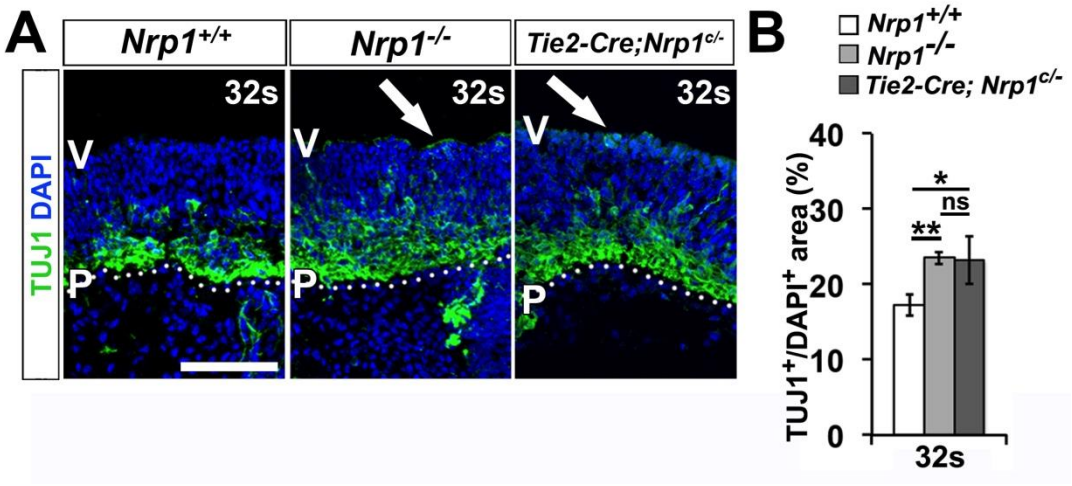

Figure 5.3 NPCs differentiate prematurely in the absence of GZ vasculature in *Nrp1*$^{-/-}$ and *Tie2-Cre; Nrp1*$^{c/-}$ hindbrains at 32s.

(**A**) 10 μm transverse sections from 32s stage-matched wildtype, *Nrp1*$^{-/-}$ and *Tie2-Cre; Nrp1*$^{c/-}$ hindbrains were labelled with TUJ1. Dotted lines demarcate the basal hindbrain surface. Scale bar: 20 μm. Arrow indicates example of ectopic TUJ1 staining in the VZ. Abbreviations: P, pial surface; V, ventricular surface.

(**B**) Quantification of TUJ1 staining, calculated as TUJ1^{+} area divided by the DAPI^{+} area (see **2.2.4**). Data are expressed as mean ± standard deviation of the mean; n≥3 for each genotype; ns (not significant) p≥0.05, * p<0.05, ** p<0.01.

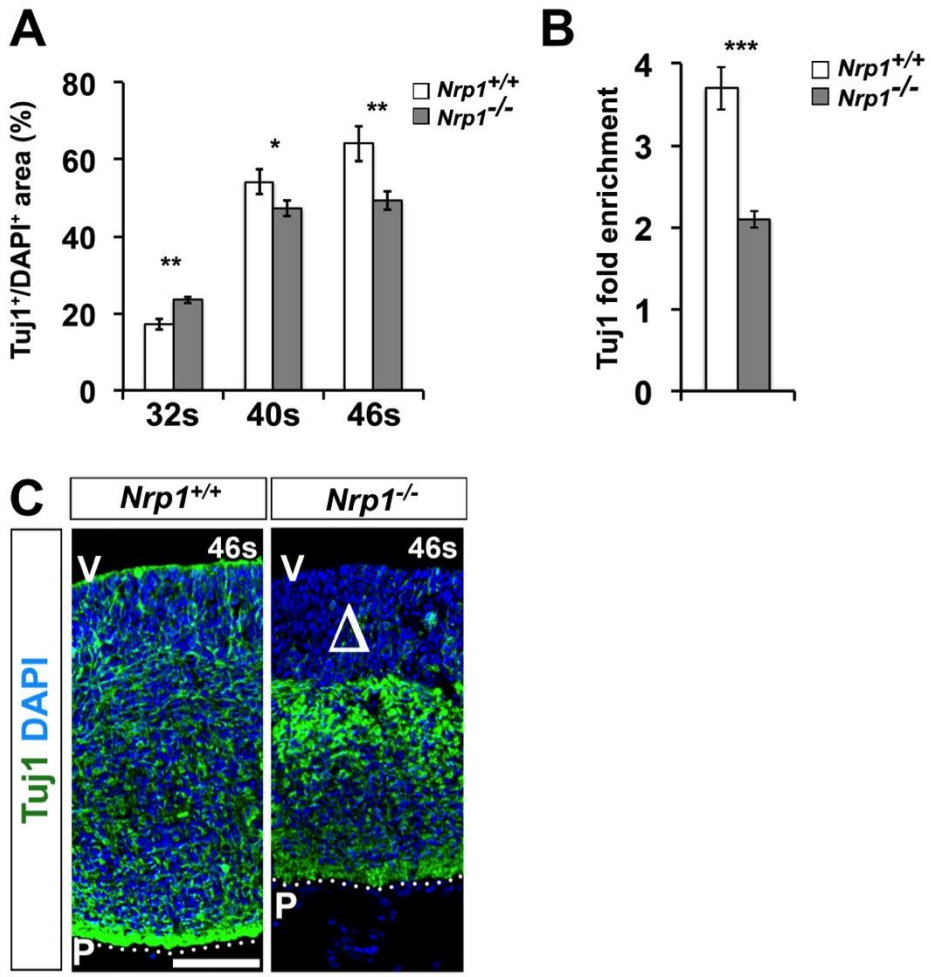

Figure 5.4 Reduced neurogenesis in *Nrp1*$^{-/-}$ hindbrains at 40s and 46s.

(**A**) Quantification of the area occupied by neurons, calculated as TUJ1^{+} area divided by the DAPI^{+} area.

(**B**) Enrichment of TUJ1 staining from 32s to 46s, calculated as TUJ1 pixel intensity at 46s divided by TUJ1 pixel intensity at 32s.

(**C**) Abnormal distribution of TUJ1 labelling in the *Nrp1*-null hindbrain. 10 µm transverse sections from hindbrains of 46s stage-matched wildtype and *Nrp1*$^{-/-}$ embryos were labelled with TUJ1. Dotted lines demarcate the basal hindbrain surface. Scale bar: 20 µm. Δ indicates lack of TUJ1 staining in the apical hindbrain of *Nrp1*-deficient hindbrains. Abbreviations: P, pial surface; V, ventricular surface.

Data are expressed as mean ± standard deviation of the mean; n≥3 for each genotype; * $p<0.05$, ** $p<0.01$, *** $p<0.001$.

5.2.3 Cell cycle analysis of hindbrain NPCs by fluorescence-activated cell sorting (FACS)

Cell cycle progression is modulated by both intrinsic and extrinsic factors in NPCs undergoing the transition from self-renewing to differentiative or neurogenic divisions (Calegari et al., 2005). Perturbing cell cycle progression, such as by prolonging G1, results in a premature switch to neurogenesis (Lange et al., 2009). I therefore asked whether progression through the cell cycle was regulated by signals derived from GZ vasculature and if the precocious neurogenesis I have observed in *Nrp1*$^{-/-}$ and *Tie2-Cre; Nrp1*$^{c/-}$ hindbrains correlates with specific perturbations of cell cycle kinetics in NPCs. To answer this question, I have used a FACS-based method to first determine the specific proportion of isolated hindbrain NPCs within each phase of the cell cycle at a given time point, as used previously (Morte et al., 2013). Secondly, following cell cycle analysis, I have quantified the relative expression of *Ccnd1* in these NPCs by qRT-PCR to determine the likely expression levels of cyclin D1, which is responsible for the transition from G1 to S-phase in embryonic NPCs (Lange et al., 2009).

I have purified hindbrain NPCs for prospective cell cycle and qRT-PCR analyses using FACS, to isolate NPCs from hindbrain tissue. Initially, I have excluded CD11b^{+} (ITGAM) macrophages and CD31^{+} (PECAM) endothelial cells (left-hand panel in **Figure 5.5A**) and then collected CD31^{-} CD133^{+} NPCs (top right-hand panel in **Figure 5.5A**; **Figure 5.5B**; (Denny et al., 2013). CD31-negative cells were excluded from the total CD133^{+} population, as endothelial progenitor cells have been reported to express CD133, and may, conceivably, also exist in the mouse hindbrain (Nguyen et al., 2009, Paprocka et al., 2011). NPCs were then analysed for cell cycle phase (**Figure 5.5B**). To collect NPCs for RNA extraction and qRT-PCR, I additionally screened CD133^{+} cells for expression of CD56 (NCAM; neural cell adhesion molecule) to exclude CD56^{hi} cells (bottom right-hand panel in **Figure 5.5A**; **Figure 5.5B**). Although CD56 expression is typical of migrating, post-mitotic neurons (Angata et al., 2007, Rieger et al., 2008), it is also expressed in the hindbrain at e9.5/25s when almost all cell types are likely to be proliferating NE (Pfaff et al., 1996). Furthermore, expression of CD56 increases progressively with differentiation (Shin et al., 2002) and as a result, FACS does not reveal a specific CD56^{-} CD133^{+}

population to classify as bonafide NPCs (see bottom right-hand panel in **Figure 5.5A**). Therefore, I have collected $CD133^{+}$ $CD56^{low}$ cells, likely to be NE and aRG, as the most accurate strategy for targeting NPCs. Whilst the sorting strategy identified a sufficiently pure population of $CD133^{+}$ $CD56^{low}$ NPCs, the final yield of progenitors was poor and represented only 0.2-0.5% of all single cells. It would therefore be important to improve the FACS protocol for future studies (see **5.3**).

For the DNA content analysis, I homogenised hindbrains, generated single cell suspensions from each sample and incubated these homogenates with 10 μg/ml Hoechst 33342 to label DNA for 30 mins at 37°C in the dark. All Hoechst staining solution was then removed and cells were labelled with fluorescently-conjugated antibodies for FACS (as described above). Owing to the relatively low yield of NPCs isolated, I retrospectively decided to exclude CD56 from digital analysis of Hoechst labelled, $CD133^{+}$ NPCs to increase the number of NPCs available for defining cell cycle progression.

$CD133^{+}$ NPCs with Hoechst labelling equalling an arbitrary ~2n value were defined as being in G1 phase (i.e. diploid), whilst NPCs with a Hoechst labelling intensity of roughly double (i.e. ~4n) were regarded as being in G2/M phase. NPCs with Hoechst labelling between these values (i.e. $2n<x<4n$) were defined as being in S-phase (Goodell et al., 1996). From FACS profiles, I therefore quantified the relative proportion of NPCs in each phase of the cell cycle and compared the percentage of NPCs in G1, S- and G2/M phases in stage-matched control and *Nrp1*$^{-/-}$ hindbrains at either 32s or 36s to determine whether GZ vasculature regulates NPC cell cycle progression (see **Figure 5.6B,C**).

Representative FACS plots taken of NPCs isolated from individual wildtype hindbrains at 32-38s exhibited substantial variation during development (**Figure 5.5C**). The fraction of NPCs in G2/M was considerably greater than in G1 at 32s, but this pattern gradually reversed over time as the proportion of progenitors in G1 increased substantially at 36s and 38s (compare left-hand panel with middle- and right-hand panels in **Figure 5.5C**). Accordingly, the fraction of NPCs in both S- and G2/M phases decrease with time, suggesting a significant shift in the relative duration of each cell cycle phase across only a few hours (32s ~e10.25; 38s ~e10.75).

Histograms displaying Hoechst labelling intensity were relatively ‘coarse’, a disadvantage of determining DNA content in a low yield of cells (Saade et al., 2013), and hindered clear definition of peaks belonging to each cell cycle phase (note the lack of smooth peaks corresponding to either S- or G2/M phases at all three time points in **Figure 5.5C**). Yet, FACS analysis of Hoechst-labelled NPCs demonstrates that the length of each cell cycle phase changes considerably over time and that FACS analysis may be used for comparing cell cycle progression between wildtype and hindbrains lacking GZ vasculature.

These findings demonstrate that hindbrain NPCs can be purified by FACS and that their ploidy can be determined following DNA labelling with Hoechst 33342. The ploidy, and therefore proportional occupancy of the different cell cycle phases, shifts over time amongst the population of NPCs, as the overall ratio of NPCs in G1 to those in S/G2/M increases from 32-38s.

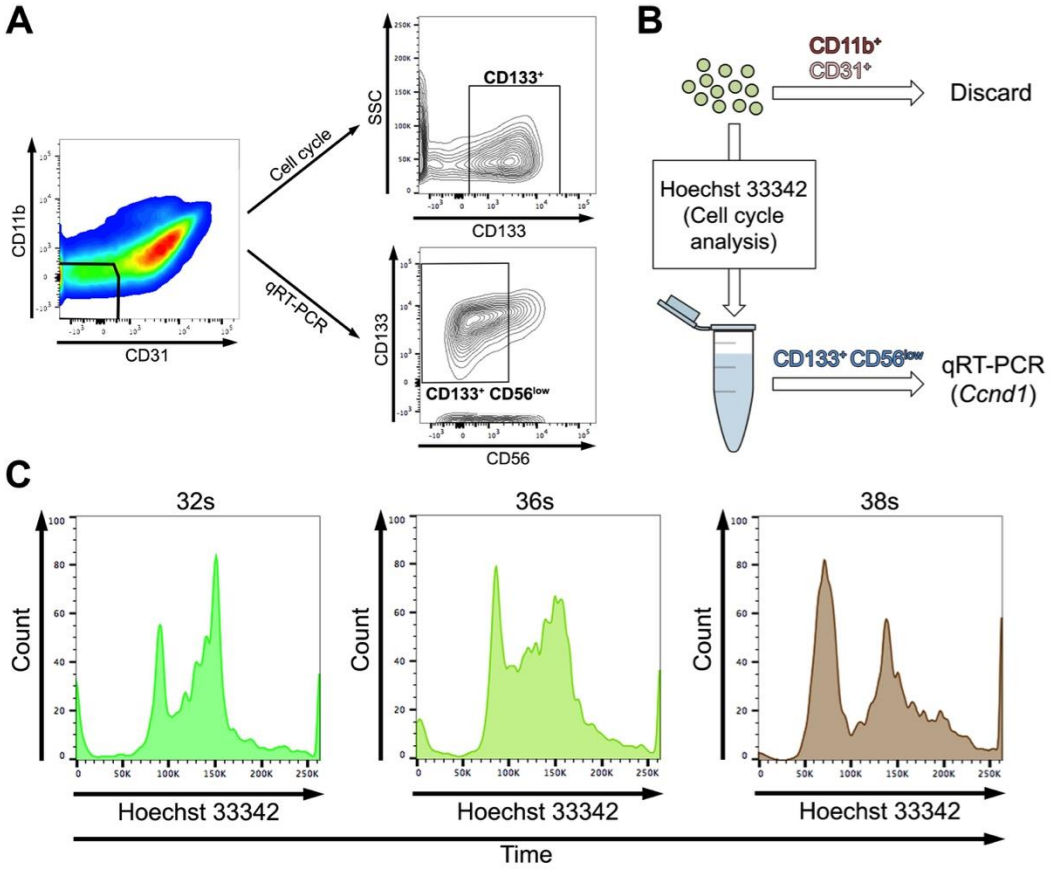

Figure 5.5 FACS analysis of hindbrain NPCs.

(**A**) Strategy for isolating hindbrain NPCs by FACS. $CD11b^+$ macrophages and $CD31^+$ endothelial cells were excluded (left panel) and the double negative cells (boxed area in the left panel) were gated for either $CD133^+$ (top right-hand panel) or $CD133^+$ $CD56^{low}$ (bottom right-hand panel) to obtain NPCs.

(**B**) Schematic representation of FACS workflow for isolating NPCs for cell cycle analysis and qRT-PCR. $CD11b^+$ and $CD31^+$ cells were excluded, Hoechst labelled $CD133^+$ NPCs were analysed for cell cycle progression and then $CD133^+$ $CD56^{low}$ cells were collected for qRT-PCR.

(**C**) Hoechst 33342 labelling intensity was used to determine the relative distribution of NPCs in different cell cycle phases. Profiles for NPCs isolated from wildtype hindbrains at three developmental stages are shown.

5.2.4 Germinal zone vasculature regulates cell cycle progression in hindbrain NPCs

I next employed FACS analysis to determine whether the fraction of NPCs in each cell cycle phase in *Nrp1*-null hindbrains was abnormal around the developmental time point when GZ vasculature is normally established. Thus, I analysed NPCs at 32s, when NPC self-renewal was lower in $Nrp1^{-/-}$ mutants (**Figure 5.1B,C**). In addition, I studied hindbrain NPCs at 36s, when I observed a specific lag in mitosis during anaphase (**Figure 4.4C**).

Surprisingly, I did not detect any changes to cell cycle progression in NPCs in $Nrp1^{-/-}$ hindbrains at 32s (**Figure 5.6A,B**) despite premature differentiation of NPCs (**Figure 5.1Figure 5.3**). Thus, the proportion of NPCs in G1 (**Figure 5.6B**, $Nrp1^{+/+}$ 23.5±2.3% vs. $Nrp1^{+/+}$ 26.0±2.4%; $p \geq 0.05$), S- (**Figure 5.6B**, $Nrp1^{+/+}$ 50.4±1.2% vs. $Nrp1^{+/+}$ 49.5±1.1%; $p \geq 0.05$) and G2/M (**Figure 5.6B**, $Nrp1^{+/+}$ 26.2±1.5% vs. $Nrp1^{+/+}$ 24.5±3.3%; $p \geq 0.05$) phases was similar between either genotype. The lack of cell cycle defects in $Nrp1^{-/-}$ hindbrains at this stage therefore suggests that $CD133^{+}$ NPCs that remain following the period of cell cycle exit prior to 32s progress normally.

In contrast, cell cycle progression of hindbrain NPCs at 36s was different in *Nrp1*-null hindbrains. Firstly, a significantly higher percentage of NPCs were retained in G1 phase, indicative of G1 lengthening (**Figure 5.6A,C**, $Nrp1^{+/+}$ 26.3±1.9% vs. $Nrp1^{+/+}$ 50.0±10.4%; $p<0.01$). Secondly, I detected a smaller proportion of NPCs in S-phase, suggesting that S-phase is shorter in NPCs in the $Nrp1^{-/-}$ hindbrain (**Figure 5.6A,C**, $Nrp1^{+/+}$ 45.8±2.6% vs. $Nrp1^{+/+}$ 23.4±8.0%; $p<0.01$). Both these observations are consistent with changes in cell cycle progression that precede a switch from self-renewing to differentiative or neurogenic cell divisions in the forebrain (Arai et al., 2011, Calegari et al., 2005). The proportion of NPCs in G2/M, however, was unchanged (**Figure 5.6A,C**, $Nrp1^{+/+}$ 27.9±2.7% vs. $Nrp1^{+/+}$ 26.8±5.2%; $p \geq 0.05$), although the G2 and M phase or specific sub-phases of mitosis cannot be resolved due to the similar DNA content in all these phases.

Ccnd1 expression levels support the results obtained by FACS analysis. I found that at 32s, expression of *Ccnd1* is normal between stage-matched control and *Nrp1*$^{-/-}$ hindbrains (**Figure 5.6D**, *Nrp1*$^{-/-}$ 1.12±0.24 factor fold change, $p \geq 0.05$). However, there is a significant downregulation of *Ccnd1* expression in NPCs at 36s in *Nrp1*$^{-/-}$ hindbrains, raising the possibility that G1 phase is prolonged (**Figure 5.6D**, *Nrp1*$^{-/-}$ 0.02±0.003 factor fold change, $p < 0.05$). Together, these observations indicate that the cell cycle slows in NPCs in *Nrp1*$^{-/-}$ hindbrains at 36s, with a specific lengthening of G1 and shortening of S phase phases. Delayed transition from G1 to S-phase may result from a substantial reduction in cyclin D1 expression. However, further experiments with additional markers are required to substantiate this possibility.

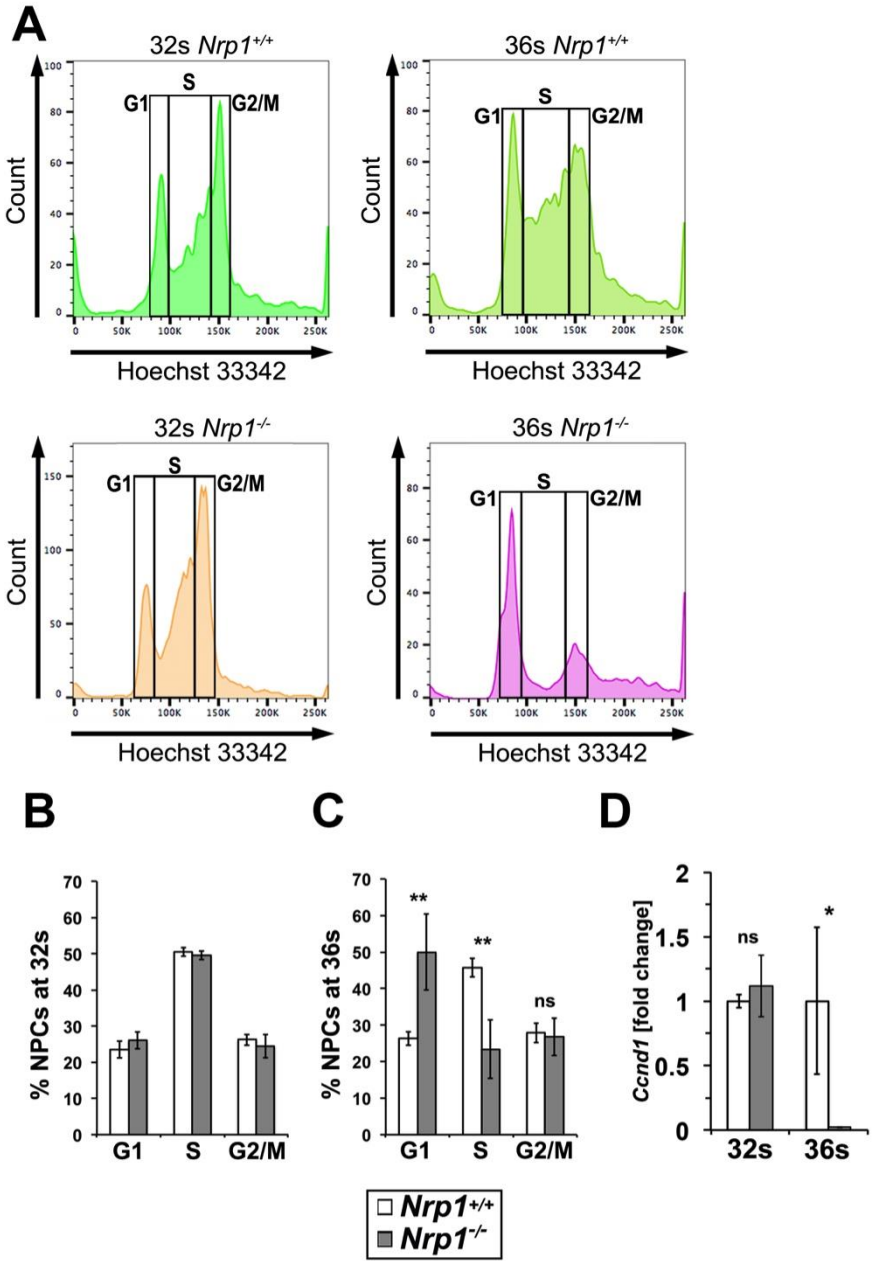

Figure 5.6 NPC cell cycle progression is perturbed at 36s, but not 32s, in *Nrp1*$^{-/-}$ hindbrains.

(**A)** Representative FACS plots for cycling CD133^{+} NPCs assayed for DNA content using Hoechst 33342 labelling intensity. Profiles for NPCs isolated from *Nrp1*$^{-/-}$and stage-matched control hindbrains at 32s and 36s are shown. 'Gates' used to define the proportion of NPCs in a specific cell cycle phase are shown as black boxes.

(**B,C)** Quantification of the fraction of CD133^{+} NPCs in each phase of the cell cycle in stage-matched control and *Nrp1*$^{-/-}$ hindbrains at 32s (**B**) and 36s (**C**). Data are

expressed as mean ± standard error of the mean, n≥3; ns (not significant) p≥0.05, ** p<0.01.

(**D**) Expression of *Ccnd1* in $CD133^{+}$ $CD56^{low}$ NPCs isolated from *Nrp1*-null and stage-matched control hindbrains at 32s and 36s. Expression levels were determined by qRT-PCR analysis, normalised to *Actb* and expressed as fold change compared to stage-matched wildtype hindbrains. Data are expressed as mean ± standard deviation of the mean, n≥3 for both genotypes; ns (not significant) p≥0.05, * p<0.05.

5.2.5 Germinal zone vasculature is essential for proper hindbrain growth

In **Figure 5.1** and **Figure 5.3**, I have shown that loss of GZ vasculature at 32s drives precocious cell cycle exit that depletes the pool of cycling NPCs and causes premature and ectopic neuronal differentiation. I further showed that smaller numbers of cycling progenitors were available at later stages of development in *Nrp1*$^{-/-}$ hindbrains (46s; **Figure 5.2**). In addition, levels of neurogenesis were significantly reduced towards the tail end of hindbrain development despite the initial increase in neuron generation at 32s **(Figure 5.4).** Taken together, these findings suggest that overall clone size of NPCs is reduced without proper GZ vascularisation. I therefore hypothesised that the overall radial growth of the hindbrain organ is impaired in *Nrp1*$^{-/-}$ mutants.

As *Nrp1*$^{-/-}$ mutant embryos in the CD1 background do not survive beyond e12.5, they can only be analysed until the 46s stage. I therefore quantified the dimensions and overall cross-sectional area of transverse hindbrain sections labelled with DAPI at this stage. Interestingly, *Nrp1*$^{-/-}$ hindbrains grew normally along the proximodistal axis (**Figure 5.7A,B**, *Nrp1*$^{+/+}$ 1979±80μm hindbrain width vs. *Nrp1*$^{-/-}$ 2055±133μm; $p \geq 0.05$). This finding agrees with a normal overall differentiation pattern of various neuronal subpopulations in these mutants (Schwarz et al., 2004). In contrast, hindbrain growth along the apicobasal axis was significantly compromised in *Nrp1*$^{-/-}$ embryos (**Figure 5.7A,C**, *Nrp1*$^{+/+}$ 418±6μm hindbrain height vs. *Nrp1*$^{-/-}$ 333±26μm; $p<0.01$). As apoptosis is not increased in *Nrp1*$^{-/-}$ hindbrains (**Figure 4.3**), this observation supports the idea that the radial expansion of individual clones is impaired following cell cycle exit of NPCs at 32s. Impaired hindbrain growth was also measurable as a reduction in the overall cross-sectional area of the NRP1-null hindbrain at 46s (**Figure 5.7A,D**, *Nrp1*$^{+/+}$ 0.58±0.015mm^2 hindbrain cross-sectional area vs. *Nrp1*$^{-/-}$ 0.47±0.05 mm^2; $p<0.05$).

Together with the finding that *Nes-Cre; Nrp1*$^{c/-}$ mutants do not have any obvious defects in NPC mitosis, but *Tie2-Cre; Nrp1*$^{c/-}$ mutants recapitulate the self-renewal defects observed in global *Nrp1*-null mutants, these findings suggest loss of GZ vascularisation impairs hindbrain growth.

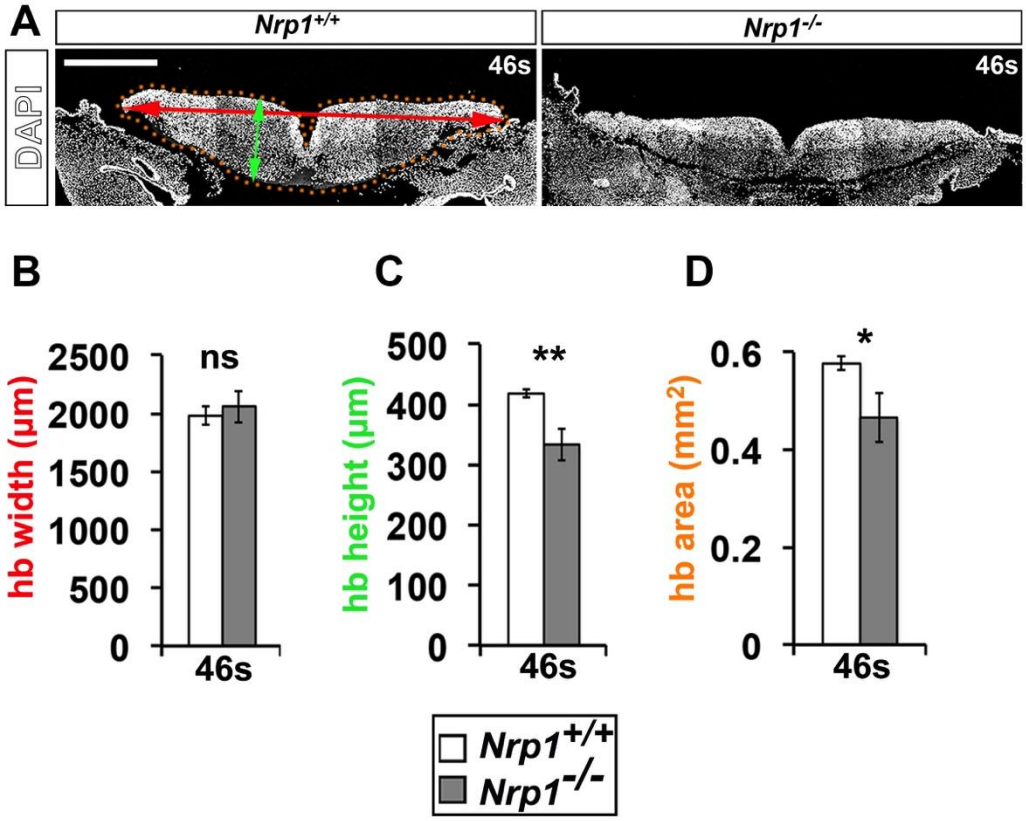

Figure 5.7 Impaired GZ vascularisation compromises hindbrain growth.

(**A**) Maximal projections of confocal tile scan z stacks of 10 µm transverse sections through 46s wildtype and *Nrp1*-null DAPI-stained hindbrains including arrows to illustrate measurements taken to determine hindbrain lateral width (red line), radial height (green line) and cross-sectional area (orange dotted outline). Scale bar: 100 µm.

(**B**) Quantification of lateral width, radial height and area of hindbrain (hb), expressed as mean ± standard deviation of the mean; n=3 for each genotype; ns (not significant) $p \geq 0.05$, * $p < 0.05$, ** $p < 0.01$.

5.2.6 The SVP does not regulate hindbrain NPCs by relieving tissue hypoxia

It was recently shown that vasculature in the developing forebrain regulates the behaviour of aRG by relieving local hypoxia (Lange et al., 2016). As *Nrp1*-deficient hindbrains are relatively avascular between 32-40s (**Figure 4.2**), I considered the possibility that insufficient oxygenation might also impair NPC self-renewal and differentiation in the developing hindbrain.

To determine whether the hindbrain of *Nrp1*$^{-/-}$ mutants is more hypoxic than in controls, I quantified the relative expression of hypoxia-induced genes *Hif1a* and *Vegfa* at 32s. I observed that the expression of both *Hif1a* (**Figure 5.8A**, 32s, *Nrp1*$^{-/-}$ 5.9±1.9 fold change increase in mRNA; $p<0.01$) and *Vegfa* (**Figure 5.8A**, 32s, *Nrp1*$^{-/-}$ 2.7±1.4 fold change increase in mRNA; $p<0.05$) was significantly upregulated in *Nrp1*-null hindbrains. I further examined whether *Nrp1*$^{-/-}$ hindbrains were hypoxic at 32s by immunolabelling for the hypoxia-responsive glucose transporter GLUT1 in *Nrp1*-null hindbrains. As GLUT1 is also expressed by the SVP (see top left-hand panel in **Figure 5.8C**) during the formation of the BBB, I calculated neural GLUT1 expression by deducting the GLUT1 labelling of vasculature from total GLUT1 labelling in the neural parenchyma. In agreement with increased expression of hypoxia-induced *Hif1a* and *Vegfa*, I also observed increased expression of GLUT1 in the *Nrp1*-null hindbrain (**Figure 5.8C,D**, 32s *Nrp1*$^{+/+}$ 59.3±2.6 arbitrary units vs. *Nrp1*$^{-/-}$ 83.6±13.2; $p<0.05$). Together, these results indicate that *Nrp1*$^{-/-}$ hindbrains are more hypoxic than control hindbrains at the time when premature NPC cell cycle exit had been detected.

In the developing forebrain, increasing atmospheric oxygen available to pregnant dams alleviates hypoxia in their embryos with impaired vascularisation and subsequently restores GLUT1 marker expression. Furthermore, increasing atmospheric oxygen also restored the differentiation of aRG to BPs to normal levels (Lange et al., 2016). To assess whether rescuing hindbrain oxygenation might also prevent precocious cell cycle exit in the *Nrp1*-null hindbrain, I housed pregnant dams in an 80% oxygen atmosphere from e9.5 before analysing embryos 24 h later (**Figure 5.8B**). This method restored the expression of GLUT1 to normal levels in *Nrp1*$^{-/-}$ hindbrains (**Figure 5.8C,D**, 32s *Nrp1*$^{+/+}$ 20% O_2 59.3±2.6 arbitrary units vs.

Nrp1$^{-/-}$ 80% O_2 60.8±5.4; p≥0.05). Thus, tissue oxygenation had been normalised in the *Nrp1*$^{-/-}$ hindbrain, as observed in the forebrain study of GPR124 mutants (Lange et al., 2016). However, and in contrast to the forebrain study, rescuing hindbrain hypoxia did not rescue the neurogenesis defect in *Nrp1*$^{-/-}$ hindbrains. Thus, a similar proportion of NPCs still underwent precocious cell cycle exit (middle graph in **Figure 5.8D**, 32s *Nrp1*$^{+/+}$ 20% O_2 84.5±5.9% $BrdU^+$ $Ki67^+$ cells/all $BrdU^+$ cells vs. *Nrp1*$^{-/-}$ 80% O_2 69.2±3.1%; p<0.01) to undergo premature neuronal differentiation (right-hand graph in **Figure 5.8D**, 32s *Nrp1*$^{+/+}$ 20% O_2 17.2±1.45% $TUJ1^+$ area/$DAPI^+$ area vs. *Nrp1*$^{-/-}$ 80% O_2 23.7±2.1%; p<0.01). Thus, whilst housing developing *Nrp1*$^{-/-}$ embryos in hyperoxia restores hindbrain oxygenation, this does not rescue defective NPC self-renewal.

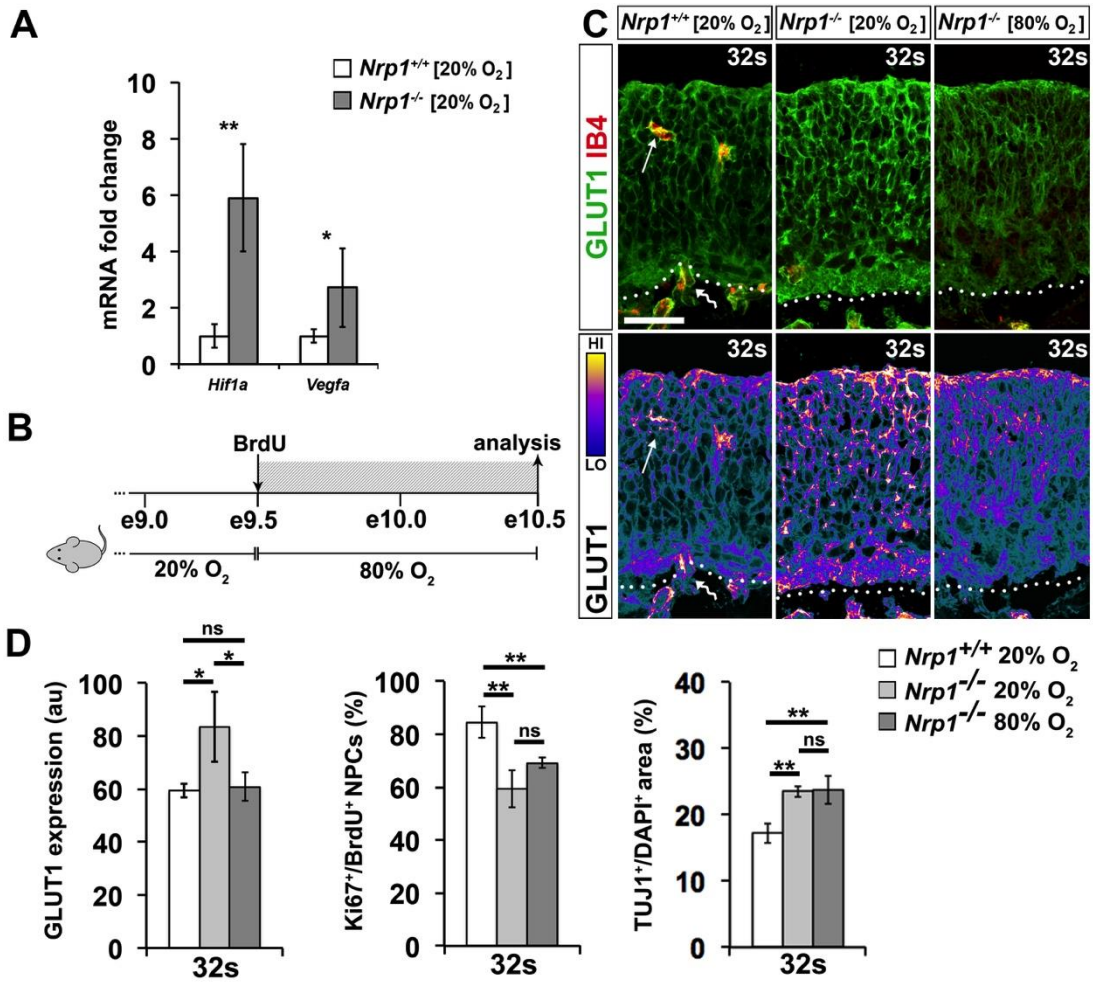

Figure 5.8 The SVP does not regulate NPCs by relieving tissue hypoxia.

(**A**) Increased expression of the hypoxia-regulated genes *Hif1a* and *Vegfa* in 32s *Nrp1*-null hindbrains. Expression levels were determined by qRT-PCR analysis, normalised to *Actb* and expressed as fold change compared to expression levels in stage-matched wildtype hindbrains.

(**B**) Schematic representation of the hypoxia rescue experiment. Pregnant dams received an intraperitoneal BrdU injection when their embryos where at e9.5 and were then transferred from normoxia to an 80% oxygen atmosphere for 24 hours before analysis e10.5. Owing to the developmental delay, embryos collected at e10.5 corresponded to 32s.

(**C**) 10 µm transverse sections from hindbrains of 32s wildtype and *Nrp1*$^{-/-}$ embryos from dams housed in 20% oxygen and *Nrp1*-null embryos from dams in an 80% oxygen environment, labelled for GLUT1 (green) and IB4 (red). 'Heatmap' for

GLUT1 staining shown in lower panels. Scale bar: 25 μm. Arrows and wavy arrows indicate the $GLUT1^+$ SVP and PNP, respectively.

(**D**) Hyperoxia rescues oxygenation of *Nrp1*-null hindbrains (left-hand graph; arbitrary units, au). NPC self-renewal (percentage of $Ki67^+BrdU^+$ double-labelled NPCs) and neuronal differentiation ($TUJ1^+$ hindbrain area), shown in middle and right-hand graphs, respectively).

Data are expressed as mean ± standard deviation of the mean; $n \geq 3$ for each genotype and oxygen level; ns (not significant) $p \geq 0.05$, * $p < 0.05$, ** $p < 0.01$.

5.2.7 Differential gene expression in the neuropilin 1-null hindbrain

My results thus far indicate that GZ vasculature is required to maintain NPC self-renewal and mitotic behaviour, and to sustain NPC mitosis in the long-term. NPCs in the developing CNS are regulated by a multitude of different extrinsic signals that make up the regulatory niche, as well as many intrinsic proteins and transcriptional regulators (described in **1.2**). Both intrinsic and extrinsic factors may therefore be involved in the regulation of hindbrain NPCs by GZ vasculature and accordingly, may vary in abundance in mouse mutants displaying compromised CNS vascularisation.

Owing to the potentially large number of candidate molecules available to interrogate in hindbrains with impaired angiogenesis, I decided to screen for the differential expression of potential genes of interest using a qRT-PCR array approach. A 96-well qRT-PCR array plate containing primer pairs for amplifying 84 different neurogenesis-associated transcripts was used (full list of genes in **Table 2.7**). In addition, array plates contained primers for 'housekeeping' genes used for normalising expression values, as well as those for experimental controls.

The five housekeeping genes used in the array were *Actb*, *B2m*, *Gapdh*, *Gusb* and *Hsp90ab1*. Owing to the potential role of NRP1 in metabolism (J. Brash, unpublished observations), *Gusb* was not used for normalising gene expression levels in the array. In addition, expression levels varied between both samples for three of out the remaining four housekeeping genes available in the array (*Actb*, *B2m* and *Gapdh*). Expression levels of *Hsp90ab1* (encoding Heat shock protein 90αb1) were the most similar between both samples; thus, I used *Hsp90ab1* as the housekeeping gene for normalising expression values across the qRT-PCR array.

I extracted RNA and subsequently generated cDNA from the hindbrains of three *Nrp1*$^{-/-}$ embryos on a mixed JF1/CD1 genetic background, as well as from three wildtype littermates at 35s. The cDNA from several embryos was pooled in order to have sufficient template material for all wells containing primer pairs. *Nrp1*$^{-/-}$ embryos on the JF1 background survive longer during gestation (Schwarz et al., 2004, Cariboni et al., 2011) and were not developmentally delayed at this time point,

thus preventing the need for stage-matching with non-littermate embryos. I have not yet demonstrated whether *Nrp1*$^{-/-}$ embryos on the JF1 genetic background possess similar angiogenesis defects to embryos on a CD1 background. However, I have performed qRT-PCR analysis for *Vegfa* (**Figure 5.8A**) and both *Bdnf* and *Ntf3* (**Figure 5.10**) in CD1 embryos to validate expression levels of these genes that are included in this qRT-PCR array (discussed below).

The majority of transcripts screened for were not 'differentially expressed' (**Table 8.1**, 15/84 genes), as defined by whether the fold change in gene expression in mutant samples relative to controls was at least twice or less than half (2.0≤ or 0.5≥) of that in control samples (**Figure 5.9A**). These thresholds were recommended by the array's manufacturer as guidance for establishing candidate genes to further analyse. However, I found that 8/84 genes (**Table 5.1**) displayed near-threshold fold changes in gene expression and therefore included these in my study (**Figure 5.9B-D**). I have classified all differentially expressed genes of interest (23/84 genes) into the following categories: those encoding VEGF-A or NRPs (**Figure 5.9B**), those encoding cytoplasmic or nuclear (i.e. 'intrinsic') molecules (**Figure 5.9C**) and those that encode membrane-bound or secreted (i.e. extrinsic) molecules (**Figure 5.9D**).

Nrp1-null hindbrains were calculated to possess almost 20-times less *Nrp1* transcript, as expected in constitutive *Nrp1* mutant embryos (**Figure 5.9B**, *Nrp1*$^{-/-}$: 0.05-factor fold change). The negligible amount of *Nrp1* expression detected in *Nrp1*$^{-/-}$ hindbrain may result from small amounts of mRNA encoding mutant *Nrp1* that do not degrade as quickly through nonsense-mediated decay and are therefore amplified during qRT-PCR. In contrast to *Nrp1*, expression of *Nrp2* increased suggesting that it may be upregulated to compensate for genetic deletion of *Nrp1* (**Figure 5.9B**, *Nrp1*$^{-/-}$: 1.84-factor fold change). *Vegfa* expression increased greatly in *Nrp1*$^{-/-}$ embryos (**Figure 5.9B**, *Nrp1*$^{-/-}$: 3.81-factor fold change) likely in response to tissue hypoxia, as mentioned previously (**Figure 5.8**). This suggests that *Nrp1*$^{-/-}$ JF1 hindbrains also possess angiogenesis defects at 35s that impair oxygenation of the neuroepithelium.

Expression of several transcripts that encode transcriptional regulators in NPCs were upregulated in *Nrp1*$^{-/-}$ hindbrains. For example, the expression of Notch

target genes *Hes1* and *Hey2* both increased (**Figure 5.9C**, *Nrp1*$^{-/-}$: *Hes1* 2.2-factor fold change, *Hey2* 1.86-factor fold change), as well as expression of *S100a6*, a marker for undifferentiated, adult NSCs (Yamada and Jinno, 2014, Karsten et al., 2003), which was also upregulated in NRP1-null samples (**Figure 5.9C**, *Nrp1*$^{-/-}$: 2.94-factor fold change). *Pax5*, which is typically expressed in early neuroectoderm (Pfeffer et al., 2002), increased as well (**Figure 5.9C**, *Nrp1*$^{-/-}$: 1.9-factor fold change). Finally, one of the most enriched transcripts in NRP1-null hindbrains was the cytoskeleton-associated gene *Flna,* encoding Filamin A, which promotes NPC cell cycle progression (**Figure 5.9C**, *Nrp1*$^{-/-}$: 3.2-factor fold change; (Lian et al., 2012).

Whilst these genes are commonly associated with the proliferation of NPCs and NSCs or the maintenance of their identity, several transcripts encoding factors promoting neuronal differentiation were also upregulated in *Nrp1*$^{-/-}$ hindbrains. *Neurod1*, the proneural TF *Mef2c* and the histone acetyltransferase *ep300* were all enriched in *Nrp1*$^{-/-}$ hindbrains (**Figure 5.9C**, *Nrp1*$^{-/-}$: *Neurod1* 1.91-factor fold change, *Mef2c* 2.2-factor fold change, *ep300* 1.86-factor fold change; Li et al., 2008, Chatterjee et al., 2013). In addition to its role in promoting neurogenesis, ep300 is involved in the NPC switch to forming astrocytes (Nakashima et al., 1999). Finally, I detected increased expression of *Hdac4* (**Figure 5.9C**, *Nrp1*$^{-/-}$: 2.45-factor fold change), which promotes the neuronal differentiation of cultured NSCs of the DG by inhibiting cell cycle progression (Micheli et al., 2016).

Many transcripts coding for extrinsic signals were also upregulated in the *Nrp1*-null hindbrain. For example, I observed increased expression of neurotrophins *Bdnf* and *Ntf3* in *Nrp1*$^{-/-}$ hindbrains at 35s, which potently induce NPC differentiation in the forebrain (Fukumitsu et al., 1998, Ghosh and Greenberg, 1995; **Figure 5.9D**, *Nrp1*$^{-/-}$: *Bdnf* 2.92-factor fold change, *Ntf3* 2.48-factor fold change). Furthermore, expression of the neurotrophin glial cell line-derived neurotrophic factor (GDNF; Pozas and Ibanez, 2005) was increased in the *Nrp1*-null hindbrain (**Figure 5.9D**, *Nrp1*$^{-/-}$: 2.81-factor fold change). Moreover, I observed increased abundance of transcripts encoding the differentiative cue BMP4 (**Figure 5.9D**, *Nrp1*$^{-/-}$: 2.08-factor fold change; Li et al., 1998). However, the *Nrp1*$^{-/-}$ hindbrain also contains greater

levels of *Nog* (**Figure 5.9D**, *Nrp1*$^{-/-}$: 1.85-factor fold change), which codes for the BMP4 antagonist Noggin (Lim et al., 2000). Thus, the abundance of either secreted factor may increase to compensate for upregulated expression of the other and consequently, may nullify any effect resulting from such amplified expression. I also detected higher levels of *Nrg1*, coding for the differentiative factor neuregulin 1 (NRG1; **Figure 5.9D**, *Nrp1*$^{-/-}$: 2.52-factor fold change; Sato et al., 2015, Liu et al., 2005b).

Finally, I observed differential expression of mRNA encoding specific extracellular or membrane-bound proteins typically associated with migrating and post-mitotic neurons. For example, expression of the axon/neuron chemorepellant SLIT2 is more abundant in the NRP1-null hindbrain, potentially compensating for reduced NRP1-mediated repulsion of progenitors or neurons (**Figure 5.9D**, *Nrp1*$^{-/-}$: 2.96-factor fold change). The NRP1-null hindbrain is also enriched for *Artn*, encoding the GDNF family member artemin, which functions as a survival factor for post-mitotic neurons (Andres et al., 2001; **Figure 5.9D**, *Nrp1*$^{-/-}$: 1.99-factor fold change), as well as for *Adora1*, which codes for the GPCR adenosine A1 receptor (**Figure 5.9D**, *Nrp1*$^{-/-}$: 3.43-factor fold change).

Lastly, the genes encoding Anaplastic lymphoma kinase (*Alk*) and the ECM protein Tenascin R (*Tnr*) were two of only three transcripts amongst the entire array to be noticeably downregulated in NRP1-null hindbrains, with the other being *Nrp1* itself (**Figure 5.9D**, *Nrp1*$^{-/-}$ *Alk*: 0.58-factor fold change, *Tnr*: 0.57-factor fold change).

Taken together, these findings demonstrate that numerous transcripts associated with NPC stemness and differentiation are regulated, either directly or indirectly, by NRP1 in the mouse embryonic hindbrain. This analysis did not distinguish which cell types express which transcripts in the mouse hindbrain. Further validation is therefore needed to determine whether differential gene expression in *Nrp1*-null hindbrains results from loss of cell autonomous NRP1 signalling in NPCs or endothelial cells, or from impaired GZ vascularisation.

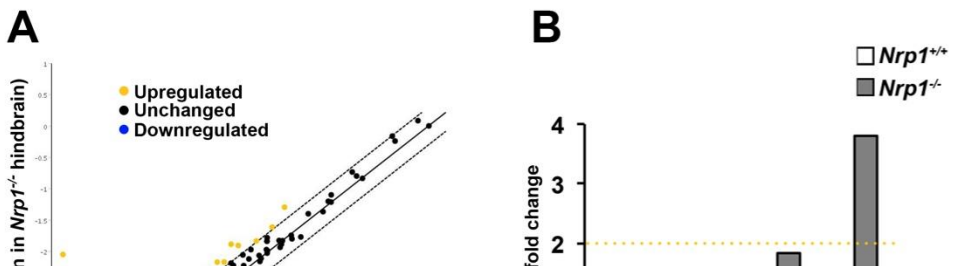

Figure 5.9 Differential gene expression of neurogenesis-associated transcripts in *Nrp1*-null hindbrains at 35s.

(**A**) Scatter plot indicating differentially and non-differentially expressed genes between wildtype and *Nrp1*$^{-/-}$ hindbrains, normalised to *Hsp90ab1*. Yellow and blue dots represent genes that are up- and downregulated in *Nrp1*-null hindbrains, respectively. Black dots are non-differentially expressed genes (i.e. those that are not >2x or <0.5x expressed in *Nrp1*-null hindbrains. Middle diagonal line represents equal gene expression levels between both genotypes, whilst parallel, flanking diagonal lines demark the >2x and <0.5x thresholds.

(**B-D**) Differentially expressed transcripts encoding VEGF-A and NRP proteins (**B**), cytoplasmic or nuclear proteins (**C**) or membrane-bound or extracellular proteins (**D**). Yellow and blue dotted lines denote the demark the >2x and <0.5x thresholds.

Table 5.1 Differentially expressed genes in qRT-PCR array.

Gene	Description	Fold change (*Nrp1*$^{-/-}$ / *Nrp1*$^{+/+}$)
Adora1	Adenosine A1 receptor	3.43
Alk	Anaplastic lymphoma kinase	0.58
Artn	Artemin	1.99
Bdnf	Brain derived neurotrophic factor	2.92
Bmp4	Bone morphogenetic protein 4	2.08
Ep300	E1A binding protein p300	2.42
Flna	Filamin, alpha	3.20
Gdnf	Glial cell line derived neurotrophic factor	2.81
Hdac4	Histone deacetylase 4	2.45
Hes1	Hairy and enhancer of split 1 (Drosophila)	2.20
Hey2	Hairy/enhancer-of-split related with YRPW motif 2	1.86
Mef2c	Myocyte enhancer factor 2C	2.03
Neurod1	Neurogenic differentiation 1	1.91
Nog	Noggin	1.85
Nrg1	Neuregulin 1	2.52
Nrp1	Neuropilin 1	0.05
Nrp2	Neuropilin 2	1.84
Ntf3	Neurotrophin 3	2.48
Pax5	Paired box gene 5	1.90
S100a6	S100 calcium binding protein A6 (calcyclin)	2.94
Slit2	Slit homolog 2 (Drosophila)	2.96
Tnr	Tenascin R	0.57
Vegfa	Vascular endothelial growth factor A	3.81
Hsp90ab1	Heat shock protein 90 alpha (cytosolic), class B member 1	1

5.2.8 Increased neurotrophin expression in the neuropilin 1-null hindbrain

The qRT-PCR array suggested that transcript levels for a number of extrinsic signalling molecules were upregulated in *Nrp1*$^{-/-}$ hindbrains, including *Bdnf* and *Ntf3* (**Figure 5.9D)**. As *Bdnf* and *Ntf3* encode BDNF and NT3, which both drive neurogenesis during development (see **1.2.3.7**), I considered them as candidate mediators of the precocious neuron production seen in hindbrains lacking GZ vasculature.

My initial quantification of *Bdnf* and *Ntf3* expression utilised cDNA pooled from three separate *Nrp1*$^{-/-}$ animals, preventing statistical comparison between genotypes as only one sample was analysed. Furthermore, these embryos were on a JF1 genetic background, in contrast to the preceding analysis that I have performed exclusively on embryos from a CD1 background. I therefore compared the expression of both genes in the latter strain at the point at which many NPCs have already undergone cell cycle exit in *Nrp1*$^{-/-}$ embryos at 32s in the *Nrp1*$^{-/-}$ CD1 hindbrain.

I found that hindbrains from *Nrp1* mutants contained significantly more *Bdnf* (**Figure 5.10**, *Nrp1*$^{-/-}$: 2.89±0.61-factor fold change; $p<0.01$) and *Ntf3* (**Figure 5.10**, *Nrp1*$^{-/-}$: 5.71±1.56-factor fold change; $p<0.01$). Thus, expression of both neurotrophins is significantly upregulated during the period of precocious cell cycle exit and neuronal differentiation. Furthermore, increased expression of both *Bdnf* and *Ntf3* directly precedes the premature decline of NPC mitosis from 40s. Therefore, the increased abundance of neurotrophins may be partly or completely responsible for reduced NPC self-renewal in hindbrains that lack GZ vasculature. Whilst this analysis validated the qRT-PCR array, it did not determine which cell type(s) express both neurotrophins at greater levels.

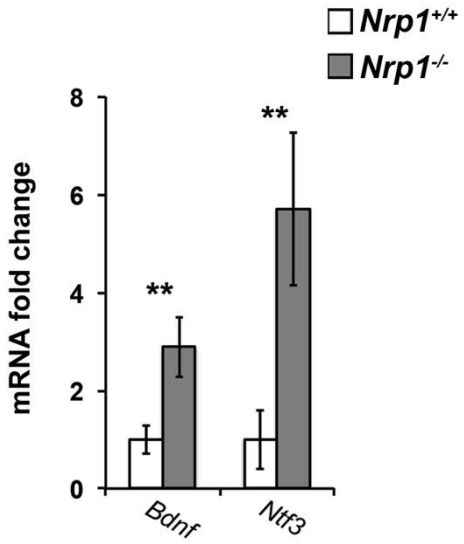

Figure 5.10 Increased expression of *Bdnf* and *Ntf3* in the *Nrp1*-null hindbrain at 32s.

Quantification of *Bdnf* and *Ntf3* expression in stage-matched control and *Nrp1*$^{-/-}$ hindbrains at 32s. Data are expressed as mean ± standard deviation of the mean; n≥3 for each genotype; ** $p<0.01$.

5.2.9 Potential angiocrine molecules regulating NPCs

I next asked whether hindbrain endothelial cells express either *Bdnf* or *Ntf3* as angiocrine signals, as well as *Serpinf1* (which encodes the neurotrophin PEDF) and two isoforms of nitric oxide synthase (*Nos1* and *Nos3*) that regulate neurogenesis in both the adult and embryonic neurogenic niches (Lameu et al., 2012, Delgado et al., 2014, Andreu-Agullo et al., 2009). I also determine whether endothelium in the hindbrain also expresses the Notch ligands DLL1, JAG1 and JAG2, which are required for maintaining NPC stemness and may also regulate hindbrain NPCs through progenitor-vessel contacts (**Figure 3.6Figure 3.8**).

For this experiment, endothelial cells were isolated by FACS by purifying YFP^+ endothelium from the hindbrains of *Tie2-Cre; Rosa*^{YFP} embryos whilst excluding $YFP^+/CD11b^+$ double-positive macrophages. I then quantified the expression of transcripts encoding the candidate molecules mentioned using qRT-PCR and normalised these values to expression of *Actb*. I then compared the expression of each gene in endothelial cells at 35s to transcript levels in the whole hindbrain, to assess the relative angiocrine contribution of each molecule.

To acquire sufficient RNA for performing qRT-PCR on endothelial cells, I pooled cDNA from three *Tie2-Cre; Rosa*^{YFP} hindbrains, thus limiting analysis of gene expression levels to technically one sample only. The expression value calculated from pooled endothelial cells was then compared to the average expression levels in cDNA obtained from pooling three whole hindbrain samples to analyse semi-quantitatively which signals were likely to be expressed by endothelium.

In addition to endothelial DLL4, which regulates tip cell specification (Hellstrom et al., 2007), *Dll1* and *Jag1* are all expressed abundantly by endothelium (**Figure 5.11**). *Jag2*, conversely, is not expressed by endothelial cells (**Figure 5.11**). Hindbrain endothelial cells also do not express *Bdnf*, *Ntf3* and *Serpinf1*, as well as nNOS (*Nos1*; **Figure 5.11**). In contrast, hindbrain endothelium may represent a source of NO, which is involved in BDNF and NT3 signalling, as I detected expression of *Nos3*, (i.e. eNOS; **Figure 5.11**). Thus, whilst endothelial cells in the

developing hindbrain at 35s do not express neurotrophins that promote neuronal differentiation, cerebrovasculature may instead modulate NPC behaviour through NO production, as well as through Notch ligands that promote stemness.

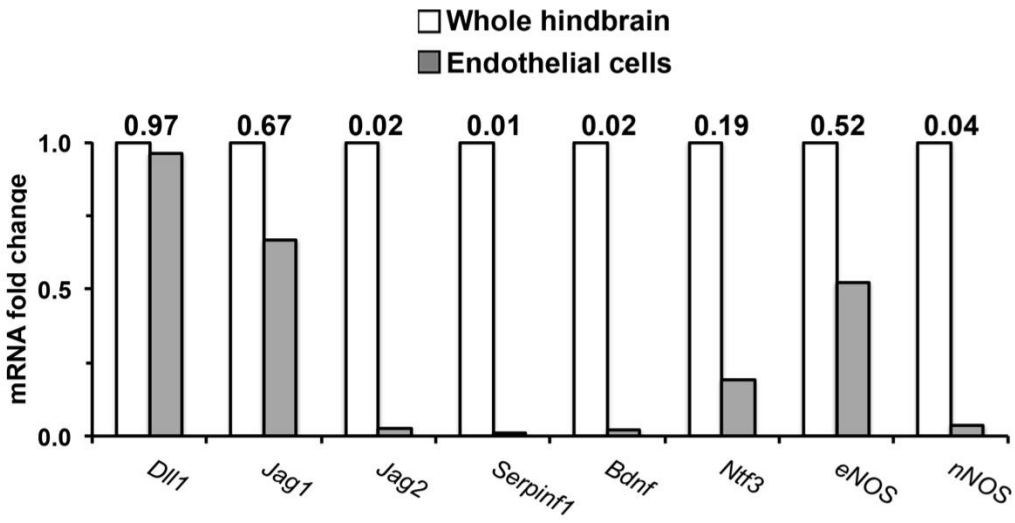

Figure 5.11 Screening candidate molecules for angiocrine signalling.

Comparison of expression levels of potential angiocrine signals in endothelial cells with whole hindbrain. Expression was determined by qRT-PCR using cDNA pooled from endothelial cells isolated from 35s *Tie2-Cre; Rosa*^{YFP} mice and comparing to cDNA pooled from three whole wildtype hindbrains. Values above bars denote fold change expression of specific transcripts in endothelial cells only.

5.3 Discussion

I have shown that in the absence of GZ vasculature, 25% more hindbrain NPCs have exited the cell cycle by 32s, and that the neuroepithelium contains significantly more TUJ1^{+} neurons at that stage (**Figure 5.1** and **Figure 5.3**; illustrated in **Figure 5.12**). Taken together, these findings demonstrate that blood vessels in the hindbrain promote NPC self-renewal. Numerous other niche signals in the developing CNS maintain stemness and self-renewal in a similar manner. For example, impaired FGF signalling from forebrain NPCs (and potentially the CSF: (Greenwood et al., 2008) results in premature NPC differentiation at the expense of expanding the NPC pool (Vaccarino et al., 1999).

The birth dating approach that I have employed labelled NPCs between 25-32s and illustrates the immediate effects of impaired GZ vascularisation on NPCs in the hindbrain. Thus, delayed ingression of radial vessels from the PNP at 25s or a failure to form an SVP by 30s result in the NPC self-renewal defects that I have described in both full and endothelial-specific *Nrp1* mutant embryos. Many of the BrdU^{+} Ki67^{-} cells that were generated excessively in hindbrains lacking GZ vasculature were already positioned near or at the pial surface, suggesting that the majority of cell cycle exit may have taken place early on. Performing birth dating experiments prior to 32s could help distinguish at what stages NPCs leave the cell cycle in the absence of hindbrain vascularisation.

Quantification of the total number of BrdU^{+} cells indicated a small but insignificant increase in the number of labelled hindbrain cells at 32s (**Figure 5.2**). This correlated with a slight increase in mitosis in the VZ that did not result from an increased number of NPCs undergoing a lag during anaphase, as I had observed at the 36s stage (**Figure 4.4**). These observations therefore indicate that, despite the large number of NPCs that have exited the cell cycle by 32s, a proportion of NPCs in *Nrp1*$^{-/-}$ hindbrains may have expanded in the absence of SVP formation. This could represent a compensatory mechanism, whereby one subset of NPCs expands in response to premature cell cycle exit of another NPC subtype. Alternatively, different subtypes may respond differently to vascular cues. Unfortunately, I cannot

yet determine whether specific NPC subpopulations respond differently to vascular cues, as little is known about NPC subtypes found in the hindbrain (in contrast to the greater understanding of forebrain progenitors).

Interestingly, I detected increased expression of the Notch target genes *Hes1* and *Hey2* in 35s *Nrp1*-null hindbrains (**Figure 5.9**). As they promote NPC stemness in the forebrain, they may similarly contribute to increased NPC proliferation in the hindbrain, or reflect an attempt to further promote NPC expansion to compensate for loss of NPCs at 32s. Alternatively, increased expression of *Hes1* and *Hey2* may reflect an adaptive response to compromised CNS vascularisation in *Nrp1*-null embryos (Fantin et al., 2015), as both genes are required for embryonic angiogenesis (Fischer et al., 2004, Kitagawa et al., 2013). It would therefore be interesting to determine which cell type in the in *Nrp1*-null hindbrain expresses increased *Hes1* and *Hey2* levels.

Ultimately, the net effect of GZ vasculature on the total cohort of hindbrain NPCs is that it sustains self-renewal and prevents neuronal differentiation, as demonstrated by a reduced proportion of cycling NPCs and increased TUJ1 labelling in $Nrp1^{-/-}$ and *Tie2-Cre;* $Nrp1^{c/-}$ embryos at 32s.

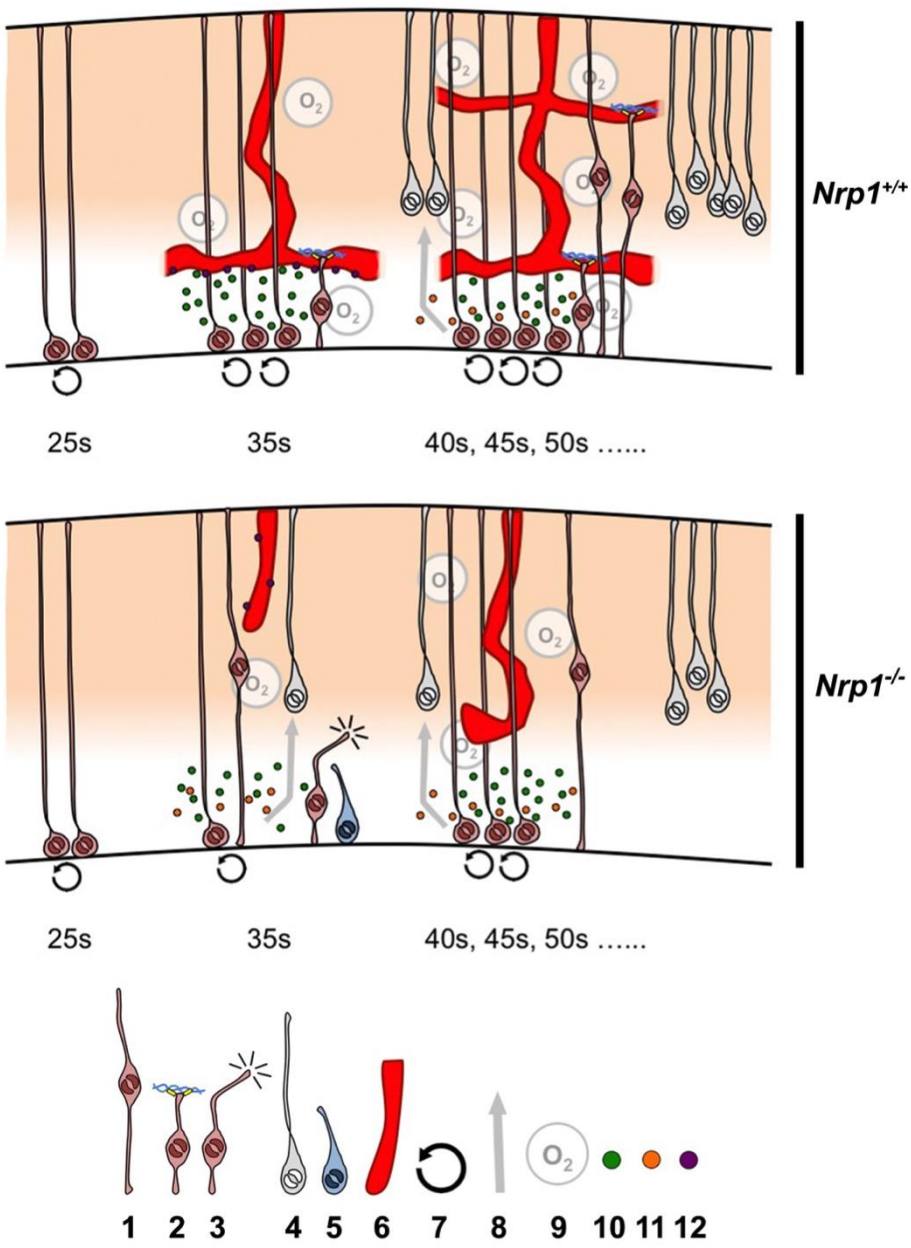

Figure 5.12 Working model for the role of blood vessels in hindbrain neurogenesis.

Upper and lower panels illustrating the hypothetical behaviour and organisation of hindbrain NPCs in wildtype (*Nrp1*$^{+/+}$) and *Nrp1*$^{-/-}$ hindbrains from 25-50s, respectively. Vasculature ensures that differentiative factors do not accumulate early in hindbrain development (at 35s) to preserve NPC self-renewal at early stages and therefore enable neurogenesis from a sufficiently large NPC pool later on. Key: 1, AP undergoing INM; 2, AP contacting vascular ECM; 3, AP without vessel contact; 4, post-mitotic neuron; 5, ectopically positioned neuron; 6, blood vessel; 7, NPC self-renewal; 8, neuronal differentiation; 9, oxygen; 10, stemness-promoting factor; 11, differentiative factor; 12, unknown vessel-derived signal.

The shift from self-renewing to either differentiative or neurogenic divisions is typically accompanied by concomitant changes in cell cycle progression, as is commonly observed in tissue culture models of NPCs and other types of stem cells. I have therefore combined Hoechst labelling with FACS analysis to determine the ploidy of cycling hindbrain $CD133^+$ NPCs and thereby assign the proportion of NPCs in each cell cycle phase at several stages from 32s onwards (**Figure 5.5**).

However, my FACS analysis may not have permitted a precise definition of cell cycle kinetics for several reasons. Firstly, the FACS plots acquired from wildtype hindbrains at 32 and 36s did not resemble typical Hoechst labelling histograms acquired by others from similar analysis of NSCs (Morte et al., 2013, Roccio et al., 2013). Secondly, the sorting strategy I used did not provide a high enough yield of NPCs at either 32s or 36s for pronounced 'peaks' corresponding to the '2n' and '4n' values for DNA content. Without prior knowledge of whether all NPC subtypes in the developing hindbrain express CD133, my targeting may have excluded other progenitor classes whose cell cycle progression may also be modulated by cerebrovasculature. Thirdly, given the different cell cycle kinetics reported for self-renewing NPCs in the forebrain and spinal cord (Calegari et al., 2005, Saade et al., 2013), it is not obvious which brain region I should base my interpretation of the hindbrain FACS plots on to interpret the changes in cell cycle phase length I have observed. For example, the ratio of NPCs in G1 compared to G2 appears to increase over time in the hindbrain, suggesting a lengthening of G1 similar to that observed in the developing forebrain (Calegari et al., 2005). However, the proportion of NPCs in S-phase did not change from 32s to 36s (i.e. with development), in contrast to both forebrain and spinal cord NPCs where S-phase decreases in length (Arai et al., 2011, Saade et al., 2013). Further characterisation of cell cycle progression in hindbrain NPCs is therefore required before I would be able to accurately interpret FACS plots to identify cell cycle perturbations in hindbrains lacking GZ vasculature.

Bearing these limitations in mind, I have begun to compare cell cycle progression of $CD133^+$ hindbrain NPCs in *Nrp1*-mutant and control embryos by FACS (**Figure 5.6**). I did not observe a difference in the proportion of NPCs in each

cell cycle phase in *Nrp1*$^{-/-}$ mutants at 32s, nor did I detect any difference in the expression of cyclin D1. This finding suggests that a proportion of NPCs, presumably those that had not exited the cell cycle by that stage, continued to cycle normally at least for some time.

In contrast to findings at 32s, I observed both an increase in the proportion of NPCs in G1 and a decrease of those in S-phase in CD133^{+} NPCs from 36s *Nrp1*-mutant compare to control hindbrains. The lengthening of G1 and shortening of S-phases agreed with a significant reduction in NPC-expressed *Ccnd1* at 36s, which encodes cyclin D1 that normally promotes the transition from G1 to S-phase and is linked to NPC division mode (Lange et al., 2009). These observations at 36s agree with the precocious decline in mitotic and cycling NPCs that occurs thereafter (**Figure 4.4** and **Figure 5.2**). Unfortunately, FACS analysis was not suitable to confirm the mitotic lag that takes place in anaphase at this stage (**Figure 4.4**), as quantifying Hoechst labelling intensity cannot differentiate between different stages of mitosis, nor can it distinguish between cells in G2 and M, when cells possess the same amount of DNA.

As I observed changes in cell cycle progression in the absence of GZ vasculature at 36s, but not at 32s, it may be worthwhile to perform another analysis at a stage just preceding 32 to examine whether cell cycle changes precede cell cycle exit of those cells that were no longer captured by the CD133 sorting strategy.

Separately, I am not confident in my quantification of *Ccnd1* expression by NPCs following FACS (**Figure 5.6**). The reduction in expression at 36s in *Nrp1* mutants is so great that it would likely prevent any future cell division from occurring, and that is clearly not the case, as NPC mitosis in *Nrp1*-null hindbrains continued after this stage (**Figure 4.4**).

In summary, my FACS analysis reveals interesting changes to cell cycle kinetics in NPCs across time, as well as in *Nrp1*-null embryos with defective GZ vascularisation. However, the strategy for studying NPC cell cycle requires optimisation and would benefit considerably from a better understanding of hindbrain NPC subtypes to enable more effective NPC targeting and to distinguish

NPC subtypes during cell cycle analysis. In an alternative and complementary approach, determining cell cycle kinetics could be performed *in situ* by using cumulative BrdU labelling (Calegari et al., 2005) or a transgenic cell cycle reporter mouse strain (Abe et al., 2013) to relate information on cell cycle progression to NPC subtypes and their anatomical position.

Even though the molecular mechanism by which hindbrain vascularisation regulates NPCs is not yet defined, the long-term effects of poor GZ vascularisation are considerably clearer. At 46s, less than half the number of $Ki67^{+}$ NPCs remains in *Nrp1*$^{-/-}$ hindbrains (**Figure 5.2**). Moreover, the reduction in $BrdU^{+}$ labelled cells at 46s, 24 h after a BrdU injection, points to further slowing in the generation of cellular progeny.

Defects in NPC mitosis and self-renewal at early stages should affect hindbrain development more so than defects that occur later on in development. This is because a reduction in the pool of APs, such as NE and aRG, reduces the number and size of the neural lineages that derive from them. For example, premature differentiation of the 'early' NPC pool compromises the growth of the neuroepithelium (e.g. Kang et al., 2009), which is analogous to the reduction in hindbrain growth that I have observed. In contrast, depletion of later forming NPCs may impair the formation of a specific neuronal subtype but overall growth of the CNS is unlikely to be affected (e.g. (Tan et al., 2016).

My analysis of NPC self-renewal at later stages shows that the proportion of NPCs undergoing cell cycle re-entry normalises in *Nrp1*-null embryos. Whilst there is a delay in radial vessel ingression and also impaired GZ vascularisation until at least 40s, the hindbrain contains a reasonable complement of endothelial cells at 46s, albeit in the form of abnormal, glomeruloid vessel structures. It is conceivable that these endothelial cells may be functionally competent to restore any angiocrine signalling or structural support that was initially missing in the poorly vascularised *Nrp1*$^{-/-}$ hindbrain at 32s. Alternatively, different NPC subtypes may possess varying responsiveness to vessel-derived cues, with some subsets resistant to poor GZ vascularisation compared to other, earlier populations that rely more on vascular regulation. This would be comparable to the importance of Wnt signalling in

maintaining the self-renewal of APs that are generated earlier on in development, but not BPs that lack contact at the apical surface of the neuroepithelium (Oliver et al., 2003, Kenney et al., 2003). Ultimately, however, re-equilibrating levels of cell cycle re-entry in mid-late hindbrain development does not balance the effect of losing early NPCs to terminal differentiation, as the pool of cycling Ki67^{+} NPCs is irreversibly depleted at 46s.

The variable responsiveness of NPC subpopulations to vessel-derived signals is highlighted by recent findings of NPCs committed to a cortical interneuron fate in the ventral forebrain (Tan et al., 2016), as well as NPCs that are regulated by tissue oxygenation in the dorsal forebrain (discussed below; (Lange et al., 2016). Nearly all progenitor processes that do not terminate at the pial surface in the medial ganglionic eminence project instead onto an SVP that runs through the neuroepithelium, and belong to interneuron-fated NPCs (Tan et al., 2016). Progenitor-vessel association is required for sustaining the division of this specified cohort of NPCs, yet NPCs do not appear to attach similarly to vessels in the dorsal forebrain and the incidence of vessel-anchored NPCs in ventral tissue varies with time (Tan et al., 2016). Thus, these observations suggest that specific subpopulations of NPCs in the developing brain exhibit a contrasting and spatiotemporal dependency on vascular regulation.

TUJ1^{+} labelling at 46s shows an unusual distribution of differentiating or post-mitotic neurons in *Nrp1*-null hindbrains (**Figure 5.4**). Firstly, the apical hindbrain is almost completely devoid of TUJ1 staining. Indeed, the enrichment of TUJ1 immunolabelling from 32s to 46s is significantly reduced in *Nrp1*$^{-/-}$ embryos compared to stage-matched controls. Secondly, TUJ1^{+} neurons appear to accumulate in the medial region of the hindbrain.

The lack of TUJ1 immunolabelling in the apical hindbrain at 46s, as well as the reduced enrichment of TUJ1^{+} neurons, indicate a slowing of neurogenesis, raising the question of which cell type normally occupies the region that completely lacks neurons in *Nrp1* mutants. I have not characterised the pattern of gliogenesis in the embryonic hindbrain in either wildtype or *Nrp1*-null hindbrains and one interesting possibility is that this region may contain prematurely-generated glia that are produced in place of neurons and/or displace TUJ1^{+} neuronal processes. As

astrogliogenesis, for example, begins from e9.5 onwards in the developing spinal cord (Deneen et al., 2006), this region in the *Nrp1*$^{-/-}$ may contain ectopically generated astrocytes following a precocious switch to gliogenesis.

Several signals promote the switch from neural to glial identity in the mammalian neurogenic niche. For example, *in utero* injection of TGF-β1 into the cortical ventricle induces precocious astrogliogenesis at the expense of neurogenesis in the mouse embryonic forebrain (Stipursky et al., 2014). I did not detect any significant difference in *Tgfb1* expression in *Nrp1*-null embryos at least at 35s (**Table 8.1**), although it possible that alternative TGFβ1 ligands promote glial commitment in NPCs. Alternatively, premature neurogenesis at 32s in *Nrp1*-null hindbrains may itself contribute to ectopic gliogenesis in the hindbrain thereafter, similar to a mechanism where neuron-derived cytokines promote glial specification in the developing cortex (Barnabe-Heider et al., 2005).

A large number of TUJ1^{+} neurons accumulate roughly halfway along the apicobasal axis and appear to have stalled during radial migration away from the VZ (**Figure 5.4**). This raises the possibility that NRP1 may be required cell autonomously to direct neuronal migration towards the pial surface by either hapto- or chemotaxis, akin to its role in guiding interneurons to the correct cortical layer (Tamamaki et al., 2003). This idea is supported by the distinct lack of BrdU^{+} labelled cells present in the basal hindbrain at 46s following a 24 h injection, suggesting that neurons formed later into hindbrain development are unable to perform radial migration. On the other hand, it would be interesting to study whether the accumulation of neurons takes place at the level of the rudimentary vessel plexus that forms at 46s in *Nrp1*-null hindbrains as this might suggest that hindbrain vasculature regulates neuronal migration by acting as a source of chemotactic cues.

I have demonstrated that NPCs in hindbrains lacking GZ vasculature undergo precocious cell cycle exit at 32s and changes in cell cycle kinetics at 36s. However, unlike in the forebrain (Lange et al., 2016), these defects do not stem from prolonged tissue hypoxia. Expression of the hypoxia-regulated markers *Hif1a*, *Vegfa* and GLUT1 is upregulated during reduced hindbrain vascularisation in *Nrp1*$^{-/-}$ mutants, but relieving hypoxia fails to restore the balance between self-renewal and

neurogenesis (**Figure 5.8**). It is possible that this difference in vascular roles in regulating neurogenesis in the hindbrain and forebrain stems from their different NPC subtypes. Thus, $TBR2^+$ BPs are abundant in the developing forebrain (Sessa et al., 2008), and prolonged hypoxia specifically impairs differentiation of APs into $TBR2^+$ BPs (Lange et al., 2016). However, $TBR2^+$ NPCs are absent from the hindbrain and spinal cord (Kwon and Hadjantonakis, 2007). Furthermore, I have observed a contrasting defect in NPC self-renewal to that demonstrated in the *Gpr124*-null forebrain (Lange et al., 2016), as defective hindbrain vascularisation instead results in increased neurogenesis (**Figure 5.1** and**Figure 5.3**). As restoring oxygenation does not explain the role of GZ vasculature in vascular regulation of hindbrain NPCs, it will be important to identify alternative mechanisms by which blood vessels communicate with NPCs.

qRT-PCR analysis in *Nrp1*-null JF1 hindbrains at 35s demonstrated that the expression of a number of secreted ligands is upregulated in the 35s *Nrp1*-null hindbrain compared to control hindbrains (**Figure 5.9**). Although I have not characterised potential angiogenesis defects *in vivo* in *Nrp1*-null JF1 hindbrains at 35s, it seems likely that they have a similar vascular phenotype as mutants on a CD1 or C57/Bl6 background, which were used in all experiments. In agreement, I detected similarly increased *Vegfa* levels in *Nrp1*-null hindbrains in CD1 and JF1 embryos, suggesting prolonged hypoxia due to vascular insufficiency **(Figure 5.8** and**Figure 5.9**).

A caveat in the array of gene expression in the *Nrp1*-null hindbrain is that it did not allow me to assign transcripts with altered expression levels to specific cell types, as at least some of the genes were expressed either by NPCs, neurons or non-neural cells such as endothelial cells. In any case, it was unlikely that the expression of differentiative factors that contributed to precocious neural differentiation was controlled cell autonomously in neural cells by NRP1, as I did not detect any defects in NPC mitosis in *Nes-Cre; Nrp1*$^{c/-}$ hindbrains, but saw defects in NPC mitotic patterns and increased premature cell cycle exit in *Tie2-Cre; Nrp1*$^{c/-}$ hindbrains (**Figure 4.7** and**Figure 5.1**). However, the increase in the expression of extrinsic

signalling ligands in the absence of GZ vasculature in *Nrp1*-null hindbrains also suggests that upregulated molecules were not endothelium-derived.

To tackle the challenge of identifying which cell types express the genes whose expression changes after NRP1 loss, I have begun to examine the transcriptome of FACS-isolated endothelium at 35s. This analysis indicates that upregulated differentiative factors such as BDNF or NTF3 (**Figure 5.10**) are not obviously expressed by endothelium, but are generated elsewhere in the neuroepithelium (**Figure 5.11**). Thus, the most parsimonious explanation for the altered patterns of gene regulation is that hindbrain vasculature inhibits the expression of genes that orchestrate the switch from self-renewing to differentiative cell divisions in a timely manner.

The upregulation of BDNF and NT3 expression in *Nrp1*$^{-/-}$ mutant hindbrain is of particular interest, given that both factors are potent differentiative and pro-survival factors during development, and I have observed increased neural differentiation marker expression, as well as decreased apoptosis (**Figure 4.3** and **Figure 5.4**). Moreover, NT3 promotes cell cycle arrest in cortical NPCs (Lukaszewicz et al., 2002), which agrees with the observation that G1 lengthening takes place in *Nrp1*$^{-/-}$ embryos at 36s, when *Ntf3* expression is considerably upregulated (**Figure 5.6**). Yet, neither BDNF nor NT3 form part of the endothelial secretome, suggesting that their increased abundance in the NRP1-deficient hindbrain results from losing vascular repression of their transcription. As CNS endothelium represents the main cell type of *Nos3* (eNOS) expression in the adult brain (Zhang et al., 2014) and hindbrain endothelial cells likely express eNOS (**Figure 5.11**) and therefore secrete NO, vessel-derived NO may form part of a regulatory framework that controls neurotrophin abundance or activity to modulate NPC self-renewal and commitment.

However, I cannot exclude that increased expression of differentiative factors such as BDNF and NT3 is an indirect consequence of precocious neurogenesis, rather than reflect the loss of repression in *Nrp1*-deficient hindbrains lacking proper vascularisation. Feedback mechanisms involving NT3 secretion by newly formed neurons, like those functioning in the developing forebrain, for example

(Parthasarathy et al., 2014), may also operate in the hindbrain following ectopic neurogenesis. In this context, it is unclear what restricts expression of these pro-differentiation factors at e8.5 or e9.5, when the neuroepithelium expands rapidly without undergoing neurogenesis, even though GZ vasculature is lacking by default in both wildtype and mutant embryos at these stages.

In addition to paracrine interactions, contact-dependent signals between vessels and NPCs may also regulate neurogenesis in the hindbrain, as there is clear vessel-progenitor contact (**Figure 3.6 -Figure 3.8**). For example, hindbrain vasculature may regulate NPC stemness through the expression of Notch ligands (**Figure 5.11**) that interact in trans with Notch receptors on NPCs, similar to JAG1 that promotes NSC quiescence in the adult brain (Ottone et al., 2014). Endothelial DLL1 may also maintain progenitor identity and proliferation by activating Notch-driven Hes family gene expression in NPCs.

5.4 Summary

In this chapter, I have examined the role of hindbrain blood vessels in the regulation of NPC self-renewal and neurogenesis. Delayed formation of GZ vasculature results in precocious cell cycle exit and neuron formation in *Nrp1*-null hindbrains, which ultimately depletes the pool of cycling NPCs at later stages in development, impairs long-term neurogenesis and attenuates hindbrain growth. NPC cell cycle kinetics are also affected in hindbrains lacking GZ vasculature. Unlike in the developing forebrain, GZ vasculature does not regulate NPC self-renewal via a role in tissue oxygenation; instead, it may do so by restricting the expression of factors known to potently induce neuronal differentiation in the developing CNS, as well as through contact-dependent regulation of NPC stemness.

Chapter 6 FINAL CONCLUSIONS AND FUTURE WORK

6.1 Summary of Conclusions and Final Remarks

During my PhD, my aims have been to understand the potential roles of VEGF-A and vasculature-derived signals in regulating mammalian NPCs during embryogenesis.

My characterisation of hindbrain neurogenesis has shown that it occurs in close spatial proximity to sprouting blood vessels, and that NPC cell division accelerates once hindbrain progenitors reside within a highly vascularised GZ. My research has also demonstrated that NPCs extend processes that contact the SVP and associated ECM, which agrees with similar observations of forebrain NPCs made by another group during my PhD. I have confirmed progenitor-vessel contact in the hindbrain using mosaic labelling of NPCs with the *Sox1-iCreER*^{T2} transgene.

My analysis of mouse mutants lacking *Nrp1* both globally and selectively in endothelial cells has demonstrated that NRP1 regulates normal mitotic behaviour of NPCs by promoting vascularisation of the hindbrain GZ. Conversely, I have also shown that NPC-expressed NRP1 is not required for sustaining NPC cell division. This finding, paired with the lack of VEGFR2 expression in NPCs, indicates that VEGF-A is unlikely to signal directly to NPCs in the same manner as in the adult brain and challenges the belief that it does so during development.

I have provided novel evidence that CNS vasculature maintains NPC self-renewal, delays the switch to neurogenesis and sustains the pool of NPCs until later stages of hindbrain development. In contrast to work carried out in the forebrain towards the end of my research project, hindbrain vasculature does not regulate neurogenesis by relieving hypoxia in the neuroepithelium. Instead, it likely does so by restricting the abundance of pro-differentiative factors that accumulate at the time when most NPCs exit the cell cycle prematurely. Therefore, my work demonstrates that vascular signals represent a vital component of the neurogenic niche that regulates embryonic NPCs and ensures sufficient CNS growth.

During my PhD, I have used my growing knowledge of the role of NRP1 to contribute to a textbook chapter concerning its function as a neural surface antigen (Tata, 2015), whilst I have also authored a peer-reviewed review article concerning the mechanisms underlying CNS vascularisation (Tata et al., 2015; see APPENDIX). Furthermore, I have recently published my findings regarding the role of GZ vasculature in embryonic neurogenesis in *Proceedings of the National Academy of Sciences* (Tata et al., 2016; see APPENDIX). In addition, I have significant data presented herein that is not included in the aforementioned manuscript and I aim to expand upon this work with additional experiments (see **6.2**) to produce a second primary research article concerning the specific mechanisms underlying angiocrine regulation of NPCs. Finally, and independently of my work on mammalian neurogenesis, I have contributed significantly to a collaborative study with another laboratory (Dr. Quenten Schwarz, U. South Australia) addressing the development and innervation of the adrenal primordia, from which a manuscript is currently in preparation

6.2 Future work

6.2.1 The spatial relationship between neurogenesis and angiogenesis

Having demonstrated that hindbrain NPCs divide within a vascularised compartment, future work could address whether mitotic NPCs are preferentially positioned near vasculature, as has been shown for perivascular forebrain BPs (Javaherian and Kriegstein, 2009). In addition, ultrascopic analysis of NPC contact with vessels using electron microscopy would determine whether NPCs attach themselves to vasculature using cell-cell junctions required for physical anchorage. Furthermore, immunolabelling for Notch and Integrin expression at these contact sites would identify if NPCs receive cell contact-dependent regulation from blood vessels.

6.2.2 Role of NRPs and VEGF in NPCs

NRP1 is not required for regulating NPC mitosis, but is expressed widely across the hindbrain neuroepithelium, posing the question of its specific role in

hindbrain progenitors. Given its importance in neurons elsewhere in the CNS (Chen et al., 2008) and apparent neuronal positioning defects in *Nrp1*-null mutants, analysis of neuronal migration in *Nestin-Cre; Nrp1*$^{c-/-}$ embryos that selectively lack NRP1 in neurons would determine whether it is required for radial migration across the hindbrain. Studying the role of NRP2 in NPCs would also reveal if it too is required during neurogenesis, given its potential role in maintaining NPC mitosis at later stages of development. Additionally, future work is also warranted to unequivocally determine whether VEGF-A signalling regulates hindbrain NPCs. Current evidence supports the idea that VEGF-A signals directly to forebrain-derived NPCs *in vitro* (Javaherian and Kriegstein, 2009, Wada et al., 2006). However, similar evidence is not yet available for hindbrain-derived NPCs. My *in vivo* evidence suggests that VEGF-A signalling through NRP1 in NPCs is not required to regulate NPC proliferation, but I have not yet determined whether NRP2 might compensate for NRP1 in this process. This could be investigated in mutants that lack VEGF signalling through NRP1 (*Nrp1*$^{D320K/D320K}$; Gelfand et al., 2014) on an *Nrp2*-null background. Moreover, exposing neurospheres derived from hindbrain NPCs to exogenous VEGF-A could confirm whether VEGF-A regulation by VEGFR2 is restricted to an *in vitro* context, given that VEGFR2 expression by NPCs was not observed *in vivo*. Finally, future experiments should address whether an alternative VEGF implicated in neurogenesis, VEGF-C, regulates hindbrain NPCs in the manner demonstrated already in mammals and amphibians (Le Bras et al., 2006).

6.2.3 Neural lineage progression in the hindbrain

The generation of specific neuronal subtypes, as well as glia, in the hindbrain remains poorly characterised and may possess a temporal correlation to angiogenesis. Comparing the birth time of various neurons and glia with the period of CNS vascularisation could identify specific neural lineages that are selectively regulated by vascular-derived signals, akin to interneurons in the forebrain (Tan et al., 2016). Future work must also identify the trend of cell cycle kinetics during the switch from self-renewing to differentiative cell divisions, given the differing patterns observed in other areas of the CNS (Saade et al., 2013, Calegari et al., 2005). Cell cycle reporter mouse strains (Abe et al., 2013) could be used to define

cell cycle progression in specific NPC subtypes, as well as in characterising the effect of angiocrine factors on NPC behaviour (see below).

6.2.4 Angiocrine signalling from embryonic CNS vasculature

The expression of several secreted ligands is upregulated in *Nrp1*$^{-/-}$ hindbrains with defective angiogenesis. As these hindbrains contain a smaller complement of endothelial cells compared to those in wildtype embryos, these factors likely derive from non-endothelial cell types and suggest that hindbrain blood vessels play an inhibitory role in regulating the expression of potential differentiative factors. Establishing the transcriptome of hindbrain endothelial cells, such as with RNAseq performed on FACS-isolated endothelium, will therefore provide insight into the likely signalling molecules generated by blood vessels in the developing CNS. From this knowledge, future work can then address which non-endothelial niche signals may be regulated by vessel-derived factors, as highlighted by differential gene expression in poorly vascularised *Nrp1*$^{-/-}$ hindbrains. Additionally, this line of inquiry may uncover new vascular signals that were not assayed for in the qRT-PCR experiments described in this thesis.

6.2.5 Functional analysis of vascular regulation of NPCs

Conditional deletion of candidate signalling molecules from endothelial cells only should confirm the role of vascular cues in sustaining NPC mitosis and self-renewal. Furthermore, endothelial-specific mouse mutants can then be applied to studying the role of vascular regulation in neural lineage and cell cycle progression, INM and transcriptional programs in NPCs. Assaying the role of vascular cues on cultured neurospheres *in vitro* could also complement experiments performed on mouse embryonic tissue. Finally, future work should examine whether mechanisms of vascular regulation of NPCs are conserved elsewhere in the nervous system, such as in the forebrain, and even whether the same regulatory mechanisms function in other species. These experiments will therefore determine how vascular regulation helps orchestrates overall CNS development as a vital component of the neurogenic niche.

Chapter 7 BIBLIOGRAPHY

AAKU-SARASTE, E., HELLWIG, A. & HUTTNER, W. B. 1996. Loss of occludin and functional tight junctions, but not ZO-1, during neural tube closure--remodeling of the neuroepithelium prior to neurogenesis. *Dev Biol,* 180**,** 664-79.

ABE, T., SAKAUE-SAWANO, A., KIYONARI, H., SHIOI, G., INOUE, K., HORIUCHI, T., NAKAO, K., MIYAWAKI, A., AIZAWA, S. & FUJIMORI, T. 2013. Visualization of cell cycle in mouse embryos with Fucci2 reporter directed by Rosa26 promoter. *Development,* 140**,** 237-46.

ABLES, J. L., DECAROLIS, N. A., JOHNSON, M. A., RIVERA, P. D., GAO, Z., COOPER, D. C., RADTKE, F., HSIEH, J. & EISCH, A. J. 2010. Notch1 is required for maintenance of the reservoir of adult hippocampal stem cells. *J Neurosci,* 30**,** 10484-92.

AGUIRRE, A., RUBIO, M. E. & GALLO, V. 2010. Notch and EGFR pathway interaction regulates neural stem cell number and self-renewal. *Nature,* 467**,** 323-7.

AHMED, S., REYNOLDS, B. A. & WEISS, S. 1995. BDNF enhances the differentiation but not the survival of CNS stem cell-derived neuronal precursors. *J Neurosci,* 15**,** 5765-78.

AKIZU, N., ESTARAS, C., GUERRERO, L., MARTI, E. & MARTINEZ-BALBAS, M. A. 2010. H3K27me3 regulates BMP activity in developing spinal cord. *Development,* 137**,** 2915-25.

ALEXANDRE, P., REUGELS, A. M., BARKER, D., BLANC, E. & CLARKE, J. D. 2010. Neurons derive from the more apical daughter in asymmetric divisions in the zebrafish neural tube. *Nat Neurosci,* 13**,** 673-9.

ALVAREZ, J. I., DODELET-DEVILLERS, A., KEBIR, H., IFERGAN, I., FABRE, P. J., TEROUZ, S., SABBAGH, M., WOSIK, K., BOURBONNIERE, L., BERNARD, M., VAN HORSSEN, J., DE VRIES, H. E., CHARRON, F. & PRAT, A. 2011. The Hedgehog pathway promotes blood-brain barrier integrity and CNS immune quiescence. *Science,* 334**,** 1727-31.

ALVAREZ-MEDINA, R., CAYUSO, J., OKUBO, T., TAKADA, S. & MARTI, E. 2008. Wnt canonical pathway restricts graded Shh/Gli patterning activity through the regulation of Gli3 expression. *Development,* 135**,** 237-47.

ANDERSON, K. D., PAN, L., YANG, X. M., HUGHES, V. C., WALLS, J. R., DOMINGUEZ, M. G., SIMMONS, M. V., BURFEIND, P., XUE, Y., WEI, Y., MACDONALD, L. E., THURSTON, G., DALY, C., LIN, H. C., ECONOMIDES, A. N., VALENZUELA, D. M., MURPHY, A. J., YANCOPOULOS, G. D. & GALE, N. W. 2011. Angiogenic sprouting into neural tissue requires Gpr124, an orphan G protein-coupled receptor. *Proc Natl Acad Sci U S A,* 108**,** 2807-12.

ANDRES, R., FORGIE, A., WYATT, S., CHEN, Q., DE SAUVAGE, F. J. & DAVIES, A. M. 2001. Multiple effects of artemin on sympathetic neurone generation, survival and growth. *Development,* 128**,** 3685-95.

ANDREU-AGULLO, C., MORANTE-REDOLAT, J. M., DELGADO, A. C. & FARINAS, I. 2009. Vascular niche factor PEDF modulates Notch-dependent stemness in the adult subependymal zone. *Nat Neurosci,* 12**,** 1514-23.

ANGATA, K., HUCKABY, V., RANSCHT, B., TERSKIKH, A., MARTH, J. D. & FUKUDA, M. 2007. Polysialic acid-directed migration and differentiation of neural precursors are essential for mouse brain development. *Mol Cell Biol,* 27**,** 6659-68.

ANTON, E. S., KREIDBERG, J. A. & RAKIC, P. 1999. Distinct functions of alpha3 and alpha(v) integrin receptors in neuronal migration and laminar organization of the cerebral cortex. *Neuron,* 22**,** 277-89.

ANTONOPOULOS, J., PAPPAS, I. S. & PARNAVELAS, J. G. 1997. Activation of the GABAA receptor inhibits the proliferative effects of bFGF in cortical progenitor cells. *Eur J Neurosci,* 9**,** 291-8.

ANTONY, J. M., PAQUIN, A., NUTT, S. L., KAPLAN, D. R. & MILLER, F. D. 2011. Endogenous microglia regulate development of embryonic cortical precursor cells. *J Neurosci Res,* 89**,** 286-98.

AQUINO, J. B., MARMIGERE, F., LALLEMEND, F., LUNDGREN, T. K., VILLAR, M. J., WEGNER, M. & ERNFORS, P. 2008. Differential expression and dynamic changes of murine NEDD9 in progenitor cells of diverse tissues. *Gene Expr Patterns,* 8**,** 217-26.

ARAI, Y., PULVERS, J. N., HAFFNER, C., SCHILLING, B., NUSSLEIN, I., CALEGARI, F. & HUTTNER, W. B. 2011. Neural stem and progenitor cells shorten S-phase on commitment to neuron production. *Nat Commun,* 2**,** 154.

ARAKAWA, Y., SENDTNER, M. & THOENEN, H. 1990. Survival effect of ciliary neurotrophic factor (CNTF) on chick embryonic motoneurons in culture: comparison with other neurotrophic factors and cytokines. *J Neurosci,* 10**,** 3507-15.

ARBEILLE, E., REYNAUD, F., SANYAS, I., BOZON, M., KINDBEITER, K., CAUSERET, F., PIERANI, A., FALK, J., MORET, F. & CASTELLANI, V. 2015. Cerebrospinal fluid-derived Semaphorin3B orients neuroepithelial cell divisions in the apicobasal axis. *Nat Commun,* 6**,** 6366.

ARNOLD, T. D., FERRERO, G. M., QIU, H., PHAN, I. T., AKHURST, R. J., HUANG, E. J. & REICHARDT, L. F. 2012. Defective retinal vascular endothelial cell development as a consequence of impaired integrin alphaVbeta8-mediated activation of transforming growth factor-beta. *J Neurosci,* 32**,** 1197-206.

ARNOLD, T. D., NIAUDET, C., PANG, M. F., SIEGENTHALER, J., GAENGEL, K., JUNG, B., FERRERO, G. M., MUKOUYAMA, Y. S., FUXE, J., AKHURST, R., BETSHOLTZ, C., SHEPPARD, D. & REICHARDT, L. F. 2014. Excessive vascular sprouting underlies cerebral hemorrhage in mice lacking alphaVbeta8-TGFbeta signaling in the brain. *Development,* 141**,** 4489-99.

ARSENIJEVIC, Y., WEISS, S., SCHNEIDER, B. & AEBISCHER, P. 2001. Insulin-like growth factor-I is necessary for neural stem cell proliferation and demonstrates distinct actions of epidermal growth factor and fibroblast growth factor-2. *J Neurosci,* 21**,** 7194-202.

ASAMI, M., PILZ, G. A., NINKOVIC, J., GODINHO, L., SCHROEDER, T., HUTTNER, W. B. & GOTZ, M. 2011. The role of Pax6 in regulating the orientation and mode of cell division of progenitors in the mouse cerebral cortex. *Development,* 138**,** 5067-78.

ASPALTER, I. M., GORDON, E., DUBRAC, A., RAGAB, A., NARLOCH, J., VIZAN, P., GEUDENS, I., COLLINS, R. T., FRANCO, C. A.,

ABRAHAMS, C. L., THURSTON, G., FRUTTIGER, M., ROSEWELL, I., EICHMANN, A. & GERHARDT, H. 2015. Alk1 and Alk5 inhibition by Nrp1 controls vascular sprouting downstream of Notch. *Nat Commun,* 6**,** 7264.

AUTIERO, M., WALTENBERGER, J., COMMUNI, D., KRANZ, A., MOONS, L., LAMBRECHTS, D., KROLL, J., PLAISANCE, S., DE MOL, M., BONO, F., KLICHE, S., FELLBRICH, G., BALLMER-HOFER, K., MAGLIONE, D., MAYR-BEYRLE, U., DEWERCHIN, M., DOMBROWSKI, S., STANIMIROVIC, D., VAN HUMMELEN, P., DEHIO, C., HICKLIN, D. J., PERSICO, G., HERBERT, J. M., COMMUNI, D., SHIBUYA, M., COLLEN, D., CONWAY, E. M. & CARMELIET, P. 2003. Role of PlGF in the intra- and intermolecular cross talk between the VEGF receptors Flt1 and Flk1. *Nat Med,* 9**,** 936-43.

AVERBUCH-HELLER, L., PRUGININ, M., KAHANE, N., TSOULFAS, P., PARADA, L., ROSENTHAL, A. & KALCHEIM, C. 1994. Neurotrophin 3 stimulates the differentiation of motoneurons from avian neural tube progenitor cells. *Proc Natl Acad Sci U S A,* 91**,** 3247-51.

AVILION, A. A., NICOLIS, S. K., PEVNY, L. H., PEREZ, L., VIVIAN, N. & LOVELL-BADGE, R. 2003. Multipotent cell lineages in early mouse development depend on SOX2 function. *Genes Dev,* 17**,** 126-40.

BAI, G., SHENG, N., XIE, Z., BIAN, W., YOKOTA, Y., BENEZRA, R., KAGEYAMA, R., GUILLEMOT, F. & JING, N. 2007. Id sustains Hes1 expression to inhibit precocious neurogenesis by releasing negative autoregulation of Hes1. *Dev Cell,* 13**,** 283-97.

BALASUBRAMANIYAN, V., BODDEKE, E., BAKELS, R., KUST, B., KOOISTRA, S., VENEMAN, A. & COPRAY, S. 2006. Effects of histone deacetylation inhibition on neuronal differentiation of embryonic mouse neural stem cells. *Neuroscience,* 143**,** 939-51.

BALLAS, N., GRUNSEICH, C., LU, D. D., SPEH, J. C. & MANDEL, G. 2005. REST and its corepressors mediate plasticity of neuronal gene chromatin throughout neurogenesis. *Cell,* 121**,** 645-57.

BARKER, N. 2014. Adult intestinal stem cells: critical drivers of epithelial homeostasis and regeneration. *Nat Rev Mol Cell Biol,* 15**,** 19-33.

BARNABE-HEIDER, F., WASYLNKA, J. A., FERNANDES, K. J., PORSCHE, C., SENDTNER, M., KAPLAN, D. R. & MILLER, F. D. 2005. Evidence that embryonic neurons regulate the onset of cortical gliogenesis via cardiotrophin-1. *Neuron,* 48**,** 253-65.

BARTLETT, P. F., BROOKER, G. J., FAUX, C. H., DUTTON, R., MURPHY, M., TURNLEY, A. & KILPATRICK, T. J. 1998. Regulation of neural stem cell differentiation in the forebrain. *Immunol Cell Biol,* 76**,** 414-8.

BAYE, L. M. & LINK, B. A. 2007. Interkinetic nuclear migration and the selection of neurogenic cell divisions during vertebrate retinogenesis. *J Neurosci,* 27**,** 10143-52.

BENEDITO, R., ROCHA, S. F., WOESTE, M., ZAMYKAL, M., RADTKE, F., CASANOVAS, O., DUARTE, A., PYTOWSKI, B. & ADAMS, R. H. 2012. Notch-dependent VEGFR3 upregulation allows angiogenesis without VEGF-VEGFR2 signalling. *Nature,* 484**,** 110-4.

BENEZRA, R., DAVIS, R. L., LOCKSHON, D., TURNER, D. L. & WEINTRAUB, H. 1990. The protein Id: a negative regulator of helix-loop-helix DNA binding proteins. *Cell,* 61**,** 49-59.

BENNER, E. J., LUCIANO, D., JO, R., ABDI, K., PAEZ-GONZALEZ, P., SHENG, H., WARNER, D. S., LIU, C., EROGLU, C. & KUO, C. T. 2013. Protective astrogenesis from the SVZ niche after injury is controlled by Notch modulator Thbs4. *Nature,* 497**,** 369-73.

BETIZEAU, M., CORTAY, V., PATTI, D., PFISTER, S., GAUTIER, E., BELLEMIN-MENARD, A., AFANASSIEFF, M., HUISSOUD, C., DOUGLAS, R. J., KENNEDY, H. & DEHAY, C. 2013. Precursor diversity and complexity of lineage relationships in the outer subventricular zone of the primate. *Neuron,* 80**,** 442-57.

BIANCO, I. H., CARL, M., RUSSELL, C., CLARKE, J. D. & WILSON, S. W. 2008. Brain asymmetry is encoded at the level of axon terminal morphology. *Neural Dev,* 3**,** 9.

BLANPAIN, C., LOWRY, W. E., PASOLLI, H. A. & FUCHS, E. 2006. Canonical notch signaling functions as a commitment switch in the epidermal lineage. *Genes Dev,* 20**,** 3022-35.

BLESCH, A., UY, H. S., GRILL, R. J., CHENG, J. G., PATTERSON, P. H. & TUSZYNSKI, M. H. 1999. Leukemia inhibitory factor augments neurotrophin expression and corticospinal axon growth after adult CNS injury. *J Neurosci,* 19**,** 3556-66.

BONAGUIDI, M. A., PENG, C. Y., MCGUIRE, T., FALCIGLIA, G., GOBESKE, K. T., CZEISLER, C. & KESSLER, J. A. 2008. Noggin expands neural stem cells in the adult hippocampus. *J Neurosci,* 28**,** 9194-204.

BOND, J., ROBERTS, E., MOCHIDA, G. H., HAMPSHIRE, D. J., SCOTT, S., ASKHAM, J. M., SPRINGELL, K., MAHADEVAN, M., CROW, Y. J., MARKHAM, A. F., WALSH, C. A. & WOODS, C. G. 2002. ASPM is a major determinant of cerebral cortical size. *Nat Genet,* 32**,** 316-20.

BOND, J., ROBERTS, E., SPRINGELL, K., LIZARRAGA, S. B., SCOTT, S., HIGGINS, J., HAMPSHIRE, D. J., MORRISON, E. E., LEAL, G. F., SILVA, E. O., COSTA, S. M., BARALLE, D., RAPONI, M., KARBANI, G., RASHID, Y., JAFRI, H., BENNETT, C., CORRY, P., WALSH, C. A. & WOODS, C. G. 2005. A centrosomal mechanism involving CDK5RAP2 and CENPJ controls brain size. *Nat Genet,* 37**,** 353-5.

BOND, J. & WOODS, C. G. 2006. Cytoskeletal genes regulating brain size. *Curr Opin Cell Biol,* 18**,** 95-101.

BORRELL, V. & MARIN, O. 2006. Meninges control tangential migration of hem-derived Cajal-Retzius cells via CXCL12/CXCR4 signaling. *Nat Neurosci,* 9**,** 1284-93.

BOUTIN, C., HARDT, O., DE CHEVIGNY, A., CORE, N., GOEBBELS, S., SEIDENFADEN, R., BOSIO, A. & CREMER, H. 2010. NeuroD1 induces terminal neuronal differentiation in olfactory neurogenesis. *Proc Natl Acad Sci U S A,* 107**,** 1201-6.

BOUVREE, K., BRUNET, I., DEL TORO, R., GORDON, E., PRAHST, C., CRISTOFARO, B., MATHIVET, T., XU, Y., SOUEID, J., FORTUNA, V., MIURA, N., AIGROT, M. S., MADEN, C. H., RUHRBERG, C., THOMAS, J. L. & EICHMANN, A. 2012. Semaphorin3A, Neuropilin-1, and PlexinA1 are required for lymphatic valve formation. *Circ Res,* 111**,** 437-45.

BOVETTI, S., HSIEH, Y. C., BOVOLIN, P., PERROTEAU, I., KAZUNORI, T. & PUCHE, A. C. 2007. Blood vessels form a scaffold for neuroblast migration in the adult olfactory bulb. *J Neurosci,* 27**,** 5976-80.

BREDT, D. S. & SNYDER, S. H. 1994. Transient nitric oxide synthase neurons in embryonic cerebral cortical plate, sensory ganglia, and olfactory epithelium. *Neuron,* 13**,** 301-13.

BRUEL-JUNGERMAN, E., DAVIS, S., RAMPON, C. & LAROCHE, S. 2006. Long-term potentiation enhances neurogenesis in the adult dentate gyrus. *J Neurosci,* 26**,** 5888-93.

BUEHLER, A., SITARAS, N., FAVRET, S., BUCHER, F., BERGER, S., PIELEN, A., JOYAL, J. S., JUAN, A. M., MARTIN, G., SCHLUNCK, G., AGOSTINI, H. T., KLAGSBRUN, M., SMITH, L. E., SAPIEHA, P. & STAHL, A. 2013. Semaphorin 3F forms an anti-angiogenic barrier in outer retina. *FEBS Lett,* 587**,** 1650-5.

BUESCHER, M., HING, F. S. & CHIA, W. 2002. Formation of neuroblasts in the embryonic central nervous system of Drosophila melanogaster is controlled by SoxNeuro. *Development,* 129**,** 4193-203.

BULTJE, R. S., CASTANEDA-CASTELLANOS, D. R., JAN, L. Y., JAN, Y. N., KRIEGSTEIN, A. R. & SHI, S. H. 2009. Mammalian Par3 regulates progenitor cell asymmetric division via notch signaling in the developing neocortex. *Neuron,* 63**,** 189-202.

BUSSMANN, J., WOLFE, S. A. & SIEKMANN, A. F. 2011. Arterial-venous network formation during brain vascularization involves hemodynamic regulation of chemokine signaling. *Development,* 138**,** 1717-26.

CALEGARI, F., HAUBENSAK, W., HAFFNER, C. & HUTTNER, W. B. 2005. Selective lengthening of the cell cycle in the neurogenic subpopulation of neural progenitor cells during mouse brain development. *J Neurosci,* 25**,** 6533-8.

CALEGARI, F. & HUTTNER, W. B. 2003. An inhibition of cyclin-dependent kinases that lengthens, but does not arrest, neuroepithelial cell cycle induces premature neurogenesis. *J Cell Sci,* 116**,** 4947-55.

CALVO, C. F., FONTAINE, R. H., SOUEID, J., TAMMELA, T., MAKINEN, T., ALFARO-CERVELLO, C., BONNAUD, F., MIGUEZ, A., BENHAIM, L., XU, Y., BARALLOBRE, M. J., MOUTKINE, I., LYYTIKKA, J., TATLISUMAK, T., PYTOWSKI, B., ZALC, B., RICHARDSON, W., KESSARIS, N., GARCIA-VERDUGO, J. M., ALITALO, K., EICHMANN, A. & THOMAS, J. L. 2011. Vascular endothelial growth factor receptor 3 directly regulates murine neurogenesis. *Genes Dev,* 25**,** 831-44.

CANOSSA, M., GIORDANO, E., CAPPELLO, S., GUARNIERI, C. & FERRI, S. 2002. Nitric oxide down-regulates brain-derived neurotrophic factor secretion in cultured hippocampal neurons. *Proc Natl Acad Sci U S A,* 99**,** 3282-7.

CAO, X., PFAFF, S. L. & GAGE, F. H. 2007. A functional study of miR-124 in the developing neural tube. *Genes Dev,* 21**,** 531-6.

CAPPELLO, S., MONZO, P. & VALLEE, R. B. 2011. NudC is required for interkinetic nuclear migration and neuronal migration during neocortical development. *Dev Biol,* 357**,** 326-35.

CARIBONI, A., DAVIDSON, K., DOZIO, E., MEMI, F., SCHWARZ, Q., STOSSI, F., PARNAVELAS, J. G. & RUHRBERG, C. 2011. VEGF signalling

controls GnRH neuron survival via NRP1 independently of KDR and blood vessels. *Development,* 138**,** 3723-33.

CARMELIET, P., DOR, Y., HERBERT, J. M., FUKUMURA, D., BRUSSELMANS, K., DEWERCHIN, M., NEEMAN, M., BONO, F., ABRAMOVITCH, R., MAXWELL, P., KOCH, C. J., RATCLIFFE, P., MOONS, L., JAIN, R. K., COLLEN, D. & KESHERT, E. 1998. Role of HIF-1alpha in hypoxia-mediated apoptosis, cell proliferation and tumour angiogenesis. *Nature,* 394**,** 485-90.

CASAROSA, S., FODE, C. & GUILLEMOT, F. 1999. Mash1 regulates neurogenesis in the ventral telencephalon. *Development,* 126**,** 525-34.

CHAMBERS, C. B., PENG, Y., NGUYEN, H., GAIANO, N., FISHELL, G. & NYE, J. S. 2001. Spatiotemporal selectivity of response to Notch1 signals in mammalian forebrain precursors. *Development,* 128**,** 689-702.

CHATTERJEE, S., MIZAR, P., CASSEL, R., NEIDL, R., SELVI, B. R., MOHANKRISHNA, D. V., VEDAMURTHY, B. M., SCHNEIDER, A., BOUSIGES, O., MATHIS, C., CASSEL, J. C., ESWARAMOORTHY, M., KUNDU, T. K. & BOUTILLIER, A. L. 2013. A novel activator of CBP/p300 acetyltransferases promotes neurogenesis and extends memory duration in adult mice. *J Neurosci,* 33**,** 10698-712.

CHAUVET, S., COHEN, S., YOSHIDA, Y., FEKRANE, L., LIVET, J., GAYET, O., SEGU, L., BUHOT, M. C., JESSELL, T. M., HENDERSON, C. E. & MANN, F. 2007. Gating of Sema3E/PlexinD1 signaling by neuropilin-1 switches axonal repulsion to attraction during brain development. *Neuron,* 56**,** 807-22.

CHEN, F. & LOTURCO, J. 2012. A method for stable transgenesis of radial glia lineage in rat neocortex by piggyBac mediated transposition. *J Neurosci Methods,* 207**,** 172-80.

CHEN, G., SIMA, J., JIN, M., WANG, K. Y., XUE, X. J., ZHENG, W., DING, Y. Q. & YUAN, X. B. 2008. Semaphorin-3A guides radial migration of cortical neurons during development. *Nat Neurosci,* 11**,** 36-44.

CHENG, A., WANG, S., CAI, J., RAO, M. S. & MATTSON, M. P. 2003. Nitric oxide acts in a positive feedback loop with BDNF to regulate neural progenitor cell proliferation and differentiation in the mammalian brain. *Dev Biol,* 258**,** 319-33.

CHENN, A. & WALSH, C. A. 2002. Regulation of cerebral cortical size by control of cell cycle exit in neural precursors. *Science,* 297**,** 365-9.

CHESNUTT, C., BURRUS, L. W., BROWN, A. M. & NISWANDER, L. 2004. Coordinate regulation of neural tube patterning and proliferation by TGFbeta and WNT activity. *Dev Biol,* 274**,** 334-47.

CHOJNACKI, A., SHIMAZAKI, T., GREGG, C., WEINMASTER, G. & WEISS, S. 2003. Glycoprotein 130 signaling regulates Notch1 expression and activation in the self-renewal of mammalian forebrain neural stem cells. *J Neurosci,* 23**,** 1730-41.

CHRISTOV, C., CHRETIEN, F., ABOU-KHALIL, R., BASSEZ, G., VALLET, G., AUTHIER, F. J., BASSAGLIA, Y., SHININ, V., TAJBAKHSH, S., CHAZAUD, B. & GHERARDI, R. K. 2007. Muscle satellite cells and endothelial cells: close neighbors and privileged partners. *Mol Biol Cell,* 18**,** 1397-409.

CICCOLINI, F. & SVENDSEN, C. N. 1998. Fibroblast growth factor 2 (FGF-2) promotes acquisition of epidermal growth factor (EGF) responsiveness in mouse striatal precursor cells: identification of neural precursors responding to both EGF and FGF-2. *J Neurosci,* 18**,** 7869-80.

CODEGA, P., SILVA-VARGAS, V., PAUL, A., MALDONADO-SOTO, A. R., DELEO, A. M., PASTRANA, E. & DOETSCH, F. 2014. Prospective identification and purification of quiescent adult neural stem cells from their in vivo niche. *Neuron,* 82**,** 545-59.

COSTA, M. R., WEN, G., LEPIER, A., SCHROEDER, T. & GOTZ, M. 2008. Par-complex proteins promote proliferative progenitor divisions in the developing mouse cerebral cortex. *Development,* 135**,** 11-22.

CUI, H., WANG, Y., HUANG, H., YU, W., BAI, M., ZHANG, L., BRYAN, B. A., WANG, Y., LUO, J., LI, D., MA, Y. & LIU, M. 2014. GPR126 protein regulates developmental and pathological angiogenesis through modulation of VEGFR2 receptor signaling. *J Biol Chem,* 289**,** 34871-85.

CULLEN, M., ELZARRAD, M. K., SEAMAN, S., ZUDAIRE, E., STEVENS, J., YANG, M. Y., LI, X., CHAUDHARY, A., XU, L., HILTON, M. B., LOGSDON, D., HSIAO, E., STEIN, E. V., CUTTITTA, F., HAINES, D. C., NAGASHIMA, K., TESSAROLLO, L. & ST CROIX, B. 2011. GPR124, an orphan G protein-coupled receptor, is required for CNS-specific vascularization and establishment of the blood-brain barrier. *Proc Natl Acad Sci U S A,* 108**,** 5759-64.

CUNNINGHAM, C. L., MARTINEZ-CERDENO, V. & NOCTOR, S. C. 2013. Microglia regulate the number of neural precursor cells in the developing cerebral cortex. *J Neurosci,* 33**,** 4216-33.

DAADI, M. M. & WEISS, S. 1999. Generation of tyrosine hydroxylase-producing neurons from precursors of the embryonic and adult forebrain. *J Neurosci,* 19**,** 4484-97.

DAHMANE, N. & RUIZ I ALTABA, A. 1999. Sonic hedgehog regulates the growth and patterning of the cerebellum. *Development,* 126**,** 3089-100.

DANEMAN, R., AGALLIU, D., ZHOU, L., KUHNERT, F., KUO, C. J. & BARRES, B. A. 2009. Wnt/beta-catenin signaling is required for CNS, but not non-CNS, angiogenesis. *Proc Natl Acad Sci U S A,* 106**,** 641-6.

DANEMAN, R., ZHOU, L., KEBEDE, A. A. & BARRES, B. A. 2010. Pericytes are required for blood-brain barrier integrity during embryogenesis. *Nature,* 468**,** 562-6.

DANIELIAN, P. S., MUCCINO, D., ROWITCH, D. H., MICHAEL, S. K. & MCMAHON, A. P. 1998. Modification of gene activity in mouse embryos in utero by a tamoxifen-inducible form of Cre recombinase. *Curr Biol,* 8**,** 1323-6.

DARLAND, D. C., CAIN, J. T., BEROSIK, M. A., SAINT-GENIEZ, M., ODENS, P. W., SCHAUBHUT, G. J., FRISCH, S., STEMMER-RACHAMIMOV, A., DARLAND, T. & D'AMORE, P. A. 2011. Vascular endothelial growth factor (VEGF) isoform regulation of early forebrain development. *Dev Biol,* 358**,** 9-22.

DE PIETRI TONELLI, D., PULVERS, J. N., HAFFNER, C., MURCHISON, E. P., HANNON, G. J. & HUTTNER, W. B. 2008. miRNAs are essential for survival and differentiation of newborn neurons but not for expansion of

neural progenitors during early neurogenesis in the mouse embryonic neocortex. *Development,* 135**,** 3911-21.

DEISSEROTH, K., SINGLA, S., TODA, H., MONJE, M., PALMER, T. D. & MALENKA, R. C. 2004. Excitation-neurogenesis coupling in adult neural stem/progenitor cells. *Neuron,* 42**,** 535-52.

DEL BENE, F., WEHMAN, A. M., LINK, B. A. & BAIER, H. 2008. Regulation of neurogenesis by interkinetic nuclear migration through an apical-basal notch gradient. *Cell,* 134**,** 1055-65.

DELGADO, A. C., FERRON, S. R., VICENTE, D., PORLAN, E., PEREZ-VILLALBA, A., TRUJILLO, C. M., D'OCON, P. & FARINAS, I. 2014. Endothelial NT-3 delivered by vasculature and CSF promotes quiescence of subependymal neural stem cells through nitric oxide induction. *Neuron,* 83**,** 572-85.

DENEEN, B., HO, R., LUKASZEWICZ, A., HOCHSTIM, C. J., GRONOSTAJSKI, R. M. & ANDERSON, D. J. 2006. The transcription factor NFIA controls the onset of gliogenesis in the developing spinal cord. *Neuron,* 52**,** 953-68.

DENNY, K. J., COULTHARD, L. G., JEANES, A., LISGO, S., SIMMONS, D. G., CALLAWAY, L. K., WLODARCZYK, B., FINNELL, R. H., WOODRUFF, T. M. & TAYLOR, S. M. 2013. C5a receptor signaling prevents folate deficiency-induced neural tube defects in mice. *J Immunol,* 190**,** 3493-9.

DJURANOVIC, S., NAHVI, A. & GREEN, R. 2012. miRNA-mediated gene silencing by translational repression followed by mRNA deadenylation and decay. *Science,* 336**,** 237-40.

DOETSCH, F., CAILLE, I., LIM, D. A., GARCIA-VERDUGO, J. M. & ALVAREZ-BUYLLA, A. 1999. Subventricular zone astrocytes are neural stem cells in the adult mammalian brain. *Cell,* 97**,** 703-16.

DOETSCH, F., PETREANU, L., CAILLE, I., GARCIA-VERDUGO, J. M. & ALVAREZ-BUYLLA, A. 2002. EGF converts transit-amplifying neurogenic precursors in the adult brain into multipotent stem cells. *Neuron,* 36**,** 1021-34.

DULABON, L., OLSON, E. C., TAGLIENTI, M. G., EISENHUTH, S., MCGRATH, B., WALSH, C. A., KREIDBERG, J. A. & ANTON, E. S. 2000. Reelin binds alpha3beta1 integrin and inhibits neuronal migration. *Neuron,* 27**,** 33-44.

DUMONT, D. J., JUSSILA, L., TAIPALE, J., LYMBOUSSAKI, A., MUSTONEN, T., PAJUSOLA, K., BREITMAN, M. & ALITALO, K. 1998. Cardiovascular failure in mouse embryos deficient in VEGF receptor-3. *Science,* 282**,** 946-9.

EHM, O., GORITZ, C., COVIC, M., SCHAFFNER, I., SCHWARZ, T. J., KARACA, E., KEMPKES, B., KREMMER, E., PFRIEGER, F. W., ESPINOSA, L., BIGAS, A., GIACHINO, C., TAYLOR, V., FRISEN, J. & LIE, D. C. 2010. RBPJkappa-dependent signaling is essential for long-term maintenance of neural stem cells in the adult hippocampus. *J Neurosci,* 30**,** 13794-807.

ELIAS, L. A. & KRIEGSTEIN, A. R. 2008. Gap junctions: multifaceted regulators of embryonic cortical development. *Trends Neurosci,* 31**,** 243-50.

ELLIS, P., FAGAN, B. M., MAGNESS, S. T., HUTTON, S., TARANOVA, O., HAYASHI, S., MCMAHON, A., RAO, M. & PEVNY, L. 2004. SOX2, a persistent marker for multipotential neural stem cells derived from embryonic stem cells, the embryo or the adult. *Dev Neurosci,* 26**,** 148-65.

ENCINAS, J. M., MICHURINA, T. V., PEUNOVA, N., PARK, J. H., TORDO, J., PETERSON, D. A., FISHELL, G., KOULAKOV, A. & ENIKOLOPOV, G. 2011. Division-coupled astrocytic differentiation and age-related depletion of neural stem cells in the adult hippocampus. *Cell Stem Cell,* 8**,** 566-79.

ERICSON, J., RASHBASS, P., SCHEDL, A., BRENNER-MORTON, S., KAWAKAMI, A., VAN HEYNINGEN, V., JESSELL, T. M. & BRISCOE, J. 1997. Pax6 controls progenitor cell identity and neuronal fate in response to graded Shh signaling. *Cell,* 90**,** 169-80.

ERSKINE, L., REIJNTJES, S., PRATT, T., DENTI, L., SCHWARZ, Q., VIEIRA, J. M., ALAKAKONE, B., SHEWAN, D. & RUHRBERG, C. 2011. VEGF signaling through neuropilin 1 guides commissural axon crossing at the optic chiasm. *Neuron,* 70**,** 951-65.

ETTNER, N., GOHRING, W., SASAKI, T., MANN, K. & TIMPL, R. 1998. The N-terminal globular domain of the laminin alpha1 chain binds to alpha1beta1 and alpha2beta1 integrins and to the heparan sulfate-containing domains of perlecan. *FEBS Lett,* 430**,** 217-21.

FAN, G., MARTINOWICH, K., CHIN, M. H., HE, F., FOUSE, S. D., HUTNICK, L., HATTORI, D., GE, W., SHEN, Y., WU, H., TEN HOEVE, J., SHUAI, K. & SUN, Y. E. 2005. DNA methylation controls the timing of astrogliogenesis through regulation of JAK-STAT signaling. *Development,* 132**,** 3345-56.

FAN, J., PONFERRADA, V. G., SATO, T., VEMARAJU, S., FRUTTIGER, M., GERHARDT, H., FERRARA, N. & LANG, R. A. 2014. Crim1 maintains retinal vascular stability during development by regulating endothelial cell Vegfa autocrine signaling. *Development,* 141**,** 448-59.

FANTIN, A., HERZOG, B., MAHMOUD, M., YAMAJI, M., PLEIN, A., DENTI, L., RUHRBERG, C. & ZACHARY, I. 2014. Neuropilin 1 (NRP1) hypomorphism combined with defective VEGF-A binding reveals novel roles for NRP1 in developmental and pathological angiogenesis. *Development,* 141**,** 556-62.

FANTIN, A., LAMPROPOULOU, A., GESTRI, G., RAIMONDI, C., SENATORE, V., ZACHARY, I. & RUHRBERG, C. 2015. NRP1 Regulates CDC42 Activation to Promote Filopodia Formation in Endothelial Tip Cells. *Cell Rep,* 11**,** 1577-90.

FANTIN, A., VIEIRA, J. M., GESTRI, G., DENTI, L., SCHWARZ, Q., PRYKHOZHIJ, S., PERI, F., WILSON, S. W. & RUHRBERG, C. 2010. Tissue macrophages act as cellular chaperones for vascular anastomosis downstream of VEGF-mediated endothelial tip cell induction. *Blood,* 116**,** 829-40.

FANTIN, A., VIEIRA, J. M., PLEIN, A., DENTI, L., FRUTTIGER, M., POLLARD, J. W. & RUHRBERG, C. 2013a. NRP1 acts cell autonomously in endothelium to promote tip cell function during sprouting angiogenesis. *Blood,* 121**,** 2352-62.

FANTIN, A., VIEIRA, J. M., PLEIN, A., MADEN, C. H. & RUHRBERG, C. 2013b. The embryonic mouse hindbrain as a qualitative and quantitative model for studying the molecular and cellular mechanisms of angiogenesis. *Nat Protoc,* 8**,** 418-29.

FARAH, M. H., OLSON, J. M., SUCIC, H. B., HUME, R. I., TAPSCOTT, S. J. & TURNER, D. L. 2000. Generation of neurons by transient expression of neural bHLH proteins in mammalian cells. *Development,* 127**,** 693-702.

FAULKNER, N. E., DUJARDIN, D. L., TAI, C. Y., VAUGHAN, K. T., O'CONNELL, C. B., WANG, Y. & VALLEE, R. B. 2000. A role for the lissencephaly gene LIS1 in mitosis and cytoplasmic dynein function. *Nat Cell Biol,* 2**,** 784-91.

FENG, Y. & WALSH, C. A. 2004. Mitotic spindle regulation by Nde1 controls cerebral cortical size. *Neuron,* 44**,** 279-93.

FERNANDEZ, V., LLINARES-BENADERO, C. & BORRELL, V. 2016. Cerebral cortex expansion and folding: what have we learned? *EMBO J,* 35**,** 1021-44.

FERRARA, N., CARVER-MOORE, K., CHEN, H., DOWD, M., LU, L., O'SHEA, K. S., POWELL-BRAXTON, L., HILLAN, K. J. & MOORE, M. W. 1996. Heterozygous embryonic lethality induced by targeted inactivation of the VEGF gene. *Nature,* 380**,** 439-42.

FIETZ, S. A., KELAVA, I., VOGT, J., WILSCH-BRAUNINGER, M., STENZEL, D., FISH, J. L., CORBEIL, D., RIEHN, A., DISTLER, W., NITSCH, R. & HUTTNER, W. B. 2010. OSVZ progenitors of human and ferret neocortex are epithelial-like and expand by integrin signaling. *Nat Neurosci,* 13**,** 690-9.

FIETZ, S. A., LACHMANN, R., BRANDL, H., KIRCHER, M., SAMUSIK, N., SCHRODER, R., LAKSHMANAPERUMAL, N., HENRY, I., VOGT, J., RIEHN, A., DISTLER, W., NITSCH, R., ENARD, W., PAABO, S. & HUTTNER, W. B. 2012. Transcriptomes of germinal zones of human and mouse fetal neocortex suggest a role of extracellular matrix in progenitor self-renewal. *Proc Natl Acad Sci U S A,* 109**,** 11836-41.

FILIPPOV, V., KRONENBERG, G., PIVNEVA, T., REUTER, K., STEINER, B., WANG, L. P., YAMAGUCHI, M., KETTENMANN, H. & KEMPERMANN, G. 2003. Subpopulation of nestin-expressing progenitor cells in the adult murine hippocampus shows electrophysiological and morphological characteristics of astrocytes. *Mol Cell Neurosci,* 23**,** 373-82.

FISCHER, A., SCHUMACHER, N., MAIER, M., SENDTNER, M. & GESSLER, M. 2004. The Notch target genes Hey1 and Hey2 are required for embryonic vascular development. *Genes Dev,* 18**,** 901-11.

FISH, J. L., KOSODO, Y., ENARD, W., PAABO, S. & HUTTNER, W. B. 2006. Aspm specifically maintains symmetric proliferative divisions of neuroepithelial cells. *Proc Natl Acad Sci U S A,* 103**,** 10438-43.

FLORIO, M., ALBERT, M., TAVERNA, E., NAMBA, T., BRANDL, H., LEWITUS, E., HAFFNER, C., SYKES, A., WONG, F. K., PETERS, J., GUHR, E., KLEMROTH, S., PRUFER, K., KELSO, J., NAUMANN, R., NUSSLEIN, I., DAHL, A., LACHMANN, R., PAABO, S. & HUTTNER, W. B. 2015. Human-specific gene ARHGAP11B promotes basal progenitor amplification and neocortex expansion. *Science,* 347**,** 1465-70.

FODE, C., MA, Q., CASAROSA, S., ANG, S. L., ANDERSON, D. J. & GUILLEMOT, F. 2000. A role for neural determination genes in specifying the dorsoventral identity of telencephalic neurons. *Genes Dev,* 14**,** 67-80.

FUENTEALBA, L. C., ROMPANI, S. B., PARRAGUEZ, J. I., OBERNIER, K., ROMERO, R., CEPKO, C. L. & ALVAREZ-BUYLLA, A. 2015. Embryonic Origin of Postnatal Neural Stem Cells. *Cell,* 161**,** 1644-55.

FUKUMITSU, H., FURUKAWA, Y., TSUSAKA, M., KINUKAWA, H., NITTA, A., NOMOTO, H., MIMA, T. & FURUKAWA, S. 1998. Simultaneous expression of brain-derived neurotrophic factor and neurotrophin-3 in Cajal-

Retzius, subplate and ventricular progenitor cells during early development stages of the rat cerebral cortex. *Neuroscience,* 84**,** 115-27.

FURUTACHI, S., MIYA, H., WATANABE, T., KAWAI, H., YAMASAKI, N., HARADA, Y., IMAYOSHI, I., NELSON, M., NAKAYAMA, K. I., HIRABAYASHI, Y. & GOTOH, Y. 2015. Slowly dividing neural progenitors are an embryonic origin of adult neural stem cells. *Nat Neurosci,* 18**,** 657-65.

GAL, J. S., MOROZOV, Y. M., AYOUB, A. E., CHATTERJEE, M., RAKIC, P. & HAYDAR, T. F. 2006. Molecular and morphological heterogeneity of neural precursors in the mouse neocortical proliferative zones. *J Neurosci,* 26**,** 1045-56.

GALCERAN, J., MIYASHITA-LIN, E. M., DEVANEY, E., RUBENSTEIN, J. L. & GROSSCHEDL, R. 2000. Hippocampus development and generation of dentate gyrus granule cells is regulated by LEF1. *Development,* 127**,** 469-82.

GALE, N. W., THURSTON, G., HACKETT, S. F., RENARD, R., WANG, Q., MCCLAIN, J., MARTIN, C., WITTE, C., WITTE, M. H., JACKSON, D., SURI, C., CAMPOCHIARO, P. A., WIEGAND, S. J. & YANCOPOULOS, G. D. 2002. Angiopoietin-2 is required for postnatal angiogenesis and lymphatic patterning, and only the latter role is rescued by Angiopoietin-1. *Dev Cell,* 3**,** 411-23.

GELFAND, M. V., HAGAN, N., TATA, A., OH, W. J., LACOSTE, B., KANG, K. T., KOPYCINSKA, J., BISCHOFF, J., WANG, J. H. & GU, C. 2014. Neuropilin-1 functions as a VEGFR2 co-receptor to guide developmental angiogenesis independent of ligand binding. *Elife,* 3**,** e03720.

GERHARDT, H. & BETSHOLTZ, C. 2003. Endothelial-pericyte interactions in angiogenesis. *Cell Tissue Res,* 314**,** 15-23.

GERHARDT, H., GOLDING, M., FRUTTIGER, M., RUHRBERG, C., LUNDKVIST, A., ABRAMSSON, A., JELTSCH, M., MITCHELL, C., ALITALO, K., SHIMA, D. & BETSHOLTZ, C. 2003. VEGF guides angiogenic sprouting utilizing endothelial tip cell filopodia. *J Cell Biol,* 161**,** 1163-77.

GERHARDT, H., RUHRBERG, C., ABRAMSSON, A., FUJISAWA, H., SHIMA, D. & BETSHOLTZ, C. 2004. Neuropilin-1 is required for endothelial tip cell guidance in the developing central nervous system. *Dev Dyn,* 231**,** 503-9.

GERTZ, C. C., LUI, J. H., LAMONICA, B. E., WANG, X. & KRIEGSTEIN, A. R. 2014. Diverse behaviors of outer radial glia in developing ferret and human cortex. *J Neurosci,* 34**,** 2559-70.

GHOSH, A. & GREENBERG, M. E. 1995. Distinct roles for bFGF and NT-3 in the regulation of cortical neurogenesis. *Neuron,* 15**,** 89-103.

GIGER, R. J., CLOUTIER, J. F., SAHAY, A., PRINJHA, R. K., LEVENGOOD, D. V., MOORE, S. E., PICKERING, S., SIMMONS, D., RASTAN, S., WALSH, F. S., KOLODKIN, A. L., GINTY, D. D. & GEPPERT, M. 2000. Neuropilin-2 is required in vivo for selective axon guidance responses to secreted semaphorins. *Neuron,* 25**,** 29-41.

GOLDMAN, S. A. 2016. Stem and Progenitor Cell-Based Therapy of the Central Nervous System: Hopes, Hype, and Wishful Thinking. *Cell Stem Cell,* 18**,** 174-88.

GOODELL, M. A., BROSE, K., PARADIS, G., CONNER, A. S. & MULLIGAN, R. C. 1996. Isolation and functional properties of murine hematopoietic stem cells that are replicating in vivo. *J Exp Med,* 183**,** 1797-806.

GOTZ, M., STOYKOVA, A. & GRUSS, P. 1998. Pax6 controls radial glia differentiation in the cerebral cortex. *Neuron,* 21**,** 1031-44.

GRAHAM, V., KHUDYAKOV, J., ELLIS, P. & PEVNY, L. 2003. SOX2 functions to maintain neural progenitor identity. *Neuron,* 39**,** 749-65.

GRAUS-PORTA, D., BLAESS, S., SENFTEN, M., LITTLEWOOD-EVANS, A., DAMSKY, C., HUANG, Z., ORBAN, P., KLEIN, R., SCHITTNY, J. C. & MULLER, U. 2001. Beta1-class integrins regulate the development of laminae and folia in the cerebral and cerebellar cortex. *Neuron,* 31**,** 367-79.

GREENWOOD, S., SWETLOFF, A., WADE, A. M., TERASAKI, T. & FERRETTI, P. 2008. Fgf2 is expressed in human and murine embryonic choroid plexus and affects choroid plexus epithelial cell behaviour. *Cerebrospinal Fluid Res,* 5**,** 20.

GREGG, C. & WEISS, S. 2005. CNTF/LIF/gp130 receptor complex signaling maintains a VZ precursor differentiation gradient in the developing ventral forebrain. *Development,* 132**,** 565-78.

GRESSENS, P., HILL, J. M., PAINDAVEINE, B., GOZES, I., FRIDKIN, M. & BRENNEMAN, D. E. 1994. Severe microcephaly induced by blockade of vasoactive intestinal peptide function in the primitive neuroepithelium of the mouse. *J Clin Invest,* 94**,** 2020-7.

GU, C., LIMBERG, B. J., WHITAKER, G. B., PERMAN, B., LEAHY, D. J., ROSENBAUM, J. S., GINTY, D. D. & KOLODKIN, A. L. 2002. Characterization of neuropilin-1 structural features that confer binding to semaphorin 3A and vascular endothelial growth factor 165. *J Biol Chem,* 277**,** 18069-76.

GU, C., RODRIGUEZ, E. R., REIMERT, D. V., SHU, T., FRITZSCH, B., RICHARDS, L. J., KOLODKIN, A. L. & GINTY, D. D. 2003. Neuropilin-1 conveys semaphorin and VEGF signaling during neural and cardiovascular development. *Dev Cell,* 5**,** 45-57.

GU, C., YOSHIDA, Y., LIVET, J., REIMERT, D. V., MANN, F., MERTE, J., HENDERSON, C. E., JESSELL, T. M., KOLODKIN, A. L. & GINTY, D. D. 2005. Semaphorin 3E and plexin-D1 control vascular pattern independently of neuropilins. *Science,* 307**,** 265-8.

GUILLEMOT, F., LO, L. C., JOHNSON, J. E., AUERBACH, A., ANDERSON, D. J. & JOYNER, A. L. 1993. Mammalian achaete-scute homolog 1 is required for the early development of olfactory and autonomic neurons. *Cell,* 75**,** 463-76.

GUO, L., YU, Q. C. & FUCHS, E. 1993. Targeting expression of keratinocyte growth factor to keratinocytes elicits striking changes in epithelial differentiation in transgenic mice. *EMBO J,* 12**,** 973-86.

GUTHRIE, S., BUTCHER, M. & LUMSDEN, A. 1991. Patterns of cell division and interkinetic nuclear migration in the chick embryo hindbrain. *J Neurobiol,* 22**,** 742-54.

HACKETT, S. F., OZAKI, H., STRAUSS, R. W., WAHLIN, K., SURI, C., MAISONPIERRE, P., YANCOPOULOS, G. & CAMPOCHIARO, P. A. 2000. Angiopoietin 2 expression in the retina: upregulation during physiologic and pathologic neovascularization. *J Cell Physiol,* 184**,** 275-84.

HAIGH, J. J., MORELLI, P. I., GERHARDT, H., HAIGH, K., TSIEN, J., DAMERT, A., MIQUEROL, L., MUHLNER, U., KLEIN, R., FERRARA, N., WAGNER, E. F., BETSHOLTZ, C. & NAGY, A. 2003. Cortical and retinal defects caused by dosage-dependent reductions in VEGF-A paracrine signaling. *Dev Biol,* 262**,** 225-41.

HAJIHOSSEINI, M. K. & DICKSON, C. 1999. A subset of fibroblast growth factors (Fgfs) promote survival, but Fgf-8b specifically promotes astroglial differentiation of rat cortical precursor cells. *Mol Cell Neurosci,* 14**,** 468-85.

HAMILTON, D. L. & ABREMSKI, K. 1984. Site-specific recombination by the bacteriophage P1 lox-Cre system. Cre-mediated synapsis of two lox sites. *J Mol Biol,* 178**,** 481-6.

HAN, J., CALVO, C. F., KANG, T. H., BAKER, K. L., PARK, J. H., PARRAS, C., LEVITTAS, M., BIRBA, U., PIBOUIN-FRAGNER, L., FRAGNER, P., BILGUVAR, K., DUMAN, R. S., NURMI, H., ALITALO, K., EICHMANN, A. C. & THOMAS, J. L. 2015. Vascular endothelial growth factor receptor 3 controls neural stem cell activation in mice and humans. *Cell Rep,* 10**,** 1158-72.

HANS, F. & DIMITROV, S. 2001. Histone H3 phosphorylation and cell division. *Oncogene,* 20**,** 3021-7.

HANSEN, D. V., LUI, J. H., PARKER, P. R. & KRIEGSTEIN, A. R. 2010. Neurogenic radial glia in the outer subventricular zone of human neocortex. *Nature,* 464**,** 554-561.

HARTFUSS, E., FORSTER, E., BOCK, H. H., HACK, M. A., LEPRINCE, P., LUQUE, J. M., HERZ, J., FROTSCHER, M. & GOTZ, M. 2003. Reelin signaling directly affects radial glia morphology and biochemical maturation. *Development,* 130**,** 4597-609.

HASHIMOTO, T., ZHANG, X. M., CHEN, B. Y. & YANG, X. J. 2006. VEGF activates divergent intracellular signaling components to regulate retinal progenitor cell proliferation and neuronal differentiation. *Development,* 133**,** 2201-10.

HATAKEYAMA, J., BESSHO, Y., KATOH, K., OOKAWARA, S., FUJIOKA, M., GUILLEMOT, F. & KAGEYAMA, R. 2004. Hes genes regulate size, shape and histogenesis of the nervous system by control of the timing of neural stem cell differentiation. *Development,* 131**,** 5539-50.

HAUBENSAK, W., ATTARDO, A., DENK, W. & HUTTNER, W. B. 2004. Neurons arise in the basal neuroepithelium of the early mammalian telencephalon: a major site of neurogenesis. *Proc Natl Acad Sci U S A,* 101**,** 3196-201.

HAUBST, N., GEORGES-LABOUESSE, E., DE ARCANGELIS, A., MAYER, U. & GOTZ, M. 2006. Basement membrane attachment is dispensable for radial glial cell fate and for proliferation, but affects positioning of neuronal subtypes. *Development,* 133**,** 3245-54.

HAYDAR, T. F., WANG, F., SCHWARTZ, M. L. & RAKIC, P. 2000. Differential modulation of proliferation in the neocortical ventricular and subventricular zones. *J Neurosci,* 20**,** 5764-74.

HEINS, N., MALATESTA, P., CECCONI, F., NAKAFUKU, M., TUCKER, K. L., HACK, M. A., CHAPOUTON, P., BARDE, Y. A. & GOTZ, M. 2002. Glial cells generate neurons: the role of the transcription factor Pax6. *Nat Neurosci,* 5**,** 308-15.

HELLSTROM, M., PHNG, L. K., HOFMANN, J. J., WALLGARD, E., COULTAS, L., LINDBLOM, P., ALVA, J., NILSSON, A. K., KARLSSON, L., GAIANO, N., YOON, K., ROSSANT, J., IRUELA-ARISPE, M. L., KALEN, M., GERHARDT, H. & BETSHOLTZ, C. 2007. Dll4 signalling through Notch1 regulates formation of tip cells during angiogenesis. *Nature,* 445**,** 776-80.

HINTON, D. R., HE, S., GRAF, K., YANG, D., HSUEH, W. A., RYAN, S. J. & LAW, R. E. 1998. Mitogen-activated protein kinase activation mediates PDGF-directed migration of RPE cells. *Exp Cell Res,* 239**,** 11-5.

HIRATSUKA, S., MINOWA, O., KUNO, J., NODA, T. & SHIBUYA, M. 1998. Flt-1 lacking the tyrosine kinase domain is sufficient for normal development and angiogenesis in mice. *Proc Natl Acad Sci U S A,* 95**,** 9349-54.

HIRATSUKA, S., NAKAO, K., NAKAMURA, K., KATSUKI, M., MARU, Y. & SHIBUYA, M. 2005. Membrane fixation of vascular endothelial growth factor receptor 1 ligand-binding domain is important for vasculogenesis and angiogenesis in mice. *Mol Cell Biol,* 25**,** 346-54.

HIROTA, S., LIU, Q., LEE, H. S., HOSSAIN, M. G., LACY-HULBERT, A. & MCCARTY, J. H. 2011. The astrocyte-expressed integrin alphavbeta8 governs blood vessel sprouting in the developing retina. *Development,* 138**,** 5157-66.

HITOSHI, S., ALEXSON, T., TROPEPE, V., DONOVIEL, D., ELIA, A. J., NYE, J. S., CONLON, R. A., MAK, T. W., BERNSTEIN, A. & VAN DER KOOY, D. 2002. Notch pathway molecules are essential for the maintenance, but not the generation, of mammalian neural stem cells. *Genes Dev,* 16**,** 846-58.

HO, V. C., DUAN, L. J., CRONIN, C., LIANG, B. T. & FONG, G. H. 2012. Elevated vascular endothelial growth factor receptor-2 abundance contributes to increased angiogenesis in vascular endothelial growth factor receptor-1-deficient mice. *Circulation,* 126**,** 741-52.

HODGE, R. D., D'ERCOLE, A. J. & O'KUSKY, J. R. 2004. Insulin-like growth factor-I accelerates the cell cycle by decreasing G1 phase length and increases cell cycle reentry in the embryonic cerebral cortex. *J Neurosci,* 24**,** 10201-10.

HODGE, R. D., KOWALCZYK, T. D., WOLF, S. A., ENCINAS, J. M., RIPPEY, C., ENIKOLOPOV, G., KEMPERMANN, G. & HEVNER, R. F. 2008. Intermediate progenitors in adult hippocampal neurogenesis: Tbr2 expression and coordinate regulation of neuronal output. *J Neurosci,* 28**,** 3707-17.

HOGLINGER, G. U., RIZK, P., MURIEL, M. P., DUYCKAERTS, C., OERTEL, W. H., CAILLE, I. & HIRSCH, E. C. 2004. Dopamine depletion impairs precursor cell proliferation in Parkinson disease. *Nat Neurosci,* 7**,** 726-35.

HOLLYDAY, M., MCMAHON, J. A. & MCMAHON, A. P. 1995. Wnt expression patterns in chick embryo nervous system. *Mech Dev,* 52**,** 9-25.

HOSOMI, S., YAMASHITA, T., AOKI, M. & TOHYAMA, M. 2003. The p75 receptor is required for BDNF-induced differentiation of neural precursor cells. *Biochem Biophys Res Commun,* 301**,** 1011-5.

HOUCK, K. A., LEUNG, D. W., ROWLAND, A. M., WINER, J. & FERRARA, N. 1992. Dual regulation of vascular endothelial growth factor bioavailability by genetic and proteolytic mechanisms. *J Biol Chem,* 267**,** 26031-7.

HSIEH, H. Y., ROBERTSON, C. L., VERMEHREN-SCHMAEDICK, A. & BALKOWIEC, A. 2010. Nitric oxide regulates BDNF release from nodose

ganglion neurons in a pattern-dependent and cGMP-independent manner. *J Neurosci Res,* 88**,** 1285-97.

HSU, Y. C., LI, L. & FUCHS, E. 2014. Emerging interactions between skin stem cells and their niches. *Nat Med,* 20**,** 847-56.

IKEYA, M., LEE, S. M., JOHNSON, J. E., MCMAHON, A. P. & TAKADA, S. 1997. Wnt signalling required for expansion of neural crest and CNS progenitors. *Nature,* 389**,** 966-70.

ILLE, F., ATANASOSKI, S., FALK, S., ITTNER, L. M., MARKI, D., BUCHMANN-MOLLER, S., WURDAK, H., SUTER, U., TAKETO, M. M. & SOMMER, L. 2007. Wnt/BMP signal integration regulates the balance between proliferation and differentiation of neuroepithelial cells in the dorsal spinal cord. *Dev Biol,* 304**,** 394-408.

IMAI, T., TOKUNAGA, A., YOSHIDA, T., HASHIMOTO, M., MIKOSHIBA, K., WEINMASTER, G., NAKAFUKU, M. & OKANO, H. 2001. The neural RNA-binding protein Musashi1 translationally regulates mammalian numb gene expression by interacting with its mRNA. *Mol Cell Biol,* 21**,** 3888-900.

IMAYOSHI, I., ISOMURA, A., HARIMA, Y., KAWAGUCHI, K., KORI, H., MIYACHI, H., FUJIWARA, T., ISHIDATE, F. & KAGEYAMA, R. 2013. Oscillatory control of factors determining multipotency and fate in mouse neural progenitors. *Science,* 342**,** 1203-8.

IMAYOSHI, I., SAKAMOTO, M., YAMAGUCHI, M., MORI, K. & KAGEYAMA, R. 2010. Essential roles of Notch signaling in maintenance of neural stem cells in developing and adult brains. *J Neurosci,* 30**,** 3489-98.

ISHIBASHI, M., ANG, S. L., SHIOTA, K., NAKANISHI, S., KAGEYAMA, R. & GUILLEMOT, F. 1995. Targeted disruption of mammalian hairy and Enhancer of split homolog-1 (HES-1) leads to up-regulation of neural helix-loop-helix factors, premature neurogenesis, and severe neural tube defects. *Genes Dev,* 9**,** 3136-48.

ISRASENA, N., HU, M., FU, W., KAN, L. & KESSLER, J. A. 2004. The presence of FGF2 signaling determines whether beta-catenin exerts effects on proliferation or neuronal differentiation of neural stem cells. *Dev Biol,* 268**,** 220-31.

IWAYAMA, T., STEELE, C., YAO, L., DOZMOROV, M. G., KARAMICHOS, D., WREN, J. D. & OLSON, L. E. 2015. PDGFRalpha signaling drives adipose tissue fibrosis by targeting progenitor cell plasticity. *Genes Dev,* 29**,** 1106-19.

JAKOBSSON, L., FRANCO, C. A., BENTLEY, K., COLLINS, R. T., PONSIOEN, B., ASPALTER, I. M., ROSEWELL, I., BUSSE, M., THURSTON, G., MEDVINSKY, A., SCHULTE-MERKER, S. & GERHARDT, H. 2010. Endothelial cells dynamically compete for the tip cell position during angiogenic sprouting. *Nat Cell Biol,* 12**,** 943-53.

JAMES, J. M., GEWOLB, C. & BAUTCH, V. L. 2009. Neurovascular development uses VEGF-A signaling to regulate blood vessel ingression into the neural tube. *Development,* 136**,** 833-41.

JAVAHERIAN, A. & KRIEGSTEIN, A. 2009. A stem cell niche for intermediate progenitor cells of the embryonic cortex. *Cereb Cortex,* 19 Suppl 1**,** i70-7.

JIN, K., ZHU, Y., SUN, Y., MAO, X. O., XIE, L. & GREENBERG, D. A. 2002. Vascular endothelial growth factor (VEGF) stimulates neurogenesis in vitro and in vivo. *Proc Natl Acad Sci U S A,* 99**,** 11946-50.

JIN, L., HU, X. & FENG, L. 2005. NT3 inhibits FGF2-induced neural progenitor cell proliferation via the PI3K/GSK3 pathway. *J Neurochem,* 93**,** 1251-61.

JOHANSSON, P. A., IRMLER, M., ACAMPORA, D., BECKERS, J., SIMEONE, A. & GOTZ, M. 2013. The transcription factor Otx2 regulates choroid plexus development and function. *Development,* 140**,** 1055-66.

JONES, P. H. & WATT, F. M. 1993. Separation of human epidermal stem cells from transit amplifying cells on the basis of differences in integrin function and expression. *Cell,* 73**,** 713-24.

JUNG, G. A., YOON, J. Y., MOON, B. S., YANG, D. H., KIM, H. Y., LEE, S. H., BRYJA, V., ARENAS, E. & CHOI, K. Y. 2008. Valproic acid induces differentiation and inhibition of proliferation in neural progenitor cells via the beta-catenin-Ras-ERK-p21Cip/WAF1 pathway. *BMC Cell Biol,* 9**,** 66.

JUNG, S., PARK, R. H., KIM, S., JEON, Y. J., HAM, D. S., JUNG, M. Y., KIM, S. S., LEE, Y. D., PARK, C. H. & SUH-KIM, H. 2010. Id proteins facilitate self-renewal and proliferation of neural stem cells. *Stem Cells Dev,* 19**,** 831-41.

KADOWAKI, M., NAKAMURA, S., MACHON, O., KRAUSS, S., RADICE, G. L. & TAKEICHI, M. 2007. N-cadherin mediates cortical organization in the mouse brain. *Dev Biol,* 304**,** 22-33.

KAGEYAMA, R., SHIMOJO, H. & IMAYOSHI, I. 2015. Dynamic expression and roles of Hes factors in neural development. *Cell Tissue Res,* 359**,** 125-33.

KALANI, M. Y., CHESHIER, S. H., CORD, B. J., BABABEYGY, S. R., VOGEL, H., WEISSMAN, I. L., PALMER, T. D. & NUSSE, R. 2008. Wnt-mediated self-renewal of neural stem/progenitor cells. *Proc Natl Acad Sci U S A,* 105**,** 16970-5.

KALTEZIOTI, V., KOUROUPI, G., OIKONOMAKI, M., MANTOUVALOU, E., STERGIOPOULOS, A., CHARONIS, A., ROHRER, H., MATSAS, R. & POLITIS, P. K. 2010. Prox1 regulates the notch1-mediated inhibition of neurogenesis. *PLoS Biol,* 8**,** e1000565.

KAN, L., JALALI, A., ZHAO, L. R., ZHOU, X., MCGUIRE, T., KAZANIS, I., EPISKOPOU, V., BASSUK, A. G. & KESSLER, J. A. 2007. Dual function of Sox1 in telencephalic progenitor cells. *Dev Biol,* 310**,** 85-98.

KANG, W., WONG, L. C., SHI, S. H. & HEBERT, J. M. 2009. The transition from radial glial to intermediate progenitor cell is inhibited by FGF signaling during corticogenesis. *J Neurosci,* 29**,** 14571-80.

KARSTEN, S. L., KUDO, L. C., JACKSON, R., SABATTI, C., KORNBLUM, H. I. & GESCHWIND, D. H. 2003. Global analysis of gene expression in neural progenitors reveals specific cell-cycle, signaling, and metabolic networks. *Dev Biol,* 261**,** 165-82.

KAWAHARA, H., IMAI, T., IMATAKA, H., TSUJIMOTO, M., MATSUMOTO, K. & OKANO, H. 2008. Neural RNA-binding protein Musashi1 inhibits translation initiation by competing with eIF4G for PABP. *J Cell Biol,* 181**,** 639-53.

KAWASAKI, T., KITSUKAWA, T., BEKKU, Y., MATSUDA, Y., SANBO, M., YAGI, T. & FUJISAWA, H. 1999. A requirement for neuropilin-1 in embryonic vessel formation. *Development,* 126**,** 4895-902.

KAWASE-KOGA, Y., LOW, R., OTAEGI, G., POLLOCK, A., DENG, H., EISENHABER, F., MAURER-STROH, S. & SUN, T. 2010. RNAase-III

enzyme Dicer maintains signaling pathways for differentiation and survival in mouse cortical neural stem cells. *J Cell Sci,* 123**,** 586-94.

KEARNEY, J. B., KAPPAS, N. C., ELLERSTROM, C., DIPAOLA, F. W. & BAUTCH, V. L. 2004. The VEGF receptor flt-1 (VEGFR-1) is a positive modulator of vascular sprout formation and branching morphogenesis. *Blood,* 103**,** 4527-35.

KENNEY, A. M., COLE, M. D. & ROWITCH, D. H. 2003. Nmyc upregulation by sonic hedgehog signaling promotes proliferation in developing cerebellar granule neuron precursors. *Development,* 130**,** 15-28.

KICHEVA, A., BOLLENBACH, T., RIBEIRO, A., VALLE, H. P., LOVELL-BADGE, R., EPISKOPOU, V. & BRISCOE, J. 2014. Coordination of progenitor specification and growth in mouse and chick spinal cord. *Science,* 345**,** 1254927.

KILPATRICK, T. J. & BARTLETT, P. F. 1995. Cloned multipotential precursors from the mouse cerebrum require FGF-2, whereas glial restricted precursors are stimulated with either FGF-2 or EGF. *J Neurosci,* 15**,** 3653-61.

KIM, J., OH, W. J., GAIANO, N., YOSHIDA, Y. & GU, C. 2011. Semaphorin 3E-Plexin-D1 signaling regulates VEGF function in developmental angiogenesis via a feedback mechanism. *Genes Dev,* 25**,** 1399-411.

KIM, S., LEHTINEN, M. K., SESSA, A., ZAPPATERRA, M. W., CHO, S. H., GONZALEZ, D., BOGGAN, B., AUSTIN, C. A., WIJNHOLDS, J., GAMBELLO, M. J., MALICKI, J., LAMANTIA, A. S., BROCCOLI, V. & WALSH, C. A. 2010. The apical complex couples cell fate and cell survival to cerebral cortical development. *Neuron,* 66**,** 69-84.

KISANUKI, Y. Y., HAMMER, R. E., MIYAZAKI, J., WILLIAMS, S. C., RICHARDSON, J. A. & YANAGISAWA, M. 2001. Tie2-Cre transgenic mice: a new model for endothelial cell-lineage analysis in vivo. *Dev Biol,* 230**,** 230-42.

KISHI, M., MIZUSEKI, K., SASAI, N., YAMAZAKI, H., SHIOTA, K., NAKANISHI, S. & SASAI, Y. 2000. Requirement of Sox2-mediated signaling for differentiation of early Xenopus neuroectoderm. *Development,* 127**,** 791-800.

KITAGAWA, M., HOJO, M., IMAYOSHI, I., GOTO, M., ANDO, M., OHTSUKA, T., KAGEYAMA, R. & MIYAMOTO, S. 2013. Hes1 and Hes5 regulate vascular remodeling and arterial specification of endothelial cells in brain vascular development. *Mech Dev,* 130**,** 458-66.

KITSUKAWA, T., SHIMIZU, M., SANBO, M., HIRATA, T., TANIGUCHI, M., BEKKU, Y., YAGI, T. & FUJISAWA, H. 1997. Neuropilin-semaphorin III/D-mediated chemorepulsive signals play a crucial role in peripheral nerve projection in mice. *Neuron,* 19**,** 995-1005.

KNOBLICH, J. A. 2001. Asymmetric cell division during animal development. *Nat Rev Mol Cell Biol,* 2**,** 11-20.

KOBLAR, S. A., TURNLEY, A. M., CLASSON, B. J., REID, K. L., WARE, C. B., CHEEMA, S. S., MURPHY, M. & BARTLETT, P. F. 1998. Neural precursor differentiation into astrocytes requires signaling through the leukemia inhibitory factor receptor. *Proc Natl Acad Sci U S A,* 95**,** 3178-81.

KOKOVAY, E., GODERIE, S., WANG, Y., LOTZ, S., LIN, G., SUN, Y., ROYSAM, B., SHEN, Q. & TEMPLE, S. 2010. Adult SVZ lineage cells

home to and leave the vascular niche via differential responses to SDF1/CXCR4 signaling. *Cell Stem Cell,* 7**,** 163-73.

KONNO, D., SHIOI, G., SHITAMUKAI, A., MORI, A., KIYONARI, H., MIYATA, T. & MATSUZAKI, F. 2008. Neuroepithelial progenitors undergo LGN-dependent planar divisions to maintain self-renewability during mammalian neurogenesis. *Nat Cell Biol,* 10**,** 93-101.

KOPAN, R. & ILAGAN, M. X. 2009. The canonical Notch signaling pathway: unfolding the activation mechanism. *Cell,* 137**,** 216-33.

KORNBLUM, H. I., HUSSAIN, R., WIESEN, J., MIETTINEN, P., ZURCHER, S. D., CHOW, K., DERYNCK, R. & WERB, Z. 1998. Abnormal astrocyte development and neuronal death in mice lacking the epidermal growth factor receptor. *J Neurosci Res,* 53**,** 697-717.

KORNBLUM, H. I., HUSSAIN, R. J., BRONSTEIN, J. M., GALL, C. M., LEE, D. C. & SEROOGY, K. B. 1997. Prenatal ontogeny of the epidermal growth factor receptor and its ligand, transforming growth factor alpha, in the rat brain. *J Comp Neurol,* 380**,** 243-61.

KOSODO, Y., ROPER, K., HAUBENSAK, W., MARZESCO, A. M., CORBEIL, D. & HUTTNER, W. B. 2004. Asymmetric distribution of the apical plasma membrane during neurogenic divisions of mammalian neuroepithelial cells. *EMBO J,* 23**,** 2314-24.

KOSODO, Y., SUETSUGU, T., SUDA, M., MIMORI-KIYOSUE, Y., TOIDA, K., BABA, S. A., KIMURA, A. & MATSUZAKI, F. 2011. Regulation of interkinetic nuclear migration by cell cycle-coupled active and passive mechanisms in the developing brain. *EMBO J,* 30**,** 1690-704.

KOSODO, Y., TOIDA, K., DUBREUIL, V., ALEXANDRE, P., SCHENK, J., KIYOKAGE, E., ATTARDO, A., MORA-BERMUDEZ, F., ARII, T., CLARKE, J. D. & HUTTNER, W. B. 2008. Cytokinesis of neuroepithelial cells can divide their basal process before anaphase. *EMBO J,* 27**,** 3151-63.

KRICHEVSKY, A. M., SONNTAG, K. C., ISACSON, O. & KOSIK, K. S. 2006. Specific microRNAs modulate embryonic stem cell-derived neurogenesis. *Stem Cells,* 24**,** 857-64.

KUHNERT, F., MANCUSO, M. R., SHAMLOO, A., WANG, H. T., CHOKSI, V., FLOREK, M., SU, H., FRUTTIGER, M., YOUNG, W. L., HEILSHORN, S. C. & KUO, C. J. 2010. Essential regulation of CNS angiogenesis by the orphan G protein-coupled receptor GPR124. *Science,* 330**,** 985-9.

KWON, G. S. & HADJANTONAKIS, A. K. 2007. Eomes::GFP-a tool for live imaging cells of the trophoblast, primitive streak, and telencephalon in the mouse embryo. *Genesis,* 45**,** 208-17.

LAIRD, P. W., ZIJDERVELD, A., LINDERS, K., RUDNICKI, M. A., JAENISCH, R. & BERNS, A. 1991. Simplified mammalian DNA isolation procedure. *Nucleic Acids Res,* 19**,** 4293.

LAKOMA, J., GARCIA-ALONSO, L. & LUQUE, J. M. 2011. Reelin sets the pace of neocortical neurogenesis. *Development,* 138**,** 5223-34.

LAMBRECHTS, D., STORKEBAUM, E., MORIMOTO, M., DEL-FAVERO, J., DESMET, F., MARKLUND, S. L., WYNS, S., THIJS, V., ANDERSSON, J., VAN MARION, I., AL-CHALABI, A., BORNES, S., MUSSON, R., HANSEN, V., BECKMAN, L., ADOLFSSON, R., PALL, H. S., PRATS, H., VERMEIRE, S., RUTGEERTS, P., KATAYAMA, S., AWATA, T., LEIGH, N., LANG-LAZDUNSKI, L., DEWERCHIN, M., SHAW, C., MOONS, L.,

VLIETINCK, R., MORRISON, K. E., ROBBERECHT, W., VAN BROECKHOVEN, C., COLLEN, D., ANDERSEN, P. M. & CARMELIET, P. 2003. VEGF is a modifier of amyotrophic lateral sclerosis in mice and humans and protects motoneurons against ischemic death. *Nat Genet,* 34**,** 383-94.

LAMEU, C., TRUJILLO, C. A., SCHWINDT, T. T., NEGRAES, P. D., PILLAT, M. M., MORAIS, K. L., LEBRUN, I. & ULRICH, H. 2012. Interactions between the NO-citrulline cycle and brain-derived neurotrophic factor in differentiation of neural stem cells. *J Biol Chem,* 287**,** 29690-701.

LAMONICA, B. E., LUI, J. H., HANSEN, D. V. & KRIEGSTEIN, A. R. 2013. Mitotic spindle orientation predicts outer radial glial cell generation in human neocortex. *Nat Commun,* 4**,** 1665.

LAMONICA, B. E., LUI, J. H., WANG, X. & KRIEGSTEIN, A. R. 2012. OSVZ progenitors in the human cortex: an updated perspective on neurodevelopmental disease. *Curr Opin Neurobiol,* 22**,** 747-53.

LANGE, C., HUTTNER, W. B. & CALEGARI, F. 2009. Cdk4/cyclinD1 overexpression in neural stem cells shortens G1, delays neurogenesis, and promotes the generation and expansion of basal progenitors. *Cell Stem Cell,* 5**,** 320-31.

LANGE, C., TURRERO GARCIA, M., DECIMO, I., BIFARI, F., EELEN, G., QUAEGEBEUR, A., BOON, R., ZHAO, H., BOECKX, B., CHANG, J., WU, C., LE NOBLE, F., LAMBRECHTS, D., DEWERCHIN, M., KUO, C. J., HUTTNER, W. B. & CARMELIET, P. 2016. Relief of hypoxia by angiogenesis promotes neural stem cell differentiation by targeting glycolysis. *EMBO J,* 35**,** 924-41.

LE BRAS, B., BARALLOBRE, M. J., HOMMAN-LUDIYE, J., NY, A., WYNS, S., TAMMELA, T., HAIKO, P., KARKKAINEN, M. J., YUAN, L., MURIEL, M. P., CHATZOPOULOU, E., BREANT, C., ZALC, B., CARMELIET, P., ALITALO, K., EICHMANN, A. & THOMAS, J. L. 2006. VEGF-C is a trophic factor for neural progenitors in the vertebrate embryonic brain. *Nat Neurosci,* 9**,** 340-8.

LEE, J., KIM, K. E., CHOI, D. K., JANG, J. Y., JUNG, J. J., KIYONARI, H., SHIOI, G., CHANG, W., SUDA, T., MOCHIZUKI, N., NAKAOKA, Y., KOMURO, I., YOO, O. J. & KOH, G. Y. 2013. Angiopoietin-1 guides directional angiogenesis through integrin alphavbeta5 signaling for recovery of ischemic retinopathy. *Sci Transl Med,* 5**,** 203ra127.

LEE, S., CHEN, T. T., BARBER, C. L., JORDAN, M. C., MURDOCK, J., DESAI, S., FERRARA, N., NAGY, A., ROOS, K. P. & IRUELA-ARISPE, M. L. 2007. Autocrine VEGF signaling is required for vascular homeostasis. *Cell,* 130**,** 691-703.

LEE, S. M., TOLE, S., GROVE, E. & MCMAHON, A. P. 2000. A local Wnt-3a signal is required for development of the mammalian hippocampus. *Development,* 127**,** 457-67.

LEHTINEN, M. K. & WALSH, C. A. 2011. Neurogenesis at the brain-cerebrospinal fluid interface. *Annu Rev Cell Dev Biol,* 27**,** 653-79.

LEHTINEN, M. K., ZAPPATERRA, M. W., CHEN, X., YANG, Y. J., HILL, A. D., LUN, M., MAYNARD, T., GONZALEZ, D., KIM, S., YE, P., D'ERCOLE, A. J., WONG, E. T., LAMANTIA, A. S. & WALSH, C. A. 2011. The

cerebrospinal fluid provides a proliferative niche for neural progenitor cells. *Neuron,* 69**,** 893-905.

LESLIE, J. D., ARIZA-MCNAUGHTON, L., BERMANGE, A. L., MCADOW, R., JOHNSON, S. L. & LEWIS, J. 2007. Endothelial signalling by the Notch ligand Delta-like 4 restricts angiogenesis. *Development,* 134**,** 839-44.

LEWIS, D. A., TRAVERS, J. B., SOMANI, A. K. & SPANDAU, D. F. 2010. The IGF-1/IGF-1R signaling axis in the skin: a new role for the dermis in aging-associated skin cancer. *Oncogene,* 29**,** 1475-85.

LI, H., RADFORD, J. C., RAGUSA, M. J., SHEA, K. L., MCKERCHER, S. R., ZAREMBA, J. D., SOUSSOU, W., NIE, Z., KANG, Y. J., NAKANISHI, N., OKAMOTO, S., ROBERTS, A. J., SCHWARZ, J. J. & LIPTON, S. A. 2008. Transcription factor MEF2C influences neural stem/progenitor cell differentiation and maturation in vivo. *Proc Natl Acad Sci U S A,* 105**,** 9397-402.

LI, H. S., WANG, D., SHEN, Q., SCHONEMANN, M. D., GORSKI, J. A., JONES, K. R., TEMPLE, S., JAN, L. Y. & JAN, Y. N. 2003. Inactivation of Numb and Numblike in embryonic dorsal forebrain impairs neurogenesis and disrupts cortical morphogenesis. *Neuron,* 40**,** 1105-18.

LI, S., HAIGH, K., HAIGH, J. J. & VASUDEVAN, A. 2013. Endothelial VEGF sculpts cortical cytoarchitecture. *J Neurosci,* 33**,** 14809-15.

LI, W., COGSWELL, C. A. & LOTURCO, J. J. 1998. Neuronal differentiation of precursors in the neocortical ventricular zone is triggered by BMP. *J Neurosci,* 18**,** 8853-62.

LIAN, G., LU, J., HU, J., ZHANG, J., CROSS, S. H., FERLAND, R. J. & SHEEN, V. L. 2012. Filamin a regulates neural progenitor proliferation and cortical size through Wee1-dependent Cdk1 phosphorylation. *J Neurosci,* 32**,** 7672-84.

LICHT, T., DOR-WOLLMAN, T., BEN-ZVI, A., ROTHE, G. & KESHET, E. 2015. Vessel maturation schedule determines vulnerability to neuronal injuries of prematurity. *J Clin Invest,* 125**,** 1319-28.

LICHT, T., GOSHEN, I., AVITAL, A., KREISEL, T., ZUBEDAT, S., EAVRI, R., SEGAL, M., YIRMIYA, R. & KESHET, E. 2011. Reversible modulations of neuronal plasticity by VEGF. *Proc Natl Acad Sci U S A,* 108**,** 5081-6.

LIEBNER, S., CORADA, M., BANGSOW, T., BABBAGE, J., TADDEI, A., CZUPALLA, C. J., REIS, M., FELICI, A., WOLBURG, H., FRUTTIGER, M., TAKETO, M. M., VON MELCHNER, H., PLATE, K. H., GERHARDT, H. & DEJANA, E. 2008. Wnt/beta-catenin signaling controls development of the blood-brain barrier. *J Cell Biol,* 183**,** 409-17.

LIM, D. A., TRAMONTIN, A. D., TREVEJO, J. M., HERRERA, D. G., GARCIA-VERDUGO, J. M. & ALVAREZ-BUYLLA, A. 2000. Noggin antagonizes BMP signaling to create a niche for adult neurogenesis. *Neuron,* 28**,** 713-26.

LIN, T., SANDUSKY, S. B., XUE, H., FISHBEIN, K. W., SPENCER, R. G., RAO, M. S. & FRANCOMANO, C. A. 2003. A central nervous system specific mouse model for thanatophoric dysplasia type II. *Hum Mol Genet,* 12**,** 2863-71.

LIU, X., HASHIMOTO-TORII, K., TORII, M., HAYDAR, T. F. & RAKIC, P. 2008. The role of ATP signaling in the migration of intermediate neuronal progenitors to the neocortical subventricular zone. *Proc Natl Acad Sci U S A,* 105**,** 11802-7.

LIU, X., WANG, Q., HAYDAR, T. F. & BORDEY, A. 2005a. Nonsynaptic GABA signaling in postnatal subventricular zone controls proliferation of GFAP-expressing progenitors. *Nat Neurosci,* 8**,** 1179-87.

LIU, Y., FORD, B. D., MANN, M. A. & FISCHBACH, G. D. 2005b. Neuregulin-1 increases the proliferation of neuronal progenitors from embryonic neural stem cells. *Dev Biol,* 283**,** 437-45.

LO, L. C., JOHNSON, J. E., WUENSCHELL, C. W., SAITO, T. & ANDERSON, D. J. 1991. Mammalian achaete-scute homolog 1 is transiently expressed by spatially restricted subsets of early neuroepithelial and neural crest cells. *Genes Dev,* 5**,** 1524-37.

LONG, K., MOSS, L., LAURSEN, L., BOULTER, L. & FFRENCH-CONSTANT, C. 2016. Integrin signalling regulates the expansion of neuroepithelial progenitors and neurogenesis via Wnt7a and Decorin. *Nat Commun,* 7**,** 10354.

LOTURCO, J. J., OWENS, D. F., HEATH, M. J., DAVIS, M. B. & KRIEGSTEIN, A. R. 1995. GABA and glutamate depolarize cortical progenitor cells and inhibit DNA synthesis. *Neuron,* 15**,** 1287-98.

LOUISSAINT, A., JR., RAO, S., LEVENTHAL, C. & GOLDMAN, S. A. 2002. Coordinated interaction of neurogenesis and angiogenesis in the adult songbird brain. *Neuron,* 34**,** 945-60.

LOULIER, K., BARRY, R., MAHOU, P., LE FRANC, Y., SUPATTO, W., MATHO, K. S., IENG, S., FOUQUET, S., DUPIN, E., BENOSMAN, R., CHEDOTAL, A., BEAUREPAIRE, E., MORIN, X. & LIVET, J. 2014. Multiplex cell and lineage tracking with combinatorial labels. *Neuron,* 81**,** 505-20.

LOULIER, K., LATHIA, J. D., MARTHIENS, V., RELUCIO, J., MUGHAL, M. R., TANG, S. C., COKSAYGAN, T., HALL, P. E., CHIGURUPATI, S., PATTON, B., COLOGNATO, H., RAO, M. S., MATTSON, M. P., HAYDAR, T. F. & FFRENCH-CONSTANT, C. 2009. beta1 integrin maintains integrity of the embryonic neocortical stem cell niche. *PLoS Biol,* 7**,** e1000176.

LU, Q. R., YUK, D., ALBERTA, J. A., ZHU, Z., PAWLITZKY, I., CHAN, J., MCMAHON, A. P., STILES, C. D. & ROWITCH, D. H. 2000. Sonic hedgehog--regulated oligodendrocyte lineage genes encoding bHLH proteins in the mammalian central nervous system. *Neuron,* 25**,** 317-29.

LUI, J. H., HANSEN, D. V. & KRIEGSTEIN, A. R. 2011. Development and evolution of the human neocortex. *Cell,* 146**,** 18-36.

LUK, K. C., KENNEDY, T. E. & SADIKOT, A. F. 2003. Glutamate promotes proliferation of striatal neuronal progenitors by an NMDA receptor-mediated mechanism. *J Neurosci,* 23**,** 2239-50.

LUKASZEWICZ, A., SAVATIER, P., CORTAY, V., GIROUD, P., HUISSOUD, C., BERLAND, M., KENNEDY, H. & DEHAY, C. 2005. G1 phase regulation, area-specific cell cycle control, and cytoarchitectonics in the primate cortex. *Neuron,* 47**,** 353-64.

LUKASZEWICZ, A., SAVATIER, P., CORTAY, V., KENNEDY, H. & DEHAY, C. 2002. Contrasting effects of basic fibroblast growth factor and neurotrophin 3 on cell cycle kinetics of mouse cortical stem cells. *J Neurosci,* 22**,** 6610-22.

LUMSDEN, A. & KRUMLAUF, R. 1996. Patterning the vertebrate neuraxis. *Science,* 274**,** 1109-15.

LYDEN, D., YOUNG, A. Z., ZAGZAG, D., YAN, W., GERALD, W., O'REILLY, R., BADER, B. L., HYNES, R. O., ZHUANG, Y., MANOVA, K. & BENEZRA, R. 1999. Id1 and Id3 are required for neurogenesis, angiogenesis and vascularization of tumour xenografts. *Nature,* 401**,** 670-7.

MA, S., KWON, H. J., JOHNG, H., ZANG, K. & HUANG, Z. 2013. Radial glial neural progenitors regulate nascent brain vascular network stabilization via inhibition of Wnt signaling. *PLoS Biol,* 11**,** e1001469.

MADISEN, L., ZWINGMAN, T. A., SUNKIN, S. M., OH, S. W., ZARIWALA, H. A., GU, H., NG, L. L., PALMITER, R. D., HAWRYLYCZ, M. J., JONES, A. R., LEIN, E. S. & ZENG, H. 2010. A robust and high-throughput Cre reporting and characterization system for the whole mouse brain. *Nat Neurosci,* 13**,** 133-40.

MAISONPIERRE, P. C., BELLUSCIO, L., FRIEDMAN, B., ALDERSON, R. F., WIEGAND, S. J., FURTH, M. E., LINDSAY, R. M. & YANCOPOULOS, G. D. 1990. NT-3, BDNF, and NGF in the developing rat nervous system: parallel as well as reciprocal patterns of expression. *Neuron,* 5**,** 501-9.

MARTHIENS, V., KAZANIS, I., MOSS, L., LONG, K. & FFRENCH-CONSTANT, C. 2010. Adhesion molecules in the stem cell niche--more than just staying in shape? *J Cell Sci,* 123**,** 1613-22.

MASUI, S., NAKATAKE, Y., TOYOOKA, Y., SHIMOSATO, D., YAGI, R., TAKAHASHI, K., OKOCHI, H., OKUDA, A., MATOBA, R., SHAROV, A. A., KO, M. S. & NIWA, H. 2007. Pluripotency governed by Sox2 via regulation of Oct3/4 expression in mouse embryonic stem cells. *Nat Cell Biol,* 9**,** 625-35.

MATSUNAGA, E., ARAKI, I. & NAKAMURA, H. 2000. Pax6 defines the di-mesencephalic boundary by repressing En1 and Pax2. *Development,* 127**,** 2357-65.

MATTIONI, T., LOUVION, J. F. & PICARD, D. 1994. Regulation of protein activities by fusion to steroid binding domains. *Methods Cell Biol,* 43 Pt A**,** 335-52.

MCCARTY, J. H. 2009. Integrin-mediated regulation of neurovascular development, physiology and disease. *Cell Adh Migr,* 3**,** 211-5.

MCCARTY, J. H., LACY-HULBERT, A., CHAREST, A., BRONSON, R. T., CROWLEY, D., HOUSMAN, D., SAVILL, J., ROES, J. & HYNES, R. O. 2005. Selective ablation of alphav integrins in the central nervous system leads to cerebral hemorrhage, seizures, axonal degeneration and premature death. *Development,* 132**,** 165-76.

MCCARTY, J. H., MONAHAN-EARLEY, R. A., BROWN, L. F., KELLER, M., GERHARDT, H., RUBIN, K., SHANI, M., DVORAK, H. F., WOLBURG, H., BADER, B. L., DVORAK, A. M. & HYNES, R. O. 2002. Defective associations between blood vessels and brain parenchyma lead to cerebral hemorrhage in mice lacking alphav integrins. *Mol Cell Biol,* 22**,** 7667-77.

MCKERCHER, S. R., TORBETT, B. E., ANDERSON, K. L., HENKEL, G. W., VESTAL, D. J., BARIBAULT, H., KLEMSZ, M., FEENEY, A. J., WU, G. E., PAIGE, C. J. & MAKI, R. A. 1996. Targeted disruption of the PU.1 gene results in multiple hematopoietic abnormalities. *EMBO J,* 15**,** 5647-58.

MCMAHON, A. P. & BRADLEY, A. 1990. The Wnt-1 (int-1) proto-oncogene is required for development of a large region of the mouse brain. *Cell,* 62**,** 1073-85.

MEGASON, S. G. & MCMAHON, A. P. 2002. A mitogen gradient of dorsal midline Wnts organizes growth in the CNS. *Development,* 129**,** 2087-98.

MEISSNER, A., MIKKELSEN, T. S., GU, H., WERNIG, M., HANNA, J., SIVACHENKO, A., ZHANG, X., BERNSTEIN, B. E., NUSBAUM, C., JAFFE, D. B., GNIRKE, A., JAENISCH, R. & LANDER, E. S. 2008. Genome-scale DNA methylation maps of pluripotent and differentiated cells. *Nature,* 454**,** 766-70.

MICHELI, L., D'ANDREA, G., LEONARDI, L. & TIRONE, F. 2016. HDAC1, HDAC4 and HDAC9 Bind to PC3/Tis21/Btg2 and Are Required for its Inhibition of Cell Cycle Progression and Cyclin D1 Expression. *J Cell Physiol*.

MIRA, H., ANDREU, Z., SUH, H., LIE, D. C., JESSBERGER, S., CONSIGLIO, A., SAN EMETERIO, J., HORTIGUELA, R., MARQUES-TORREJON, M. A., NAKASHIMA, K., COLAK, D., GOTZ, M., FARINAS, I. & GAGE, F. H. 2010. Signaling through BMPR-IA regulates quiescence and long-term activity of neural stem cells in the adult hippocampus. *Cell Stem Cell,* 7**,** 78-89.

MIRZADEH, Z., MERKLE, F. T., SORIANO-NAVARRO, M., GARCIA-VERDUGO, J. M. & ALVAREZ-BUYLLA, A. 2008. Neural stem cells confer unique pinwheel architecture to the ventricular surface in neurogenic regions of the adult brain. *Cell Stem Cell,* 3**,** 265-78.

MISSON, J. P., EDWARDS, M. A., YAMAMOTO, M. & CAVINESS, V. S., JR. 1988. Identification of radial glial cells within the developing murine central nervous system: studies based upon a new immunohistochemical marker. *Brain Res Dev Brain Res,* 44**,** 95-108.

MIYATA, T., KAWAGUCHI, A., OKANO, H. & OGAWA, M. 2001. Asymmetric inheritance of radial glial fibers by cortical neurons. *Neuron,* 31**,** 727-41.

MIYATA, T., KAWAGUCHI, A., SAITO, K., KAWANO, M., MUTO, T. & OGAWA, M. 2004. Asymmetric production of surface-dividing and non-surface-dividing cortical progenitor cells. *Development,* 131**,** 3133-45.

MIZUTANI, K., YOON, K., DANG, L., TOKUNAGA, A. & GAIANO, N. 2007. Differential Notch signalling distinguishes neural stem cells from intermediate progenitors. *Nature,* 449**,** 351-5.

MORIN, X., JAOUEN, F. & DURBEC, P. 2007. Control of planar divisions by the G-protein regulator LGN maintains progenitors in the chick neuroepithelium. *Nat Neurosci,* 10**,** 1440-8.

MORTE, M. I., CARREIRA, B. P., MACHADO, V., CARMO, A., NUNES-CORREIA, I., CARVALHO, C. M. & ARAUJO, I. M. 2013. Evaluation of proliferation of neural stem cells in vitro and in vivo. *Curr Protoc Stem Cell Biol,* Chapter 2**,** Unit 2D 14.

MURCIANO, A., ZAMORA, J., LOPEZ-SANCHEZ, J. & FRADE, J. M. 2002. Interkinetic nuclear movement may provide spatial clues to the regulation of neurogenesis. *Mol Cell Neurosci,* 21**,** 285-300.

NAGASE, T., NAGASE, M., YOSHIMURA, K., FUJITA, T. & KOSHIMA, I. 2005. Angiogenesis within the developing mouse neural tube is dependent on

sonic hedgehog signaling: possible roles of motor neurons. *Genes Cells,* 10**,** 595-604.

NAGY, A. 2000. Cre recombinase: the universal reagent for genome tailoring. *Genesis,* 26**,** 99-109.

NAKAMURA-ISHIZU, A., KURIHARA, T., OKUNO, Y., OZAWA, Y., KISHI, K., GODA, N., TSUBOTA, K., OKANO, H., SUDA, T. & KUBOTA, Y. 2012. The formation of an angiogenic astrocyte template is regulated by the neuroretina in a HIF-1-dependent manner. *Dev Biol,* 363**,** 106-14.

NAKAO, T., ISHIZAWA, A. & OGAWA, R. 1988. Observations of vascularization in the spinal cord of mouse embryos, with special reference to development of boundary membranes and perivascular spaces. *Anat Rec,* 221**,** 663-77.

NAKASHIMA, K., YANAGISAWA, M., ARAKAWA, H., KIMURA, N., HISATSUNE, T., KAWABATA, M., MIYAZONO, K. & TAGA, T. 1999. Synergistic signaling in fetal brain by STAT3-Smad1 complex bridged by p300. *Science,* 284**,** 479-82.

NAMIHIRA, M., KOHYAMA, J., SEMI, K., SANOSAKA, T., DENEEN, B., TAGA, T. & NAKASHIMA, K. 2009. Committed neuronal precursors confer astrocytic potential on residual neural precursor cells. *Dev Cell,* 16**,** 245-55.

NGUYEN, V. A., FURHAPTER, C., OBEXER, P., STOSSEL, H., ROMANI, N. & SEPP, N. 2009. Endothelial cells from cord blood CD133+CD34+ progenitors share phenotypic, functional and gene expression profile similarities with lymphatics. *J Cell Mol Med,* 13**,** 522-34.

NIOLA, F., ZHAO, X., SINGH, D., CASTANO, A., SULLIVAN, R., LAURIA, M., NAM, H. S., ZHUANG, Y., BENEZRA, R., DI BERNARDO, D., IAVARONE, A. & LASORELLA, A. 2012. Id proteins synchronize stemness and anchorage to the niche of neural stem cells. *Nat Cell Biol,* 14**,** 477-87.

NOCTOR, S. C., FLINT, A. C., WEISSMAN, T. A., DAMMERMAN, R. S. & KRIEGSTEIN, A. R. 2001. Neurons derived from radial glial cells establish radial units in neocortex. *Nature,* 409**,** 714-20.

NOCTOR, S. C., FLINT, A. C., WEISSMAN, T. A., WONG, W. S., CLINTON, B. K. & KRIEGSTEIN, A. R. 2002. Dividing precursor cells of the embryonic cortical ventricular zone have morphological and molecular characteristics of radial glia. *J Neurosci,* 22**,** 3161-73.

NOCTOR, S. C., MARTINEZ-CERDENO, V., IVIC, L. & KRIEGSTEIN, A. R. 2004. Cortical neurons arise in symmetric and asymmetric division zones and migrate through specific phases. *Nat Neurosci,* 7**,** 136-44.

NORDEN, C., YOUNG, S., LINK, B. A. & HARRIS, W. A. 2009. Actomyosin is the main driver of interkinetic nuclear migration in the retina. *Cell,* 138**,** 1195-208.

NOVITCH, B. G., CHEN, A. I. & JESSELL, T. M. 2001. Coordinate regulation of motor neuron subtype identity and pan-neuronal properties by the bHLH repressor Olig2. *Neuron,* 31**,** 773-89.

OHTANI, N., GOTO, T., WAEBER, C. & BHIDE, P. G. 2003. Dopamine modulates cell cycle in the lateral ganglionic eminence. *J Neurosci,* 23**,** 2840-50.

OHTSUKA, T., ISHIBASHI, M., GRADWOHL, G., NAKANISHI, S., GUILLEMOT, F. & KAGEYAMA, R. 1999. Hes1 and Hes5 as notch effectors in mammalian neuronal differentiation. *EMBO J,* 18**,** 2196-207.

OHTSUKA, T., SAKAMOTO, M., GUILLEMOT, F. & KAGEYAMA, R. 2001. Roles of the basic helix-loop-helix genes Hes1 and Hes5 in expansion of neural stem cells of the developing brain. *J Biol Chem,* 276**,** 30467-74.

OKABE, K., KOBAYASHI, S., YAMADA, T., KURIHARA, T., TAI-NAGARA, I., MIYAMOTO, T., MUKOUYAMA, Y. S., SATO, T. N., SUDA, T., EMA, M. & KUBOTA, Y. 2014. Neurons limit angiogenesis by titrating VEGF in retina. *Cell,* 159**,** 584-96.

OLIVER, T. G., GRASFEDER, L. L., CARROLL, A. L., KAISER, C., GILLINGHAM, C. L., LIN, S. M., WICKRAMASINGHE, R., SCOTT, M. P. & WECHSLER-REYA, R. J. 2003. Transcriptional profiling of the Sonic hedgehog response: a critical role for N-myc in proliferation of neuronal precursors. *Proc Natl Acad Sci U S A,* 100**,** 7331-6.

OOSTHUYSE, B., MOONS, L., STORKEBAUM, E., BECK, H., NUYENS, D., BRUSSELMANS, K., VAN DORPE, J., HELLINGS, P., GORSELINK, M., HEYMANS, S., THEILMEIER, G., DEWERCHIN, M., LAUDENBACH, V., VERMYLEN, P., RAAT, H., ACKER, T., VLEMINCKX, V., VAN DEN BOSCH, L., CASHMAN, N., FUJISAWA, H., DROST, M. R., SCIOT, R., BRUYNINCKX, F., HICKLIN, D. J., INCE, C., GRESSENS, P., LUPU, F., PLATE, K. H., ROBBERECHT, W., HERBERT, J. M., COLLEN, D. & CARMELIET, P. 2001. Deletion of the hypoxia-response element in the vascular endothelial growth factor promoter causes motor neuron degeneration. *Nat Genet,* 28**,** 131-8.

ORTEGA, S., ITTMANN, M., TSANG, S. H., EHRLICH, M. & BASILICO, C. 1998. Neuronal defects and delayed wound healing in mice lacking fibroblast growth factor 2. *Proc Natl Acad Sci U S A,* 95**,** 5672-7.

OSTREM, B. E., LUI, J. H., GERTZ, C. C. & KRIEGSTEIN, A. R. 2014. Control of outer radial glial stem cell mitosis in the human brain. *Cell Rep,* 8**,** 656-64.

OTTONE, C., KRUSCHE, B., WHITBY, A., CLEMENTS, M., QUADRATO, G., PITULESCU, M. E., ADAMS, R. H. & PARRINELLO, S. 2014. Direct cell-cell contact with the vascular niche maintains quiescent neural stem cells. *Nat Cell Biol,* 16**,** 1045-56.

OWENS, D. F. & KRIEGSTEIN, A. R. 1998. Patterns of intracellular calcium fluctuation in precursor cells of the neocortical ventricular zone. *J Neurosci,* 18**,** 5374-88.

PACKER, A. N., XING, Y., HARPER, S. Q., JONES, L. & DAVIDSON, B. L. 2008. The bifunctional microRNA miR-9/miR-9* regulates REST and CoREST and is downregulated in Huntington's disease. *J Neurosci,* 28**,** 14341-6.

PAEK, H., GUTIN, G. & HEBERT, J. M. 2009. FGF signaling is strictly required to maintain early telencephalic precursor cell survival. *Development,* 136**,** 2457-65.

PALMA, V. & RUIZ I ALTABA, A. 2004. Hedgehog-GLI signaling regulates the behavior of cells with stem cell properties in the developing neocortex. *Development,* 131**,** 337-45.

PALMEIRIM, I., HENRIQUE, D., ISH-HOROWICZ, D. & POURQUIE, O. 1997. Avian hairy gene expression identifies a molecular clock linked to vertebrate segmentation and somitogenesis. *Cell,* 91**,** 639-48.

PAPROCKA, M., KRAWCZENKO, A., DUS, D., KANTOR, A., CARREAU, A., GRILLON, C. & KIEDA, C. 2011. CD133 positive progenitor endothelial cell lines from human cord blood. *Cytometry A,* 79**,** 594-602.

PARIDAEN, J. T. & HUTTNER, W. B. 2014. Neurogenesis during development of the vertebrate central nervous system. *EMBO Rep,* 15**,** 351-64.

PARIDAEN, J. T., WILSCH-BRAUNINGER, M. & HUTTNER, W. B. 2013. Asymmetric inheritance of centrosome-associated primary cilium membrane directs ciliogenesis after cell division. *Cell,* 155**,** 333-44.

PARK, J. E., KELLER, G. A. & FERRARA, N. 1993. The vascular endothelial growth factor (VEGF) isoforms: differential deposition into the subepithelial extracellular matrix and bioactivity of extracellular matrix-bound VEGF. *Mol Biol Cell,* 4**,** 1317-26.

PARK, J. K., WILLIAMS, B. P., ALBERTA, J. A. & STILES, C. D. 1999. Bipotent cortical progenitor cells process conflicting cues for neurons and glia in a hierarchical manner. *J Neurosci,* 19**,** 10383-9.

PARKER, M. W., XU, P., LI, X. & VANDER KOOI, C. W. 2012. Structural basis for selective vascular endothelial growth factor-A (VEGF-A) binding to neuropilin-1. *J Biol Chem,* 287**,** 11082-9.

PARTHASARATHY, S., SRIVATSA, S., NITYANANDAM, A. & TARABYKIN, V. 2014. Ntf3 acts downstream of Sip1 in cortical postmitotic neurons to control progenitor cell fate through feedback signaling. *Development,* 141**,** 3324-30.

PASSEMARD, S., EL GHOUZZI, V., NASSER, H., VERNEY, C., VODJDANI, G., LACAUD, A., LEBON, S., LABURTHE, M., ROBBERECHT, P., NARDELLI, J., MANI, S., VERLOES, A., GRESSENS, P. & LELIEVRE, V. 2011. VIP blockade leads to microcephaly in mice via disruption of Mcph1-Chk1 signaling. *J Clin Invest,* 121**,** 3071-87.

PAWLISZ, A. S. & FENG, Y. 2011. Three-dimensional regulation of radial glial functions by Lis1-Nde1 and dystrophin glycoprotein complexes. *PLoS Biol,* 9**,** e1001172.

PEIRSON, S. N., BUTLER, J. N. & FOSTER, R. G. 2003. Experimental validation of novel and conventional approaches to quantitative real-time PCR data analysis. *Nucleic Acids Res,* 31**,** e73.

PETERSEN, P. H., ZOU, K., HWANG, J. K., JAN, Y. N. & ZHONG, W. 2002. Progenitor cell maintenance requires numb and numblike during mouse neurogenesis. *Nature,* 419**,** 929-34.

PETERSEN, P. H., ZOU, K., KRAUSS, S. & ZHONG, W. 2004. Continuing role for mouse Numb and Numbl in maintaining progenitor cells during cortical neurogenesis. *Nat Neurosci,* 7**,** 803-11.

PEUNOVA, N. & ENIKOLOPOV, G. 1995. Nitric oxide triggers a switch to growth arrest during differentiation of neuronal cells. *Nature,* 375**,** 68-73.

PEVNY, L. H., SOCKANATHAN, S., PLACZEK, M. & LOVELL-BADGE, R. 1998. A role for SOX1 in neural determination. *Development,* 125**,** 1967-78.

PFAFF, S. L., MENDELSOHN, M., STEWART, C. L., EDLUND, T. & JESSELL, T. M. 1996. Requirement for LIM homeobox gene Isl1 in motor neuron generation reveals a motor neuron-dependent step in interneuron differentiation. *Cell,* 84**,** 309-20.

PFEFFER, P. L., PAYER, B., REIM, G., DI MAGLIANO, M. P. & BUSSLINGER, M. 2002. The activation and maintenance of Pax2 expression at the mid-

hindbrain boundary is controlled by separate enhancers. *Development,* 129**,** 307-18.

PICARD, D. 1994. Regulation of protein function through expression of chimaeric proteins. *Curr Opin Biotechnol,* 5**,** 511-5.

PILAZ, L. J., MCMAHON, J. J., MILLER, E. E., LENNOX, A. L., SUZUKI, A., SALMON, E. & SILVER, D. L. 2016. Prolonged Mitosis of Neural Progenitors Alters Cell Fate in the Developing Brain. *Neuron,* 89**,** 83-99.

PILAZ, L. J., PATTI, D., MARCY, G., OLLIER, E., PFISTER, S., DOUGLAS, R. J., BETIZEAU, M., GAUTIER, E., CORTAY, V., DOERFLINGER, N., KENNEDY, H. & DEHAY, C. 2009. Forced G1-phase reduction alters mode of division, neuron number, and laminar phenotype in the cerebral cortex. *Proc Natl Acad Sci U S A,* 106**,** 21924-9.

PILZ, G. A., SHITAMUKAI, A., REILLO, I., PACARY, E., SCHWAUSCH, J., STAHL, R., NINKOVIC, J., SNIPPERT, H. J., CLEVERS, H., GODINHO, L., GUILLEMOT, F., BORRELL, V., MATSUZAKI, F. & GOTZ, M. 2013. Amplification of progenitors in the mammalian telencephalon includes a new radial glial cell type. *Nat Commun,* 4**,** 2125.

PLEIN, A., CALMONT, A., FANTIN, A., DENTI, L., ANDERSON, N. A., SCAMBLER, P. J. & RUHRBERG, C. 2015. Neural crest-derived SEMA3C activates endothelial NRP1 for cardiac outflow tract septation. *J Clin Invest,* 125**,** 2661-76.

POLAKIS, P. 2012. Wnt signaling in cancer. *Cold Spring Harb Perspect Biol,* 4.

PONTI, G., OBERNIER, K. & ALVAREZ-BUYLLA, A. 2013. Lineage progression from stem cells to new neurons in the adult brain ventricular-subventricular zone. *Cell Cycle,* 12**,** 1649-50.

POPKEN, G. J., HODGE, R. D., YE, P., ZHANG, J., NG, W., O'KUSKY, J. R. & D'ERCOLE, A. J. 2004. In vivo effects of insulin-like growth factor-I (IGF-I) on prenatal and early postnatal development of the central nervous system. *Eur J Neurosci,* 19**,** 2056-68.

POSOKHOVA, E., SHUKLA, A., SEAMAN, S., VOLATE, S., HILTON, M. B., WU, B., MORRIS, H., SWING, D. A., ZHOU, M., ZUDAIRE, E., RUBIN, J. S. & ST CROIX, B. 2015. GPR124 functions as a WNT7-specific coactivator of canonical beta-catenin signaling. *Cell Rep,* 10**,** 123-30.

POZAS, E. & IBANEZ, C. F. 2005. GDNF and GFRalpha1 promote differentiation and tangential migration of cortical GABAergic neurons. *Neuron,* 45**,** 701-13.

QIAN, X., DAVIS, A. A., GODERIE, S. K. & TEMPLE, S. 1997. FGF2 concentration regulates the generation of neurons and glia from multipotent cortical stem cells. *Neuron,* 18**,** 81-93.

RAAB, S., BECK, H., GAUMANN, A., YUCE, A., GERBER, H. P., PLATE, K., HAMMES, H. P., FERRARA, N. & BREIER, G. 2004. Impaired brain angiogenesis and neuronal apoptosis induced by conditional homozygous inactivation of vascular endothelial growth factor. *Thromb Haemost,* 91**,** 595-605.

RADAKOVITS, R., BARROS, C. S., BELVINDRAH, R., PATTON, B. & MULLER, U. 2009. Regulation of radial glial survival by signals from the meninges. *J Neurosci,* 29**,** 7694-705.

RAIMONDI, C., BRASH, J. T., FANTIN, A. & RUHRBERG, C. 2016. NRP1 function and targeting in neurovascular development and eye disease. *Prog Retin Eye Res,* 52**,** 64-83.

RAIMONDI, C., FANTIN, A., LAMPROPOULOU, A., DENTI, L., CHIKH, A. & RUHRBERG, C. 2014. Imatinib inhibits VEGF-independent angiogenesis by targeting neuropilin 1-dependent ABL1 activation in endothelial cells. *J Exp Med,* 211**,** 1167-83.

RAKIC, P. 1972. Mode of cell migration to the superficial layers of fetal monkey neocortex. *J Comp Neurol,* 145**,** 61-83.

RAKIC, P. 1995. A small step for the cell, a giant leap for mankind: a hypothesis of neocortical expansion during evolution. *Trends Neurosci,* 18**,** 383-8.

RAMIREZ-CASTILLEJO, C., SANCHEZ-SANCHEZ, F., ANDREU-AGULLO, C., FERRON, S. R., AROCA-AGUILAR, J. D., SANCHEZ, P., MIRA, H., ESCRIBANO, J. & FARINAS, I. 2006. Pigment epithelium-derived factor is a niche signal for neural stem cell renewal. *Nat Neurosci,* 9**,** 331-9.

RASH, B. G., LIM, H. D., BREUNIG, J. J. & VACCARINO, F. M. 2011. FGF signaling expands embryonic cortical surface area by regulating Notch-dependent neurogenesis. *J Neurosci,* 31**,** 15604-17.

RASIN, M. R., GAZULA, V. R., BREUNIG, J. J., KWAN, K. Y., JOHNSON, M. B., LIU-CHEN, S., LI, H. S., JAN, L. Y., JAN, Y. N., RAKIC, P. & SESTAN, N. 2007. Numb and Numbl are required for maintenance of cadherin-based adhesion and polarity of neural progenitors. *Nat Neurosci,* 10**,** 819-27.

RHEINWALD, J. G. & GREEN, H. 1977. Epidermal growth factor and the multiplication of cultured human epidermal keratinocytes. *Nature,* 265**,** 421-4.

RIEGER, S., VOLKMANN, K. & KOSTER, R. W. 2008. Polysialyltransferase expression is linked to neuronal migration in the developing and adult zebrafish. *Dev Dyn,* 237**,** 276-85.

RIZZOTI, K., BRUNELLI, S., CARMIGNAC, D., THOMAS, P. Q., ROBINSON, I. C. & LOVELL-BADGE, R. 2004. SOX3 is required during the formation of the hypothalamo-pituitary axis. *Nat Genet,* 36**,** 247-55.

ROCCIO, M., SCHMITTER, D., KNOBLOCH, M., OKAWA, Y., SAGE, D. & LUTOLF, M. P. 2013. Predicting stem cell fate changes by differential cell cycle progression patterns. *Development,* 140**,** 459-70.

ROGERS, C. D., HARAFUJI, N., ARCHER, T., CUNNINGHAM, D. D. & CASEY, E. S. 2009. Xenopus Sox3 activates sox2 and geminin and indirectly represses Xvent2 expression to induce neural progenitor formation at the expense of non-neural ectodermal derivatives. *Mech Dev,* 126**,** 42-55.

ROPER, K., CORBEIL, D. & HUTTNER, W. B. 2000. Retention of prominin in microvilli reveals distinct cholesterol-based lipid micro-domains in the apical plasma membrane. *Nat Cell Biol,* 2**,** 582-92.

ROWITCH, D. H., B, S. J., LEE, S. M., FLAX, J. D., SNYDER, E. Y. & MCMAHON, A. P. 1999. Sonic hedgehog regulates proliferation and inhibits differentiation of CNS precursor cells. *J Neurosci,* 19**,** 8954-65.

RUHRBERG, C., GERHARDT, H., GOLDING, M., WATSON, R., IOANNIDOU, S., FUJISAWA, H., BETSHOLTZ, C. & SHIMA, D. T. 2002. Spatially restricted patterning cues provided by heparin-binding VEGF-A control blood vessel branching morphogenesis. *Genes Dev,* 16**,** 2684-98.

RUIZ DE ALMODOVAR, C., COULON, C., SALIN, P. A., KNEVELS, E., CHOUNLAMOUNTRI, N., POESEN, K., HERMANS, K., LAMBRECHTS, D., VAN GEYTE, K., DHONDT, J., DRESSELAERS, T., RENAUD, J.,

ARAGONES, J., ZACCHIGNA, S., GEUDENS, I., GALL, D., STROOBANTS, S., MUTIN, M., DASSONVILLE, K., STORKEBAUM, E., JORDAN, B. F., ERIKSSON, U., MOONS, L., D'HOOGE, R., HAIGH, J. J., BELIN, M. F., SCHIFFMANN, S., VAN HECKE, P., GALLEZ, B., VINCKIER, S., CHEDOTAL, A., HONNORAT, J., THOMASSET, N., CARMELIET, P. & MEISSIREL, C. 2010. Matrix-binding vascular endothelial growth factor (VEGF) isoforms guide granule cell migration in the cerebellum via VEGF receptor Flk1. *J Neurosci,* 30**,** 15052-66.

RUIZ DE ALMODOVAR, C., FABRE, P. J., KNEVELS, E., COULON, C., SEGURA, I., HADDICK, P. C., AERTS, L., DELATTIN, N., STRASSER, G., OH, W. J., LANGE, C., VINCKIER, S., HAIGH, J., FOUQUET, C., GU, C., ALITALO, K., CASTELLANI, V., TESSIER-LAVIGNE, M., CHEDOTAL, A., CHARRON, F. & CARMELIET, P. 2011. VEGF mediates commissural axon chemoattraction through its receptor Flk1. *Neuron,* 70**,** 966-78.

SAADE, M., GUTIERREZ-VALLEJO, I., LE DREAU, G., RABADAN, M. A., MIGUEZ, D. G., BUCETA, J. & MARTI, E. 2013. Sonic hedgehog signaling switches the mode of division in the developing nervous system. *Cell Rep,* 4**,** 492-503.

SAKAKIBARA, S., IMAI, T., HAMAGUCHI, K., OKABE, M., ARUGA, J., NAKAJIMA, K., YASUTOMI, D., NAGATA, T., KURIHARA, Y., UESUGI, S., MIYATA, T., OGAWA, M., MIKOSHIBA, K. & OKANO, H. 1996. Mouse-Musashi-1, a neural RNA-binding protein highly enriched in the mammalian CNS stem cell. *Dev Biol,* 176**,** 230-42.

SANSOM, S. N., GRIFFITHS, D. S., FAEDO, A., KLEINJAN, D. J., RUAN, Y., SMITH, J., VAN HEYNINGEN, V., RUBENSTEIN, J. L. & LIVESEY, F. J. 2009. The level of the transcription factor Pax6 is essential for controlling the balance between neural stem cell self-renewal and neurogenesis. *PLoS Genet,* 5**,** e1000511.

SATO, T., SATO, F., KAMEZAKI, A., SAKAGUCHI, K., TANIGOME, R., KAWAKAMI, K. & SEHARA-FUJISAWA, A. 2015. Neuregulin 1 Type II-ErbB Signaling Promotes Cell Divisions Generating Neurons from Neural Progenitor Cells in the Developing Zebrafish Brain. *PLoS One,* 10**,** e0127360.

SATO, T., VAN ES, J. H., SNIPPERT, H. J., STANGE, D. E., VRIES, R. G., VAN DEN BORN, M., BARKER, N., SHROYER, N. F., VAN DE WETERING, M. & CLEVERS, H. 2011. Paneth cells constitute the niche for Lgr5 stem cells in intestinal crypts. *Nature,* 469**,** 415-8.

SATO, T. N., TOZAWA, Y., DEUTSCH, U., WOLBURG-BUCHHOLZ, K., FUJIWARA, Y., GENDRON-MAGUIRE, M., GRIDLEY, T., WOLBURG, H., RISAU, W. & QIN, Y. 1995. Distinct roles of the receptor tyrosine kinases Tie-1 and Tie-2 in blood vessel formation. *Nature,* 376**,** 70-4.

SAUER, F. 1935. Mitosis in the neural tube. *The Journal of Comparative Neurology.,* 62**,** 377-405.

SCARDIGLI, R., BAUMER, N., GRUSS, P., GUILLEMOT, F. & LE ROUX, I. 2003. Direct and concentration-dependent regulation of the proneural gene Neurogenin2 by Pax6. *Development,* 130**,** 3269-81.

SCHANZER, A., WACHS, F. P., WILHELM, D., ACKER, T., COOPER-KUHN, C., BECK, H., WINKLER, J., AIGNER, L., PLATE, K. H. & KUHN, H. G.

2004. Direct stimulation of adult neural stem cells in vitro and neurogenesis in vivo by vascular endothelial growth factor. *Brain Pathol,* 14**,** 237-48.

SCHENK, J., WILSCH-BRAUNINGER, M., CALEGARI, F. & HUTTNER, W. B. 2009. Myosin II is required for interkinetic nuclear migration of neural progenitors. *Proc Natl Acad Sci U S A,* 106**,** 16487-92.

SCHOLZEN, T. & GERDES, J. 2000. The Ki-67 protein: from the known and the unknown. *J Cell Physiol,* 182**,** 311-22.

SCHWARZ, Q., GU, C., FUJISAWA, H., SABELKO, K., GERTSENSTEIN, M., NAGY, A., TANIGUCHI, M., KOLODKIN, A. L., GINTY, D. D., SHIMA, D. T. & RUHRBERG, C. 2004. Vascular endothelial growth factor controls neuronal migration and cooperates with Sema3A to pattern distinct compartments of the facial nerve. *Genes Dev,* 18**,** 2822-34.

SCHWARZ, Q., MADEN, C. H., VIEIRA, J. M. & RUHRBERG, C. 2009. Neuropilin 1 signaling guides neural crest cells to coordinate pathway choice with cell specification. *Proc Natl Acad Sci U S A,* 106**,** 6164-9.

SCOTT, E. W., SIMON, M. C., ANASTASI, J. & SINGH, H. 1994. Requirement of transcription factor PU.1 in the development of multiple hematopoietic lineages. *Science,* 265**,** 1573-7.

SEGAL, R. A. 2003. Selectivity in neurotrophin signaling: theme and variations. *Annu Rev Neurosci,* 26**,** 299-330.

SEIDNER, G., ALVAREZ, M. G., YEH, J. I., O'DRISCOLL, K. R., KLEPPER, J., STUMP, T. S., WANG, D., SPINNER, N. B., BIRNBAUM, M. J. & DE VIVO, D. C. 1998. GLUT-1 deficiency syndrome caused by haploinsufficiency of the blood-brain barrier hexose carrier. *Nat Genet,* 18**,** 188-91.

SESSA, A., MAO, C. A., HADJANTONAKIS, A. K., KLEIN, W. H. & BROCCOLI, V. 2008. Tbr2 directs conversion of radial glia into basal precursors and guides neuronal amplification by indirect neurogenesis in the developing neocortex. *Neuron,* 60**,** 56-69.

SHEN, Q., WANG, Y., KOKOVAY, E., LIN, G., CHUANG, S. M., GODERIE, S. K., ROYSAM, B. & TEMPLE, S. 2008. Adult SVZ stem cells lie in a vascular niche: a quantitative analysis of niche cell-cell interactions. *Cell Stem Cell,* 3**,** 289-300.

SHEN, Q., ZHONG, W., JAN, Y. N. & TEMPLE, S. 2002. Asymmetric Numb distribution is critical for asymmetric cell division of mouse cerebral cortical stem cells and neuroblasts. *Development,* 129**,** 4843-53.

SHIBATA, M., NAKAO, H., KIYONARI, H., ABE, T. & AIZAWA, S. 2011. MicroRNA-9 regulates neurogenesis in mouse telencephalon by targeting multiple transcription factors. *J Neurosci,* 31**,** 3407-22.

SHIMIZU, M., MURAKAMI, Y., SUTO, F. & FUJISAWA, H. 2000. Determination of cell adhesion sites of neuropilin-1. *J Cell Biol,* 148**,** 1283-93.

SHIMOJO, H., OHTSUKA, T. & KAGEYAMA, R. 2008. Oscillations in notch signaling regulate maintenance of neural progenitors. *Neuron,* 58**,** 52-64.

SHIN, M. H., LEE, E. G., LEE, S. H., LEE, Y. S. & SON, H. 2002. Neural cell adhesion molecule (NCAM) promotes the differentiation of hippocampal precursor cells to a neuronal lineage, especially to a glutamatergic neural cell type. *Exp Mol Med,* 34**,** 401-10.

SHITAMUKAI, A., KONNO, D. & MATSUZAKI, F. 2011. Oblique radial glial divisions in the developing mouse neocortex induce self-renewing

progenitors outside the germinal zone that resemble primate outer subventricular zone progenitors. *J Neurosci,* 31**,** 3683-95.

SHITAMUKAI, A. & MATSUZAKI, F. 2012. Control of asymmetric cell division of mammalian neural progenitors. *Dev Growth Differ,* 54**,** 277-86.

SIEGENTHALER, J. A., ASHIQUE, A. M., ZARBALIS, K., PATTERSON, K. P., HECHT, J. H., KANE, M. A., FOLIAS, A. E., CHOE, Y., MAY, S. R., KUME, T., NAPOLI, J. L., PETERSON, A. S. & PLEASURE, S. J. 2009. Retinoic acid from the meninges regulates cortical neuron generation. *Cell,* 139**,** 597-609.

SILLER, K. H. & DOE, C. Q. 2009. Spindle orientation during asymmetric cell division. *Nat Cell Biol,* 11**,** 365-74.

SMART, I. H. 1972. Proliferative characteristics of the ependymal layer during the early development of the mouse diencephalon, as revealed by recording the number, location, and plane of cleavage of mitotic figures. *J Anat,* 113**,** 109-29.

SMITH, K. M., MARAGNOLI, M. E., PHULL, P. M., TRAN, K. M., CHOUBEY, L. & VACCARINO, F. M. 2014. Fgfr1 inactivation in the mouse telencephalon results in impaired maturation of interneurons expressing parvalbumin. *PLoS One,* 9**,** e103696.

SNAPYAN, M., LEMASSON, M., BRILL, M. S., BLAIS, M., MASSOUH, M., NINKOVIC, J., GRAVEL, C., BERTHOD, F., GOTZ, M., BARKER, P. A., PARENT, A. & SAGHATELYAN, A. 2009. Vasculature guides migrating neuronal precursors in the adult mammalian forebrain via brain-derived neurotrophic factor signaling. *J Neurosci,* 29**,** 4172-88.

SOMMER, L., MA, Q. & ANDERSON, D. J. 1996. neurogenins, a novel family of atonal-related bHLH transcription factors, are putative mammalian neuronal determination genes that reveal progenitor cell heterogeneity in the developing CNS and PNS. *Mol Cell Neurosci,* 8**,** 221-41.

SONG, M. R. & GHOSH, A. 2004. FGF2-induced chromatin remodeling regulates CNTF-mediated gene expression and astrocyte differentiation. *Nat Neurosci,* 7**,** 229-35.

SORIANO, E. & DEL RIO, J. A. 2005. The cells of cajal-retzius: still a mystery one century after. *Neuron,* 46**,** 389-94.

SPEMANN, H. & MANGOLD, H. 1924. Über Induktion von Embryonalanlagen durch Implantation artfremder Organisatoren. . *Roux's Arch. EntwMech. Org.,* 100**,** 599-638.

SRINIVAS, S., WATANABE, T., LIN, C. S., WILLIAM, C. M., TANABE, Y., JESSELL, T. M. & COSTANTINI, F. 2001. Cre reporter strains produced by targeted insertion of EYFP and ECFP into the ROSA26 locus. *BMC Dev Biol,* 1**,** 4.

STALMANS, I., NG, Y. S., ROHAN, R., FRUTTIGER, M., BOUCHE, A., YUCE, A., FUJISAWA, H., HERMANS, B., SHANI, M., JANSEN, S., HICKLIN, D., ANDERSON, D. J., GARDINER, T., HAMMES, H. P., MOONS, L., DEWERCHIN, M., COLLEN, D., CARMELIET, P. & D'AMORE, P. A. 2002. Arteriolar and venular patterning in retinas of mice selectively expressing VEGF isoforms. *J Clin Invest,* 109**,** 327-36.

STENMAN, J. M., RAJAGOPAL, J., CARROLL, T. J., ISHIBASHI, M., MCMAHON, J. & MCMAHON, A. P. 2008. Canonical Wnt signaling

regulates organ-specific assembly and differentiation of CNS vasculature. *Science,* 322**,** 1247-50.

STENZEL, D., WILSCH-BRAUNINGER, M., WONG, F. K., HEUER, H. & HUTTNER, W. B. 2014. Integrin alphavbeta3 and thyroid hormones promote expansion of progenitors in embryonic neocortex. *Development,* 141**,** 795-806.

STIPURSKY, J., FRANCIS, D., DEZONNE, R. S., BERGAMO DE ARAUJO, A. P., SOUZA, L., MORAES, C. A. & ALCANTARA GOMES, F. C. 2014. TGF-beta1 promotes cerebral cortex radial glia-astrocyte differentiation in vivo. *Front Cell Neurosci,* 8**,** 393.

STUBBS, D., DEPROTO, J., NIE, K., ENGLUND, C., MAHMUD, I., HEVNER, R. & MOLNAR, Z. 2009. Neurovascular congruence during cerebral cortical development. *Cereb Cortex,* 19 Suppl 1**,** i32-41.

SUCHTING, S., FREITAS, C., LE NOBLE, F., BENEDITO, R., BREANT, C., DUARTE, A. & EICHMANN, A. 2007. The Notch ligand Delta-like 4 negatively regulates endothelial tip cell formation and vessel branching. *Proc Natl Acad Sci U S A,* 104**,** 3225-30.

SULLIVAN, K. F. 1988. Structure and utilization of tubulin isotypes. *Annu Rev Cell Biol,* 4**,** 687-716.

SUN, G., YU, R. T., EVANS, R. M. & SHI, Y. 2007. Orphan nuclear receptor TLX recruits histone deacetylases to repress transcription and regulate neural stem cell proliferation. *Proc Natl Acad Sci U S A,* 104**,** 15282-7.

SUN, Y., JIN, K., XIE, L., CHILDS, J., MAO, X. O., LOGVINOVA, A. & GREENBERG, D. A. 2003. VEGF-induced neuroprotection, neurogenesis, and angiogenesis after focal cerebral ischemia. *J Clin Invest,* 111**,** 1843-51.

SURI, C., JONES, P. F., PATAN, S., BARTUNKOVA, S., MAISONPIERRE, P. C., DAVIS, S., SATO, T. N. & YANCOPOULOS, G. D. 1996. Requisite role of angiopoietin-1, a ligand for the TIE2 receptor, during embryonic angiogenesis. *Cell,* 87**,** 1171-80.

SUZUKI, S. C. & TAKEICHI, M. 2008. Cadherins in neuronal morphogenesis and function. *Dev Growth Differ,* 50 Suppl 1**,** S119-30.

SUZUKI, Y., YANAGISAWA, M., YAGI, H., NAKATANI, Y. & YU, R. K. 2010. Involvement of beta1-integrin up-regulation in basic fibroblast growth factor- and epidermal growth factor-induced proliferation of mouse neuroepithelial cells. *J Biol Chem,* 285**,** 18443-51.

TAI, C. Y., DUJARDIN, D. L., FAULKNER, N. E. & VALLEE, R. B. 2002. Role of dynein, dynactin, and CLIP-170 interactions in LIS1 kinetochore function. *J Cell Biol,* 156**,** 959-68.

TAKAGI, S., KASUYA, Y., SHIMIZU, M., MATSUURA, T., TSUBOI, M., KAWAKAMI, A. & FUJISAWA, H. 1995. Expression of a cell adhesion molecule, neuropilin, in the developing chick nervous system. *Dev Biol,* 170**,** 207-22.

TAKEBAYASHI, H., YOSHIDA, S., SUGIMORI, M., KOSAKO, H., KOMINAMI, R., NAKAFUKU, M. & NABESHIMA, Y. 2000. Dynamic expression of basic helix-loop-helix Olig family members: implication of Olig2 in neuron and oligodendrocyte differentiation and identification of a new member, Olig3. *Mech Dev,* 99**,** 143-8.

TAM, S. J., RICHMOND, D. L., KAMINKER, J. S., MODRUSAN, Z., MARTIN-MCNULTY, B., CAO, T. C., WEIMER, R. M., CARANO, R. A., VAN

BRUGGEN, N. & WATTS, R. J. 2012. Death receptors DR6 and TROY regulate brain vascular development. *Dev Cell,* 22**,** 403-17.

TAMAMAKI, N., FUJIMORI, K., NOJYO, Y., KANEKO, T. & TAKAUJI, R. 2003. Evidence that Sema3A and Sema3F regulate the migration of GABAergic neurons in the developing neocortex. *J Comp Neurol,* 455**,** 238-48.

TAMMELA, T., ZARKADA, G., NURMI, H., JAKOBSSON, L., HEINOLAINEN, K., TVOROGOV, D., ZHENG, W., FRANCO, C. A., MURTOMAKI, A., ARANDA, E., MIURA, N., YLA-HERTTUALA, S., FRUTTIGER, M., MAKINEN, T., EICHMANN, A., POLLARD, J. W., GERHARDT, H. & ALITALO, K. 2011. VEGFR-3 controls tip to stalk conversion at vessel fusion sites by reinforcing Notch signalling. *Nat Cell Biol,* 13**,** 1202-13.

TAMMELA, T., ZARKADA, G., WALLGARD, E., MURTOMAKI, A., SUCHTING, S., WIRZENIUS, M., WALTARI, M., HELLSTROM, M., SCHOMBER, T., PELTONEN, R., FREITAS, C., DUARTE, A., ISONIEMI, H., LAAKKONEN, P., CHRISTOFORI, G., YLA-HERTTUALA, S., SHIBUYA, M., PYTOWSKI, B., EICHMANN, A., BETSHOLTZ, C. & ALITALO, K. 2008. Blocking VEGFR-3 suppresses angiogenic sprouting and vascular network formation. *Nature,* 454**,** 656-60.

TAN, X., LIU, W. A., ZHANG, X. J., SHI, W., REN, S. Q., LI, Z., BROWN, K. N. & SHI, S. H. 2016. Vascular Influence on Ventral Telencephalic Progenitors and Neocortical Interneuron Production. *Dev Cell,* 36**,** 624-38.

TAO, Y., BLACK, I. B. & DICICCO-BLOOM, E. 1997. In vivo neurogenesis is inhibited by neutralizing antibodies to basic fibroblast growth factor. *J Neurobiol,* 33**,** 289-96.

TATA, M., RUHRBERG, C. & FANTIN, A. 2015. Vascularisation of the central nervous system. *Mech Dev,* 138 Pt 1**,** 26-36.

TATA, M., TILLO, M., RUHRBERG, C. 2015. Neuropilins in Development and Disease of the Nervous System *In:* PRUSZAK, J. (ed.) *Neural Surface Antigens: From Basic Biology to Biomedical Applications.* 1st ed.: Academic Press.

TATA, M., WALL, I., JOYCE, A., VIEIRA, J.M.V., KESSARIS, N. & RUHRBERG, C. 2016. Regulation of embryonic neurogenesis by germinal zone vasculature. *Proc Natl Acad Sci U S A,* 113(47), 13414-13419

TAVAZOIE, M., VAN DER VEKEN, L., SILVA-VARGAS, V., LOUISSAINT, M., COLONNA, L., ZAIDI, B., GARCIA-VERDUGO, J. M. & DOETSCH, F. 2008. A specialized vascular niche for adult neural stem cells. *Cell Stem Cell,* 3**,** 279-88.

TAVERNA, E., GOTZ, M. & HUTTNER, W. B. 2014. The cell biology of neurogenesis: toward an understanding of the development and evolution of the neocortex. *Annu Rev Cell Dev Biol,* 30**,** 465-502.

TAVERNA, E., HAFFNER, C., PEPPERKOK, R. & HUTTNER, W. B. 2012. A new approach to manipulate the fate of single neural stem cells in tissue. *Nat Neurosci,* 15**,** 329-37.

TAVERNA, E. & HUTTNER, W. B. 2010. Neural progenitor nuclei IN motion. *Neuron,* 67**,** 906-14.

THEILER, K. 1989. *The House Mouse: Atlas of Embryonic Development.*, Springer-Verlag.

THORED, P., WOOD, J., ARVIDSSON, A., CAMMENGA, J., KOKAIA, Z. & LINDVALL, O. 2007. Long-term neuroblast migration along blood vessels in an area with transient angiogenesis and increased vascularization after stroke. *Stroke,* 38**,** 3032-9.

TILLO, M., ERSKINE, L., CARIBONI, A., FANTIN, A., JOYCE, A., DENTI, L. & RUHRBERG, C. 2015. VEGF189 binds NRP1 and is sufficient for VEGF/NRP1-dependent neuronal patterning in the developing brain. *Development,* 142**,** 314-9.

TONG, C. K., CHEN, J., CEBRIAN-SILLA, A., MIRZADEH, Z., OBERNIER, K., GUINTO, C. D., TECOTT, L. H., GARCIA-VERDUGO, J. M., KRIEGSTEIN, A. & ALVAREZ-BUYLLA, A. 2014. Axonal control of the adult neural stem cell niche. *Cell Stem Cell,* 14**,** 500-11.

TOVAR, Y. R. L. B., ZEPEDA, A. & TAPIA, R. 2007. Vascular endothelial growth factor prevents paralysis and motoneuron death in a rat model of excitotoxic spinal cord neurodegeneration. *J Neuropathol Exp Neurol,* 66**,** 913-22.

TOZUKA, Y., FUKUDA, S., NAMBA, T., SEKI, T. & HISATSUNE, T. 2005. GABAergic excitation promotes neuronal differentiation in adult hippocampal progenitor cells. *Neuron,* 47**,** 803-15.

TSUDA, S., KITAGAWA, T., TAKASHIMA, S., ASAKAWA, S., SHIMIZU, N., MITANI, H., SHIMA, A., TSUTSUMI, M., HORI, H., NARUSE, K., ISHIKAWA, Y. & TAKEDA, H. 2010. FAK-mediated extracellular signals are essential for interkinetic nuclear migration and planar divisions in the neuroepithelium. *J Cell Sci,* 123**,** 484-96.

TSUNEKAWA, Y., BRITTO, J. M., TAKAHASHI, M., POLLEUX, F., TAN, S. S. & OSUMI, N. 2012. Cyclin D2 in the basal process of neural progenitors is linked to non-equivalent cell fates. *EMBO J,* 31**,** 1879-92.

TUNG, J. W., HEYDARI, K., TIROUVANZIAM, R., SAHAF, B., PARKS, D. R., HERZENBERG, L. A. & HERZENBERG, L. A. 2007. Modern flow cytometry: a practical approach. *Clin Lab Med,* 27**,** 453-68, v.

VACCARINO, F. M., SCHWARTZ, M. L., RABALLO, R., NILSEN, J., RHEE, J., ZHOU, M., DOETSCHMAN, T., COFFIN, J. D., WYLAND, J. J. & HUNG, Y. T. 1999. Changes in cerebral cortex size are governed by fibroblast growth factor during embryogenesis. *Nat Neurosci,* 2**,** 848.

VALLEE, R. B. & TSAI, J. W. 2006. The cellular roles of the lissencephaly gene LIS1, and what they tell us about brain development. *Genes Dev,* 20**,** 1384-93.

VASUDEVAN, A., LONG, J. E., CRANDALL, J. E., RUBENSTEIN, J. L. & BHIDE, P. G. 2008. Compartment-specific transcription factors orchestrate angiogenesis gradients in the embryonic brain. *Nat Neurosci,* 11**,** 429-39.

VENERE, M., HAN, Y. G., BELL, R., SONG, J. S., ALVAREZ-BUYLLA, A. & BLELLOCH, R. 2012. Sox1 marks an activated neural stem/progenitor cell in the hippocampus. *Development,* 139**,** 3938-49.

VICARIO-ABEJON, C., JOHE, K. K., HAZEL, T. G., COLLAZO, D. & MCKAY, R. D. 1995. Functions of basic fibroblast growth factor and neurotrophins in the differentiation of hippocampal neurons. *Neuron,* 15**,** 105-14.

VIEIRA, J. M., SCHWARZ, Q. & RUHRBERG, C. 2007. Selective requirements for NRP1 ligands during neurovascular patterning. *Development,* 134**,** 1833-43.

VISVANATHAN, J., LEE, S., LEE, B., LEE, J. W. & LEE, S. K. 2007. The microRNA miR-124 antagonizes the anti-neural REST/SCP1 pathway during embryonic CNS development. *Genes Dev,* 21**,** 744-9.

VITI, J., GULACSI, A. & LILLIEN, L. 2003. Wnt regulation of progenitor maturation in the cortex depends on Shh or fibroblast growth factor 2. *J Neurosci,* 23**,** 5919-27.

WADA, T., HAIGH, J. J., EMA, M., HITOSHI, S., CHADDAH, R., ROSSANT, J., NAGY, A. & VAN DER KOOY, D. 2006. Vascular endothelial growth factor directly inhibits primitive neural stem cell survival but promotes definitive neural stem cell survival. *J Neurosci,* 26**,** 6803-12.

WANG, T. W., STROMBERG, G. P., WHITNEY, J. T., BROWER, N. W., KLYMKOWSKY, M. W. & PARENT, J. M. 2006. Sox3 expression identifies neural progenitors in persistent neonatal and adult mouse forebrain germinative zones. *J Comp Neurol,* 497**,** 88-100.

WANG, X., TSAI, J. W., IMAI, J. H., LIAN, W. N., VALLEE, R. B. & SHI, S. H. 2009. Asymmetric centrosome inheritance maintains neural progenitors in the neocortex. *Nature,* 461**,** 947-55.

WANG, Y., RATTNER, A., ZHOU, Y., WILLIAMS, J., SMALLWOOD, P. M. & NATHANS, J. 2012. Norrin/Frizzled4 signaling in retinal vascular development and blood brain barrier plasticity. *Cell,* 151**,** 1332-44.

WILCOCK, A. C., SWEDLOW, J. R. & STOREY, K. G. 2007. Mitotic spindle orientation distinguishes stem cell and terminal modes of neuron production in the early spinal cord. *Development,* 134**,** 1943-54.

WILLIAMS, B. P., PARK, J. K., ALBERTA, J. A., MUHLEBACH, S. G., HWANG, G. Y., ROBERTS, T. M. & STILES, C. D. 1997. A PDGF-regulated immediate early gene response initiates neuronal differentiation in ventricular zone progenitor cells. *Neuron,* 18**,** 553-62.

WILSCH-BRAUNINGER, M., PETERS, J., PARIDAEN, J. T. & HUTTNER, W. B. 2012. Basolateral rather than apical primary cilia on neuroepithelial cells committed to delamination. *Development,* 139**,** 95-105.

WITTKO, I. M., SCHANZER, A., KUZMICHEV, A., SCHNEIDER, F. T., SHIBUYA, M., RAAB, S. & PLATE, K. H. 2009. VEGFR-1 regulates adult olfactory bulb neurogenesis and migration of neural progenitors in the rostral migratory stream in vivo. *J Neurosci,* 29**,** 8704-14.

WODARZ, A. & NUSSE, R. 1998. Mechanisms of Wnt signaling in development. *Annu Rev Cell Dev Biol,* 14**,** 59-88.

WOOD, H. B. & EPISKOPOU, V. 1999. Comparative expression of the mouse Sox1, Sox2 and Sox3 genes from pre-gastrulation to early somite stages. *Mech Dev,* 86**,** 197-201.

WOODS, C. G., BOND, J. & ENARD, W. 2005. Autosomal recessive primary microcephaly (MCPH): a review of clinical, molecular, and evolutionary findings. *Am J Hum Genet,* 76**,** 717-28.

WU, Y., LIU, Y., LEVINE, E. M. & RAO, M. S. 2003. Hes1 but not Hes5 regulates an astrocyte versus oligodendrocyte fate choice in glial restricted precursors. *Dev Dyn,* 226**,** 675-89.

XU, Q., WANG, Y., DABDOUB, A., SMALLWOOD, P. M., WILLIAMS, J., WOODS, C., KELLEY, M. W., JIANG, L., TASMAN, W., ZHANG, K. & NATHANS, J. 2004. Vascular development in the retina and inner ear:

control by Norrin and Frizzled-4, a high-affinity ligand-receptor pair. *Cell,* 116**,** 883-95.

YAMADA, J. & JINNO, S. 2014. S100A6 (calcyclin) is a novel marker of neural stem cells and astrocyte precursors in the subgranular zone of the adult mouse hippocampus. *Hippocampus,* 24**,** 89-101.

YANG, Y. T., WANG, C. L. & VAN AELST, L. 2012. DOCK7 interacts with TACC3 to regulate interkinetic nuclear migration and cortical neurogenesis. *Nat Neurosci,* 15**,** 1201-10.

YE, W., SHIMAMURA, K., RUBENSTEIN, J. L., HYNES, M. A. & ROSENTHAL, A. 1998. FGF and Shh signals control dopaminergic and serotonergic cell fate in the anterior neural plate. *Cell,* 93**,** 755-66.

YE, X., SMALLWOOD, P. & NATHANS, J. 2011. Expression of the Norrie disease gene (Ndp) in developing and adult mouse eye, ear, and brain. *Gene Expr Patterns,* 11**,** 151-5.

YE, X., WANG, Y., CAHILL, H., YU, M., BADEA, T. C., SMALLWOOD, P. M., PEACHEY, N. S. & NATHANS, J. 2009. Norrin, frizzled-4, and Lrp5 signaling in endothelial cells controls a genetic program for retinal vascularization. *Cell,* 139**,** 285-98.

YILMAZ, O. H., KATAJISTO, P., LAMMING, D. W., GULTEKIN, Y., BAUER-ROWE, K. E., SENGUPTA, S., BIRSOY, K., DURSUN, A., YILMAZ, V. O., SELIG, M., NIELSEN, G. P., MINO-KENUDSON, M., ZUKERBERG, L. R., BHAN, A. K., DESHPANDE, V. & SABATINI, D. M. 2012. mTORC1 in the Paneth cell niche couples intestinal stem-cell function to calorie intake. *Nature,* 486**,** 490-5.

YOON, K. J., KOO, B. K., IM, S. K., JEONG, H. W., GHIM, J., KWON, M. C., MOON, J. S., MIYATA, T. & KONG, Y. Y. 2008. Mind bomb 1-expressing intermediate progenitors generate notch signaling to maintain radial glial cells. *Neuron,* 58**,** 519-31.

YOSHIDA, N., HISHIYAMA, S., YAMAGUCHI, M., HASHIGUCHI, M., MIYAMOTO, Y., KAMINOGAWA, S. & HISATSUNE, T. 2003. Decrease in expression of alpha 5 beta 1 integrin during neuronal differentiation of cortical progenitor cells. *Exp Cell Res,* 287**,** 262-71.

YOUSIF, L. F., DI RUSSO, J. & SOROKIN, L. 2013. Laminin isoforms in endothelial and perivascular basement membranes. *Cell Adh Migr,* 7**,** 101-10.

ZARKADA, G., HEINOLAINEN, K., MAKINEN, T., KUBOTA, Y. & ALITALO, K. 2015. VEGFR3 does not sustain retinal angiogenesis without VEGFR2. *Proc Natl Acad Sci U S A,* 112**,** 761-6.

ZHANG, J., WOODHEAD, G. J., SWAMINATHAN, S. K., NOLES, S. R., MCQUINN, E. R., PISAREK, A. J., STOCKER, A. M., MUTCH, C. A., FUNATSU, N. & CHENN, A. 2010a. Cortical neural precursors inhibit their own differentiation via N-cadherin maintenance of beta-catenin signaling. *Dev Cell,* 18**,** 472-9.

ZHANG, X., HUANG, C. T., CHEN, J., PANKRATZ, M. T., XI, J., LI, J., YANG, Y., LAVAUTE, T. M., LI, X. J., AYALA, M., BONDARENKO, G. I., DU, Z. W., JIN, Y., GOLOS, T. G. & ZHANG, S. C. 2010b. Pax6 is a human neuroectoderm cell fate determinant. *Cell Stem Cell,* 7**,** 90-100.

ZHANG, Y., CHEN, K., SLOAN, S. A., BENNETT, M. L., SCHOLZE, A. R., O'KEEFFE, S., PHATNANI, H. P., GUARNIERI, P., CANEDA, C., RUDERISCH, N., DENG, S., LIDDELOW, S. A., ZHANG, C.,

DANEMAN, R., MANIATIS, T., BARRES, B. A. & WU, J. Q. 2014. An RNA-sequencing transcriptome and splicing database of glia, neurons, and vascular cells of the cerebral cortex. *J Neurosci,* 34**,** 11929-47.

ZHAO, S., NICHOLS, J., SMITH, A. G. & LI, M. 2004. SoxB transcription factors specify neuroectodermal lineage choice in ES cells. *Mol Cell Neurosci,* 27**,** 332-42.

ZHONG, W., JIANG, M. M., SCHONEMANN, M. D., MENESES, J. J., PEDERSEN, R. A., JAN, L. Y. & JAN, Y. N. 2000. Mouse numb is an essential gene involved in cortical neurogenesis. *Proc Natl Acad Sci U S A,* 97**,** 6844-9.

ZHONG, W., JIANG, M. M., WEINMASTER, G., JAN, L. Y. & JAN, Y. N. 1997. Differential expression of mammalian Numb, Numblike and Notch1 suggests distinct roles during mouse cortical neurogenesis. *Development,* 124**,** 1887-97.

ZHOU, Y. & NATHANS, J. 2014. Gpr124 controls CNS angiogenesis and blood-brain barrier integrity by promoting ligand-specific canonical wnt signaling. *Dev Cell,* 31**,** 248-56.

ZHOU, Y., WANG, Y., TISCHFIELD, M., WILLIAMS, J., SMALLWOOD, P. M., RATTNER, A., TAKETO, M. M. & NATHANS, J. 2014. Canonical WNT signaling components in vascular development and barrier formation. *J Clin Invest,* 124**,** 3825-46.

ZHU, G., MEHLER, M. F., ZHAO, J., YU YUNG, S. & KESSLER, J. A. 1999. Sonic hedgehog and BMP2 exert opposing actions on proliferation and differentiation of embryonic neural progenitor cells. *Dev Biol,* 215**,** 118-29.

ZHU, J., MOTEJLEK, K., WANG, D., ZANG, K., SCHMIDT, A. & REICHARDT, L. F. 2002. beta8 integrins are required for vascular morphogenesis in mouse embryos. *Development,* 129**,** 2891-903.

Chapter 8 APPENDIX

Table 8.1 Fold change enrichment for all transcripts assayed for in qRT-PCR array.

Gene	Description	Fold change (*Nrp1*$^{-/-}$ *expression / Nrp1*$^{+/+}$ *expression)*
Ache	Acetylcholinesterase	1.1155
Adora1	Adenosine A1 receptor	3.4339
Adora2a	Adenosine A2a receptor	1.6057
Alk	Anaplastic lymphoma kinase	0.5815
Apbb1	Amyloid beta (A4) precursor protein-binding, family B, member 1	0.8717
Apoe	Apolipoprotein E	1.7154
App	Amyloid beta (A4) precursor protein	1.0137
Artn	Artemin	1.9914
Ascl1	Achaete-scute complex homolog 1 (Drosophila)	0.9387
Bcl2	B-cell leukemia/lymphoma 2	1.3072
Bdnf	Brain derived neurotrophic factor	2.9168
Bmp2	Bone morphogenetic protein 2	1.6923
Bmp4	Bone morphogenetic protein 4	2.0833
Bmp8b	Bone morphogenetic protein 8b	1.7442
Cdk5r1	Cyclin-dependent kinase 5, regulatory subunit 1	0.9553
Cdk5rap2	CDK5 regulatory subunit associated protein 2	1.6612
Chrm2	Cholinergic receptor, muscarinic 2, cardiac	0.6375
Creb1	CAMP responsive element binding protein 1	1.5247
Cxcl1	Chemokine (C-X-C motif) ligand 1	0.7974
Dcx	Doublecortin	0.8322
Dlg4	Discs, large homolog 4 (Drosophila)	1.6348
Dll1	Delta-like 1 (Drosophila)	1.135
Drd2	Dopamine receptor D2	1.7685
Dvl3	Dishevelled 3, dsh homolog (Drosophila)	1.0508
Efnb1	Ephrin B1	1.3287
Egf	Epidermal growth factor	1.2943
Ep300	E1A binding protein p300	2.4189
Erbb2	V-erb-b2 erythroblastic leukemia viral oncogene homolog 2, neuro/glioblastoma derived oncogene homolog (avian)	1.068
Fgf2	Fibroblast growth factor 2	1.195

Flna	Filamin, alpha	3.2048
Gdnf	Glial cell line derived neurotrophic factor	2.8084
Gpi1	Glucose phosphate isomerase 1	1.6666
Grin1	Glutamate receptor, ionotropic, NMDA1 (zeta 1)	0.9433
Hdac4	Histone deacetylase 4	2.4491
Hes1	Hairy and enhancer of split 1 (Drosophila)	2.2017
Hey1	Hairy/enhancer-of-split related with YRPW motif 1	0.9759
Hey2	Hairy/enhancer-of-split related with YRPW motif 2	1.8598
Heyl	Hairy/enhancer-of-split related with YRPW motif-like	1.3584
Il3	Interleukin 3	0.7974
Mdk	Midkine	1.5134
Mef2c	Myocyte enhancer factor 2C	2.0329
Mll1	Myeloid/lymphoid or mixed-lineage leukemia 1	1.2592
Mtap2	Microtubule-associated protein 2	1.1272
Ndn	Necdin	0.8983
Ndp	Norrie disease (pseudoglioma) (human)	1.0356
Neurod1	Neurogenic differentiation 1	1.9075
Neurog1	Neurogenin 1	1.2998
Neurog2	Neurogenin 2	0.9155
Nf1	Neurofibromatosis 1	1.1321
Nog	Noggin	1.848
Notch1	Notch gene homolog 1 (Drosophila)	0.9562
Notch2	Notch gene homolog 2 (Drosophila)	1.4488
Nr2e3	Nuclear receptor subfamily 2, group E, member 3	0.7974
Nrcam	Neuron-glia-CAM-related cell adhesion molecule	0.9857
Nrg1	Neuregulin 1	2.5214
Nrp1	Neuropilin 1	0.0518
Nrp2	Neuropilin 2	1.8358
Ntf3	Neurotrophin 3	2.4795
Ntn1	Netrin 1	0.7171
Odz1	Odd Oz/ten-m homolog 1 (Drosophila)	0.6482
Olig2	Oligodendrocyte transcription factor 2	0.883
Pafah1b1	Platelet-activating factor acetylhydrolase, isoform 1b, subunit 1	0.8977
Pard3	Par-3 (partitioning defective 3) homolog (C. elegans)	1.5146
Pax3	Paired box gene 3	0.9914
Pax5	Paired box gene 5	1.8993

Pax6	Paired box gene 6	0.8065
Pou3f3	POU domain, class 3, transcription factor 3	0.6706
Pou4f1	POU domain, class 4, transcription factor 1	1.4447
Ptn	Pleiotrophin	1.1291
Rac1	RAS-related C3 botulinum substrate 1	1.2656
Robo1	Roundabout homolog 1 (Drosophila)	1.7707
Rtn4	Reticulon 4	1.3123
S100a6	S100 calcium binding protein A6 (calcyclin)	2.9448
S100b	S100 protein, beta polypeptide, neural	0.9592
Shh	Sonic hedgehog	0.8864
Slit2	Slit homolog 2 (Drosophila)	2.9609
Sod1	Superoxide dismutase 1, soluble	0.9813
Sox2	SRY-box containing gene 2	1.0999
Sox3	SRY-box containing gene 3	0.685
Stat3	Signal transducer and activator of transcription 3	1.0148
Tgfb1	Transforming growth factor, beta 1	1.2092
Th	Tyrosine hydroxylase	1.5681
Tnr	Tenascin R	0.5717
Vegfa	Vascular endothelial growth factor A	3.811
Actb	Actin, beta	1.6562
B2m	Beta-2 microglobulin	1.2698
Gapdh	Glyceraldehyde-3-phosphate dehydrogenase	1.9558
Gusb	Glucuronidase, beta	330.8235
Hsp90ab1	Heat shock protein 90 alpha (cytosolic), class B member 1	1
MGDC	Mouse Genomic DNA Contamination	0.7974
RTC	Reverse Transcription Control	0.7323
RTC	Reverse Transcription Control	0.6401
RTC	Reverse Transcription Control	0.7487
PPC	Positive PCR Control	0.8012
PPC	Positive PCR Control	0.776
PPC	Positive PCR Control	0.7459

Table 8.2 Number of embryos analysed.

Figure	Genotype	Developmental stage (sample size)
4.2B	*Nrp1*$^{+/+}$	32s (6), 36s (3), 40s (4)
	Nrp1$^{-/-}$	32s (4), 36s (4) 40s (5)
4.3	*Nrp1*$^{+/+}$	32s (3), 40s (4), 46s (3)
	Nrp1$^{-/-}$	32s (3), 40s (3) 46s (3)
4.4B-D	*Nrp1*$^{+/+}$	25s (4), 32s (3), 36s (3), 40s (3), 42s (3) 46s (5)
	Nrp1$^{-/-}$	25s (3), 32s (6), 36s (3), 40s (4), 42s (6), 46s (3)
4.5B	*Nrp1*$^{+/+}$	32s (4), 36s (3), 40s (4)
	Nrp1$^{-/-}$	32s (3), 36s (4), 40s (5)
4.7D	*Nrp1*$^{c/+}$	36s (3), 42s (5), 45s (6), 49s (3)
	Tie2-Cre; Nrp1$^{c/-}$	36s (5), 42s (3), 45s (7), 49s (7)
4.7E	*Nrp1*$^{c/+}$	36s (3), 42s (6), 51s (3)
	Nes-Cre; Nrp1$^{c/-}$	36s (3), 42s (4), 51s (3)
4.8	*Nrp1*$^{+/+}$*Nrp2*$^{+/+}$	49s (4)
	Nrp1$^{+/Sema}$ *Nrp2*$^{+/-}$	49s (6)
	Nrp1$^{+/+}$ *Nrp2*$^{-/-}$	49s (2)
	Nrp1$^{Sema/Sema}$ *Nrp2*$^{-/-}$	49s (3)
4.10	*Pu.1*$^{+/+}$	50s (3)
	Pu.1$^{-/-}$	50s (3)
5.1C	*Nrp1*$^{+/+}$	32s (3)
	Nrp1$^{-/-}$	32s (3)
	Tie2-Cre; Nrp1$^{c/-}$	32s (5)
5.2B-D	*Nrp1*$^{+/+}$	32s (3), 40s (3), 46s (3)
	Nrp1$^{-/-}$	32s (3), 40s (3), 46s (3)
5.3A	*Nrp1*$^{+/+}$	32s (3)
	Nrp1$^{-/-}$	32s (3)
	Tie2-Cre; Nrp1$^{c/-}$	32s (5)
5.4A	*Nrp1*$^{+/+}$	32s (3), 40s (3), 46s (3)
	Nrp1$^{-/-}$	32s (3), 40s (3), 46s (3)
5.6B,C	*Nrp1*$^{+/+}$	32 (5), 36s (10)
	Nrp1$^{-/-}$	32 (5), 36s (3)
5.6D	*Nrp1*$^{+/+}$	32 (4), 36s (8)
	Nrp1$^{-/-}$	32 (5), 36s (3)
5.7	*Nrp1*$^{+/+}$	46s (3)

	Nrp1$^{-/-}$	46s (3)
5.8A	*Nrp1*$^{+/+}$	32s (4)
	Nrp1$^{-/-}$	32s (4)
5.8D	*Nrp1*$^{+/+}$ 20% O_2	32s (3)
	Nrp1$^{-/-}$ 20% O_2	32s (3)
	Nrp1$^{-/-}$ 80% O_2	32s (3)
5.9	*Nrp1*$^{+/+}$	35s (3 embryos pooled)
	Nrp1$^{-/-}$	35s (3 embryos pooled)
5.10	*Nrp1*$^{+/+}$	32s (4)
	Nrp1$^{-/-}$	32s (5)
5.11	Wildtype	35s (3 embryos pooled)
	Tie2-Cre; Rosa^{YFP}	35s (3 embryos pooled)

LIST OF SUPPORTING PUBLICATIONS

Tata M, Tillo M and Ruhrberg C (2015) Neuropilins in Development and Disease of the Nervous System In: *Neural Surface Antigens: From Basic Biology to Biomedical Applications*. 1st ed. London: Academic Press Inc. pp. 65-75

Tata M, Ruhrberg C and Fantin A (2015) Vascularisation of the central nervous system. *Mechanisms of Development* 138(1):26-36

Tata M, Wall I, Joyce A, Vieira J, Kessaris N and Ruhrberg C (2016) Regulation of embryonic neurogenesis by germinal zone vasculature. *Proceedings of the National Academy.* 113(47):13414-13419